Motion representation in hMT+/V5: Influence of cross-modal inputs and visual deprivation

Motion representation in hMT+/V5: Influence of cross-modal inputs and visual deprivation

Mohamed REZK

Thèse présentée en vue de l'obtention du grade de Docteur en sciences psychologiques et de l'éducation

Promoter

Prof. Dr. Olivier COLLIGNON (UCLouvain, Belgium)

Accompanying committee

Prof. Dr. Valérie GOFFAUX (UCLouvain, Belgium)
Prof. Dr. André MOURAUX, MD (UCLouvain, Belgium)

Collection de thèses de l'Université catholique de Louvain, 2021

President

Prof. Dr. Valérie GOFFAUX (UCLouvain, Belgium)

Accompanying committee and jury

Prof. Dr. Olivier COLLIGNON (UCLouvain, Belgium)
Prof. Dr. André MOURAUX, MD (UCLouvain, Belgium)
Prof. Dr. Holly BRIDGE (University of Oxford, United Kingdom)
Prof. Dr. Georgios KELIRIS (University of Antwerp, Belgium)

Table of contents

Résumé ... *13*
Abstract ... *15*
Chapter 1: Introduction ... *21*
Functional specialization in the visual cortex ... *21*
Functional specialization of MT/V5 ... *22*
Cortical route for visual motion processing ... *23*
How does visual information reach MT/V5? ... 23
Is V1 necessary for visual motion information to reach MT/V5? ... 24
Blindsight ... 25
Riddoch Syndrome ... 25
Subcortical routes for visual motion processing ... *26*
Organization of MT/V5 ... *27*
The distinction between MT and MST ... 29
The origin of functional specialization in the visual cortex ... *30*
[i] Visual features selectivity ... 30
[ii] hierarchy of information processing ... 31
[iii] Biased connectivity hypothesis ... 31
Auditory motion processing ... *32*
Cortical pathway for auditory motion processing ... 33
Multi-sensory motion processing: Behavior ... 33
Multi-sensory motion processing: Brain ... 34
Arguments supporting multisensory motion processing in hMT+/V5 ... 36
Arguments supporting uni-sensory visual motion processing in hMT+/V5 ... 37
The impact of visual deprivation on the development of the visual system ... *39*
Orientation and Direction Deprivation ... 39
Monocular visual deprivation ... 40
Early transient and complete visual deprivation ... 40
Permanent congenital/early blindness ... 42
Functional reorganization of the visual system ... 43
Impact of the age of blindness onset ... 44
The connectivity architecture of the visual system in the visually deprived ... *45*
Methods used to investigate brain activity ... *48*
fMRI and univariate analyses ... 48
Multivariate pattern analysis (MVPA) ... 50
Split-half correlation ... 50
Pattern classification ... 51
Representational similarity analysis (RSA) ... 56
Brain connectivity ... 58
Task-based functional connectivity ... 58

Resting state functional connectivity 59
Summary *61*
References *62*
Chapter 2 ..... *91*
Shared representation of visual and auditory motion directions in the human middle-temporal cortex *91*
Introduction *91*
Methods *92*
Participants 92
Training 92
Experimental design 93
Stimuli 93
Visual motion localizer 94
Auditory motion localizer 94
Directional motion decoding experiment 95
MRI acquisition 95
fMRI preprocessing 96
Eye tracker experiment 96
Behavioral Analysis 97
Univariate analysis 97
Beta parameter estimates 98
Functional connectivity analysis (PPI) 99
Multivariate pattern analysis (MVPA) 100
ROI definition for MVPA 100
Experiment 1 (visual and auditory motion localizer) 100
Experiment 2 (Directional motion decoding experiment) 102
Results *107*
Experiment 1: Motion Localizers 107
Visual and auditory motion localizers 107
Beta parameter estimates in auditory and visual motion selective regions 107
Functional connectivity analysis 109
Motion versus static decoding 110
Experiment 2: Directional motion decoding 111
Within-modality decoding 111
Cross-modal decoding 111
Modality decoding 113
Representational similarity analysis 113
Pattern correlations 114
Differential pattern correlation 116
Discussion *117*
References *122*
Supplementary materials *130*
Chapter 3 ..... *145*
Introduction *145*

Materials and methods ... *146*
Participants ... 146
Visual tests ... 147
Assessment of visual acuity ... 147
Assessment of contrast sensitivity ... 147
Assessment of motion sensitivity ... 147
fMRI experiments ... 148
Stimuli ... 148
Experimental design (Experiment I): Motion selectivity Experiment ... 149
Experimental design (Experiment II): Directional motion decoding experiment ... 149
MRI acquisition ... 150
fMRI preprocessing ... 150
Experiment 1 (Motion selectivity experiment) ... 150
Experiment 2 (Directional motion decoding experiment) ... 153
Structural analysis ... 157
Experiment III (Resting-State) ... 157
Participants ... 157
MRI acquisition ... 157
Regions of interest ... 158
Resting-state functional connectivity analysis ... 158
Results ... *159*
Visual tests ... 159
Assessment of visual acuity ... 159
Assessment of contrast sensitivity ... 159
Behavioral results: ... 159
Experiment I: Motion selectivity ... 160
Correlation ... 162
Functional connectivity analysis (PPI) ... 162
Retinotopic motion selectivity ... 164
Experiment II: Directional motion decoding experiment ... 166
Control Analysis 1: Group-level hMT+/V5 ROI ... 167
Control Analysis 2: Individual-level hMT+/V5 ROI ... 167
Split-half correlation ... 169
Structural analysis ... 170
Experiment III: Resting-state ... 172
Discussion ... *173*
References ... *178*
Supplementary materials ... *187*
Chapter 4 ... *205*
Impact of blindness onset on the connectivity profile of hMT+/V5 ... *205*
Introduction ... *205*
Materials & Methods ... *207*
Participants ... 207
fMRI Acquisition ... 207
fMRI data preprocessing ... 208

Functional connectivity 208
Connectivity within-visual system 209
ROIs Definition 209
ROI-to-ROI functional connectivity 209
Similarities of average fingerprints across groups 209
Connectivity across different sensory systems 210
ROIs Definition 210
ROI-to-ROI functional connectivity 210
Similarities of average fingerprints across groups 210
Connectivity across the whole brain 211
Seed-to-voxel functional connectivity 211
Group Classification 211
Results 212
Connectivity within the visual system 212
ROI-to-ROI connectivity 212
Similarities of average fingerprints across groups 214
Connectivity across sensory systems 216
ROI-to-ROI connectivity 216
Similarities of average fingerprints across groups 217
Seed-to-voxel analysis 219
Group Classification 219
Discussion 222
References 227
Supplementary materials 234
Chapter 5 243
Discussion 243
The aim of the thesis 243
The nature of motion processing in hMT+/V5 243
Format of representation 244
Multisensory motion processing in hMT+/V5 245
Development of the visual motion system in the early blind 245
Development of the visual motion system in the late blind 250
Development of the visual motion system in the cataract-reversal patients 251
Is hMT+/V5 immune to change 252
Cross-modal reorganization in the cataract-reversal patients 252
Connectivity architecture of the visual motion system in the cataract-reversal patients 253
Functional connectivity and plasticity 254
Limitations of inferring functional reorganization from resting-state connectivity 255
Models of the development of the visual motion system 258
Typical visual development 258
Brief early visual deprivation 259
Early permanent visual deprivation 260

Late visual deprivation 261
Summary *262*
References *263*
List of publications *277*

List of figures

Figure 1.1 Visual pathways to MT/V5 according to Felleman & Van Essen (1991). *24*
Figure 1.2 Optical imaging of area MT/V5 in owl monkey. *28*
Figure 1.3 A 3D representation of the columnar organization of MT/V5 in the macaque. *28*
Figure 1.4 Columnar organization of MT/V5 in humans using high-field MRI. *29*
Figure 1.5 The recruitment of hMT+/V5 during motion processing from different modalities. *35*
Figure 1.6 An illustration of unimodal, multi-modal, and supra-modal regions. ... *39*
Figure 1.7 Effect of visual deprivation due to cataract on global motion processing. *41*
Figure 1.8 Cross-modal plasticity in the early blind and the late blind. *45*
Figure 1.9 Resting-state functional connectivity changes in the early blind. *47*
Figure 1.10 Split-half correlation analysis. *51*
Figure 1.11 A graphical illustration of multivariate pattern classification. *53*
Figure 1.12 Linear classifiers (SVM and LDA) *55*
Figure 1.13 Representational similarity analysis (RSA). *57*
Figure 2.1 Univariate results from the visual and the auditory motion localizers. *108*
Figure 2.2 PPI analysis. *109*
Figure 2.3 Motion versus static decoding. *110*
Figure 2.4 Directional motion decoding experiment. *112*
Figure 2.5 Multivariate analyses from the directional motion decoding experiment. *115*
Figure S2.1 Within-modality Within-axis classification. *131*
Figure S2.2 Control analysis for the cross-modal decoding. *132*
Figure S2.3 Eye movements. *134*
Figure 3.1 Univariate results from the motion selectivity experiment. *161*
Figure 3.2 Correlation analysis in the cataract-reversal patients. *163*
Figure 3.3 PPI Analysis in the motion selectivity experiment. *164*
Figure 3.4 Beta parameter estimates for different retinotopic regions in V1. ..... *165*
Figure 3.5 MVPA results from the directional motion experiment in V1 and MT. *166*

Figure 3.6 MVPA results from the directional motion experiment in the functionally-defined hMT+/V5. ..... *168*
Figure 3.7 Split-half correlation results. *170*
Figure 3.8 Structural analysis results *171*
Figure 3.9 Resting-state functional connectivity analysis. *172*
Figure 3.10 Resting-state seed-to-voxel functional connectivity. *173*
Figure S3.1 Supplementary analysis for the motion selectivity experiment. *187*
Figure S3.2 Effect of varying the number of features on motion direction decoding in V1 ..... *188*
Figure S3.3 Correlation between the duration of visual deprivation and motion direction classification. *189*
Figure S3.4 Correlation between the behavioral motion direction discrimination threshold and motion direction classification. *190*
Figure S3.5 Correlation between visual acuity and motion direction classification. *191*
Figure S3.6 Correlation between contrast sensitivity and motion direction classification. *192*
Figure S3.7 Variability of the MRI signal from the eyes. *193*
Figure S3.8 Motion direction decoding from the eyes. *194*
Figure 4.1 ROI-to-ROI functional connectivity in the visual motion system. *213*
Figure 4.2 Functional connectivity differences between the EB and the LB within the visual motion network. *214*
Figure 4.3 Connectivity fingerprint of hMT within the visual motion system. *215*
Figure 4.4 ROI-to-ROI functional connectivity of hMT+/V5 with different sensory networks *216*
Figure 4.5 Connectivity changes of hMT+/V5 with the different sensory networks due to early visual deprivation. *217*
Figure 4.6 Multisensory connectivity fingerprint of hMT+/V5. ..... *218*
Figure 4.7 Seed-to-voxel analysis *220*
Figure 4.8 Group Classification based on the hMT+/V5 connectivity fingerprint. *221*
Figure 4.9 Mixture-of-experts model. *224*
Figure S4.1 Connectivity fingerprint of V1 within the visual motion system. *234*
Figure S4.2 Connectivity fingerprint of V2 within the visual motion system. *235*
Figure S4.3 Connectivity fingerprint of V3v and V3a within the visual motion system. *236*
Figure S4.4 Connectivity fingerprint of V3b and V3d within the visual motion system. *237*
Figure S4.5 Connectivity fingerprint of LGN and hMT within the visual motion system. *238*

Figure S4.6 The correlation analysis of the average connectivity fingerprint of the different visual regions within the visual motion system. 239
Figure 5.1 Auditory motion plane decoding in the early blind 247
Figure 5.2 Auditory motion direction decoding in the early blind 248
Figure 5.3 Structural connectivity between hMT+/V5 and PT. 249
Figure 5.4 Models of the development of the visual motion system. 259

List of tables

Table S2.1 Results of the univariate analysis from the visual and the auditory motion localizers. 135
Table S2.2 Peak coordinates of the individually defined regions of interest. 136
Table S2.3 Psychophysiological interactions (PPI) from the visual and the auditory motion localizers. 137
Table S2.4 Within-modality classification results. 138
Table S2.5 RSA analysis and the comparison of the RSA models' correlation. 139
Table S2.6 Split-half correlation results and the comparison between the SHC values in the different conditions. 140
Table S3.1 Cataract-reversal patients' information. 195
Table S3.2 Peak coordinates of the individually defined hMT+/V5. 196
Table S3.3 Results of the univariate analysis from the motion selectivity experiment. 197
Table S3.4 Correlation between motion selectivity and duration of visual deprivation. 198
Table S3.5 Psychophysiological interactions (PPI) from the motion selectivity experiment. 200
Table S3.6 Directional motion classification results. 201
Table S4.1 Connectivity changes of hMT+/V5 with the different sensory networks due to early visual deprivation. 240
Table S4.2 Seed-to-voxel analysis. 241

Résumé

La recherche présentée dans cette thèse étudie la représentation intermodale du mouvement dans hMT+/V5 et l'impact de la privation visuelle sur cette région à l'aide de l'imagerie par résonance magnétique fonctionnelle (IRMf). hMT+/V5 est une région de la voie visuelle dorsale qui est connue pour être dédiée au traitement de l'information liée au mouvement visuel. Pour comprendre comment hMT+/V5 représente cette information à travers les sens et comment cette représentation se développe en l'absence d'expérience visuelle, nous avons réalisé les études suivantes:

Dans la première étude, nous avons utilisé l'IRMf pour caractériser la représentation des directions du mouvements visuel et auditif dans hMT+/V5, après avoir défini cette région fonctionnellement chez chaque participant. Nous avons montré que les directions des mouvements auditifs et visuels peuvent être décodées de manière fiable dans hMT+/V5. De plus, la direction de mouvement dans une modalité sensorielle peut être prédite à partir des profils d'activité induits par une autre modalité sensorielle. Malgré les informations partagées sur la direction du mouvement entre les modalités sensorielles, les stimuli visuels et auditifs ont produit des réponses opposées au niveau des voxels de hMT+/V5. Nos résultats ont mis en évidence une représentation complexe des informations de mouvement multisensorielle dans hMT+/V5.

Dans la deuxième étude, nous avons étudié comment l'absence d'expérience visuelle pendant une courte et ransitoire période en début de vie façonne le développement du réseau de mouvement visuel à l'aide de l'IRMf. Nos résultats suggèrent qu'une période précoce et brève de privation visuelle conduit à un recrutement réduit des zones visuelles primaires (V1) lors du traitement des informations de mouvement par rapport aux participants contrôles appariés avec un développement visuel typique. Le recrutement réduit dans le cortex visuel primaire chez les patients était corrélé avec la durée de la privation visuelle. Les analyses univariées et multivariées n'ont montré aucune altération du traitement l'information du mouvement visuel dans la région hMT+/V5 chez les patients. Les résultats suggèrent qu'une période brève et transitoire de privation visuelle au début de la vie a un impact sur le réseau de traitement de l'information du mouvement qui est spécifique à la région : V1 étant affecté de manière permanente tandis que hMT+/V5 montre une certaine résilience à la privation visuelle.

Dans la troisième étude, nous avons étudié l'architecture de la connectivité au repos de la région hMT+/V5 avec d'autres régions du réseau du mouvement visuel chez les personnes aveugles précoces (*early blind* - EB) et tardives (*late blind* - LB). Nos résultats

ont démontré que le profil de connectivité de hMT+/V5 avec les différentes zones du réseau du mouvement visuel était très similaire dans tous les groupes et ne dépendait pas de l'expérience visuelle. De plus, nous avons étudié le profil de connectivité de hMT+/V5 avec les réseaux sensoriels non visuels, et avons trouvé une connectivité réduite avec le cortex somatosensoriel pendant le repos chez les EB. En outre, le profil de connectivité de hMT+/V5 avec les différents réseaux sensoriels était différent entre les EB et les voyants. En revanche, il n'y avait aucune différence dans le profil de connectivité de hMT+/V5 entre le LB et les voyants. Ces résultats démontrent que la cécité précoce, mais pas la cécité acquise tardivement, a un impact sur l'architecture de la connectivité de hMT+/V5 avec des réseaux non visuels.

Dans l'ensemble, nos résultats suggèrent: [1] hMT+/V5 représente les informations de mouvement de manière multisensorielle avec des informations partagées entre les sens. [2] La privation visuelle précoce et brève a un impact spécifique sur le réseau de mouvement, affectant principalement les zones visuelles primaires mais laissant la région hMT+/V5 relativement préservée. [3] L'âge d'apparition de la privation visuelle affecte le profil de connectivité multisensorielle de hMT+/V5.

Abstract

The research presented in this thesis investigates the cross-modal representation of motion information in hMT+/V5 and the impact of visual deprivation using functional magnetic resonance imaging (fMRI). hMT+/V5 is a region in the dorsal visual pathway that is known to be dedicated to processing visual motion. To unravel how hMT+/V5 represents motion information across the senses and how it develops in the absence of visual experience, we performed the following studies:

In the first study, we relied on fMRI recordings to characterize the representation of visual and auditory motion directions in individually and functionally defined hMT+/V5. We showed that auditory and visual motion directions can be reliably decoded in hMT+/V5. Additionally, motion directions in one modality can be predicted from the activity patterns elicited by the other modality. Despite shared motion-direction information across the senses, vision and audition produced opposite voxel-wise responses in hMT+/V5. Our results revealed a multi-faced representation of multisensory motion information in hMT+/V5.

In the second study, we investigated how the absence of early visual experience in cataract-reversal patients shapes the development of the visual motion network using fMRI. Our results suggest that an early and brief period of visual deprivation leads to a reduced recruitment of the early visual areas while processing motion information when compared to matched controls with typical visual development. The reduced recruitment in the early visual cortex in cataract-reversal patients correlated with the duration of visual deprivation. Univariate and multivariate analyses showed no impairments in visual motion processing in the higher order visual motion area hMT+/V5 in the cataract-reversal patients. The results suggested that a brief and transient period of visual deprivation early in life has a region-specific impact on the visual motion network with V1 being permanently affected while hMT+/V5 shows some resilience to deprivation.

In the third study, we investigated the resting-state connectivity architecture of hMT+/V5 with other regions within the visual motion network in early blind (EB) and late blind (LB) people. Our results demonstrated that the connectivity profile of hMT+/V5 with the different areas within the visual motion network was highly similar in all groups, and was not dependent on visual experience. Additionally, we investigated the connectivity profile of hMT+/V5 with the non-visual sensory networks, and found reduced connectivity with the somatosensory cortex during rest in the EB. Moreover, the connectivity profile of hMT+/V5 with the different sensory networks was not similar in the EB and the sighted. In

contrast, there was no difference in the connectivity profile of hMT+/V5 between the LB and the sighted. These results demonstrate that blindness onset impacts the connectivity architecture of hMT+/V5 with non-visual networks. While hMT+/V5 reorganizes its resting connectivity profile as a consequence of early visual deprivation, the hMT+/V5 connectivity architecture was not significantly affected in the LB.

Overall, our findings suggest: [1] hMT+/V5 represents motion information in a multisensory fashion with shared information between the senses. [2] Early and brief visual deprivation has a region-specific impact on the motion network, mostly affecting early visual areas but leaving hMT+/V5 somehow functionally preserved. [3] The age of onset of visual deprivation affects the multisensory connectivity profile of hMT+/V5.

Keywords: hMT+/V5, fMRI, MVPA, visual, auditory, motion, plasticity, deprivation, blindness, connectivity.

Acknowledgments

This PhD journey and this thesis was a product of many months of research and hard work that wouldn't have been possible without the help and the support from many people to whom I am very grateful.

First and foremost, I would like to thank my supervisor, Prof. Olivier Collignon, for his support and motivation throughout the previous years, and for providing me with the opportunities that made me where I am today. All the work that I was a part of wouldn't have seen the light without his supervision and guidance. Thank you for that. I learned a lot from you, and I am grateful for this opportunity. There were moments of ups and downs during this journey. I appreciate your motivation on the up days, and pushing me to first enjoy it and celebrate it, and then to move forward and to do bigger achievements. I also appreciate your understanding, support, and patience in the down days which definitely made it easier. I also want to thank you for creating a lab with a collaborative atmosphere rather than a competitive one. Thank you very much.

I also want to thank the accompanying committee Prof. André Mouraux and Prof. Valérie Goffaux for following my progress during my PhD, and for their valuable time, discussions, and advice that helped me progress in my journey. I would also like to thank Prof. Holly Bridge and Prof. Georgios Keliris for joining the doctoral committee, and for their time and effort in reading this thesis, and for the stimulating discussions that improved my work. Thank you very much. I truly appreciate it.

The work done in this thesis can't be mentioned without acknowledging the huge effort of Ceren in creating the sound system of the lab, and the help and support of Ceren, Stephanie, and Stefania in acquiring the data and analyzing it. Thank you for your patience and for the long fruitful discussions. I would also like to thank our collaborators Prof. Jorge Jovicich, Prof. Daphne Maurer, and Prof. Terri Lewis for their valuable help and support.

To my lab members and dear friends, thank you for being a big part of this journey, and for making it exciting and enjoyable. There is so much to tell and to thank all of you. Francesca and Jyothi, thank you for being the closest friends, and for being there whenever it was needed. I am very lucky and grateful for our friendship. Ceren and Siddharth, thank you for your support, and for our long discussions both professional or personal. Remi, thank you for your support and for sparking my curiosity about new domains. Stefania, Roberta, Marco, Fede, and Ane, thank you for all the nice times and experiences we had together. To my dear IPSY friends, Cathy, Kirsten, and Christiane, thank you for the nice times, discussions, and most definitely, thank you Kirsten for the "Cake Time" that we missed in the last year.

I want to thank Virginie Crollen (and Lucas of course) for all the help and support since I first arrived in Belgium, and for being like a family to me here. Thank you so much.

My dear friends, Yanina, Deniz, Hicret, Francesca, Nihan, Mario, Andrea, and Badr. Thank you for being such great friends, and for maintaining our strong connection after all these years without being affected by distance or time. Barbara, a big thank you for your continuous support, patience, help, and encouragement that I am very grateful for. My dear lifelong Egyptian friends, Amr, Hatem, M. Samir, despite being all on different continents, you have always been there, and encouraged me in every step of the way. Thank you. Your friendship and brotherhood are so valuable to me.

Last, but not least, my dear family. Thank you all for the support and encouragement throughout the years. Being far from you, especially in the good and the hard times, was not easy, and I appreciate your support nonetheless. To my mother, Amani, thank you for everything. There are so many things to be thankful for, trying to enumerate them would be unfair. Thank you for everything. My aunt, Faten, thank you for inspiring me to follow this path at a very early stage in my life. You opened my eyes to a different world. My grandmother, thank you for raising me to be the person who I am today, and thank you for everything you did for me in my life. My sisters, Mai & Mahinour, thank you for your care, love, and for being always close. My beautiful niece, Kenda, thank you for the happiness, positivity and love that you always bring to me. I can't wait to see you grow up, and to see the path that will inspire you.

أخيرًا وليس آخرًا، عائلتي العزيزة. شكرا لكم جميعا على الدعم والتشجيع على مر السنين. لم يكن الابتعاد عنكم، خاصة في الأوقات السعيدة والصعبة، أمرًا سهلاً، وأنا أقدر دعمكم رغم ذلك. لأمي، أماني، أشكرك على كل شيء. هناك الكثير من الأشياء التي يجب أن أكون شاكرا لها، ومحاولة حصرها ستكون غير عادلة. شكرا لك على كل شيء. خالتي، فاتن، أشكرك على إلهامي لاتباع هذا المسار في مرحلة مبكرة من حياتي. لقد فتحتي عيني على عالم مختلف. جدتي، أشكرك على تربيتي لأكون الشخص الذي أنا عليه اليوم، وأشكرك على كل ما فعلته من أجلي في حياتي. شقيقاتي مي و ماهينور، أشكركم على اهتمامكم وحبكم وعلى قربكم الدائم. ابنة أختي الجميلة كندا، أشكرك على السعادة والإيجابية والحب الذي تجلبيه لي دائمًا. لا أستطيع الانتظار لرؤيتك تكبرين، وأرى المسار الذي سيلهمك

To my partner, Zeyneb, thank you for your tremendous support throughout this journey, and for always giving me hope and positivity during the difficult times. My life would never be the same without you. I am a better person because of you. Thank you for being there for me, and for making me dream of an inspiring future, and for helping me to get there together. Thank you.

Chapter 1

Introduction

Chapter 1: Introduction

Motion perception is a crucial perceptual skill for the survival of living organisms. We rely on motion information in our daily life to perceive and to navigate our environment. Vision is one of the most reliable sources of information that guide our perception and our actions. However, our environment is multisensory in nature and is rich in information from different sensory modalities. Despite relying strongly on visual properties to process motion information, motion information can however be extracted from non-visual modalities as audition or touch. More importantly, integrating motion information from different sensory modalities allows us to have an enhanced perception of motion, and to interact more efficiently with our environment. Therefore, it is crucial to understand how our brain processes motion information, and how multisensory motion information are represented and integrated in the brain.

Functional specialization in the visual cortex

The processing of complex visual information to reach a coherent perception occurs in the visual system starting from the early striate visual cortex (V1) to higher-order visual regions. Early animal studies demonstrated that different regions along the visual hierarchy have specific functions of visual processing. For instance, neurons in the early visual cortex have a preference for stimuli **in** a certain orientation, and in a specific location in the visual field (Hubel & Wiesel, 1959, 1968). Regions in the extrastriate cortex also showed functional preference to specific domains. A region in the visual cortex, known as V4, is recruited during color processing (Baker et al., 1981; Zeki, 1973, 1978), and another region in the middle temporal cortex, called MT (also called V5), is recruited during motion processing (Dubner & Zeki, 1971; Zeki, 1974, 1978). When a chemical lesion was applied to MT/V5 in rhesus monkeys by ibotenic acid injection, the coherence thresholds required for motion direction discrimination were elevated (Newsome & Paré, 1988). This was selective to motion processing and did not affect contrast discrimination. These findings strengthened the notion of functional specialization in the visual system where different visual regions perform specific cognitive functions and computations. Moreover, these regions are connected together in a distributed hierarchical fashion, and information flows from low-level processing regions to higher-order functional regions (Figure 1.1; Felleman & Van Essen, 1991). The two-stream hypothesis (also known as the what/where pathways) suggested that visual information is transmitted through two main routes that depends on the presented information and the performed task (Mishkin et al., 1983; Ungerleider & Haxby, 1994). For object recognition and perception, information flows from the early visual cortex to the inferior-temporal cortex (ventral stream/what pathway). The ventral stream also represents animacy category information ranging from inanimate objects to birds and mammals (Caramazza & Shelton, 1998; Connolly et al., 2012; Sha et

al., 2015). When performing localization tasks, motion processing, or executing visually guided actions, information flows from the early striate cortex to the posterior parietal cortex (dorsal stream/where pathway) (Goodale & Milner, 1992).

Similarly, in humans, the visual system is functionally organized with different regions having a preference to perform specific perceptual/cognitive functions. The fusiform face area (FFA) has a preference for processing faces (Kanwisher et al., 1997; McCarthy et al., 1997), the extrastriate body area (EBA) has a preference for processing body parts (Downing et al., 2001), the parahippocampal place area (PPA) has a preference for processing scenes (Epstein & Kanwisher, 1998), V4 is activated during processing color (Bartels & Zeki, 2004; Zeki et al., 1991), and hMT/V5 (human homologue of MT/V5) is recruited during processing motion (Zeki et al., 1991). A disruption in any of these functional regions due to a cortical lesion could lead to selective deficits in processing their functional domains. For example, cortical lesions in the FFA can lead to deficits in face processing (Barton et al., 2002). Lesions in V4 can lead to deficits in seeing color (achromatopsia) (Damasio et al., 1980; Pearlman et al., 1979), and bilateral lesions in hMT/V5 lead to deficits in motion processing (Zihl et al., 1983).

In the present thesis, we will focus on the visual motion system, and how motion information is represented in the brain. Moreover, we will investigate the development of the visual motion system, and how the presence/absence of visual input at birth can alter its typical development.

Functional specialization of MT/V5

Studies in the non-human primates demonstrated that an extrastriate region in the middle temporal cortex (MT) is dedicated to processing visual motion. MT/V5 is tuned to process motion direction information and has motion direction selective cells (Dubner & Zeki, 1971; Zeki, 1978). Similarly in humans, hMT/V5 is recruited during visual motion processing (J. D. G. Watson et al., 1993; Zeki et al., 1991) and represents visual motion direction information (Kamitani & Tong, 2006; Tootell, Reppas, Dale, et al., 1995). When this region is damaged in primates, visual motion processing is impaired (Newsome & Paré, 1988). Similarly in humans, when applying Transcranial Magnetic Stimulation (TMS) to hMT/V5 leading to a temporary disruption, or when a lesion is present in hMT/V5, motion perception in the visual modality is highly impaired (Beckers & Zeki, 1995; Zihl et al., 1983). These findings indicated that MT/V5 (or hMT/V5 in humans) is a cornerstone region for processing visual motion information.

Cortical route for visual motion processing

How does visual information reach MT/V5?

When light hits the retina, visual information is transferred from the ganglion cells to the brain through the optic nerve. Around 10% of the optic tract fibers convey information through the tectopulvinar pathway which projects to the superior colliculus and then to the posterior pulvinar in the thalamus. The majority of the optic tract fibers follow the geniculostriate pathway which projects to the lateral geniculate nucleus (LGN) in the thalamus and then to the striate early visual cortex (Figure 1.1). The LGN is organized in a multi-layer fashion comprising the magnocellular, the parvocellular, and the koniocellular layers. The output from these layers is mediated to the early visual cortex through the magnocellular and the parvocellular pathways. While the parvocellular pathway is involved in processing high spatial information, shape, size, and color, the magnocellular pathway is crucial for tasks involving high temporal resolution, spatial processing, location, speed, and motion direction processing (Schiller et al., 1990). It is suggested that most of the input arriving to the extrastriate regions in the dorsal visual stream is coming from the magnocellular pathway through V1 (Born & Bradley, 2005; Shipp & Zeki, 1989; Yabuta et al., 2001). There is also a small proportion of connections that project directly from the LGN to MT through the koniocellular pathway (Sincich et al., 2004; but see below the section discussing subcortical routes for visual motion processing).

Primate studies demonstrated that cortical feedforward connections to MT/V5 arrive from earlier visual regions as (but not limited to) V1, V2, V3, and V3A (Felleman & Van Essen, 1991; Maunsell & van Essen, 1983). Interestingly, most of the input is coming from V1 through direct highly myelinated cortico-cortical axons ensuring rapid synaptic transmission (Rockland, 1989, 1995). Responses in MT/V5 could be observed after only 2 ms following the elicited response in V1 advocating for the direct monosynaptic communication between the two regions (Movshon & Newsome, 1996). Information is then transmitted from MT to a specialized region in the medial superior temporal cortex (MST) which performs additional specialized motion computations as optic flow motion processing (Duffy & Wurtz, 1991; Komatsu & Wurtz, 1988). It is important to note that when talking about MT and MST and other motion selective regions in the vicinity of MT combined, the extended region is referred to as hMT+/V5 (human MT complex).

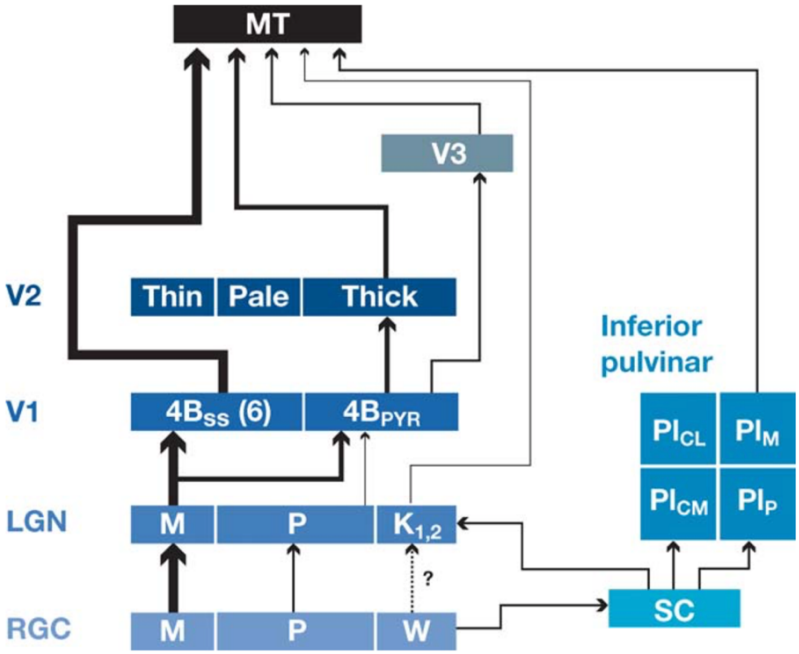


Figure 1.1 Visual pathways to MT/V5 according to Felleman & Van Essen (1991).
The line thickness indicates the magnitude of the connections between two different regions. The strongest connections are direct feedforward connections between V1 and MT/V5. In addition to the feedforward cortical connections, there are connections of lower magnitude arriving from subcortical structures as the Lateral Geniculate Nucleus (LGN), and the superior colliculus (SC) through the inferior pulvinar (PI). The arrow thickness represents the strength of the connections. The thickest lines represent direct cortical connections between brain regions. M: magnocellular pathway; P: parvocellular pathway; K: koniocellular pathway; RGC: retinal ganglion cells. Figure adapted from (Born & Bradley, 2005).

Is V1 necessary for visual motion information to reach MT/V5?

Since most of the input arriving to MT/V5 is originating from V1 through cortico-cortical connections, it is plausible that the disruption of V1 could prevent the delivery of motion information to MT/V5. However, disrupting the early visual cortex or its removal in non-human primates did not completely abolish the responsiveness of MT/V5 to visual motion. Despite having weaker responses after the removal of the striate cortex, MT/V5 was still responsive to visual motion and showed motion direction selectivity (Rodman et al., 1989). Moreover, neuropsychological studies in humans demonstrated that V1 is not the only route for motion information to reach MT/V5. This was initially inspired by two

neuropsychological cases known as blindsight (Weiskrantz et al., 1974) and Riddoch syndrome (Riddoch, 1917; Zeki & Ffytche, 1998).

Blindsight

Blindsight is a case where individuals who have lesions in (part of) the early visual cortex are rendered blind in a part of their visual field. Blindsight is the ability of the individual to perform a visual task above chance-level even though they are not consciously aware of perceiving the visual stimulus (Weiskrantz et al., 1974). For instance, blindsight individuals who have a lesion in the ventral right V1 will have a blind spot in the upper-left visual field, and will not consciously perceive visual stimuli in their blind spot. However, when performing a visual motion detection task in their blind spot location, they perform above chance without being aware of the visual stimuli (Stoerig & Cowey, 1997; Weiskrantz et al., 1974). This suggests that motion information is being processed despite the damaged V1, and despite the absence of conscious awareness. These findings were supported by neuroimaging studies demonstrating that patients with blindsight have an intact connection between the LGN and hMT/V5 which is the most likely route for motion information to reach hMT/V5 (Ajina, Pestilli, et al., 2015; Ajina & Bridge, 2018, 2019).

Riddoch Syndrome

Patients with Riddoch syndrome suffer from a lesion in the early visual cortex, however they can perform certain visual tasks and respond to visual stimuli in their blind spot while being consciously aware of the presented moving stimuli (Arcaro et al., 2019; Riddoch, 1917; Zeki & Ffytche, 1998). The difference between Riddoch syndrome and blindsight is conscious awareness of motion. Unlike blindsight patients who are not consciously aware of static or moving stimuli, Riddoch syndrome patients are only consciously aware of moving objects or stimuli. One of the most famous cases is patient G.Y. who was cortically blind due to a lesion in V1, and had an intact hMT/V5. G.Y. was able to discriminate motion, but not brightness (Morland et al., 1999). Furthermore, G.Y. was consciously aware of the nature and the direction of the visual stimuli. Neuroimaging revealed that hMT/V5 was activated during visual motion processing. This suggested that visual input can reach hMT/V5 through parallel subcortical pathway that bypasses V1, and that it is sufficient for conscious awareness and successful motion direction discrimination (Barbur et al., 1993). It was later suggested that mainly fast motion information is processed through subcortical pathways bypassing V1, while slow motion information would be processed through the cortical V1 pathway. This hypothesis was suggested as in patient G.Y., the responses to fast motion were preserved and were similar to the elicited activity in the control subjects in hMT/V5. In contrast, slow motion, pattern offset, and pattern reversal stimuli failed to elicit responses in hMT/V5 in G.Y. (Ffytche et al., 1996). These findings were later confirmed with other patients with Riddoch Syndrome where the

patients reported visual awareness in their blind visual fields and were able to discriminate visual motion directions. Therefore, the primary visual cortex or back-projections to it are not necessary for visual awareness and are not the only route for delivering motion information to hMT/V5 (Arcaro et al., 2019; Ffytche & Zeki, 2011).

In another case study with a patient with Riddoch syndrome, the patient showed activation in several extrastriate areas of the lesioned hemisphere. Magnetoencephalographic recordings indicated that evoked activity occurred earlier in the higher-order visual areas (V4 and V5) than in the early visual areas (V2/V3) adjacent to the lesion. fMRI analysis showed an increased functional connectivity between areas V4 and V5 of the lesioned hemisphere in comparison with the same areas in the intact hemisphere during the presentation of color changes. This added more evidence that visual perception after the V1 lesion in Riddoch syndrome is mediated by subcortical pathways that bypass V1 and project first to higher-order visual areas (as V4 and hMT/V5) and subsequently to lower-order visual areas as V2/V3 (Schoenfeld et al., 2002).

Subcortical routes for visual motion processing

In the previous section, the neuropsychological studies demonstrated that motion information can be delivered to MT/V5 through subcortical pathways. However, the subcortical route was not only present in the case of lesions in the early visual cortex, but also in healthy individuals with typical visual development. Electroencephalography (EEG) studies in humans showed that using alternating visual checkerboard stimuli, a visual evoked potential (VEP) component, with an onset of 30-45 ms, was located in the vicinity of hMT/V5 (Buchner et al., 1997). This early component was independent of a second activity, which started around 50-70 ms, and was located within the early visual cortex (V1). These results provide further evidence for a very fast input to V5 even before the activation of V1 in healthy individuals. In another study, TMS was applied to either hMT/V5 or V1 for a period of 100 ms after visual stimulus onset. Applying TMS on hMT/V5 led to a massive decrease in performance of visual motion discrimination after around 30-40 ms from the stimulus onset. When TMS was applied to V1, disruption of visual motion discrimination was observed after 60-70 ms of the stimulus onset. These results suggested that multiple pathways exist between the retina and hMT/V5. One slower pathway that passes through V1, and another fast subcortical pathway that bypasses V1 and delivers visual information to V5 even before V1 (Beckers & Zeki, 1995).

Supporting evidence for the subcortical connections to MT/V5 comes from tracer studies in non-human primates demonstrating the existence of direct connections between subcortical structures [as the pulvinar and the LGN] and MT/V5 (Maunsell & van Essen, 1983; Mundinano et al., 2019; Sincich et al., 2004; Ungerleider et al., 1984). Similarly in humans, diffusion weighted imaging studies demonstrated the presence of direct

subcortical connections between the LGN in the thalamus and hMT/V5 bypassing V1 (Bridge et al., 2008). This can allow visual information to reach hMT/V5 earlier than it reaches V1 (Buchner et al., 1997; Gaglianese et al., 2012).

In summary, this section discussed the possible routes for visual information to reach MT/V5 through direct cortico-cortical connections from the early visual cortex (Rockland, 1989, 1995), or though subcortical-cortical connections between the [LGN and the pulvinar] and MT/V5 (Sincich et al., 2004; Ungerleider et al., 1984). In the following section, we discuss how MT/V5 is organized and how it represents visual motion information.

Organization of MT/V5

Seminal non-human primate studies demonstrated that MT/V5 neurons show selectivity for motion speed (Rodman & Albright, 1987) and direction (Albright, 1984; Albright et al., 1984b; Baker et al., 1981; Dubner & Zeki, 1971; Zeki, 1974, 1980). MT/V5 is a unique structure as it was the first extrastriate structure to be found highly myelinated after birth (Flechsig, 1901). It was even suggested to be considered a primary sensory area due to its high myelination and its strong connectivity to the primary visual cortex. This similarity with the early visual cortex is not limited to the degree of myelination but also with the way it is organized. Interestingly, MT/V5 has a columnar organization (Albright et al., 1984b; Dubner & Zeki, 1971; Malonek et al., 1994) similar to that in the early striate cortex (Hubel et al., 1977; Mountcastle, 1997). The columnar organization of MT/V5 is expressed in the presence of cortical columns having neurons that show a preferential activity for a specific motion direction. Moreover, there is an axis-of-motion columnar organization where neighboring cortical columns show a gradual and smooth change in the preferred motion direction, with these columns located side by side with another set of columns preferring the opposite direction (Figure 1.2 and 1.3)

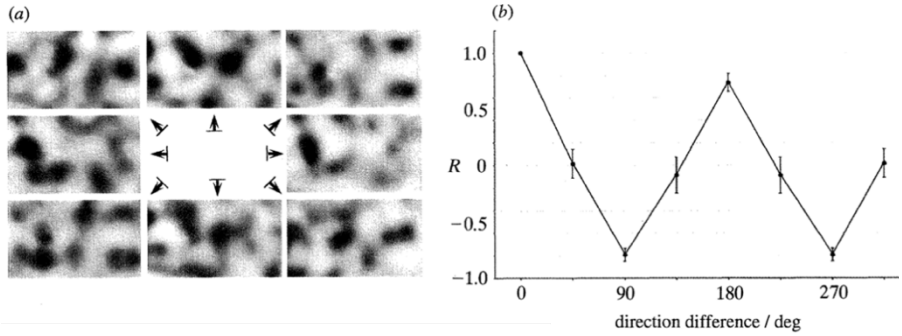


Figure 1.2 Optical imaging of area MT/V5 in owl monkey.
[a] Optical maps in MT/V5 when processing moving grating information in eight different directions. The optical maps of each motion direction showed high similarity with the maps from the opposite motion direction in the same plane. [b] The correlation analysis between the different maps from the different motion directions demonstrated that there was a very high correlation with the maps from the opposite direction. This correlation gradually decreased as the motion direction moved away from the preferred direction reaching lowest correlation at orthogonal directions. These results suggest an axis-of-motion organization in MT/V5. Figure adapted from (Malonek et al., 1994).

It is important to note that this model does not suggest that MT/V5 cells are only selective to one direction. The responsiveness of MT/V5 cells to different motion directions is somehow more complex. About 60% of MT/V5 cells responded only to one specific motion direction, while around 24% responded strongly to one direction and to a lesser extent the opposite direction. A smaller proportion of neurons responded equally to opposite directions (8%), or to motion (8%) regardless of the direction (Albright et al., 1984b).

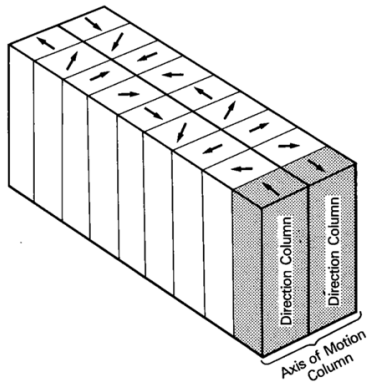


Figure 1.3 A 3D representation of the columnar organization of MT/V5 in the macaque.
Columns show a gradual and systemic transition in the preferred motion direction, with frequent 180° reversals. This leads to an axis-of-motion columnar organization in MT/V5. Figure adapted from (Albright et al., 1984b).

The representation of visual motion directions in humans was probed using machine learning and pattern classification techniques where the perceived visual motion directions were predicted from the elicited activity patterns in hMT/V5 (Kamitani & Tong, 2006). Moreover, ultra-high field (7T) fMRI studies also revealed an axis-of-motion columnar organization in hMT/V5 (Figure 1.4; Zimmermann et al., 2011) similar to that present in non-human primates (Albright et al., 1984b).

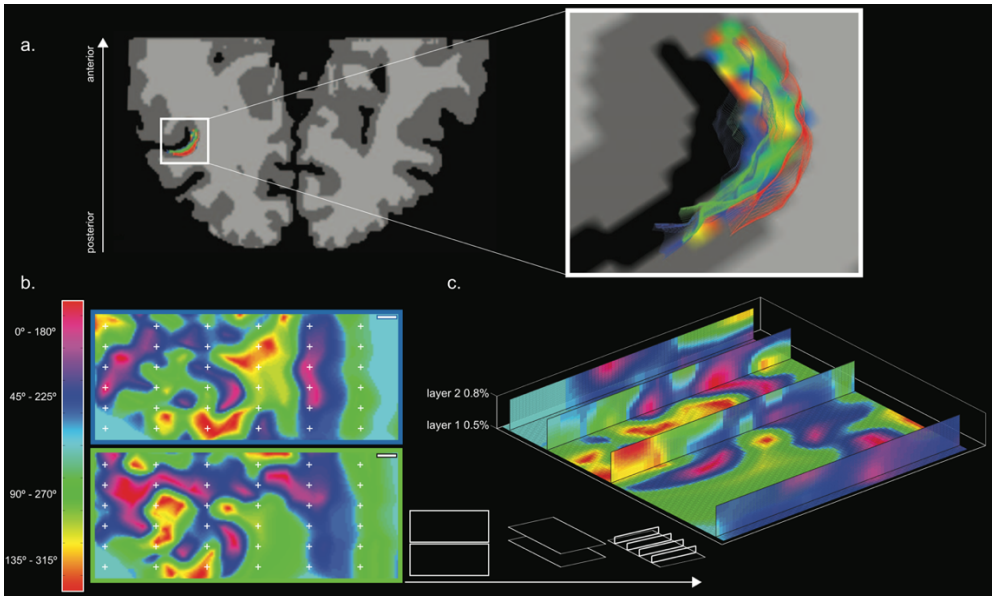


Figure 1.4 Columnar organization of MT/V5 in humans using high-field MRI.
MT/V5 voxels show a preference for different axes of motion. The high-field MRI results demonstrate an axis-of-motion columnar organization in humans similar to that organization demonstrated in the macaque (Albright et al., 1984b). *Figure is adapted from (Zimmermann et al., 2011).*

The distinction between MT and MST

MST is another cortical region that is selective to motion and is anatomically close to MT, and receives feedforward input from MT (Maunsell & van Essen, 1983; Ungerleider & Desimone, 1986). However, there are different properties for MT and MST. MST has larger receptive fields than MT in primates (Desimone & Ungerleider, 1986; Van Essen et al., 1981) and humans (Amano et al., 2009). MST is involved in processing optic flow motion or similar kinds of motion in primates (Duffy & Wurtz, 1991, 1997) and humans (A. T. Smith et al., 2006), which is not the case for MT (Lagae et al., 1994). It has been suggested that MT and MST can be defined separately in humans based on retinotopic properties and the recruitment during ipsi-lateral motion stimulation. MT is retinotopically organized, and does not respond to peripheral ipsi-lateral stimulation due to its small

receptive field size. Oppositely, MST is not retinotopically organized, and responds to peripheral stimulation in both ipsi- and contra-lateral hemifields due to its larger receptive field (Huk et al., 2002). Depending on the presented stimuli, and the way of how and where it is presented, MT and MST can be defined separately or together in humans. But as discussed earlier, when MT and MST are defined together without distinction, it is referred to as the human MT complex (hMT+/V5).

The origin of functional specialization in the visual cortex

Where does the functional organization emerge from? What drives a certain region as hMT+/V5 to perform a specific function as motion processing in a respective anatomical location? While these questions don't have a definitive answer yet, there are different hypotheses explaining the origin of the functional organization of the visual cortex (Op de Beeck et al., 2019). Three main hypotheses have been proposed: [i] Visual features selectivity; [ii] hierarchy of information processing; [iii] Biased connectivity hypothesis.

[i] Visual features selectivity

Within the ventral stream, responses to faces or words seem to be located in regions preferring foveal information, while responses to scenes are in regions preferring peripheral stimuli (Hasson et al., 2002; Larsson & Heeger, 2006; Levy et al., 2001; Schwarzlose et al., 2008). Moreover, regions processing faces seem to prefer round shapes while regions processing places prefer lines (Bracci & Op de Beeck, 2016; Hong et al., 2016; Op De Beeck et al., 2006; Rajimehr et al., 2011). The preference of these regions for specific retinotopic locations, shapes, or spatial frequencies might drive the emergence of the category selectivity and the functional organization of the visual system.

In the dorsal stream, MT neurons have a preference for foveal stimuli (Van Essen et al., 1981). Additionally, they are tuned for different visual properties as motion direction (Albright et al., 1984b), speed (Maunsell & Van Essen, 1983), contrast (Pack et al., 2005), and stimulus size (Allman et al., 1985; Felleman & Kaas, 1984). The tuning of MT neurons to these visual properties altogether could potentially drive MT to process translational visual motion information. Compared with MT, MST has a larger receptive field size (Desimone & Ungerleider, 1986; Van Essen et al., 1981). Additionally it is sensitive to large-field stimuli, and responds to circular and expanding/contracting patterns of motion (Duffy & Wurtz, 1991, 1997; Smith et al., 2006). The sensitivity of MST to these properties could drive its function to process optic flow information (Duffy & Wurtz, 1991, 1997). The differences in the retinotopic properties and the receptive field sizes between MT and MST (Amano et al., 2009; Desimone & Ungerleider, 1986; Van Essen et al., 1981) could allow them to process different kinds of motion information.

[ii] hierarchy of information processing

The visual system is arranged in a hierarchical fashion where information is transferred from lower-level processing areas to higher-level regions. Even functional-specific regions as the FFA that is known for processing faces can be divided to submodules performing different levels of computational complexity (Weiner et al., 2010; Weiner & Grill-Spector, 2012). When looking at the visual motion system, we see different levels of computations starting from local motion processing in the early visual cortex (Hubel & Wiesel, 1962, 1968) to global motion processing in higher-order visual motion areas (Braddick et al., 2001; Britten et al., 1993; Newsome & Paré, 1988; Rees et al., 2000). Even within the higher-order visual motion areas, we see a distinction between MT and MST which process motion information at different levels of complexity, with MT processing translational motion and MST processing optic flow motion (Duffy & Wurtz, 1991; Lagae et al., 1994; A. T. Smith et al., 2006). This hypothesis suggests that the development of a functionally specialized region depends on the input it receives from the previous region in the visual information processing hierarchy, which will allow it to perform more complex computations.

[iii] Biased connectivity hypothesis

Another hypothesis suggests that the functional organization of the visual system is driven by the connectivity architecture of the visual system (Hannagan et al., 2015). For instance, the regions processing faces (as the occipital face area (OFA) and the fusiform face area (FFA)) are more connected to each other than with other regions (as the STS) (Davies-Thompson & Andrews, 2012; Gschwind et al., 2012), while the region processing visual words (VWFA) is connected to the language network in the left hemisphere (Bouhali et al., 2014; Stevens et al., 2017). Such connectivity architecture could drive the development of these functionally specialized regions in the visual cortex. hMT+/V5 is strongly connected to the early visual cortex. Most of the feedforward input arriving to hMT+/V5 is coming directly from V1 through highly myelinated cortico-cortical connections (Rockland, 1989, 1995). The processing of local motion information in V1 (Hubel & Wiesel, 1962, 1968) could drive hMT+/V5 to perform the same function (motion processing) on a more global scale due to its larger receptive field size (Felleman & Kaas, 1984). Additionally, the axis-of-motion organization in hMT+/V5 (Albright et al., 1984b; Dubner & Zeki, 1971; Malonek et al., 1994) is similar to the columnar organization of the early visual cortex (Hubel et al., 1977; Mountcastle, 1997). It is highly plausible that the early-established and strong connectivity between V1 and hMT+/V5 impacts the function and the organization of hMT+/V5. This notion is supported by studies suggesting that the structural connectivity could be used as a predictor of the functional role of different visual regions (Osher et al., 2016; Saygin et al., 2012).

It is important to emphasize that it is highly unlikely that these different hypotheses are mutually exclusive, or that only one of them can fully explain the organization of the visual system. For example, while the FFA seems to prefer more foveal stimuli (Larsson & Heeger, 2006; Levy et al., 2001) as supported by the visual selectivity features hypothesis, it is also connected to other regions processing faces (Davies-Thompson & Andrews, 2012; Gschwind et al., 2012) as supported by the biased connectivity hypothesis. Similar patterns of results can also be seen in the visual motion network. hMT+/V5 processes global motion information (Braddick et al., 2001; Newsome & Paré, 1988) compared with the local motion information processing in V1 (Hubel & Wiesel, 1962, 1968) as supported by the hierarchy of information processing hypothesis. The differences between local and global motion processing could also be attributed to the receptive field sizes of the neurons in these areas (Duffy & Wurtz, 1991; Felleman & Kaas, 1984) as supported by the visual features' selectivity hypothesis. The columnar organization of hMT+/V5 and its function could be driven by the strong connectivity with the early visual cortex (Felleman & Van Essen, 1991; Maunsell & van Essen, 1983; Rockland, 1989, 1995) as supported by the biased connectivity hypothesis. Therefore, it is important to consider these different propositions and the possibility of integrating these findings into a common framework.

In this section, we discussed the visual motion system, and how motion information arrives to hMT+/V5. Additionally, we discussed how hMT+/V5 is organized, and how it represents motion direction information. In the next section, we will discuss auditory motion processing and the debates regarding multisensory processing of motion information in hMT+/V5.

Auditory motion processing

Animals and humans rely on motion cues not only from the visual modality, but also from other non-visual modalities as the auditory and the tactile modality. Relying on different sensory modalities and integrating motion information from different modalities is beneficial for our survival, and to have a better perception of our environment (Soto-Faraco et al., 2002; Soto-Faraco, Kingstone, Calvert, et al., 2004). Similar to the visual motion network (J. D. G. Watson et al., 1993; Zeki et al., 1991), there is a dedicated network for processing auditory motion encompassing *planum temporale*, Heschl's Gyrus and the superior temporal cortex (Alink et al., 2012; Baumgart et al., 1999; J. W. Lewis et al., 2000). Auditory motion perception depends on interaural time differences, interaural level differences, and spectral properties of sounds (Blauert, 1997; Grothe et al., 2010; Middlebrooks, 2015; Middlebrooks et al., 2002).

Cortical pathway for auditory motion processing

Sounds enter the ear arriving at the cochlea and stimulate the hair cells where the different frequencies of these sounds stimulate different hair cells. Auditory information is then transferred through the auditory nerve to the medulla and then to the inferior colliculus in the midbrain. Information is then passed to the medial geniculate nucleus in the thalamus and then to the auditory cortex. Similar to how the visual system represents visual information in the form of retinotopic maps, the auditory system represents auditory information in the frequency domain in a tonotopic organization. Auditory spatial and non-spatial information is processed in two auditory streams (Hackett & Kaas, 2004; Rauschecker & Tian, 2000) analogous to the dorsal and the ventral pathways in vision. The auditory "what" pathway is suggested to be involved in non-spatial object recognition processes (J. H. Kaas & Hackett, 1999; Romanski et al., 1999), while the auditory "where" pathway processes spatial and auditory motion information (Rauschecker & Tian, 2000). The *planum temporale* (PT) is a region that is posterior to the Heschl's gyrus within the Sylvian fissure and is known to be involved in several functions as perception of music (Zatorre et al., 1994), speech perception (Binder et al., 1996; Giraud & Price, 2001), spatial information processing (Warren et al., 2002), and auditory motion processing (Baumgart et al., 1999; J. W. Lewis et al., 2000). Focusing on auditory motion, PT shows enhanced recruitment when processing auditory motion stimuli when compared to auditory static stimuli (Battal et al., 2019; Baumgart et al., 1999; Krumbholz et al., 2005; J. W. Lewis et al., 2000; Pavani et al., 2002; Warren et al., 2002). Additionally, auditory motion information could be decoded from the activity patterns in PT (Alink et al., 2012; Battal et al., 2018, 2019; Dormal et al., 2016; Jiang et al., 2014, 2016). Moreover, neuropsychological case studies demonstrated that the resection of the posterior superior temporal gyrus (including PT) led to deficits in perceiving auditory motion (Ducommun et al., 2004). All these findings suggest that PT is a cornerstone region for processing auditory motion information.

So far, we have talked about auditory motion processing within the auditory network, and we previously discussed visual motion processing within the visual system. The next section discusses the multi-sensory processing of motion information from different sensory modalities, and how motion information is represented in multisensory motion processing regions (i.e., hMT+/V5).

Multi-sensory motion processing: Behavior

Integrating motion information from multiple senses can lead to enhanced perception of motion (Meyer et al., 2005; Soto-Faraco et al., 2002; Soto-Faraco, Kingstone, Calvert, et al., 2004). When visual and auditory motion stimuli are presented simultaneously and are moving in opposite directions, the behavioral performance in

motion direction discrimination is reduced (Soto-Faraco, Kingstone, & Spence, 2004). Moving visual stimuli can bias the perception of auditory motion direction (Soto-Faraco, Kingstone, & Spence, 2004), and auditory motion stimuli can bias the perception of visual motion direction (Meyer & Wuerger, 2001). These results suggest that the information from the different modalities is integrated in the brain leading to a coherent percept of motion direction. There is a clear interplay between the different modalities when processing motion information. It was demonstrated that adaptation to visual motion directions can lead to a motion after-effect in the tactile modality, and adaptation to tactile motion directions leads to a visual motion after-effect (Konkle et al., 2009). The transfer of the adaptation effect across modalities suggests a shared neural mechanism for motion processing across modalities.

Multi-sensory motion processing: Brain

Studies have suggested that the integration of multisensory motion signals occurs in higher-order multi-sensory regions such as the superior temporal sulcus (Baumann & Greenlee, 2007; Beauchamp, 2005) or the parietal cortex (Lewis et al., 2000). Further evidence showed that multi-modal motion information is integrated in hMT+/V5 (Alink et al., 2008; Scheef et al., 2009; von Saldern & Noppeney, 2013). Thus, the classic modular view of the brain, where visual/auditory areas process only visual/auditory information, might be questionable. Recent evidence showed that the representation of different categories when using auditory stimuli could be found even in the early visual cortex (Vetter et al., 2014). Furthermore, when watching audio-visual vocalization clips compared to when listening to the same audio without video, some cells in the auditory cortex in primates showed enhanced neural responses while others showed reduced responses. These results suggest that multi-sensory interactions could even occur at the level of primary sensory cortices and not only at higher-level association areas (Ghazanfar et al., 2005). The interaction between primary sensory cortices is further supported by studies demonstrating direct anatomical connections between the early visual cortex and the auditory cortex in the primate brain (Falchier et al., 2002), and that disrupting brain activity in the occipital cortex by applying TMS can lead to deficits in tactile orientation discrimination (Zangaladze et al., 1999). The recent views suggest that the primate brain is multi-sensory in nature including the regions that were typically considered early uni-sensory regions (Ghazanfar & Schroeder, 2006). While a region is dominantly responsive to one modality (e.g., vision), it may contain information from another sensory modality (e.g., auditory) even though the level of recruitment is less in the non-dominant modality.

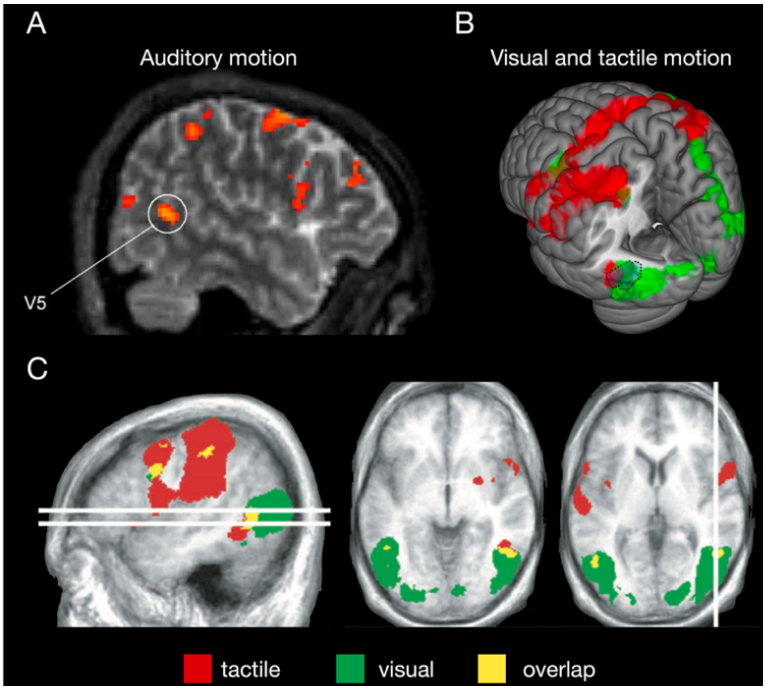


Figure 1.5 The recruitment of hMT+/V5 during motion processing from different modalities.
[A] hMT+/V5 was recruited during auditory motion processing (Poirier et al., 2005). [B, C] The recruitment of different regions during tactile (in red) and visual motion processing (in green). The activations from tactile and the visual motion overlapped in the anterior part of hMT+/V5. Figures adapted from [A] (Poirier et al., 2005), [B] (Van Kemenade et al., 2014), and [C] (Ricciardi et al., 2007).

As previously discussed, there is multi-sensory motion information in hMT+/V5 (Alink et al., 2008; Scheef et al., 2009; von Saldern & Noppeney, 2013). Additionally, hMT+/V5 is recruited when processing auditory motion information (Figure 1.5; Poirier et al., 2005). The evidence from primates studies reveals the existence of direct projections from the middle lateral belt region of the auditory cortex to area MT (Majka et al., 2019). Moreover, hMT+/V5 was recruited during tactile motion processing (Figure 1.5; Hagen et al., 2002; Ricciardi et al., 2007; Van Kemenade et al., 2014). The anterior subdivision of hMT+/V5 is recruited during tactile motion processing, and shows enhanced connectivity with the somatosensory cortex during tactile motion processing (Ricciardi et al., 2007; Sani et al., 2010). Recent advancements in multivariate analysis techniques offered new tools that are more sensitive than traditional fMRI analysis such as univariate techniques (see below the section detailing the methods used to investigate brain activity). Multivariate pattern analysis (MVPA) demonstrated that despite the lower level of univariate recruitment of hMT+/V5 to non-visual motion, motion information was present in

hMT+/V5 during auditory (Battal et al., 2018; Dormal et al., 2016; Strnad et al., 2013) and tactile motion processing (Van Kemenade et al., 2014).

According to the metamodal theory of the brain (Pascual-Leone & Hamilton, 2001), a functional region is organized to perform a specific function, and is not dependent on the dominant sensory input modality. Therefore, according to the metamodal theory, hMT+/V5 is an abstracted motion processing region that is indifferent to the input modality, but is specialized to process motion information. While this theory can explain why we may find motion information from different modalities in hMT+/V5, it does not address the format of representation of visual and auditory motion information. In other words, while visual and auditory motion information can be present in hMT+/V5, we cannot know whether the representation of visual motion is similar to or identical to the representation of auditory motion. Relying on overlapping activations to infer similar computations or abstracted representation (Pascual-Leone & Hamilton, 2001; Ricciardi et al., 2007) could be misleading as a single region (e.g. *planum temporale*) could be recruited during performing different cognitive tasks while performing different kinds of computations (Baumgart et al., 1999; Binder et al., 1996; Lewis et al., 2000; Warren et al., 2002; Zatorre et al., 1994). In other words, hMT+/V5 could be recruited during processing visual and auditory motion, however, the processing of motion information from the different modalities could be completely different. Moreover, despite the presented evidence of the multi-sensory processing of motion information in hMT+/V5, there are studies that do not support these findings and still advocate for a uni-sensory visual processing of motion information in hMT+/V5. Therefore, we will discuss the arguments that are in favor of a multisensory processing of motion information in hMT+/V5, and the arguments advocating for a uni-sensory visual motion processing in hMT+/V5.

Arguments supporting multisensory motion processing in hMT+/V5

Different studies have suggested that hMT+/V5 is recruited during auditory and tactile motion processing (Hagen et al., 2002; Poirier et al., 2005; Ricciardi et al., 2007). Different non-visual motion conditions or directions could be decoded from the activity patterns in hMT+/V5 (Battal et al., 2018; Dormal et al., 2016; Strnad et al., 2013; Van Kemenade et al., 2014). Additionally, applying TMS to hMT+/V5 impaired tactile motion direction discrimination (Amemiya et al., 2017). These studies altogether promoted the idea that auditory/tactile motion information is present in hMT+/V5. However, there were different interpretations about how hMT+/V5 encodes motion information. Some studies interpreted these findings as an evidence for hMT+/V5 (or a subdivision of hMT+/V5) being supra-modal or abstracted from the sensory input (Ricciardi et al., 2007; Sani et al., 2010). Another study suggested that visual and tactile motion direction information are represented in hMT+/V5, however, when using cross-modal decoding, the cross-modal

classifier was not able to discriminate the motion directions across modalities. Therefore, the authors concluded that there was no shared information between the two modalities, and that hMT+/V5 is a multi-modal region with separate neural populations processing motion information from the different modalities separately (Van Kemenade et al., 2014).

Arguments supporting uni-sensory visual motion processing in hMT+/V5

Oppositely, there are also studies advocating for the modular visual nature of hMT+/V5. Case studies with individuals having bilateral damage in hMT+/V5 showed deficits in visual motion processing but not in auditory motion processing (Zihl et al., 1983, 1991). Initially it was proposed that different subdivisions of hMT+/V5 respond differently to different modalities where hMT is a unimodal visual area, and tactile motion information is represented only in MST (Beauchamp et al., 2007). However, this view was later updated and it was proposed that neither MT and MST represent tactile information (Jiang et al., 2015). Similarly in the auditory modality, some studies found no evidence of auditory motion processing in hMT+/V5 (Alink et al., 2012; Jiang et al., 2014; Saenz et al., 2008), or even found a deactivation in hMT+/V5 during auditory motion processing (Lewis et al., 2000). These results supported the unimodal view of hMT+/V5.

These authors of the above-mentioned studies further claim that the results obtained from the studies advocating for the multi-modal/supra-modal nature of hMT+/V5 are a byproduct of an inaccurate definition of hMT+/V5 or preprocessing strategies. Multi-modal regions are in close proximity to hMT+/V5 (Beauchamp, 2005), therefore including these regions can lead to false positive results. Similarly, applying spatial smoothing can lead to spill-over effects from neighboring multi-modal regions (Beauchamp et al., 2007; Jiang et al., 2015). The study by Jiang and colleagues demonstrated that when individually-defining hMT+/V5 (MT and MST), and avoiding smoothing, no enhanced recruitment was observed in MT or MST (Jiang et al., 2015). Accordingly, if hMT+/V5 was properly defined and spatial smoothing was avoided, we should not find auditory (or tactile) motion information in hMT+/V5.

The first aim of the present thesis will therefore be to investigate the multisensory nature of motion processing in hMT+/V5. The second chapter of the present thesis is dedicated to the question of whether hMT+/V5 is a purely unimodal visual area as previously suggested, or whether in fact there is non-visual motion information in hMT+/V5 when it is accurately defined and when methodological confounds are avoided and controlled for.

Since we investigated the uni-/multi-/supra-modal nature of motion processing in hMT+/V5, it is important to elaborate on the meanings of these terms. Unfortunately, these

terms are interpreted differently among researchers, and therefore it is necessary to clearly define them in the current thesis (Ricciardi & Pietrini, 2011; Spence et al., 2009; Voss & Zatorre, 2012). The following definitions are what is meant when we refer to unimodal, multi-modal, and supra-modal in the present thesis.

A unimodal region is a region that contains neurons that respond to or contain information from only one sensory modality (Figure 1.6A, B).

A Multi-modal region is a region with different sets of neurons, with different preferences for different modalities. While a region responds to information from different modalities, the response profile is modulated and affected by the input modality. It does not necessarily mean the neurons preferring different modalities does not interact with each other (Figure 1.6C).

A supra-modal region is a region that contains neurons that respond equally to a certain stimulus across modalities and is not modulated by the sensory modality. Here supra-modality is defined as being indifferent to and unaffected by the sensory input modality (Figure 1.6D).

In the next section, we will discuss how the multisensory processing in hMT+/V5 can shape its development, and how hMT+/V5 reorganizes in the case of visual deprivation.

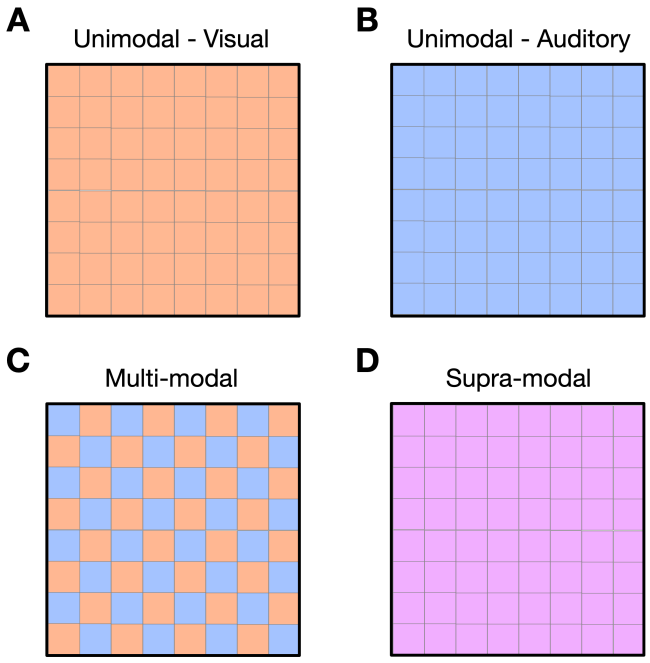


Figure 1.6 An illustration of unimodal, multi-modal, and supra-modal regions.
A representation of unimodal regions where all the neurons/voxels contain information [A] only from the visual modality, or [B] only from the auditory modality. [C] A representation of a multi-modal region which contains information from the visual and the auditory modality, however, neurons/voxels have different preferences for the visual and the auditory modalities. [D] A representation of a supra-modal region which contains the same information regardless of the sensory modality, and is not modulated by the sensory input.

The impact of visual deprivation on the development of the visual system

Understanding what drives the development of the visual system is not limited to investigating how it reacts to visual stimuli, but also by investigating how it develops in the presence/absence of visual input. Seminal studies in animals used visual deprivation as a model to understand the development and plasticity of the visual cortex. This was implemented by using different kinds of deprivation such as feature deprivation, monocular deprivation, or binocular deprivation.

Orientation and Direction Deprivation

Visual deprivation can be applied to a specific visual feature (as orientation or motion direction) while still having visual experience. Neurons in the early visual cortex

show orientation and direction selectivity for stimuli presented in their receptive fields. A neuron that is selective to a specific orientation (e.g., horizontal orientation) will show an enhanced response for a presented stimulus in its receptive field in the horizontal orientation than for a stimulus in a different orientation (e.g., vertical). If the animal is reared in an environment of stripes with only one orientation present (e.g., horizontal), and is not exposed to other orientations, the percentage of neurons preferring the presented orientation (e.g., horizontal) will be much higher (Blakemore & Cooper, 1970; Hirsch & Spinelli, 1970). Similarly, for motion selectivity, neurons that are selective to a specific motion direction show enhanced responses when the presented stimulus is moving in the preferred direction than when moving in another direction. If an animal is reared in an environment with dot patterns moving in only one direction (e.g., rightward motion), and is deprived from perceiving other motion directions, the percentage of neurons preferring the presented motion direction (e.g., rightward motion) will be very high (Cynader et al., 1975; Daw & Wyatt, 1976). However, with training on the deprived motion directions, motion selectivity for the deprived directions in the early visual cortex is enhanced (Li et al., 2008; Van Hooser et al., 2012).

Monocular visual deprivation

Monocular visual deprivation in kittens from birth led to most cells in the visual cortex losing their responsiveness to stimuli from the deprived eye (Hubel & Wiesel, 1970; Wiesel & Hubel, 1963a, 1965a). Interestingly, the effects arising from visual deprivation were prominent when visual deprivation occurred early in life. When cats were visually deprived at an adult stage in their life, these effects were minimal (Hubel & Wiesel, 1970). Similar results were later demonstrated in primates (Le Vay et al., 1980). These results led to the conclusion that there is a critical period early in life where the presence/absence of visual input influences the development of the visual cortex. Therefore, it is necessary to investigate how the visual system develops in the absence of visual experience.

Early transient and complete visual deprivation

The absence of visual input during the critical period early in life has a strong impact on the development of the visual system (Hubel et al., 1977; Hubel & Wiesel, 1970; Wiesel & Hubel, 1965b). It is necessary to understand the duration of that critical window, and how does the presence/absence of visual experience during this window impact the development of the visual system (Maurer, 2017; Maurer et al., 2005). Studies in ferrets proposed that directional selectivity in the visual cortex requires visual experience to develop (Li et al., 2006, 2008). Unlike orientation selectivity and ocular dominance that were present following eye opening, direction selectivity in ferrets was absent. However, it developed gradually with visual experience (Li et al., 2006); but see other findings in mice suggesting that direction selectivity is independent from visual experience (Rochefort et al.,

2011). Behavioral studies in kittens demonstrated that visual deprivation during the first six weeks of life leads to permanent deficits in the perception of global motion (Mitchell et al., 2009).

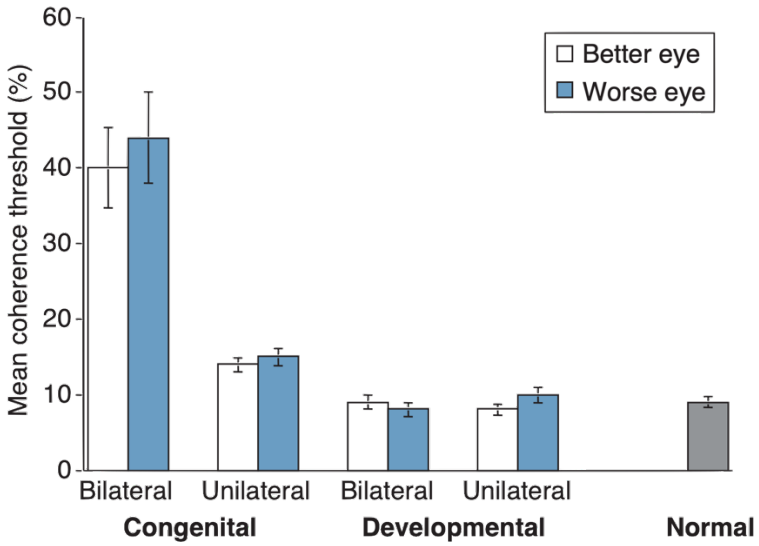


Figure 1.7 Effect of visual deprivation due to cataract on global motion processing.
The figure illustrates the required motion coherence thresholds to discriminate different motion directions in cataract-reversal patients and their matched controls. Deficits in global motion processing were most prominent in patients who had a history of congenital and bilateral cataract. Figure is adapted from (Maurer et al., 2005)

Human studies in the cataract-reversal patients provided a window to understand how the lack of visual experience early in life even for a brief period can change the typical development of the visual motion system (Ellemberg et al., 2002; Grady et al., 2014; Maurer, 2017; Maurer et al., 2007). Cataract-reversal patients who were deprived from visual experience for a period of less than eight months showed strong deficits in discriminating visual motion directions despite being tested after years of visual experience following the cataract removal surgery. These deficits were specific to patients who had a history of congenital and dense bilateral cataract (Figure 1.7, Ellemberg et al., 2002; Maurer et al., 2005). Brief early visual deprivation not only affected visual processing in visual areas, but also affected the integration of multi-sensory information in multi-sensory regions probably due to relying on the more reliable auditory signal (de Heering et al., 2016; Guerreiro, Erfort, et al., 2015). This is potentially due to the recruitment of the visual cortex in the cataract reversal patients during auditory processing (Collignon et al., 2015). Indeed, the absence of visual input early in life even for a short period of time seems to

trigger a long-lasting cross-modal reorganization of the visual cortex (Collignon et al., 2015). This enhancement in auditory or non-visual processing is accompanied by deficiencies in visual processing (Bottari et al., 2018; de Heering et al., 2016; Ellemberg et al., 2002). It has been suggested that the reduced performance in processing global motion in vision is a result of deficits in neural processing in hMT+/V5 (Ellemberg et al., 2002; Maurer et al., 2005). However, the neural correlates of visual motion processing in cataract reversal patients have not been comprehensively tested.

In the present thesis we addressed this question of how the visual motion system is altered due to an early and a brief period of visual deprivation using fMRI. In the third chapter, we tested how the absence of visual input during the sensitive period early in life impacts visual motion processing and the development of different regions (as V1 and hMT+/V5) in the visual motion system. Moreover, we investigated the connectivity between low-level and high-level visual areas when processing visual motion information, and the impact of brief early visual deprivation on the connectivity profile of hMT+/V5.

In the next section, we discuss how permanent visual deprivation impacts the functional organization of the visual system, and we address how the onset of visual deprivation impacts the organization of hMT+/V5, and its connectivity profile with different brain networks.

Permanent congenital/early blindness

As previously discussed, early visual deprivation alters the normal development of the visual cortex (Hubel et al., 1977; Wiesel & Hubel, 1963a, 1965a). Interestingly, studies in the early blind (EB) demonstrated that their occipital cortex is not dormant even during rest (Veraart et al., 1990; Wanet-Defalque et al., 1988), and in fact also responds to tactile (Büchel et al., 1998; Pietrini et al., 2004; Sadato et al., 1996) and auditory stimuli (Weeks et al., 2000). In addition to non-visual sensory stimuli, the occipital cortex responded to higher order cognitive functions such as language (Bedny et al., 2011; Burton et al., 2002) and memory (Amedi et al., 2003). Disrupting the occipital's activity by using TMS leads to impairments in sound localization (Collignon et al., 2007), verbal memory (Amedi et al., 2004) and Braille identification (Cohen et al., 1997). Single case studies also supported these findings. A proficient blind braille reader lost her ability to read braille following a bilateral occipital lesion due to a stroke (Hamilton et al., 2000). All these findings indicate that the presence/absence of visual input during the sensitive period early in life has a strong impact on the development of the "visual" system.

Functional reorganization of the visual system

The reorganization of the visual system in the EB seems to follow certain functional organizational principles. For instance, the visual word form area (VWFA), which responds to visual words in the sighted, is recruited during braille reading in the EB (Reich et al., 2011). The category selectivity observed in the sighted in the ventral stream is preserved in the EB when stimulated with non-visual stimuli (Mahon et al., 2009; Pietrini et al., 2004). Similarly in the dorsal stream, which is specialized in processing visual spatial and motion information in the sighted, the functional organization is preserved in the EB. Areas in the right dorsal stream were preferentially recruited when performing auditory localization tasks (Collignon et al., 2011; Gougoux et al., 2005; Weeks et al., 2000). Additionally, hMT+/V5 was recruited in the EB during auditory (Battal et al., 2018; Bedny et al., 2010; Dormal et al., 2016; Jiang et al., 2014; Poirier et al., 2006; Strnad et al., 2013; Wolbers, Zahorik, et al., 2011) and tactile motion processing (Ricciardi et al., 2007).

One suggested theory explaining this cross-modal reorganization to process non-visual information is Hebbian competition. At birth, there are connections between the different sensory cortices. Depending on the available sensory inputs, the connections can be either strengthened or pruned (Hebb, 1949). In the presence of visual experience, and because of the visual pathway from the retina to the early visual cortex, visual information arrives faster to the occipital cortex than other regions, therefore the occipital cortex processes visual information, and some of the connections between the occipital cortex and the auditory cortex are pruned away for efficiency. In the absence of visual input, no visual information arrives to the visual cortex. Therefore, the "visual" cortex is reorganized to process non-visual information with enhancing connections between the occipital cortex and the cortical/subcortical auditory regions (Hebb, 1949).

Hebbian competition can explain why the visual cortex is strongly recruited when processing non-visual information, however, it doesn't explain why a certain region like hMT+/V5 maintains its functional role as a motion processor (Bedny et al., 2010; Dormal et al., 2016; Poirier et al., 2006), or why VWFA is recruited during processing non-visual words (Reich et al., 2011). As previously discussed, the question of how does functional specialization emerge in the brain doesn't have a definitive answer. Different theories have been proposed to explain the origin of functional specialization. The three main theories were visual features selectivity, hierarchy of information processing, and the biased connectivity hypothesis. While the visual features selectivity hypothesis was promising in explaining the functional role of many visual regions (Op de Beeck et al., 2019; Silson et al., 2015), it fails to explain the maintenance of the functional role of different functional regions in the congenital visually deprived as they didn't have any visual experience.

The biased connectivity hypothesis (Hannagan et al., 2015), on the other hand, seems to be the most promising theory to explain cross-modal reorganization in the EB. The interest in investigating this hypothesis increased in the field as it provides a mechanistic explanation where other theories failed. The VWFA, which processes visual words in the sighted (Cohen et al., 2000; McCandliss et al., 2003), is recruited during braille reading in the early blind (Reich et al., 2011). The maintenance of the functional role of this region, despite not being in the visual modality, is most likely attributed to its strong connectivity to the language network (Bouhali et al., 2014; Stevens et al., 2017). Recent evidence suggested that the visual motion area hMT+/V5 actually processes motion information from non-visual modalities in the sighted individuals (Battal et al., 2018; Dormal et al., 2016; Poirier et al., 2005; Strnad et al., 2013; Van Kemenade et al., 2014). This is most likely due to the observed functional and structural connectivity of hMT+/V5 (or its sub-regions) to the auditory and the tactile sensory networks (Gurtubay-Antolin et al., 2020; Sani et al., 2010). In the case of early visual deprivation, hMT+/V5 shows enhanced recruitment in the early blind than the sighted controls during processing tactile and auditory motion information (Battal et al., 2018; Dormal et al., 2016; Jiang et al., 2016). The observed reorganization leading to enhanced processing and maintenance of its functional role could be driven by the connectivity architecture of hMT+/V5 to the different sensory networks (Gurtubay-Antolin et al., 2020; Sani et al., 2010).

Impact of the age of blindness onset

As suggested by animal studies (Hubel & Wiesel, 1970; Le Vay et al., 1980), visual deprivation in humans at a later stage in life has a much lesser impact on the reorganization of the visual cortex. For instance, the occipital cortex is recruited during braille reading in EB, but not late blind. Applying TMS to the occipital cortex during braille-reading leads to impairments in the EB and not the LB (L. G. Cohen et al., 1999). hMT+/V5 showed significant recruitment during auditory motion processing in the EB, but not in the LB (Bedny et al., 2010). That is not to say that there is no evident reorganization in the visual cortex of the LB. Cross-modal plasticity is observed in the visual cortex of the LB during performing auditory tasks (Collignon et al., 2013; Voss et al., 2006), however, it is significantly less than that observed in the EB (Figure 1.8; Collignon et al., 2013). While cortical reorganization is possible at a later stage in life, the presence/absence of visual input during the early critical period in life strongly impacts the organization and the development of the visual system (Voss, 2013).

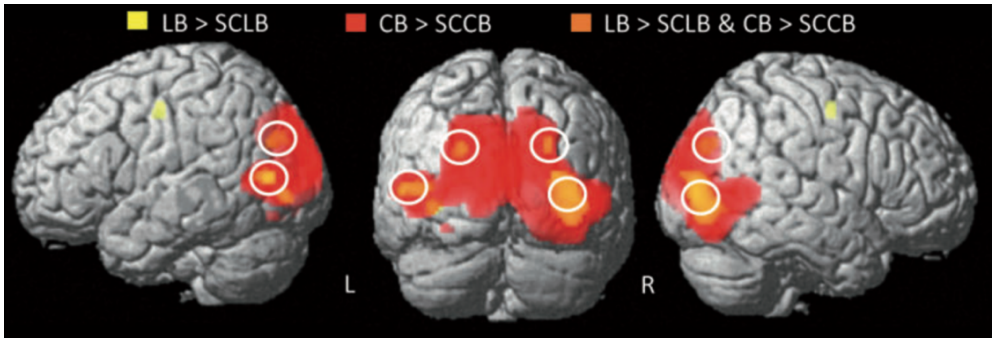


Figure 1.8 Cross-modal plasticity in the early blind and the late blind.
When comparing the early blind (EB) with their matched control group (SCEB), and the late blind (LB) with their matched control group (SCLB), the EB and LB showed enhanced recruitment of the occipital cortex when processing auditory information as a result of cross-modal plasticity. While both EB and LB showed cross-modal reorganization of the visual system during auditory processing, the reorganization in the LB was much less pronounced than that observed in the EB in terms of magnitude or anatomical location. Figure adapted from (Collignon et al., 2013).

The connectivity architecture of the visual system in the visually deprived

Resting-state functional connectivity has been used to understand the communication between different brain regions during rest (Biswal et al., 1995). The resting connectivity profile of a functional region seems to reflect its functional role and organization to a certain extent. For instance, looking at the connectivity of the left motor cortex, it was found that at rest, this region is connected to the contra-lateral motor cortex (Biswal et al., 1995). Similarly, when taking the posterior cingulate cortex (a part of the default mode network (DMN)) as seed region, it shows strong connectivity with other regions belonging to the DMN (Fox et al., 2005). Studying connectivity is not only important to reveal the communication between different brain regions, but also could potentially explain the emergence of functional specialization in the brain. As previously discussed, the biased connectivity hypothesis suggests that the emergence of functionally-specialized regions could be dependent on the connectivity architecture of a specific region (Hannagan et al., 2015; Op de Beeck et al., 2019; Osher et al., 2016). Therefore, investigating the connectivity architecture of hMT+/V5 in the visually-deprived can provide some insights into its development and its functional role in motion processing following visual deprivation.

Studies investigating motion processing in the EB and LB suggested that the reorganization of hMT+/V5 to process auditory motion information is unique to the EB and is not present in the LB (Bedny et al., 2010). Interestingly, other studies investigating

auditory spatial processing in the dorsal stream demonstrated that there was cross-modal recruitment of the visual cortex in the EB and the LB when processing auditory information. However, the magnitude and the extent of this cross-modal recruitment in the LB was less than that observed in the EB (Collignon et al., 2013). Considering the proposed role of connectivity on the development of functionally specialized regions in the brain (Hannagan et al., 2015; Op de Beeck et al., 2019), it is necessary to investigate the connectivity architecture of hMT+/V5 in the case of early and late visual deprivation. Except for few studies (Qin et al., 2015; Sabbah et al., 2016), most connectivity studies in the blind individuals focused only on early visual deprivation (Bedny et al., 2011; Burton et al., 2014; Liu et al., 2007) or anophthalmic individuals (Watkins et al., 2012). Moreover, most of these studies focused on the visual cortex globally and its connectivity with other brain networks (Figure 1.9; Burton et al., 2014; Liu et al., 2007), and were not specifically investigating hMT+/V5. Our main goal in the present thesis is to understand the organization and the development of hMT+/V5 and the visual motion system. Therefore, in the fourth chapter of the present thesis, we tested the impact of blindness onset on the connectivity architecture of hMT+/V5 within the visual motion network and across different sensory networks.

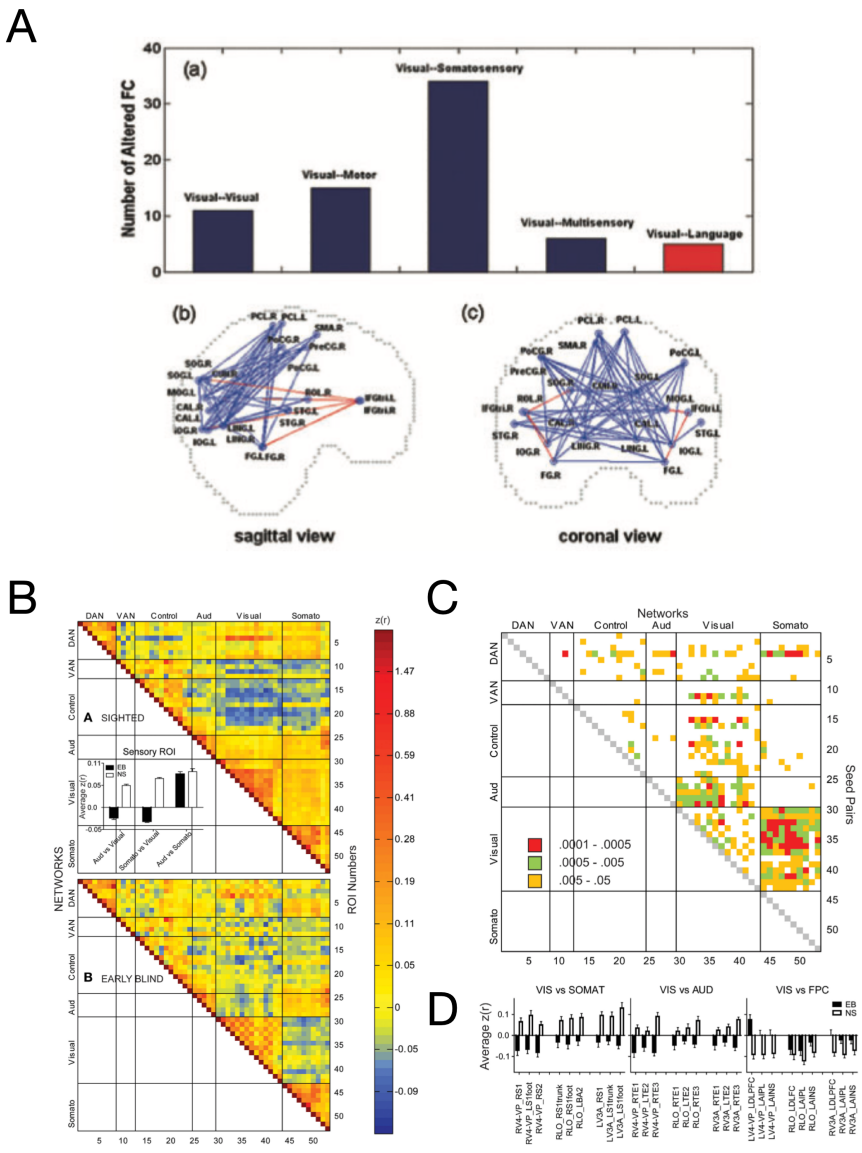


Figure 1.9 Resting-state functional connectivity changes in the early blind.

[A] The visual cortex in the EB shows reduced connectivity (in blue) with the somato-sensory and the motor cortex, and enhanced connectivity (in red) with frontal language regions (Liu et al., 2007). [B] A visualization of the connectivity matrix between different networks in the sighted and the EB (Burton et al., 2014). [C, D] Group differences in the resting state connectivity between different networks demonstrating reduced connectivity between the visual cortex and the auditory and somatosensory cortex. Figures are adapted from (Burton et al., 2014; Liu et al., 2007).

Methods used to investigate brain activity

Neuroimaging techniques became a popular and an effective method to measure brain activity non-invasively. Different neuroimaging techniques (as fMRI, electroencephalography (EEG), and Magnetoencephalography (MEG)) rely on different principles, and each method has its advantages and disadvantages. While EEG and MEG have a high temporal resolution, they have a low spatial resolution. Oppositely, while fMRI has a low temporal resolution, it has a high spatial resolution. The choice of the optimal neuroimaging technique depends on the experimental question and the experimental design. For our experiments, fMRI is a more suitable technique to answer our research questions as we need high spatial resolution to accurately define hMT+/V5 in each subject and to investigate the elicited activity patterns in hMT+/V5 when processing motion information. Therefore, we used fMRI in our experiments, and relied on different analytical techniques that will be detailed hereafter.

fMRI and univariate analyses

fMRI relies on the magnetic properties of oxygenated and deoxygenated hemoglobin cells. De-oxy hemoglobin has strong paramagnetic properties which leads to higher distortion in the magnetic field produced by the MRI magnet. As the recorded signal from the fMRI relies on the magnetic properties of oxy- and deoxyhemoglobin, the measured signal is referred to as the blood oxygen-level-dependent (BOLD) signal (Ogawa et al., 1990). The BOLD signal is an indirect measure of neural activity. When there is an increase in neural activity, oxygen consumption increases to produce sufficient energy. The depletion of oxygen leads to the conversion of the oxyhemoglobin to deoxyhemoglobin. The decrease in the oxy/deoxy-hemoglobin ratio triggers the body to provide more energy to these neurons. It leads to a strong increase in blood volume and blood flow (Buxton et al., 1998). The massive income of oxyhemoglobin leads to an increase in the BOLD signal. The hemodynamic response function (HRF) is a measure of how the BOLD signal evolves over time following a neuron's stimulation (Hoge & Pike, 2001a, 2001b). The HRF is characterized by an initial dip in the first 1-2 seconds (Malonek & Grinvald, 1996) followed by an increase of the BOLD response reaching maximum peak after 4-6 seconds, and then gradually returning to baseline after ~15 seconds. The HRF function varies across individuals and also across different regions (Aguirre et al., 1998b). This is attributed to the different vascularity of different brain regions. Therefore, directly comparing the activation of different brain regions to the same task is not feasible.

In a standard univariate analysis, the HRF is convolved with the presented stimuli and the different conditions to predict the BOLD activity in each voxel independently (Boynton et al., 1996). This is performed using a General Linear model (GLM) relying on

multiple linear regression which estimates the contribution (β) of the different predictors (X) to the recorded brain activity (Y).

$$Y = X\beta + \varepsilon$$

The univariate analysis using the GLM massively improved our understanding of the brain organization and the functional specialization of brain networks. For instance, univariate analyses were used to discover regions dedicated to processing faces (Kanwisher et al., 1997), body parts (Downing et al., 2001), and scenes (Aguirre et al., 1998a; Epstein & Kanwisher, 1998). In the visual motion system, hMT+/V5 is typically defined by contrasting brain responses to moving stimuli with responses to static stimuli (J. D. G. Watson et al., 1993; Zeki et al., 1991). Even sub-regions of hMT+/V5 as MT and MST can be distinguished using univariate analysis techniques (Huk et al., 2002). However, there are limitations to univariate analyses if we want to address specific questions. For instance, while hMT+/V5 is strongly recruited when processing motion information from different directions, we don't observe any activation-level differences between the responses to the different directions. While non-human primate studies using single-cell recordings suggest a columnar organization of MT (Albright et al., 1984b), it is difficult to observe this organization in humans using fMRI due to the relatively low spatial resolution of the fMRI when compared to invasive electrophysiology techniques in animals (usually around 3000 μm isotropic voxels compared to the resolution of the cortical columns (~300-600 μm) in the primate MT (Albright et al., 1984b). Other techniques such as repetition suppression (or adaptation leading to motion after-effect) were used to address the question of motion direction representation in hMT+/V5 (Culham et al., 1999; Tootell, Reppas, Dale, et al., 1995). Additionally, recent advancements in neuroimaging techniques and specifically high-field MRI made it possible to observe a large-scale columnar organization of MT (Zimmermann et al., 2011). However, even using high-field imaging, it is not easy to address the format of representation of motion directions in hMT+/V5. How does hMT+/V5 represent motion directions from different sensory modalities? Is the representation of motion abstracted from the sensory input? Or is it multi-modal and represents each modality differently? Several studies used univariate techniques and relied on overlapping activations to infer similar computations or abstracted representation (Pascual-Leone & Hamilton, 2001; Ricciardi et al., 2007). However, the recruitment of the same region in two different tasks does not necessarily indicate that identical computations are performed. Therefore, instead of being limited to the single voxel (univariate) analysis, we employ multivariate pattern analysis to investigate the above-mentioned questions.

Multivariate pattern analysis (MVPA)

In the beginning of the last decade, the notion of pure functional specialization came to question. Haxby and colleagues introduced the idea of distributed representation opposing the classical view of centralized representation. For instance, regions typically known to process faces showed the strongest recruitment for stimuli with faces, however, other stimuli without faces still elicited a lesser response in these regions (Haxby et al., 2000). The presence of a response in these regions for non-face stimuli suggested that certain computations are being performed. Soon after, the idea of looking at the distributed activity pattern altogether rather than voxel-wise activation level was introduced (Haxby et al., 2001). The appeal of using MVPA was motivated by how it addressed the limitations of univariate analyses. It provided a tool that was much needed to address questions that were unanswerable by univariate techniques.

MVPA introduced new assumptions that were against the traditional assumptions of univariate analyses, yet they were accepted due to evolved understanding of the brain organization. MVPA doesn't look at individual voxels, but rather looks at an ensemble of voxels together and extracting information from the relation between the different voxels. This is totally different from the univariate techniques which look at each voxel in isolation for statistical analysis. Additionally, univariate analysis looks at the activation level in individual voxels. If the activation level passed a predetermined statistical threshold, then we would infer that this voxel is recruited during performing the specified task. On the other hand, MVPA does not consider by default low activation as an indicator of absence of information or just noise. In fact, it considers it as a potential source of information. If the distributed activity pattern reveals information about a specific task or cognitive function, that would be an indicator of the presence of information in the ensemble of voxels. Even when excluding maximally responsive voxels, the activity patterns in the ventral occipito-temporal cortex (vOTC) were consistent for the different categories (Haxby et al., 2001). These findings strengthened the notion that computations in the brain are not limited to maximum recruitment levels, and that a region may potentially contain information regarding other categories that don't massively activate this region. That is not to underestimate the important role of univariate analyses relying on activation levels, but rather to emphasize another source of information which is the global activity pattern and the relation between different voxels altogether. There are different ways to conduct multivariate analyses, and new techniques continue to be introduced in the field. Here we discuss the most popular techniques and the ones that we will use in our experiments.

Split-half correlation

Split-half correlation (SHC) is performed by dividing the different experimental runs into odd and even runs. In a certain region-of-interest (ROI), the activity patterns

elicited by different categories or tasks are extracted for the odd and the even runs independently. The within-category SHC is computed by correlating the activity pattern to a certain category in the odd run with that in the even run. If the patterns from the odd and even runs are significantly correlated, this would suggest that there is reliable and stable information about this category across the different runs. To perform across-category SHC, the activity patterns elicited by one category in the odd runs are correlated with those from the other categories in the even runs (and vice versa). This technique was introduced by Haxby and colleagues (2001). They demonstrated that the within-category SHC was higher than the across-category SHC (Figure 1.10). Even when removing the most responsive voxels in these regions, the SHC results were not affected highlighting the presence of stable distributed representation of different categories in the vOTC (Haxby et al., 2001).

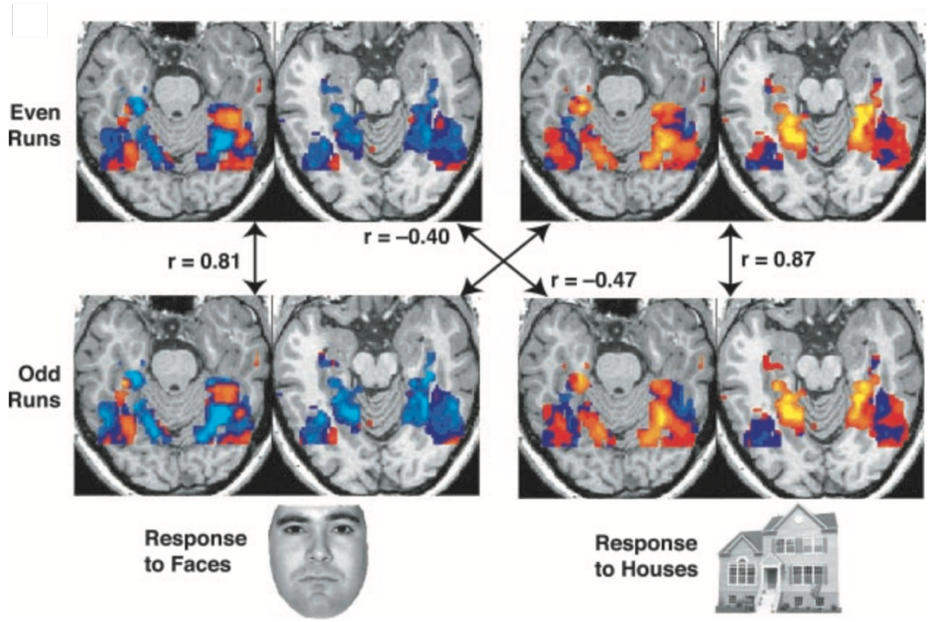


Figure 1.10 Split-half correlation analysis.
This analysis was first introduced by Haxby and colleagues (2011) where they estimated the activity patterns in the ventral occipito-temporal cortex (vOTC) in the odd and even runs of the experiment when processing different categories (here faces and houses). The correlation values across even and odd runs were higher within-categories than across-categories. This demonstrates that there are distributed activity patterns that are stable and consistent across runs within each category. Figure adapted from (Haxby et al., 2001).

Pattern classification

The field of cognitive neuroscience adopted more from the field of machine learning and pattern classification which led to additional analysis techniques other than

pattern correlations. Using pattern classification technique, a classifier is trained on different features (voxels) in a certain brain region to discriminate different categories. The classifier is then tested on an independent set of data. If it could successfully predict the different categories from the activity patterns, this would indicate that there is useful category information in the area that the classifier was able to learn and use to predict the new independent data (Figure 1.11). The technique can also be applied across the whole brain rather than a single region. A whole brain searchlight analysis is performed by creating a region of interest (e.g., a sphere) in which the classification analysis is performed. The sphere is then moved across the whole brain where each voxel in the brain gets to be the center of that sphere and the decoding analysis is performed. The results in a whole brain map reveal which regions contained discriminatory information between the different conditions that the decoder tries to classify (Kriegeskorte et al., 2006).

The nature of the brain signal that contributes to the decoding analysis is still in debate. Some studies suggested that MVPA can have access to sub-voxel resolution information (also known as hyperacuity; (Haynes & Rees, 2006; Kamitani & Tong, 2005). According to this view, within each voxel, there is an unequal distribution of cortical columns with different preferences leading to consistent biases of individual voxels to different conditions. Therefore, a pattern classifier can pick up on these consistent biases and learn to discriminate the different conditions (Haynes & Rees, 2006; Kamitani & Tong, 2005). On the other hand, other studies demonstrated that eliminating high frequency pattern information by smoothing the patterns does not have a negative impact on the classification results (Op de Beeck, 2010). Additionally, other studies suggested that the successful classification is driven by larger coarse scale information, and not necessarily depending on high frequency information as cortical column organization (Beckett et al., 2012; Freeman et al., 2011; Shmuel et al., 2010). However, the two explanations are not necessarily mutually exclusive. Recent studies demonstrated that orientation information is unlikely to be due to low-spatial information alone. Information at different scales from high frequency spatial information to large scale biases do contribute to orientation decoding (Sengupta et al., 2017), and that orientation information is present at different spatial scales (Swisher et al., 2010). The influence of spatial frequency can also depend on the decoded task. For instance, using the same auditory stimuli, Gardumi and colleagues showed that the decoding accuracy of different vowels increased with higher spatial resolution. However, when classifying the speaker identity on the same stimuli, no enhancement in decoding was observed with higher spatial resolution (Gardumi et al., 2016). These results suggest that both high spatial frequency information and coarse large-scale information contribute to the classification process. Whether one of them or both of them contribute to the classification process depends on the task in question (Gardumi et al., 2016).

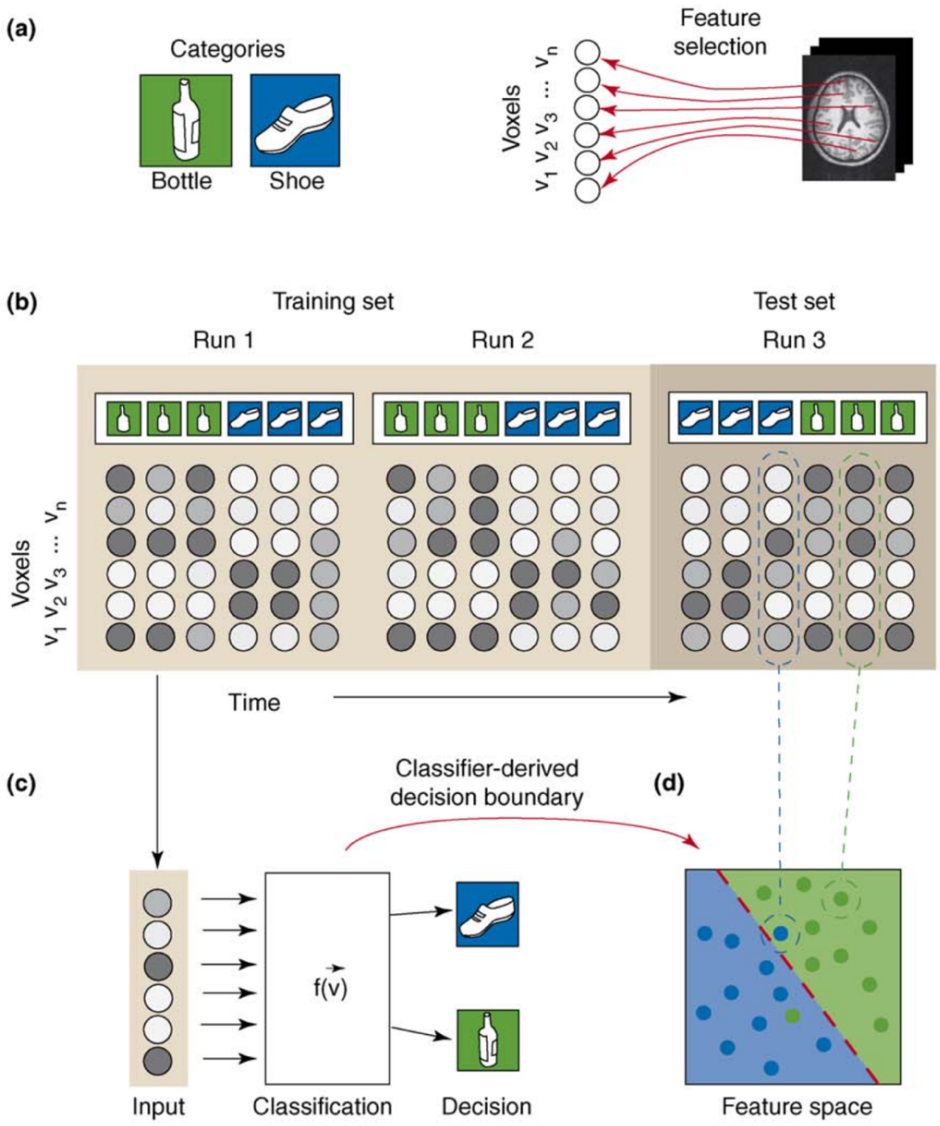


Figure 1.11 A graphical illustration of multivariate pattern classification.
In this example, we are interested in differentiating the representation of two categories (here bottle and shoe). [a] We choose our features (voxels) of interest. These features could be chosen from a region of interest or by using a feature-selection technique. [b] The activity pattern from these voxels is estimated when processing the two categories in each run and each presentation. [c] A classifier is then trained to discriminate between these two categories by finding the optimal decision boundary that separates the two categories in the high-dimensional representational space. The classifier is then tested on new independent data to predict the categories of the test data. If category information is present in these features (or voxels), the classifier should be able to predict the tested categories above chance level. Figure adapted from (Norman et al., 2006).

Moreover, the classification analysis in a certain region does not only depend on the investigated activity pattern or its spatial resolution. There are other factors that contribute to the classification process. For instance, the choice of the classifier can impact the classification results as each classifier works in a different way. Studies have suggested that linear classifiers (as support vector machines (SVM) and linear discriminant analysis (LDA) classifiers) are the best choice for neuroimaging pattern classification (Misaki et al., 2010).

Support vector machine (SVM) classifier

An SVM classifier finds a decision boundary (hyperplane) that separates the exemplars from the different categories. In SVM, the optimal hyperplane is the one that maximizes the margin between the decision boundary and the support vectors (Figure 1.12). There are two necessary parameters for running an SVM-classifier. These are the kernel type (whether linear or nonlinear) and the regularization parameter (often called the C-parameter). In neuroimaging, the usage of non-linear kernels is not recommended as it is harder to interpret and would require us to use much less features and more data (Misaki et al., 2010). There is no predetermined right choice for the C-parameter, a high value of C-parameter (low regularization) will lead to minimal mis-classifications in the training data, however, this might lead to overfitting. Oppositely, a small C-parameter (more regularization) will lead to some misclassifications in the training data, however, the classifier will be more general and less prone to overfitting. Too much regularization will lead to underfitting the training data. Therefore, it is important to find the right balance to avoid both overfitting and underfitting. Ideally, part of the data would be used to estimate the hyperparameters (as the C-parameter), and wouldn't be used later in the training and testing phases. However, this needs a huge amount of data which is not practically feasible in MRI experiments most of the time. The convention in the field is to use a C-parameter of 1 which represents a good compromise to avoid both overfitting and underfitting.

Linear discriminant analysis (LDA) classifier

The LDA classifier performs a dimensionality reduction of the activity patterns from a high multi-dimensional space to a lower dimensional space. The LDA classifier finds the optimal plane on which the data from the different categories have maximum separation, and projects it to that lower-dimensional plane. The decision boundary is defined on that plane where the classes are highly separated (Figure 1.12). The classifier is then tested on independent data, and it predicts the likelihood of the classes that the test data belong to (McLachlan, 2004).

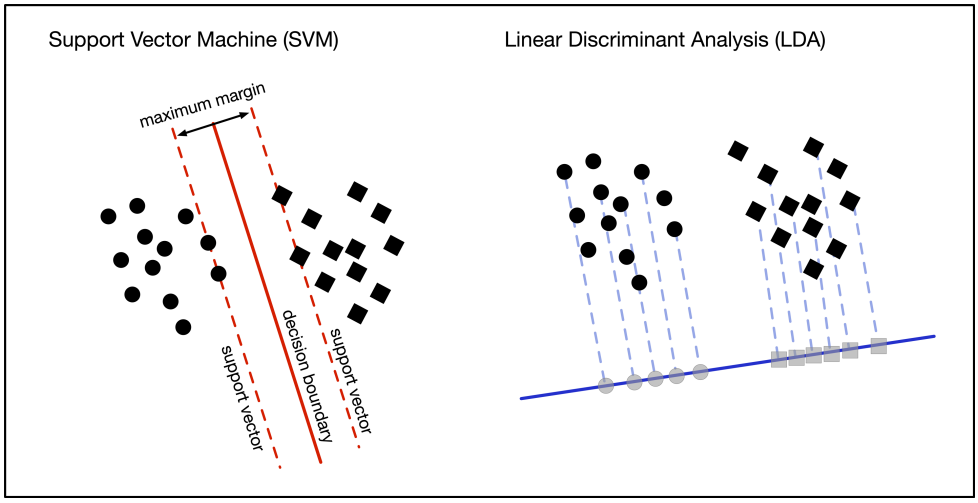


Figure 1.12 Linear classifiers (SVM and LDA)
A representation of how two types of linear classifiers classify the same data. A linear support vector machine classifier tries to find the optimal decision boundary that maximizes the distance between the two support vectors. The classifier then predicts the label of the tested data depending on its location from the decision boundary. A Linear discriminant analysis classifier projects the data to a lower dimensional plane which gives maximum separability between the two categories. The label of the tested data is predicted by projecting it to the lower dimensional plane, and estimating the maximum likelihood of the category that it belongs to.

Limitations of pattern classification techniques

Pattern classification looks at how distinct the different patterns are from each other, and it doesn't tell us much about the similarity between the representation of different exemplars in the multi-dimensional representational space. Another downside in pattern classification is that a classifier needs to be trained and tested on the same subject. This is a limitation as it prevents us from addressing interesting questions. For instance, if we want to investigate whether a special population (e.g., early blind) processes auditory motion in the same way as the sighted processes visual motion information, hypothetically one could train a decoder in the sighted individuals and then test it on blind individuals. However, this is not recommended nor ideal in practice. When training a classifier on one subject and testing it on another subject, we cannot assume that a certain voxel is identical across individuals. We cannot also assume that all voxels elicit the same response leading to an identical response profile and representation in a brain region across individuals. This is reflected in the higher classification accuracies when the training and testing of the classifier occur in the same subject rather than training and testing in different subjects (Haxby et al., 2011). Indeed, across-subject classification can be significantly above chance (van den Hurk et al., 2017), However, the significant classification most likely stems from a

large-scale organization (Downing et al., 2006) rather than a fine-grained activation pattern. New techniques are being introduced to overcome this limitation. A recent technique, known as hyperalignment, was introduced recently where the patterns are transformed from a native voxel subject space to a higher dimensional common space. The transformation of patterns from a subject space to a common functional multi-dimensional space across individuals allows for across-subject classification with comparable accuracy to that from within-subject classification (Haxby et al., 2011, 2014, 2020).

Representational similarity analysis (RSA)

RSA investigates the relation between different response patterns in a multi-dimensional space (Kriegeskorte, Mur, & Bandettini, 2008). RSA offers additional insights to those that could be inferred from pattern classification by relying on using a distance metric to evaluate the (dis)similarity of the representation of different categories or stimuli. The distance metrics could be a correlation, Euclidean, or Mahalanobis distance (Kriegeskorte, Mur, & Bandettini, 2008; Walther et al., 2016). Using these metrics, we can have a statistical measure of similarity between the representation of different categories (Figure 1.13). RSA investigates the representational geometry of the category representations and the (dis)similarity relation between the different categories. By looking at distance metrics and similarity relations, we transcend the multi-dimensional feature (voxels) space. Therefore, RSA allows us to compare representations across brain regions, individuals, groups, neuroimaging modalities (as fMRI, MEG, and single cell recordings), or even species (Kriegeskorte, Mur, & Bandettini, 2008; Kriegeskorte, Mur, Ruff, et al., 2008).

Additionally, RSA allows to test different theories and models regarding how information is represented in the brain. For instance, creating models based on low-level features of the stimuli as luminance, silhouette, frequency and then comparing which models better explains the observed data in a certain brain region. We can also build categorical models based on semantic or categorical distinctions or even behavioral responses (Bracci & Op de Beeck, 2016; Connolly et al., 2012; Kriegeskorte, Mur, Ruff, et al., 2008; Mattioni et al., 2020). Categorical modelling provides a good way to relate behavioral perception with multivariate brain representations.

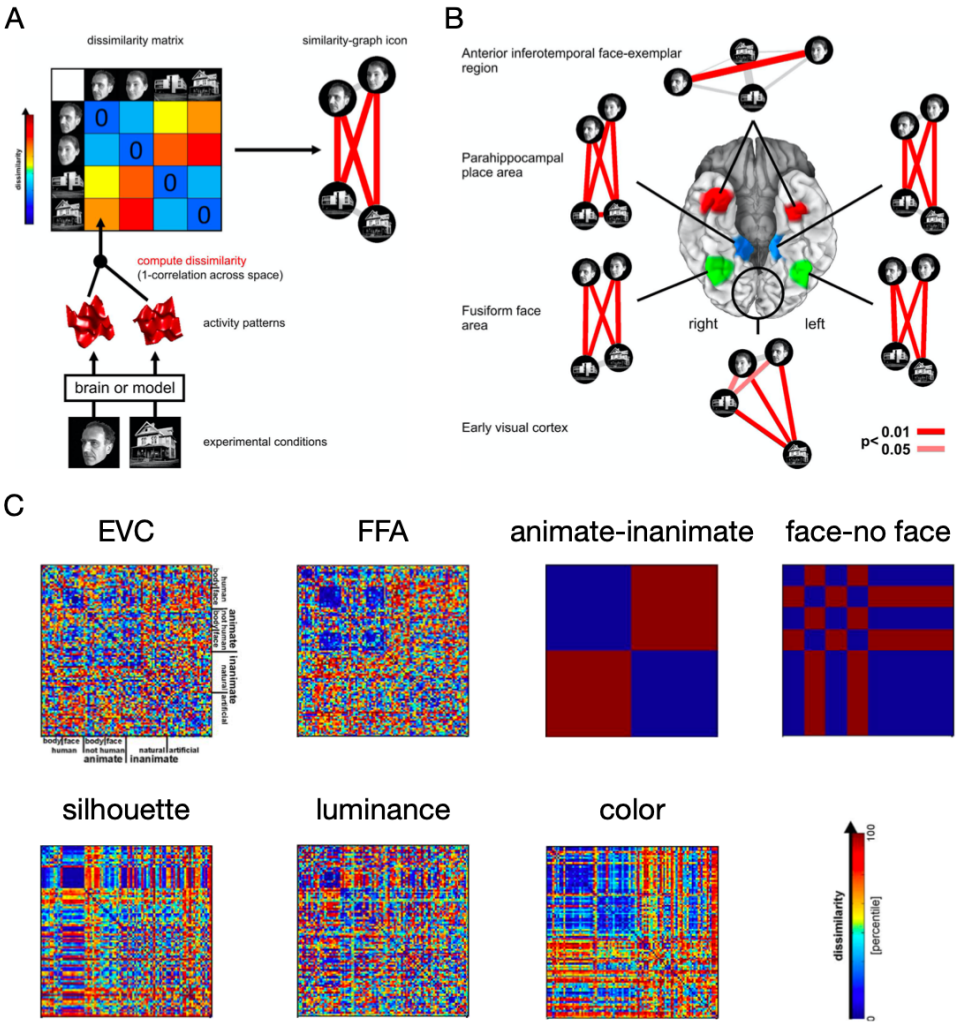


Figure 1.13 Representational similarity analysis (RSA).

RSA looks at the representational geometry of different categories and how (dis)similar they are from each other. [a] In this example, we look at the elicited activity pattern for faces and houses in a brain region. The distance metric used to measure the dissimilarity between the two patterns in this example is correlation (but see also other possible distance metrics (Kriegeskorte, Mur, & Bandettini, 2008; Walther et al., 2016)). The distance between all category pairs is computed in a dissimilarity matrix. [B] for instance in FFA and PPA, the patterns from faces have low dissimilarity, and also have high dissimilarity from the patterns from houses. This is expected as these regions are category selective, and it is not surprising that the within-category responses are less dissimilar than the across-category responses. Oppositely, in the early visual cortex, the dissimilarity between exemplars is based on low-level visual features rather than categorical distinctions. [C] The dissimilarity between different categories can be extracted from different regions of interest as in early visual cortex or the fusiform face areas. For example, FFA has low dissimilarity between face exemplars and high dissimilarity with other categories. Another way is to create categorical theoretical models

(as the animate-inanimate model or the face-no face model) and correlate these theoretical models with neural dissimilarity measures, and find regions that represent information in a way similar to that theoretical model. We can also create models reflecting the low-level properties of the stimuli (as silhouette, luminance, or color), and use these models to find brain regions that represent low-level information in a similar fashion to the theoretical model. Figure is adapted and modified from (Kriegeskorte, Mur, & Bandettini, 2008).

Brain connectivity

Previously mentioned techniques (both univariate and multivariate methods) investigated local information within a certain region. The univariate techniques looked at the recruitment of a brain region during performing a task, and the multivariate techniques looked at the pattern information within the region. While both of the methods provide insight regarding the local information within individual regions, it does not tell us about the flow of information between distant brain regions or the connectivity between them. The connectivity between regions can be assessed on the structural level by tracking white matter fibers between a seed region and target regions (Assaf & Pasternak, 2008; Basser et al., 1994; Hagmann et al., 2003), or on the functional level with correlations between BOLD signals between different regions. Here we focus on functional connectivity using task-based and resting-state methods.

Task-based functional connectivity

Psycho-physiological interaction (PPI) is a way to investigate task-based brain connectivity and the communication between brain regions during performing a specific task (Friston et al., 1997). This technique relies on identifying a seed region of interest, and extracting the activity time course from this region. An interaction term (PPI) is then created by calculating the element-by-element product of the demeaned time course from the seed ROI (physiological term) and the task (psychological) regressor. The different regressors are entered in a GLM and the PPI interaction term is estimated. Voxels that show a positive PPI effect are more correlated with the seed region during one task over the other.

There are two mainstream ways to perform the PPI analysis. This is due to the psychological and physiological factors being sampled at different time resolutions and with different offsets. The psychological term is measured in real time while the physiological term is measured with a lag and different resolution as we are measuring the HRF rather than direct neural responses. It has been suggested that the PPI term should be calculated at the same scale for both physiological and psychological terms. The first approach is to work on neural responses rather than hemodynamic responses by performing a deconvolution of the extracted time series before calculating the PPI term as implemented in the SPM software (Gitelman et al., 2003). However, there is no guarantee that the

deconvolved time series results in the real elicited neural responses. Another approach is to work in the HRF time scale by convolving the psychological term with the HRF before calculating the PPI term as implemented in the FSL software (O'Reilly et al., 2012).

There are some limitations to PPI analysis. PPI suffers from low statistical power. This is due to the interaction term having to some degree a similar time course with the physiological and the psychological term as it was created by multiplying the two, and therefore cannot be completely independent. Therefore, the estimation of the PPI term is likely to be under-powered due to a varying degree of collinearity and similarity with other regressors (O'Reilly et al., 2012). Additionally, while PPI provides some correlational information between different regions, it does not provide information regarding directionality or causality as inferred by other connectivity techniques as granger causality or dynamic causal modelling (Friston et al., 2003; Granger, 1969).

Resting state functional connectivity

Resting state functional connectivity is based on functional correlations. Biswal et al. (1995) demonstrated that the extracted BOLD signal time series from the motor cortex correlated with the contralateral motor cortex and other areas involved in motor functions. The raw BOLD signal is highly affected by many sources of noise. For instance, head motion can have a strong effect on resting state connectivity results even after the classical motion correction procedures like spatial realignment of brain volumes (Power et al., 2012; Satterthwaite et al., 2012; Van Dijk et al., 2012).Moreover, physiological processes such as cardiac pulsation can lead systemic fluctuations in the brain especially near large blood vessels (Dagli et al., 1999). Respiration and systemic chest movements can lead to systemic changes in the magnetic field and therefore could produce artifactual brain correlations (Brosch et al., 2002; Raj et al., 2001). A methodological approach known as "component-based noise correction" (CompCorr) approach was introduced to account for such artifacts. This method uses information from the white matter, and the cerebral spinal fluid (CSF), where BOLD signal is not expected, to estimate noise components using principal component analysis. Noise components are then regressed out from the data before computing correlations between different regions (Behzadi et al., 2007). The functional correlation can be measured using an ROI-to-ROI or a seed-to-voxel approach. In the ROI-to-ROI approach, a pairwise correlation of the BOLD signal is computed between all regions which is represented in a connectivity matrix. In the seed-to-voxel approach, the signal from the seed region is extracted and correlated with the signal from each voxel in the brain resulting in a whole brain functional connectivity map. The correlation values are then compared to zero, or between groups in the case of multiple groups. These results would give us an indication of the connectivity or the correlation between different brain regions in different brain networks.

To understand the functional role of hMT+/V5 in processing motion information, we investigated the task-based connectivity of hMT+/V5 when processing motion information using PPI in chapter 2 and 3. In chapter 4, we investigated the connectivity profile of hMT+/V5 with the visual, the auditory, and the tactile sensory networks using resting-state functional connectivity.

Summary

The aim of the present thesis is to investigate the organization and the development of the visual motion system, with an emphasis on the visual motion area hMT+/V5. We aimed to investigate three main questions:

[1] Is there a unimodal, or multi-modal, or abstracted representation of motion direction information in hMT+/V5?

[2] How does early and brief visual deprivation impact the processing of visual motion information within the visual motion network?

[3] Does the blindness onset impact the resting-state connectivity architecture of hMT+/V5 within the visual motion network and with other sensory networks?

References

Aguirre, G. K., Zarahn, E., & D'Esposito, M. (1998a). An area within human ventral cortex sensitive to "Building" stimuli. *Neuron*.

Aguirre, G. K., Zarahn, E., & D'Esposito, M. (1998b). The variability of human, BOLD hemodynamic responses. *NeuroImage*. https://doi.org/10.1006/nimg.1998.0369

Ajina, S., & Bridge, H. (2018). Blindsight relies on a functional connection between hMT+ and the lateral geniculate nucleus, not the pulvinar. *PLOS Biology*, *16*(7), e2005769. https://doi.org/10.1371/journal.pbio.2005769

Ajina, S., & Bridge, H. (2019). Subcortical pathways to extrastriate visual cortex underlie residual vision following bilateral damage to V1. *Neuropsychologia*, *128*(January 2018), 140–149. https://doi.org/10.1016/j.neuropsychologia.2018.01.007

Ajina, S., Pestilli, F., Rokem, A., Kennard, C., & Bridge, H. (2015). Human blindsight is mediated by an intact geniculo-extrastriate pathway. *ELife*, *4*(OCTOBER2015), 1–23. https://doi.org/10.7554/eLife.08935

Albright, T. D. (1984). Direction and orientation selectivity of neurons in visual area MT of the macaque Direction and Orientation Selectivity of Neurons in Visual Area MT of the Macaque. *Journal of Neurophysiology*, *52*(6), 1106–1130. https://doi.org/10.1152/jn.1984.52.6.1106

Albright, T. D., Desimone, R., & Gross, C. G. (1984). Columnar organization of directionally selective cells in visual area MT of the macaque. *Journal of Neurophysiology*, *51*(1), 16–31. https://doi.org/10.1152/jn.1984.51.1.16

Alink, A., Euler, F., Kriegeskorte, N., Singer, W., & Kohler, A. (2012). Auditory motion direction encoding in auditory cortex and high-level visual cortex. *Human Brain Mapping*, *33*(4), 969–978. https://doi.org/10.1002/hbm.21263

Alink, A., Singer, W., & Muckli, L. (2008). Capture of Auditory Motion by Vision Is Represented by an Activation Shift from Auditory to Visual Motion Cortex. *Journal of Neuroscience*, *28*(11), 2690–2697. https://doi.org/10.1523/JNEUROSCI.2980-07.2008

Allman, J., Miezin, F., & McGuinness, E. (1985). Stimulus specific responses from beyond the classical receptive field: Neurophysiological mechanisms for local-global comparisons in visual neurons. In *Annual Review of Neuroscience*. https://doi.org/10.1146/annurev.neuro.8.1.407

Amano, K., Wandell, B. A., & Dumoulin, S. O. (2009). Visual Field Maps, Population Receptive Field Sizes, and Visual Field Coverage in the Human MT+ Complex.

Journal of Neurophysiology, *102*(5), 2704–2718. https://doi.org/10.1152/jn.00102.2009

Amedi, A., Floel, A., Knecht, S., Zohary, E., & Cohen, L. G. (2004). *Transcranial magnetic stimulation of the occipital pole interferes with verbal processing in blind subjects*. *7*(11), 1266–1270. https://doi.org/10.1038/nn1328

Amedi, A., Raz, N., Pianka, P., Malach, R., & Zohary, E. (2003). Early "visual" cortex activation correlates with superior verbal memory performance in the blind. *Nat. Neurosci.*, *6*(7), 758–766. https://doi.org/10.1038/nn1072

Amemiya, T., Beck, B., Walsh, V., Gomi, H., & Haggard, P. (2017). Visual area V5/hMT+ contributes to perception of tactile motion direction: A TMS study. *Scientific Reports*, *7*(December 2016), 1–7. https://doi.org/10.1038/srep40937

Arcaro, M. J., Thaler, L., Quinlan, D. J., Monaco, S., Khan, S., Valyear, K. F., Goebel, R., Dutton, G. N., Goodale, M. A., Kastner, S., & Culham, J. C. (2019). Psychophysical and neuroimaging responses to moving stimuli in a patient with the Riddoch phenomenon due to bilateral visual cortex lesions. *Neuropsychologia*, *128*(May), 150–165. https://doi.org/10.1016/j.neuropsychologia.2018.05.008

Assaf, Y., & Pasternak, O. (2008). Diffusion tensor imaging (DTI)-based white matter mapping in brain research: A review. In *Journal of Molecular Neuroscience*. https://doi.org/10.1007/s12031-007-0029-0

Baker, J. F., Petersen, S. E., Newsome, W. T., & Allman, J. M. (1981). Visual response properties of neurons in four extrastriate visual areas of the owl monkey (Aotus trivirgatus): A quantitative comparison of medial, dorsomedial, dorsolateral, and middle temporal areas. *Journal of Neurophysiology*, *45*(3), 397–416. https://doi.org/10.1152/jn.1981.45.3.397

Barbur, J. L., Watson, J. D. G., Frackowiak, R. S. J., & Zeki, S. (1993). Conscious visual perception without V1. *Brain*, *116*(6), 1293–1302. https://doi.org/10.1093/brain/116.6.1293

Bartels, A., & Zeki, S. (2004). *Functional Brain Mapping During Free Viewing of Natural Scenes*. *5*, 75–85. https://doi.org/10.1002/hbm.10153

Barton, J. J. S., Press, D. Z., Keenan, J. P., & O'Connor, M. (2002). Lesions of the fusiform face area impair perception of facial configuration in prosopagnosia. *Neurology*, *58*(1), 71–78. https://doi.org/10.1212/WNL.58.1.71

Basser, P. J., Mattiello, J., & LeBihan, D. (1994). MR diffusion tensor spectroscopy and imaging. *Biophysical Journal*. https://doi.org/10.1016/S0006-3495(94)80775-1

Battal, C., Rezk, M., Mattioni, S., Bottini, R., Bertonati, G., Occelli, V., Targher, S., & Collignon, O. (2018). Decoding auditory motion direction and location in hMT+/V5 and Planum Temporale of sighted and blind individuals. *Journal of Vision*, *18*(10), 436. https://doi.org/10.1167/18.10.436

Battal, C., Rezk, M., Mattioni, S., Vadlamudi, J., & Collignon, O. (2019). Representation of auditory motion directions and sound source locations in the human planum temporale. *The Journal of Neuroscience*, *39*(12), 2218–2289. https://doi.org/10.1523/JNEUROSCI.2289-18.2018

Baumann, O., & Greenlee, M. W. (2007). Neural correlates of coherent audiovisual motion perception. *Cerebral Cortex*, *17*(6), 1433–1443. https://doi.org/10.1093/cercor/bhl055

Baumgart, F., Gaschler-Markefski, B., Woldorff, M. G., Heinze, H.-J., & Scheich, H. (1999). A movement-sensitive area in auditory cortex. *Nature*, *400*(6746), 724–726. https://doi.org/10.1038/23390

Beauchamp, M. S. (2005). See me, hear me, touch me: Multisensory integration in lateral occipital-temporal cortex. *Current Opinion in Neurobiology*, *15*(2), 145–153. https://doi.org/10.1016/j.conb.2005.03.011

Beauchamp, M. S., Yasar, N. E., Kishan, N., & Ro, T. (2007). Human MST But Not MT Responds to Tactile Stimulation. *Journal of Neuroscience*, *27*(31), 8261–8267. https://doi.org/10.1523/JNEUROSCI.0754-07.2007

Beckers, G., & Zeki, S. (1995). The consequences of inactivating areas V1 and V5 on visual motion perception. *Brain*, *118*(1), 49–60. https://doi.org/10.1093/brain/118.1.49

Beckett, A., Peirce, J. W., Sanchez-Panchuelo, R. M., Francis, S., & Schluppeck, D. (2012). Contribution of large scale biases in decoding of direction-of-motion from high-resolution fMRI data in human early visual cortex. *NeuroImage*, *63*(3), 1623–1632. https://doi.org/10.1016/j.neuroimage.2012.07.066

Bedny, M., Konkle, T., Pelphrey, K., Saxe, R., & Pascual-Leone, A. (2010). Sensitive period for a multimodal response in human visual motion area MT/MST. *Current Biology*, *20*(21), 1900–1906. https://doi.org/10.1016/j.cub.2010.09.044

Bedny, M., Pascual-Leone, A., Dodell-Feder, D., Fedorenko, E., & Saxe, R. (2011). Language processing in the occipital cortex of congenitally blind adults. *Proceedings of the National Academy of Sciences*, *108*(11), 4429–4434. https://doi.org/10.1073/pnas.1014818108

Behzadi, Y., Restom, K., Liau, J., & Liu, T. T. (2007). A component based noise correction method (CompCor) for BOLD and perfusion based fMRI. *NeuroImage*, *37*(1), 90–101. https://doi.org/10.1016/j.neuroimage.2007.04.042

Binder, J. R., Frost, J. A., Hammeke, T. A., Rao, S. M., & Cox, R. W. (1996). Function of the left planum temporale in auditory and linguistic processing. *Brain*. https://doi.org/10.1093/brain/119.4.1239

Biswal, B., Zerrin Yetkin, F., Haughton, V. M., & Hyde, J. S. (1995). Functional connectivity in the motor cortex of resting human brain using echo-planar mri. *Magnetic Resonance in Medicine*, *34*(4), 537–541. https://doi.org/10.1002/mrm.1910340409

Blakemore, C., & Cooper, G. F. (1970). Development of the brain depends on the visual environment. *Nature*, *228*(5270), 477–478.

Blauert, J. (1997). *Spatial hearing: the psychophysics of human sound localization*. MIT press.

Born, R. T., & Bradley, D. C. (2005). Structure and Function of Visual Area MT. *Annual Review of Neuroscience*, *28*(March), 157–189. https://doi.org/10.1146/annurev.neuro.26.041002.131052

Bottari, D., Kekunnaya, R., Hense, M., Troje, N. F., Sourav, S., & Röder, B. (2018). Motion processing after sight restoration: No competition between visual recovery and auditory compensation. *NeuroImage*, *167*(October 2017), 284–296. https://doi.org/10.1016/j.neuroimage.2017.11.050

Bouhali, F., Schotten, M. T. De, Pinel, P., Poupon, C., Universite, S., Atomique, E., Bm, I., & Yvette, G. (2014). *Anatomical Connections of the Visual Word Form Area*. *34*(46), 15402–15414. https://doi.org/10.1523/JNEUROSCI.4918-13.2014

Boynton, G. M., Engel, S. A., Glover, G. H., & Heeger, D. J. (1996). Linear systems analysis of functional magnetic resonance imaging in human V1. *Journal of Neuroscience*. https://doi.org/10.1523/jneurosci.16-13-04207.1996

Bracci, S., & Op de Beeck, H. (2016). Dissociations and Associations between Shape and Category Representations in the Two Visual Pathways. *Journal of Neuroscience*, *36*(2), 432–444. https://doi.org/10.1523/JNEUROSCI.2314-15.2016

Braddick, O. J., O'Brien, J. M. D., Wattam-Bell, J., Atkinson, J., Hartley, T., & Turner, R. (2001). Brain areas sensitive to coherent visual motion. *Perception*, *30*(1), 61–72. https://doi.org/10.1068/p3048

Bridge, H., Thomas, O., Jbabdi, S., & Cowey, A. (2008). Changes in connectivity after visual cortical brain damage underlie altered visual function. *Brain*, *131*(6), 1433–1444. https://doi.org/10.1093/brain/awn063

Britten, K. H., Shadlen, M. N., Newsome, W. T., & Movshon, J. A. (1993). Responses of

neurons in macaque MT to stochastic motion signals. *Visual Neuroscience*. https://doi.org/10.1017/S0952523800010269

Brosch, J. R., Talavage, T. M., Ulmer, J. L., & Nyenhuis, J. A. (2002). Simulation of human respiration in fMRI with a mechanical model. *IEEE Transactions on Biomedical Engineering*. https://doi.org/10.1109/TBME.2002.1010854

Büchel, C., Price, C. J., Frackowiak, R. S. J., & Friston, K. (1998). Different activation patterns in the visual cortex of late and congentially blind subjects. *Brain*, *121*, 409–419.

Buchner, H., Gobbelé, R., Wagner, M., Fuchs, M., Waberski, T. D., & Beckmann, R. (1997). Fast visual evoked potential input into human area V5. *NeuroReport*, *8*(11), 2419–2422. https://doi.org/10.1097/00001756-199707280-00002

Burton, H., Snyder, A. Z., Diamond, J. B., & Raichle, M. E. (2002). Adaptive Changes in Early and Late Blind: A fMRI Study of Verb Generation to Heard Nouns. *Journal of Neurophysiology*, *88*(6), 3359–3371. https://doi.org/10.1152/jn.00129.2002

Burton, H., Snyder, A. Z., & Raichle, M. E. (2014). Resting state functional connectivity in early blind humans. *Frontiers in Systems Neuroscience*, *8*(April), 1–13. https://doi.org/10.3389/fnsys.2014.00051

Buxton, R. B., Wong, E. C., & Frank, L. R. (1998). Dynamics of blood flow and oxygenation changes during brain activation: the balloon model. *Magnetic Resonance in Medicine*, *39*(6), 855–864.

Caramazza, A., & Shelton, J. R. (1998). Domain-specific knowledge systems in the brain: The animate-inanimate distinction. *Journal of Cognitive Neuroscience*, *10*(1), 1–34. https://doi.org/10.1162/089892998563752

Cohen, L., Dehaene, S., Naccache, L., Lehéricy, S., Dehaene-Lambertz, G., Hénaff, M.-A., & Michel, F. (2000). The visual word form area: Spatial and temporal characterization of an initial stage of reading in normal subjects and posterior split-brain patients. *Brain*, *123*(2), 291–307. https://doi.org/10.1093/brain/123.2.291

Cohen, L. G., Celnik, P., Pascual-Leone, A., Corwell, B., Faiz, L., Dambrosia, J., Honda, M., Sadato, N., Gerloff, C., Catala´, M. D., & Hallett, M. (1997). Functional relevance of cross-modal plasticity in blind humans. *Nature*, *389*(6647), 180–183. https://doi.org/10.1038/38278

Cohen, L. G., Weeks, R. A., Sadato, N., Celnik, P., Ishii, K., & Hallett, M. (1999). Period of susceptibility for cross-modal plasticity in the blind. *Annals of Neurology*, *45*(4), 451–460. https://doi.org/10.1002/1531-8249(199904)45:4<451::AID-ANA6>3.0.CO;2-B

Collignon, O., Dormal, G., Albouy, G., Vandewalle, G., Voss, P., Phillips, C., & Lepore, F. (2013). Impact of blindness onset on the functional organization and the connectivity of the occipital cortex. *Brain*, *136*(9), 2769–2783. https://doi.org/10.1093/brain/awt176

Collignon, O., Dormal, G., De Heering, A., Lepore, F., Lewis, T. L., & Maurer, D. (2015). Long-Lasting Crossmodal Cortical Reorganization Triggered by Brief Postnatal Visual Deprivation. *Current Biology*, *25*(18), 2379–2383. https://doi.org/10.1016/j.cub.2015.07.036

Collignon, O., Lassonde, M., Lepore, F., Bastien, D., & Veraart, C. (2007). Functional cerebral reorganization for auditory spatial processing and auditory substitution of vision in early blind subjects. *Cerebral Cortex*, *17*(2), 457–465. https://doi.org/10.1093/cercor/bhj162

Collignon, O., Vandewalle, G., Voss, P., Albouy, G., Charbonneau, G., Lassonde, M., & Lepore, F. (2011). Functional specialization for auditory-spatial processing in the occipital cortex of congenitally blind humans. *Proceedings of the National Academy of Sciences*, *108*(11), 4435–4440. https://doi.org/10.1073/pnas.1013928108

Connolly, A. C., Guntupalli, J. S., Gors, J., Hanke, M., Halchenko, Y. O., Wu, Y.-C., Abdi, H., & Haxby, J. V. (2012). The Representation of Biological Classes in the Human Brain. *Journal of Neuroscience*, *32*(8), 2608–2618. https://doi.org/10.1523/JNEUROSCI.5547-11.2012

Culham, J. C., Dukelow, S. P., Vilis, T., Hassard, F. A., Gati, J. S., Menon, R. S., & Goodale, M. A. (1999). Recovery of fMRI activation in Motion Area MT following storage of the motion aftereffect. *Journal of Neurophysiology*. https://doi.org/10.1152/jn.1999.81.1.388

Cynader, M., Berman, N., & Hein, A. (1975). Cats raised in a one-directional world: effects on receptive fields in visual cortex and superior colliculus. *Experimental Brain Research*, *22*(3), 267–280.

Dagli, M. S., Ingeholm, J. E., & Haxby, J. V. (1999). Localization of cardiac-induced signal change in fMRI. *NeuroImage*. https://doi.org/10.1006/nimg.1998.0424

Damasio, A., Yamada, T., Damasio, H., Corbett, J., & McKee, J. (1980). Central achromatopsia: Behavioral, anatomic, and physiologic aspects. *Neurology*, *30*(10), 1064–1064. https://doi.org/10.1212/WNL.30.10.1064

Davies-Thompson, J., & Andrews, T. J. (2012). Intra- and interhemispheric connectivity between face-selective regions in the human brain. *Journal of Neurophysiology*. https://doi.org/10.1152/jn.01171.2011

Daw, N. W., & Wyatt, H. J. (1976). Kittens reared in a unidirectional environment: evidence for a critical period. *The Journal of Physiology*, *257*(1), 155–170.

de Heering, A., Dormal, G., Pelland, M., Lewis, T., Maurer, D., & Collignon, O. (2016). A Brief Period of Postnatal Visual Deprivation Alters the Balance between Auditory and Visual Attention. *Current Biology*, *26*(22), 3101–3105. https://doi.org/10.1016/j.cub.2016.10.014

Desimone, R., & Ungerleider, L. G. (1986). Multiple visual areas in the caudal superior temporal sulcus of the macaque. *Journal of Comparative Neurology*. https://doi.org/10.1002/cne.902480203

Dormal, G., Rezk, M., Yakobov, E., Lepore, F., & Collignon, O. (2016). Auditory motion in the sighted and blind: Early visual deprivation triggers a large-scale imbalance between auditory and "visual" brain regions. *NeuroImage*, *134*, 630–644. https://doi.org/10.1016/j.neuroimage.2016.04.027

Downing, P. E., Chan, A.-Y., Peelen, M. V, Dodds, C. M., & Kanwisher, N. (2006). Domain specificity in visual cortex. *Cerebral Cortex*, *16*(10), 1453–1461.

Downing, P. E., Jiang, Y., Shuman, M., & Kanwisher, N. (2001). A Cortical Area Selective for Visual Processing of the Human Body. *Science*, *293*(5539), 2470–2473. https://doi.org/10.1126/science.1063414

Dubner, R., & Zeki, S. (1971). Response properties and receptive fields of cells in an anatomically defined region of the superior temporal sulcus in the monkey. *Brain Research*, *35*(2), 528–532. https://doi.org/10.1016/0006-8993(71)90494-X

Ducommun, C. Y., Michel, C. M., Clarke, S., Adriani, M., Seeck, M., Landis, T., & Blanke, O. (2004). Cortical Motion Deafness. *Neuron*, *43*(6), 765–777. https://doi.org/10.1016/j.neuron.2004.08.020

Duffy, C. J., & Wurtz, R. H. (1991). Sensitivity of MST neurons to optic flow stimuli. II. Mechanisms of response selectivity revealed by small-field stimuli. *Journal of Neurophysiology*, *65*(6), 1346–1359. https://doi.org/10.1152/jn.1991.65.6.1346

Duffy, C. J., & Wurtz, R. H. (1997). Medial superior temporal area neurons respond to speed patterns in optic flow. *Journal of Neuroscience*. https://doi.org/10.1523/JNEUROSCI.17-08-02839.1997

Ellemberg, D., Lewis, T. L., Maurer, D., Brar, S., & Brent, H. P. (2002). Better perception of global motion after monocular than after binocular deprivation. *Vision Research*, *42*(2), 169–179. https://doi.org/10.1016/S0042-6989(01)00278-4

Epstein, R., & Kanwisher, N. (1998). A cortical representation of the local visual

environment. *Nature*, *392*(6676), 598–601. https://doi.org/10.1038/33402

Falchier, A., Clavagnier, S., Barone, P., & Kennedy, H. (2002). Anatomical Evidence of Multimodal Integration in Primate Striate Cortex. *The Journal of Neuroscience*, *22*(13), 5749–5759. https://doi.org/10.1523/JNEUROSCI.22-13-05749.2002

Felleman, D. J., & Kaas, J. H. (1984). Receptive-field properties of neurons in middle temporal visual area (MT) of owl monkeys. *Journal of Neurophysiology*, *52*(3), 488–513. https://doi.org/10.1152/jn.1984.52.3.488

Felleman, D. J., & Van Essen, D. C. (1991). Distributed Hierarchical Processing in the Primate Cerebral Cortex. *Cerebral Cortex*, *1*(1), 1–47. https://doi.org/10.1093/cercor/1.1.1

Ffytche, D. H., Guy, C. N., & Zeki, S. (1996). Motion specific responses from a blind hemifield. *Brain*, *119*(6), 1971–1982. https://doi.org/10.1093/brain/119.6.1971

Ffytche, D. H., & Zeki, S. (2011). The primary visual cortex, and feedback to it, are not necessary for conscious vision. *Brain*, *134*(1), 247–257. https://doi.org/10.1093/brain/awq305

Flechsig, P. (1901). Developmental (myelogenetic) localisation of the cerebral cortex in the human subject. *The Lancet*.

Fox, M. D., Snyder, A. Z., Vincent, J. L., Corbetta, M., Van Essen, D. C., & Raichle, M. E. (2005). The human brain is intrinsically organized into dynamic, anticorrelated functional networks. *Proceedings of the National Academy of Sciences of the United States of America*. https://doi.org/10.1073/pnas.0504136102

Freeman, J., Brouwer, G. J., Heeger, D. J., & Merriam, E. P. (2011). Orientation Decoding Depends on Maps, Not Columns. *Journal of Neuroscience*, *31*(13), 4792–4804. https://doi.org/10.1523/JNEUROSCI.5160-10.2011

Friston, K. ., Buechel, C., Fink, G. ., Morris, J., Rolls, E., & Dolan, R. . (1997). Psychophysiological and Modulatory Interactions in Neuroimaging. *NeuroImage*, *6*(3), 218–229. https://doi.org/10.1006/nimg.1997.0291

Friston, K. J., Harrison, L., & Penny, W. (2003). Dynamic causal modelling. *NeuroImage*. https://doi.org/10.1016/S1053-8119(03)00202-7

Gaglianese, A., Costagli, M., Bernardi, G., Ricciardi, E., & Pietrini, P. (2012). Evidence of a direct influence between the thalamus and hMT+ independent of V1 in the human brain as measured by fMRI. *NeuroImage*, *60*(2), 1440–1447. https://doi.org/10.1016/j.neuroimage.2012.01.093

Gardumi, A., Ivanov, D., Hausfeld, L., Valente, G., Formisano, E., & Uludağ, K. (2016). The effect of spatial resolution on decoding accuracy in fMRI multivariate pattern analysis. *NeuroImage*, *132*, 32–42. https://doi.org/10.1016/j.neuroimage.2016.02.033

Ghazanfar, A. A., Maier, J. X., Hoffman, K. L., & Logothetis, N. K. (2005). Multisensory integration of dynamic faces and voices in rhesus monkey auditory cortex. *Journal of Neuroscience*. https://doi.org/10.1523/JNEUROSCI.0799-05.2005

Ghazanfar, A. A., & Schroeder, C. (2006). Is neocortex essentially multisensory? *Trends in Cognitive Sciences*, *10*(6), 278–285. https://doi.org/10.1016/j.tics.2006.04.008

Giraud, A. L., & Price, C. J. (2001). The constraints functional neuroimaging places on classical models of auditory word processing. *Journal of Cognitive Neuroscience*. https://doi.org/10.1162/08989290152541421

Gitelman, D. R., Penny, W. D., Ashburner, J., & Friston, K. J. (2003). Modeling regional and psychophysiologic interactions in fMRI: the importance of hemodynamic deconvolution. *NeuroImage*, *19*(1), 200–207. https://doi.org/10.1016/S1053-8119(03)00058-2

Goodale, M. A., & Milner, A. D. (1992). Separate visual pathways for perception and action. *Trends in Neurosciences*, *15*(1), 20–25. https://doi.org/10.1016/0166-2236(92)90344-8

Gougoux, F., Zatorre, R. J., Lassonde, M., Voss, P., & Lepore, F. (2005). A functional neuroimaging study of sound localization: Visual cortex activity predicts performance in early-blind individuals. *PLoS Biology*, *3*(2), 0324–0333. https://doi.org/10.1371/journal.pbio.0030027

Grady, C. L., Mondloch, C. J., Lewis, T. L., & Maurer, D. (2014). Early visual deprivation from congenital cataracts disrupts activity and functional connectivity in the face network. *Neuropsychologia*, *57*(1), 122–139. https://doi.org/10.1016/j.neuropsychologia.2014.03.005

Granger, C. W. J. (1969). Investigating Causal Relations by Econometric Models and Cross-spectral Methods. *Econometrica*. https://doi.org/10.2307/1912791

Grothe, B., Pecka, M., & McAlpine, D. (2010). Mechanisms of sound localization in mammals. In *Physiological Reviews*. https://doi.org/10.1152/physrev.00026.2009

Gschwind, M., Pourtois, G., Schwartz, S., Van De Ville, D., & Vuilleumier, P. (2012). White-matter connectivity between face-responsive regions in the human brain. *Cerebral Cortex*. https://doi.org/10.1093/cercor/bhr226

Guerreiro, M. J. S., Erfort, M. V., Henssler, J., Putzar, L., & Röder, B. (2015). Increased

visual cortical thickness in sight-recovery individuals. *Human Brain Mapping*, *36*(12), 5265–5274. https://doi.org/10.1002/hbm.23009

Gurtubay-Antolin, A., Battal, C., Maffei, C., Rezk, M., Mattioni, S., Jovicich, J., & Collignon, O. (2020). Direct structural connections between auditory and visual motion selective regions in humans. *BioRxiv*, 2020.06.11.145490. https://doi.org/10.1101/2020.06.11.145490

Hackett, T. A., & Kaas, J. H. (2004). *Auditory Cortex in Primates: Functional Subdivisions and Processing Streams.* MIT Press.

Hagen, M. C., Franzén, O., McGlone, F., Essick, G., Dancer, C., & Pardo, J. V. (2002). Tactile motion activates the human middle temporal/V5 (MT/V5) complex. *European Journal of Neuroscience*, *16*(5), 957–964. https://doi.org/10.1046/j.1460-9568.2002.02139.x

Hagmann, P., Thiran, J. P., Jonasson, L., Vandergheynst, P., Clarke, S., Maeder, P., & Meuli, R. (2003). DTI mapping of human brain connectivity: Statistical fibre tracking and virtual dissection. *NeuroImage*. https://doi.org/10.1016/S1053-8119(03)00142-3

Hamilton, R., Keenan, J. P., Catala, M., & Pascual-Leone, A. (2000). Alexia for Braille following bilateral occipital stroke in an early blind woman. *NeuroReport*. https://doi.org/10.1097/00001756-200002070-00003

Hannagan, T., Amedi, A., Cohen, L., Dehaene-lambertz, G., & Dehaene, S. (2015). Origins of the specialization for letters and numbers in ventral occipitotemporal cortex. *Trends in Cognitive Sciences*, *19*(7), 374–382. https://doi.org/10.1016/j.tics.2015.05.006

Hasson, U., Levy, I., Behrmann, M., Hendler, T., & Malach, R. (2002). Eccentricity bias as an organizing principle for human high-order object areas. *Neuron*, *34*(3), 479–490. https://doi.org/10.1016/S0896-6273(02)00662-1

Haxby, J. V., Connolly, A. C., & Guntupalli, J. S. (2014). Decoding Neural Representational Spaces Using Multivariate Pattern Analysis. *Annual Review of Neuroscience*, *37*, 435–456. https://doi.org/10.1146/annurev-neuro-062012-170325

Haxby, J. V., Gobbini, M. I., Furey, M. L., Ishai, A., Schouten, J. L., & Pietrini, P. (2001). Distrubuted and Overlapping Representations of Face and Objects in Ventral Temporal Cortex. *Science*, *293*(5539), 2425–2430. https://doi.org/10.1126/science.1063736

Haxby, J. V., Guntupalli, J. S., Connolly, A. C., Halchenko, Y. O., Conroy, B. R., Gobbini, M. I., Hanke, M., & Ramadge, P. J. (2011). A common, high-dimensional model of the representational space in human ventral temporal cortex. *Neuron*, *72*(2), 404–416. https://doi.org/10.1016/j.neuron.2011.08.026

Haxby, J. V., Guntupalli, J. S., Nastase, S. A., & Feilong, M. (2020). Hyperalignment: Modeling shared information encoded in idiosyncratic cortical topographies. *ELife*, *9*, 1–26. https://doi.org/10.7554/eLife.56601

Haxby, J. V., Hoffman, E. A., & Gobbini, M. I. (2000). The distributed human neural system for face perception. *Trends in Cognitive Sciences*, *4*(6), 223–233. https://doi.org/10.1016/S1364-6613(00)01482-0

Haynes, J.-D., & Rees, G. (2006). Decoding mental states from brain activity in humans. *Nature Reviews Neuroscience*, *7*(7), 523–534. https://doi.org/10.1038/nrn1931

Hebb, D. O. (1949). *The organization of behavior: a neuropsychological theory*. J. Wiley; Chapman & Hall.

Hirsch, H. V. B., & Spinelli, D. N. (1970). Visual experience modifies distribution of horizontally and vertically oriented receptive fields in cats. *Science*, *168*(3933), 869–871.

Hoge, R. D., & Pike, G. B. (2001a). Oxidative metabolism and the detection of neuronal activation via imaging. *Journal of Chemical Neuroanatomy*. https://doi.org/10.1016/S0891-0618(01)00114-4

Hoge, R. D., & Pike, G. B. (2001b). Quantitative measurement using fMRI. *Functional Magnetic Resonance Imaging: An Introduction to Methods*, 159–174.

Hong, H., Yamins, D. L. K., Majaj, N. J., & Dicarlo, J. J. (2016). Explicit information for category-orthogonal object properties increases along the ventral stream. *Nature Neuroscience*, *19*(4), 613–622. https://doi.org/10.1038/nn.4247

Hubel, D. H., & Wiesel, T. N. (1959). Receptive fields of single neurones in the cat's striate cortex. *The Journal of Physiology*. https://doi.org/10.1113/jphysiol.1959.sp006308

Hubel, D. H., & Wiesel, T. N. (1962). Receptive fields, binocular interaction and functional architecture in the cat's visual cortex. *The Journal of Physiology*, *160*(1), 106–154. https://doi.org/10.1113/jphysiol.1962.sp006837

Hubel, D. H., & Wiesel, T. N. (1968). Receptive fields and functional architecture of monkey striate cortex. *The Journal of Physiology*, *195*(1), 215–243. https://doi.org/10.1113/jphysiol.1968.sp008455

Hubel, D. H., & Wiesel, T. N. (1970). The period of susceptibility to the physiological effects of unilateral eye closure in kittens. *The Journal of Physiology*, *206*(2), 419–436. http://www.ncbi.nlm.nih.gov/pubmed/5498493

Hubel, D. H., Wiesel, T. N., & LeVay, S. (1977). Plasticity of ocular dominance columns in

monkey striate cortex. *Philosophical Transactions of the Royal Society of London. Series B, Biological Sciences*, *278*(961), 377–409. https://doi.org/10.1098/rstb.1977.0050

Huk, A. C., Dougherty, R. F., & Heeger, D. J. (2002). Retinotopy and functional subdivision of human areas MT and MST. *The Journal of Neuroscience : The Official Journal of the Society for Neuroscience*, *22*(16), 7195–7205. https://doi.org/20026661

Jiang, F., Beauchamp, M. S., & Fine, I. (2015). Re-examining overlap between tactile and visual motion responses within hMT + and STS. *NeuroImage*, *119*, 187–196. https://doi.org/10.1016/j.neuroimage.2015.06.056

Jiang, F., Stecker, G. C., Boynton, G. M., & Fine, I. (2016). Early Blindness Results in Developmental Plasticity for Auditory Motion Processing within Auditory and Occipital Cortex. *Frontiers in Human Neuroscience*, *10*(July). https://doi.org/10.3389/fnhum.2016.00324

Jiang, F., Stecker, G. C., & Fine, I. (2014). Auditory motion processing after early blindness. *Journal of Vision*, *14*(13), 4–4. https://doi.org/10.1167/14.13.4

Kaas, J. H., & Hackett, T. A. (1999). 'What' and 'where' processing in auditory cortex. *Nature Neuroscience*.

Kamitani, Y., & Tong, F. (2005). Decoding the visual and subjective contents of the human brain. *Nature Neuroscience*, *8*(5), 679–685. https://doi.org/10.1038/nn1444

Kamitani, Y., & Tong, F. (2006). Decoding Seen and Attended Motion Directions from Activity in the Human Visual Cortex. *Current Biology*, *16*(11), 1096–1102. https://doi.org/10.1016/j.cub.2006.04.003

Kanwisher, N., McDermott, J., & Chun, M. M. (1997). The Fusiform Face Area: A Module in Human Extrastriate Cortex Specialized for Face Perception. *The Journal of Neuroscience*, *17*(11), 4302–4311. https://doi.org/10.1523/JNEUROSCI.17-11-04302.1997

Komatsu, H., & Wurtz, R. H. (1988). Relation of cortical areas MT and MST to pursuit eye movements. I. Localization and visual properties of neurons. *Journal of Neurophysiology*, *60*(2), 580–603. https://doi.org/10.1152/jn.1988.60.2.580

Konkle, T., Wang, Q., Hayward, V., & Moore, C. I. (2009). Motion Aftereffects Transfer between Touch and Vision. *Current Biology*, *19*(9), 745–750. https://doi.org/10.1016/j.cub.2009.03.035

Kriegeskorte, N., Goebel, R., & Bandettini, P. (2006). Information-based functional brain mapping. *Proceedings of the National Academy of Sciences*, *103*(10), 3863–3868.

https://doi.org/10.1073/pnas.0600244103

Kriegeskorte, N., Mur, M., & Bandettini, P. (2008). Representational similarity analysis – connecting the branches of systems neuroscience. *Frontiers in Systems Neuroscience*, *2*, 4. https://doi.org/10.3389/neuro.06.004.2008

Kriegeskorte, N., Mur, M., Ruff, D. A., Kiani, R., Bodurka, J., Esteky, H., Tanaka, K., & Bandettini, P. A. (2008). Matching Categorical Object Representations in Inferior Temporal Cortex of Man and Monkey. *Neuron*, *60*(6), 1126–1141. https://doi.org/10.1016/j.neuron.2008.10.043

Krumbholz, K., Schönwiesner, M., Rübsamen, R., Zilles, K., Fink, G. R., & Von Cramon, D. Y. (2005). Hierarchical processing of sound location and motion in the human brainstem and planum temporale. *European Journal of Neuroscience*, *21*(1), 230–238.

Lagae, L., Maes, H., Raiguel, S., Xiao, D. K., & Orban, G. A. (1994). Responses of macaque STS neurons to optic flow components: A comparison of areas MT and MST. *Journal of Neurophysiology*. https://doi.org/10.1152/jn.1994.71.5.1597

Larsson, J., & Heeger, D. J. (2006). Two retinotopic visual areas in human lateral occipital cortex. *Journal of Neuroscience*, *26*(51), 13128–13142. https://doi.org/10.1523/JNEUROSCI.1657-06.2006

Le Vay, S., Wiesel, T. N., & Hubel, D. H. (1980). The development of ocular dominance columns in normal and visually deprived monkeys. *Journal of Comparative Neurology*, *191*(1), 1–51. https://doi.org/10.1002/cne.901910102

Levy, I., Hasson, U., Avidan, G., Hendler, T., & Malach, R. (2001). Center-periphery organization of human object areas. *Nature Neuroscience*, *4*(5), 533–539. https://doi.org/10.1038/87490

Lewis, J. W., Beauchamp, M. S., & DeYoe, E. A. (2000). A comparison of visual and auditory motion processing in human cerebral cortex. *Cerebral Cortex (New York, N.Y. : 1991)*, *10*(9), 873–888. https://doi.org/10.1093/cercor/10.9.873

Li, Y., Fitzpatrick, D., & White, L. E. (2006). The development of direction selectivity in ferret visual cortex requires early visual experience. *Nature Neuroscience*, *9*(5), 676–681. https://doi.org/10.1038/nn1684

Li, Y., Van Hooser, S. D., Mazurek, M., White, L. E., & Fitzpatrick, D. (2008). Experience with moving visual stimuli drives the early development of cortical direction selectivity. *Nature*, *456*(7224), 952–956. https://doi.org/10.1038/nature07417

Liu, Y., Yu, C., Liang, M., Li, J., Tian, L., Zhou, Y., Qin, W., Li, K., & Jiang, T. (2007). Whole brain functional connectivity in the early blind. *Brain*, *130*(8), 2085–2096.

https://doi.org/10.1093/brain/awm121

Mahon, B. Z., Anzellotti, S., Schwarzbach, J., Zampini, M., & Caramazza, A. (2009). Category-Specific Organization in the Human Brain Does Not Require Visual Experience. *Neuron*, *63*(3), 397–405. https://doi.org/10.1016/j.neuron.2009.07.012

Majka, P., Rosa, M. G. P., Bai, S., Chan, J. M., Huo, B. X., Jermakow, N., Lin, M. K., Takahashi, Y. S., Wolkowicz, I. H., Worthy, K. H., Rajan, R., Reser, D. H., Wójcik, D. K., Okano, H., & Mitra, P. P. (2019). Unidirectional monosynaptic connections from auditory areas to the primary visual cortex in the marmoset monkey. *Brain Structure and Function*. https://doi.org/10.1007/s00429-018-1764-4

Malonek, D., & Grinvald, A. (1996). Interactions between electrical activity and cortical microcirculation revealed by imaging spectroscopy: implications for functional brain mapping. *Science*, *272*(5261), 551–554.

Malonek, D., Tootell, R., & Grinvald, A. (1994). Optical imaging reveals the functional architecture of neurons processing shape and motion in owl monkey area MT. *Proc. R. Soc. Lond. B*, *258*(1352), 109–119.

Mattioni, S., Rezk, M., Battal, C., Bottini, R., Cuculiza Mendoza, K. E., Oosterhof, N. N., & Collignon, O. (2020). Categorical representation from sound and sight in the ventral occipito-temporal cortex of sighted and blind. *ELife*, *9*, 1–33. https://doi.org/10.7554/eLife.50732

Maunsell, J. H., & van Essen, D. C. (1983). The connections of the middle temporal visual area (MT) and their relationship to a cortical hierarchy in the macaque monkey. *The Journal of Neuroscience : The Official Journal of the Society for Neuroscience*, *3*(12), 2563–2586.

Maunsell, J. H., & Van Essen, D. C. (1983). Functional properties of neurons in middle temporal visual area of the macaque monkey. I. Selectivity for stimulus direction, speed, and orientation. *Journal of Neurophysiology*, *49*(5), 1127–1147. https://doi.org/10.1152/jn.1983.49.5.1127

Maurer, D. (2017). Critical periods re-examined: Evidence from children treated for dense cataracts. *Cognitive Development*, *42*, 27–36. https://doi.org/10.1016/j.cogdev.2017.02.006

Maurer, D., Lewis, T. L., & Mondloch, C. J. (2005). Missing sights: Consequences for visual cognitive development. *Trends in Cognitive Sciences*, *9*(3 SPEC. ISS.), 144–151. https://doi.org/10.1016/j.tics.2005.01.006

Maurer, D., Mondloch, C. J., & Lewis, T. L. (2007). Sleeper effects. *Developmental Science*, *10*(1), 40–47. https://doi.org/10.1111/j.1467-7687.2007.00562.x

McCandliss, B. D., Cohen, L., & Dehaene, S. (2003). The visual word form area: Expertise for reading in the fusiform gyrus. *Trends in Cognitive Sciences*. https://doi.org/10.1016/S1364-6613(03)00134-7

McCarthy, G., Puce, A., Gore, J. C., & Allison, T. (1997). Face-Specific Processing in the Human Fusiform Gyrus. *Journal of Cognitive Neuroscience*, *9*(5), 605–610. https://doi.org/10.1162/jocn.1997.9.5.605

McLachlan, G. J. (2004). *Discriminant analysis and statistical pattern recognition* (Vol. 544). John Wiley & Sons.

Meyer, G. F., & Wuerger, S. M. (2001). Cross-modal integration of auditory and visual motion signals. *NeuroReport*, *12*(11), 2557–2560. https://doi.org/10.1097/00001756-200108080-00053

Meyer, G. F., Wuerger, S. M., Röhrbein, F., & Zetzsche, C. (2005). Low-level integration of auditory and visual motion signals requires spatial co-localisation. *Experimental Brain Research*, *166*(3–4), 538–547. https://doi.org/10.1007/s00221-005-2394-7

Middlebrooks, J. C. (2015). Sound localization. In *Handbook of Clinical Neurology* (1st ed., Vol. 129, pp. 99–116). Elsevier B.V. https://doi.org/10.1016/B978-0-444-62630-1.00006-8

Middlebrooks, J. C., Xu, L., Furukawa, S., & Macpherson, E. A. (2002). Cortical neurons that localize sounds. In *Neuroscientist*. https://doi.org/10.1177/107385840200800112

Misaki, M., Kim, Y., Bandettini, P. A., & Kriegeskorte, N. (2010). Comparison of multivariate classifiers and response normalizations for pattern-information fMRI. *NeuroImage*, *53*(1), 103–118. https://doi.org/10.1016/j.neuroimage.2010.05.051

Mishkin, M., Ungerleider, L. G., & Macko, K. A. (1983). Object vision and spatial vision: two cortical pathways. In *Trends in Neurosciences*. https://doi.org/10.1016/0166-2236(83)90190-X

Mitchell, D. E., Kennie, J., & Kung, D. (2009). Development of Global Motion Perception Requires Early Postnatal Exposure to Patterned Light. *Current Biology*, *19*(8), 645–649. https://doi.org/10.1016/j.cub.2009.02.038

Morland, A. B., Jones, S. R., Finlay, A. L., Deyzac, E., Lê, S., & Kemp, S. (1999). Visual perception of motion, luminance and colour in a human hemianope. *Brain*, *122*(6), 1183–1198. https://doi.org/10.1093/brain/122.6.1183

Mountcastle, V. B. (1997). The columnar organization of the neocortex. *Brain*, *120*(4), 701–722. https://doi.org/10.1093/brain/120.4.701

Movshon, J. A., & Newsome, W. T. (1996). Visual Response Properties of Striate Cortical Neurons Projecting to Area MT in Macaque Monkeys. *The Journal of Neuroscience*, *16*(23), 7733–7741. https://doi.org/10.1523/JNEUROSCI.16-23-07733.1996

Mundinano, I. C., Kwan, W. C., & Bourne, J. A. (2019). Retinotopic specializations of cortical and thalamic inputs to area MT. *Proceedings of the National Academy of Sciences of the United States of America*, *116*(46), 23326–23331. https://doi.org/10.1073/pnas.1909799116

Newsome, W. T., & Paré, E. B. (1988). A selective impairment of motion perception following lesions of the middle temporal visual area (MT). *The Journal of Neuroscience : The Official Journal of the Society for Neuroscience*, *8*(6), 2201–2211. https://doi.org/10.1055/s-1999-184

Norman, K. A., Polyn, S. M., Detre, G. J., & Haxby, J. V. (2006). Beyond mind-reading: multi-voxel pattern analysis of fMRI data. *Trends in Cognitive Sciences*, *10*(9), 424–430. https://doi.org/10.1016/j.tics.2006.07.005

O'Reilly, J. X., Woolrich, M. W., Behrens, T. E. J., Smith, S. M., & Johansen-Berg, H. (2012). Tools of the trade: Psychophysiological interactions and functional connectivity. *Social Cognitive and Affective Neuroscience*, *7*(5), 604–609. https://doi.org/10.1093/scan/nss055

Ogawa, S., Lee, T.-M., Kay, A. R., & Tank, D. W. (1990). Brain magnetic resonance imaging with contrast dependent on blood oxygenation. *Proceedings of the National Academy of Sciences*, *87*(24), 9868–9872.

Op de Beeck, H. P. (2010). Against hyperacuity in brain reading: Spatial smoothing does not hurt multivariate fMRI analyses? *NeuroImage*, *49*(3), 1943–1948. https://doi.org/10.1016/j.neuroimage.2009.02.047

Op De Beeck, H. P., Baker, C. I., DiCarlo, J. J., & Kanwisher, N. G. (2006). Discrimination training alters object representations in human extrastriate cortex. *Journal of Neuroscience*, *26*(50), 13025–13036. https://doi.org/10.1523/JNEUROSCI.2481-06.2006

Op de Beeck, H. P., Pillet, I., & Ritchie, J. B. (2019). Factors Determining Where Category-Selective Areas Emerge in Visual Cortex. *Trends in Cognitive Sciences*, 1–14. https://doi.org/10.1016/j.tics.2019.06.006

Osher, D. E., Saxe, R. R., Koldewyn, K., Gabrieli, J. D. E., Kanwisher, N., & Saygin, Z. M. (2016). *Structural Connectivity Fingerprints Predict Cortical Selectivity for Multiple Visual Categories across Cortex*. *January 2015*, 1668–1683. https://doi.org/10.1093/cercor/bhu303

Pack, C. C., Hunter, J. N., & Born, R. T. (2005). Contrast dependence of suppressive influences in cortical area MT of alert macaque. *Journal of Neurophysiology*, *93*(3), 1809–1815. https://doi.org/10.1152/jn.00629.2004

Pascual-Leone, A., & Hamilton, R. (2001). The metamodal organization of the brain. In *Progress in Brain Research* (pp. 427–445). https://doi.org/10.1016/S0079-6123(01)34028-1

Pavani, F., Macaluso, E., Warren, J. D., Driver, J., & Griffiths, T. D. (2002). A Common Cortical Substrate Activated by Horizontal and Vertical Sound Movement in the Human Brain. *Current Biology*, *12*(18), 1584–1590. https://doi.org/10.1016/S0960-9822(02)01143-0

Pearlman, A. L., Birch, J., & Meadows, J. C. (1979). Cerebral color blindness: An acquired defect in hue discrimination. *Annals of Neurology*, *5*(3), 253–261. https://doi.org/10.1002/ana.410050307

Pietrini, P., Furey, M. L., Ricciardi, E., Gobbini, M. I., Wu, W.-H. C., Cohen, L., Guazzelli, M., & Haxby, J. V. (2004). Beyond sensory images: Object-based representation in the human ventral pathway. *Proceedings of the National Academy of Sciences*, *101*(15), 5658–5663. https://doi.org/10.1073/pnas.0400707101

Poirier, C., Collignon, O., DeVolder, A. G., Renier, L., Vanlierde, A., Tranduy, D., & Scheiber, C. (2005). Specific activation of the V5 brain area by auditory motion processing: An fMRI study. *Cognitive Brain Research*, *25*(3), 650–658. https://doi.org/10.1016/j.cogbrainres.2005.08.015

Poirier, C., Collignon, O., Scheiber, C., Renier, L., Vanlierde, A., Tranduy, D., Veraart, C., & De Volder, A. G. (2006). Auditory motion perception activates visual motion areas in early blind subjects. *NeuroImage*, *31*(1), 279–285. https://doi.org/10.1016/j.neuroimage.2005.11.036

Power, J. D., Barnes, K. A., Snyder, A. Z., Schlaggar, B. L., & Petersen, S. E. (2012). Spurious but systematic correlations in functional connectivity MRI networks arise from subject motion. *NeuroImage*, *59*(3), 2142–2154. https://doi.org/10.1016/j.neuroimage.2011.10.018

Qin, W., Xuan, Y., Liu, Y., Jiang, T., & Yu, C. (2015). Functional connectivity density in congenitally and late blind subjects. *Cerebral Cortex*, *25*(9), 2507–2516. https://doi.org/10.1093/cercor/bhu051

Raj, D., Anderson, A. W., & Gore, J. C. (2001). Respiratory effects in human functional magnetic resonance imaging due to bulk susceptibility changes. *Physics in Medicine and Biology*. https://doi.org/10.1088/0031-9155/46/12/318

Rajimehr, R., Devaney, K. J., Bilenko, N. Y., Young, J. C., & Tootell, R. B. H. (2011). The "parahippocampal place area" responds preferentially to high spatial frequencies in humans and monkeys. *PLoS Biology*, *9*(4). https://doi.org/10.1371/journal.pbio.1000608

Rauschecker, J. P., & Tian, B. (2000). Mechanisms and streams for processing of "what" and "where" in auditory cortex. *Proceedings of the National Academy of Sciences*, *97*(22), 11800–11806.

Rees, G., Friston, K., & Koch, C. (2000). A direct quantitative relationship between the functional properties of human and macaque V5. *Nature Neuroscience*, *3*(7), 716–723. https://doi.org/10.1038/76673

Reich, L., Szwed, M., Cohen, L., & Amedi, A. (2011). A ventral visual stream reading center independent of visual experience. *Current Biology*, *21*(5), 363–368. https://doi.org/10.1016/j.cub.2011.01.040

Ricciardi, E., & Pietrini, P. (2011). New light from the dark: What blindness can teach us about brain function. *Current Opinion in Neurology*, *24*(4), 357–363. https://doi.org/10.1097/WCO.0b013e328348bdbf

Ricciardi, E., Vanello, N., Sani, L., Gentili, C., Scilingo, E. P., Landini, L., Guazzelli, M., Bicchi, A., Haxby, J. V., & Pietrini, P. (2007). The Effect of Visual Experience on the Development of Functional Architecture in hMT+. *Cerebral Cortex*, *17*(12), 2933–2939. https://doi.org/10.1093/cercor/bhm018

Riddoch, G. (1917). Dissociation of visual perceptions due to occipital injuries, with especial reference to appreciation of movement. *Brain*, *40*(1), 15–57. https://doi.org/10.1093/brain/40.1.15

Rochefort, N. L., Narushima, M., Grienberger, C., Marandi, N., Hill, D. N., & Konnerth, A. (2011). Development of direction selectivity in mouse cortical neurons. *Neuron*, *71*(3), 425–432. https://doi.org/10.1016/j.neuron.2011.06.013

Rockland, K. S. (1989). Bistratified Distribution Of Terminal Arbors Of Individual Axons Projecting From Area Vi To Middle Temporal Area (Mt) In The Macaque Monkey. *Visual Neuroscience*. https://doi.org/10.1017/S0952523800004466

Rockland, K. S. (1995). Morphology of individual axons projecting from area V2 to MT in the macaque. *Journal of Comparative Neurology*. https://doi.org/10.1002/cne.903550105

Rodman, H. R., & Albright, T. D. (1987). Coding of visual stimulus velocity in area MT of the macaque. *Vision Research*, *27*(12), 2035–2048. https://doi.org/10.1016/0042-6989(87)90118-0

Rodman, H. R., Gross, C. G., & Albright, T. D. (1989). Afferent basis of visual response properties in area MT of the macaque. I. Effects of striate cortex removal. *Journal of Neuroscience*, *9*(6), 2033–2050. https://doi.org/10.1523/jneurosci.09-06-02033.1989

Romanski, L. M., Tian, B., Fritz, J. B., Mishkin, M., Goldman-Rakic, P. S., & Rauschecker, J. P. (1999). "What,' "where' and "how' in auditory cortex. Reply. *Nature Neuroscience*.

Sabbah, N., Authié, C. N., Sanda, N., Mohand-Saïd, S., Sahel, J.-A. A., Safran, A. B., Habas, C., & Amedi, A. (2016). Increased functional connectivity between language and visually deprived areas in late and partial blindness. *NeuroImage*, *136*, 162–173. https://doi.org/10.1016/j.neuroimage.2016.04.056

Sadato, N., Pascual-Leone, A., Grafman, J., Ibañez, V., Deiber, M.-P., Dold, G., & Hallett, M. (1996). Activation of the primary visual cortex by Braille reading in blind subjects. *Nature*, *380*(6574), 526–528. https://doi.org/10.1038/380526a0

Saenz, M., Lewis, L. B., Huth, A. G., Fine, I., & Koch, C. (2008). Visual Motion Area MT+/V5 Responds to Auditory Motion in Human Sight-Recovery Subjects. *Journal of Neuroscience*, *28*(20), 5141–5148. https://doi.org/10.1523/JNEUROSCI.0803-08.2008

Sani, L., Ricciardi, E., Gentili, C., Vanello, N., Haxby, J. V., & Pietrini, P. (2010). Effects of Visual Experience on the Human MT+ Functional Connectivity Networks: An fMRI Study of Motion Perception in Sighted and Congenitally Blind Individuals. *Frontiers in Systems Neuroscience*, *4*, 159. https://doi.org/10.3389/fnsys.2010.00159

Satterthwaite, T. D., Wolf, D. H., Loughead, J., Ruparel, K., Elliott, M. A., Hakonarson, H., Gur, R. C., & Gur, R. E. (2012). NeuroImage Impact of in-scanner head motion on multiple measures of functional connectivity : Relevance for studies of neurodevelopment in youth ☆. *NeuroImage*, *60*(1), 623–632. https://doi.org/10.1016/j.neuroimage.2011.12.063

Saygin, Z. M., Osher, D. E., Koldewyn, K., Reynolds, G., Gabrieli, J. D. E., & Saxe, R. R. (2012). Anatomical connectivity patterns predict face selectivity in the fusiform gyrus. *Nature Neuroscience*, *15*(2), 321–327. https://doi.org/10.1038/nn.3001

Scheef, L., Boecker, H., Daamen, M., Fehse, U., Landsberg, M. W., Granath, D. O., Mechling, H., & Effenberg, A. O. (2009). Multimodal motion processing in area V5/MT: Evidence from an artificial class of audio-visual events. *Brain Research*, *1252*, 94–104. https://doi.org/10.1016/j.brainres.2008.10.067

Schiller, P. H., Logothetis, N. K., & Charles, E. R. (1990). Functions of the colour-opponent and broad-band channels of the visual system. *Nature*, *343*(6253), 68–70. https://doi.org/10.1038/343068a0

Schoenfeld, M. A., Noesselt, T., Poggel, D., Tempelmann, C., Hopf, J. M., Woldorff, M. G., Heinze, H. J., & Hillyard, S. A. (2002). Analysis of pathways mediating preserved vision after striate cortex lesions. *Annals of Neurology*, *52*(6), 814–824. https://doi.org/10.1002/ana.10394

Schwarzlose, R. F., Swisher, J. D., Dang, S., & Kanwisher, N. (2008). The distribution of category and location information across object-selective regions in human visual cortex. *Proceedings of the National Academy of Sciences of the United States of America*, *105*(11), 4447–4452. https://doi.org/10.1073/pnas.0800431105

Sengupta, A., Yakupov, R., Speck, O., Pollmann, S., & Hanke, M. (2017). The effect of acquisition resolution on orientation decoding from V1 BOLD fMRI at 7 T. *NeuroImage*, *148*(January), 64–76. https://doi.org/10.1016/j.neuroimage.2016.12.040

Sha, L., Haxby, J. V., Abdi, H., Guntupalli, J. S., Oosterhof, N. N., Halchenko, Y. O., & Connolly, A. C. (2015). The Animacy Continuum in the Human Ventral Vision Pathway. *Journal of Cognitive Neuroscience*, *27*(4), 665–678. https://doi.org/10.1162/jocn_a_00733

Shipp, S., & Zeki, S. (1989). The Organization of Connections between Areas V5 and V1 in Macaque Monkey Visual Cortex. *European Journal of Neuroscience*, *1*(4), 309–332. https://doi.org/10.1111/j.1460-9568.1989.tb00798.x

Shmuel, A., Chaimow, D., Raddatz, G., Ugurbil, K., & Yacoub, E. (2010). Mechanisms underlying decoding at 7 T: Ocular dominance columns, broad structures, and macroscopic blood vessels in V1 convey information on the stimulated eye. *NeuroImage*, *49*(3), 1957–1964. https://doi.org/10.1016/j.neuroimage.2009.08.040

Silson, E. H., Chan, A. W. Y., Reynolds, R. C., Kravitz, D. J., & Baker, C. I. (2015). A retinotopic basis for the division of high-level scene processing between lateral and ventral human occipitotemporal cortex. *Journal of Neuroscience*. https://doi.org/10.1523/JNEUROSCI.0137-15.2015

Sincich, L. C., Park, K. F., Wohlgemuth, M. J., & Horton, J. C. (2004). Bypassing V1: a direct geniculate input to area MT. *Nature Neuroscience*, *7*(10), 1123–1128. https://doi.org/10.1038/nn1318

Smith, A. T., Wall, M. B., Williams, A. L., & Singh, K. D. (2006). Sensitivity to optic flow in human cortical areas MT and MST. *European Journal of Neuroscience*, *23*(2), 561–569. https://doi.org/10.1111/j.1460-9568.2005.04526.x

Soto-Faraco, S., Kingstone, A., Calvert, G., Spence, C., & Stein, B. E. (2004). Multisensory Integration of Dynamic Information. *The Handbook of Multisensory Processes*.

Soto-Faraco, S., Kingstone, A., & Spence, C. (2004). Cross-Modal Dynamic Capture:

Congruency Effects in the Perception of Motion Across Sensory Modalities. *Journal of Experimental Psychology: Human Perception and Performance*, *30*(2), 330–345. https://doi.org/10.1037/0096-1523.30.2.330

Soto-Faraco, S., Lyons, J., Gazzaniga, M., Spence, C., & Kingstone, A. (2002). The ventriloquist in motion: Illusory capture of dynamic information across sensory modalities. *Cognitive Brain Research*, *14*(1), 139–146. https://doi.org/10.1016/S0926-6410(02)00068-X

Spence, C., Senkowski, D., & Röder, B. (2009). Crossmodal processing. *Experimental Brain Research*, *198*(2–3), 107–111. https://doi.org/10.1007/s00221-009-1973-4

Stevens, W. D., Kravitz, D. J., Peng, C. S., Tessler, M. H., & Martin, A. (2017). Privileged functional connectivity between the visual word form area and the language system. *Journal of Neuroscience*. https://doi.org/10.1523/JNEUROSCI.0138-17.2017

Stoerig, P., & Cowey, A. (1997). Blindsight in man and monkey. *Brain*, *120*(3), 535–559. https://doi.org/10.1093/brain/120.3.535

Strnad, L., Peelen, M. V., Bedny, M., & Caramazza, A. (2013). Multivoxel Pattern Analysis Reveals Auditory Motion Information in MT+ of Both Congenitally Blind and Sighted Individuals. *PLoS ONE*, *8*(4). https://doi.org/10.1371/journal.pone.0063198

Swisher, J. D., Gatenby, J. C., Gore, J. C., Wolfe, B. A., Moon, C.-H., Kim, S.-G., & Tong, F. (2010). Multiscale Pattern Analysis of Orientation-Selective Activity in the Primary Visual Cortex. *Journal of Neuroscience*, *30*(1), 325–330. https://doi.org/10.1523/JNEUROSCI.4811-09.2010

Tootell, R. B. H., Reppas, J. B., Dale, A. M., Look, R. B., Sereno, M. I., Malach, R., Brady, T. J., & Rosen, B. R. (1995). Visual motion aftereffect in human cortical area MT revealed by functional magnetic resonance imaging. *Nature*, *375*(6527), 139–141. https://doi.org/10.1038/375139a0

Ungerleider, L. G., & Desimone, R. (1986). Cortical connections of visual area MT in the macaque. *Journal of Comparative Neurology*, *248*(2), 190–222. https://doi.org/10.1002/cne.902480204

Ungerleider, L. G., Desimone, R., Galkin, T. W., & Mishkin, M. (1984). Subcortical projections of area MT in the macaque. *The Journal of Comparative Neurology*, *223*(3), 368–386. https://doi.org/10.1002/cne.902230304

Ungerleider, L. G., & Haxby, J. V. (1994). “What” and “where” in the human brain. *Current Opinion in Neurobiology*, *4*(2), 157–165. https://doi.org/10.1016/0959-4388(94)90066-3

van den Hurk, J., Van Baelen, M., & Op de Beeck, H. P. (2017). Development of visual category selectivity in ventral visual cortex does not require visual experience. *Proceedings of the National Academy of Sciences*, *114*(22), E4501–E4510. https://doi.org/10.1073/pnas.1612862114

Van Dijk, K. R. A., Sabuncu, M. R., & Buckner, R. L. (2012). The influence of head motion on intrinsic functional connectivity MRI. *NeuroImage*, *59*(1), 431–438. https://doi.org/10.1016/j.neuroimage.2011.07.044

Van Essen, D. C., Maunsell, J. H. R., & Bixby, J. L. (1981). The middle temporal visual area in the macaque: Myeloarchitecture, connections, functional properties and topographic organization. *Journal of Comparative Neurology*, *199*(3), 293–326. https://doi.org/10.1002/cne.901990302

Van Hooser, S. D., Li, Y., Christensson, M., Smith, G. B., White, L. E., & Fitzpatrick, D. (2012). Initial neighborhood biases and the quality of motion stimulation jointly influence the rapid emergence of direction preference in visual cortex. *Journal of Neuroscience*, *32*(21), 7258–7266.

Van Kemenade, B. M., Seymour, K., Wacker, E., Spitzer, B., Blankenburg, F., & Sterzer, P. (2014). Tactile and visual motion direction processing in hMT+/V5. *NeuroImage*, *84*, 420–427. https://doi.org/10.1016/j.neuroimage.2013.09.004

Veraart, C., De Volder, A. G., Wanet-Defalque, M. C., Bol, A., Michel, C., & Goffinet, A. M. (1990). Glucose utilization in human visual cortex is abnormally elevated in blindness of early onset but decreased in blindness of late onset. *Brain Research*, *510*(1), 115–121.

Vetter, P., Smith, F. W., & Muckli, L. (2014). Decoding sound and imagery content in early visual cortex. *Current Biology*, *24*(11), 1256–1262. https://doi.org/10.1016/j.cub.2014.04.020

von Saldern, S., & Noppeney, U. (2013). Sensory and Striatal Areas Integrate Auditory and Visual Signals into Behavioral Benefits during Motion Discrimination. *Journal of Neuroscience*, *33*(20), 8841–8849. https://doi.org/10.1523/JNEUROSCI.3020-12.2013

Voss, P. (2013). Sensitive and critical periods in visual sensory deprivation. *Frontiers in Psychology*, *4*(SEP), 1–13. https://doi.org/10.3389/fpsyg.2013.00664

Voss, P., Gougoux, F., Lassonde, M., Zatorre, R. J., & Lepore, F. (2006). A positron emission tomography study during auditory localization by late-onset blind individuals. *NeuroReport*, *17*(4), 383–388. https://doi.org/10.1097/01.wnr.0000204983.21748.2d

Voss, P., & Zatorre, R. J. (2012). Organization and reorganization of sensory-deprived cortex. *Current Biology*, *22*(5), R168–R173. https://doi.org/10.1016/j.cub.2012.01.030

Walther, A., Nili, H., Ejaz, N., Alink, A., Kriegeskorte, N., & Diedrichsen, J. (2016). Reliability of dissimilarity measures for multi-voxel pattern analysis. *NeuroImage*, *137*, 188–200. https://doi.org/10.1016/j.neuroimage.2015.12.012

Wanet-Defalque, M.-C., Veraart, C., De Volder, A., Metz, R., Michel, C., Dooms, G., & Goffinet, A. (1988). High metabolic activity in the visual cortex of early blind human subjects. *Brain Research*, *446*(2), 369–373.

Warren, J. D., Zielinski, B. A., Green, G. G. R., Rauschecker, J. P., & Griffiths, T. D. (2002). Perception of Sound-Source Motion by the Human Brain. *Neuron*, *34*(1), 139–148. https://doi.org/10.1016/S0896-6273(02)00637-2

Watkins, K. E., Cowey, A., Alexander, I., Filippini, N., Kennedy, J. M., Smith, S. M., Ragge, N., & Bridge, H. (2012). Language networks in anophthalmia: Maintained hierarchy of processing in "visual" cortex. *Brain*, *135*(5), 1566–1577. https://doi.org/10.1093/brain/aws067

Watson, J. D. G., Myers, R., Frackowiak, R. S. J., Hajnal, J. V., Woods, R. P., Mazziotta, J. C., Shipp, S., & Zeki, S. (1993). Area V5 of the Human Brain: Evidence from a Combined Study Using Positron Emission Tomography and Magnetic Resonance Imaging. *Cerebral Cortex*, *3*(2), 79–94. https://doi.org/10.1093/cercor/3.2.79

Weeks, R., Horwitz, B., Aziz-Sultan, A., Tian, B., Wessinger, C. M., Cohen, L. G., Hallett, M., & Rauschecker, J. P. (2000). A Positron Emission Tomographic Study of Auditory Localization in the Congenitally Blind. *The Journal of Neuroscience*, *20*(7), 2664–2672. https://doi.org/10.1523/JNEUROSCI.20-07-02664.2000

Weiner, K. S., & Grill-Spector, K. (2012). The improbable simplicity of the fusiform face area. *Trends in Cognitive Sciences*, *16*(5), 251–254. https://doi.org/10.1016/j.tics.2012.03.003

Weiner, K. S., Sayres, R., Vinberg, J., & Grill-spector, K. (2010). *fMRI-Adaptation and Category Selectivity in Human Ventral Temporal Cortex : Regional Differences Across Time Scales*. 3349–3365. https://doi.org/10.1152/jn.01108.2009.

Weiskrantz, L., Warrington, E. K., Sanders, M. D., & Marshall, J. (1974). Visual Capacity in the Hemianopic Field Following a Restricted Occipital Ablation. *Brain*, *97*(4), 709–728. https://doi.org/10.1093/brain/97.4.709

Wiesel, T. N., & Hubel, D. H. (1963). Responses in Striate Deprived of Vision Cortex of One Eye. *Journal of Neurophysiology*, *26*(6), 1003–1017.

Wiesel, T. N., & Hubel, D. H. (1965a). Comparison of the effects of unilateral and bilateral eye closure on cortical unit responses in kittens. *Journal of Neurophysiology*, *28*(6), 1029–1040. https://doi.org/10.1152/jn.1965.28.6.1029

Wiesel, T. N., & Hubel, D. H. (1965b). Extent of recovery from the effects of visual deprivation in kittens. *Journal of Neurophysiology*, *28*(6), 1060–1072. https://doi.org/10.1152/jn.1965.28.6.1060

Wolbers, T., Zahorik, P., & Giudice, N. A. (2011). Decoding the direction of auditory motion in blind humans. *NeuroImage*, *56*(2), 681–687. https://doi.org/10.1016/j.neuroimage.2010.04.266

Yabuta, N. H., Sawatari, A., & Callaway, E. M. (2001). Two functional channels from primary visual cortex to dorsal visual cortical areas. *Science*. https://doi.org/10.1126/science.1057916

Zangaladze, A., Epstein, C. M., Grafton, S. T., & Sathian, K. (1999). *Involvement of visual cortex in tactile discrimination of orientation*. *401*(October), 587–590.

Zatorre, R. J., Evans, A. C., & Meyer, E. (1994). Neural mechanisms underlying melodic perception and memory for pitch. *Journal of Neuroscience*. https://doi.org/10.1523/jneurosci.14-04-01908.1994

Zeki, S. (1973). Colour coding in rhesus monkey prestriate cortex. *Brain Research*, *53*(2), 422–427. https://doi.org/10.1016/0006-8993(73)90227-8

Zeki, S. (1974). Functional organization of a visual area in the posterior bank of the superior temporal sulcus of the rhesus monkey. *The Journal of Physiology*, *236*(3), 549–573. https://doi.org/10.1113/jphysiol.1974.sp010452

Zeki, S. (1978). Uniformity and diversity of structure and function in rhesus monkey prestriate visual cortex. *The Journal of Physiology*, *277*(1), 273–290. https://doi.org/10.1113/jphysiol.1978.sp012272

Zeki, S. (1980). The response properties of cells in the middle temporal area (area MT) of owl monkey visual cortex. *Proc. R. Soc. Lond. B*, *207*(1167), 239–248.

Zeki, S., & Ffytche, D. H. (1998). The Riddoch syndrome: insights into the neurobiology of conscious vision. *Brain*, *121*(1), 25–45. https://doi.org/10.1093/brain/121.1.25

Zeki, S., Watson, J. D. G., Lueck, C., Friston, K., Kennard, C., & Frackowiak, R. (1991). A direct demonstration of functional specialization in human visual cortex. *The Journal of Neuroscience*, *11*(3), 641–649. https://doi.org/10.1523/JNEUROSCI.11-03-00641.1991

Zihl, J., Von Cramon, D., & Mai, N. (1983). Selective disturbance of movement vision after bilateral brain damage. *Brain*, *106*(2), 313–340. https://doi.org/10.1093/brain/106.2.313

Zihl, J., Von Cramon, D., Mai, N., & Schmid, C. H. (1991). Disturbance of movement vision after bilateral posterior brain damage: Further evidence and follow up observations. *Brain*, *114*(5), 2235–2252. https://doi.org/10.1093/brain/114.5.2235

Zimmermann, J., Goebel, R., de Martino, F., van de Moortele, P. F., Feinberg, D., Adriany, G., Chaimow, D., Shmuel, A., Uğurbil, K., & Yacoub, E. (2011). Mapping the organization of axis of motion selective features in human area mt using high-field fmri. *PLoS ONE*, *6*(12), 1–10. https://doi.org/10.1371/journal.pone.0028716

Chapter 2

Shared representation of visual and auditory motion directions in the human middle-temporal cortex

Mohamed Rezk[1], Stephanie Cattoir[2], Ceren Battal[1], Valeria Occelli[2], Stefania Mattioni[1], & Olivier Collignon[1,2]

[1]Institut de Recherche en Sciences Psychologiques (IPSY) and Institute of Neuroscience (IoNS), Louvain Bionics, Crossmodal Perception and Plasticity Lab, Universite catholique de Louvain (UCL), 1348 Louvain-la-Neuve, Belgium [2]Center for Mind/Brain Sciences (CIMeC), University of Trento, 38068 Rovereto, Italy

---

The human occipito-temporal region hMT+/V5 is well known for processing visual motion direction. Here, we demonstrate that hMT+/V5 also represents the direction of auditory motion in a format partially aligned with the one used to code visual motion. We show that auditory and visual motion directions can be reliably decoded in individually localized hMT+/V5 and that motion directions in one modality can be predicted from the activity patterns elicited by the other modality. Despite shared motion-direction information across the senses, vision and audition, however, overall produce opposite voxel-wise responses in hMT+/V5. Our results reveal a multifaced representation of multisensory motion signals in hMT+/V5 and have broader implications for our understanding of how we consider the division of sensory labor between brain regions dedicated to a specific perceptual function.

Article published in Current Biology: Rezk, M., Cattoir, S., Battal, C., Occelli, V., Mattioni, S., & Collignon, O. (2020). Shared Representation of Visual and Auditory Motion Directions in the Human Middle-Temporal Cortex. *Current Biology*.

Chapter 2

Shared representation of visual and auditory motion directions in the human middle-temporal cortex

Introduction

In primates, the visual cortex evolved a region in the middle-temporal cortex (MT) that is highly specialized to process visual motion (Baker et al., 1981; Zeki, 1974, 1980). One hallmark organizational feature of this region, first disclosed using electrophysiological recording in animals, is the presence of cortical columns that are preferentially tuned to a specific direction/axis of visual motion (Albright et al., 1984a). Motion preference (Zeki et al., 1991) and directional selectivity (Tootell, Reppas, Dale, et al., 1995; Zimmermann et al., 2011) was also probed using functional Magnetic Resonance Imaging (fMRI) in the human homologue of MT (hereafter hMT+/V5). These studies promoted hMT+/V5 as one cornerstone region in the visual system showing reliable functional preference for processing visual motion direction.

Is hMT+/V5 uniquely visual? It was recently suggested that hMT+/V5 might also be involved in processing motion information from non-visual modalities (Dormal et al., 2016; Hagen et al., 2002; Poirier et al., 2005; Ricciardi et al., 2007; Van Kemenade et al., 2014; Wacker et al., 2011). If true, this has major implication on how we classically consider the division of sensory labor between brain regions dedicated to a specific perceptual or cognitive function (Calvert & Thesen, 2004; Schroeder & Foxe, 2005). This would suggest that regions typically considered as purely unisensory may in fact show some level of abstraction by implementing canonical perceptual computations across the senses (Driver & Spence, 2000; Pascual-Leone & Hamilton, 2001; Ricciardi et al., 2013). However, the idea that hMT+/V5 involves in motion processing other than for vision remains controversial and has notably been challenged by studies suggesting that the overlap between brain activity elicited by visual and non-visual motion is an artifactual byproduct of smoothing fMRI activity maps or by using group-level rather than individually-defined hMT+/V5 (Beauchamp et al., 2007; Chaplin et al., 2018; Dormal et al., 2016; Jiang et al., 2014, 2015; Poirier et al., 2005; Ricciardi et al., 2007; Saenz et al., 2008; Van Kemenade et al., 2014).

Unlike univariate techniques, multivariate pattern analyses (MVPA) were able to dissociate information about visual motion direction in hMT+/V5 (Beckett et al., 2012; Kamitani & Tong, 2006). Interestingly, planes of auditory motion were successfully

decoded in hMT+/V5 (Battal et al., 2018; Dormal et al., 2016). Although these results suggest that auditory motion information may be represented in hMT+/V5, whether the representation of motion direction is similar across sensory modalities remains unsolved. In other words, the idea that hMT+/V5 can share an abstracted representation of directional motion across the senses has never been tested. In this context, MVPA and in particular cross-modal classification methods represent an appealing application of machine learning to operationalize the presence of abstracted brain representations (Kaplan et al., 2015). The goal of this study was to use fMRI to characterize the representation of visual and auditory motion in individually-defined hMT+/V5.

Methods

Participants

Twenty-four individuals participated in the experiment (12 males, mean age ± SD= 27.68 ± 5.11 years, age range= 20 - 41 years). All participants were right-handed and had normal or corrected-to-normal vision, and self-reported normal audition. Participants had no reported history of psychiatric or neurological problems. One subject was excluded from the analysis due to excessive head motion and very low behavioral performance in discriminating visual and auditory motion directions during fMRI acquisition suggesting no attention to the task. All participants were naive to the purpose of the experiment. The protocol was approved by the research ethics committee in University of Trento and the Center for Mind/Brain Sciences (CIMeC). A written consent was acquired from all participants. Participants were monetarily compensated for their participation.

Training

Prior to testing, participants underwent a two-parts training session. First, the participants were trained in MRI-like conditions for the auditory motion direction discrimination task to get familiarized with the procedure and to ensure the best sound perception inside the scanner. Participants were asked to lie down during the training session to get familiarized with the space shift of the motion sound when they are in the scanner. They were trained using in-ear-plugs under the headphones while loud fMRI acquisition noise was played from a speaker behind their head. The training for the auditory motion direction discrimination task in the decoding experiment lasted for a maximum of 30 minutes or until the participants performed two complete training runs without any mistakes. Each training run had 8 blocks with 4 auditory motion directions and 2 repetitions per direction. The percentage of correct responses and feedback was provided at the end of each run. Training for visual motion direction discrimination with 100% coherence in MRI-like conditions was not necessary due to the easiness of the task (all participants reach ceiling effect without training). After the auditory training in MRI-like conditions was over,

the participants performed a 1-run training session containing both visual and auditory blocks (2 modalities x 4 directions x 1 repetition) while sitting in front of the computer with MRI noise played in the background.

Experimental design

Stimuli

Visual Stimuli: Visual stimuli were projected on a screen (frame rate: 60 Hz; screen resolution: 1024 x 768 pixels; mean luminance: 109 cd/m^2) behind the scanner via an EMP 7900 Epson projector. Participants viewed the screen (distance from head= 134 cm) through a mirror mounted on the MRI head coil. Participants performed a task in each experiment by responding with a Lumina MR-compatible response button. Visual stimuli consisted of random dot kinematograms (RDK) within an invisible circular aperture of 8 visual degrees centered around a white fixation cross. Each visual event was composed of 300 white dots (diameter= 0.1°) on a black background. Motion dots had a speed of 4°/s and a limited dot lifetime of 200 ms. The use of the limited lifetime ensures that motion direction discrimination could be achieved by relying on the global motion perception rather than focusing on a single dot (Bex et al., 2003). Dots moved in one of four possible motion directions [upward, downward, rightward, and leftward] with 100% coherence level (Figure 2.4A). Each visual motion event lasted 1.2 s. In the visual static condition, each static event had RDKs of 300 dots that remained static. The location of the dots was randomized in each event.

Auditory Stimuli: To provide an externalized and ecological sensation of auditory motion and accurate motion localization in the MRI, we recorded the auditory stimuli using in-ear binaural microphones (Møller, 1992) in a semi-anechoic room for each subject individually prior to the scanning session (Zoom H4n digital wave recorder – 200 m, with microphones Master Series - Sound Professionals-TFB-2). Participants were positioned at the center of the sound setup with their head on a chin-rest, facing one vertical and one horizontal semi-circular sound bar of 31 speakers each. The sound bars had a radius of 1.1m and provided a fixed distance (1.1m) between each speaker and the participant's head (Figure 2.4B). The position of the horizontal bar was at the same level of the subject's ear level, and the position of the vertical bar was at the participant's mid-sagittal plane. Pink noise (duration 1.2 s, fade in/out of 50 ms each) was divided in 31 equal segments and was replayed sequentially in the 31 corresponding speakers, to create smooth sensation of motion (no gap or overlap between the different segments). The sound's level was constant at 65 dB from the subject's head position. Four translational motion directions were recorded [upward, downward, rightward, and leftward]. Motion speed was 2 m/s and covered 120° of the subject's peripheral space. For the target detection task, similar motion stimuli with faster speed (4 m/s) and shorter duration (0.6 s) were recorded. An additional

static condition was recorded at the central speaker, located at the intersection of the horizontal and vertical planes of the sound bars. Static events had a duration of 1.2 s for the normal event, and 0.6 s for the target event. The recordings from each participant were re-played inside the MRI scanner for the auditory motion localizer and the directional motion decoding experiment. By using such sound system and in-ear recording in each subject, the auditory stimuli are convolved with each individuals' own pinna and head related transfer function producing a vivid auditory perception of the external space.

Visual motion localizer

We implemented a traditional visual motion localizer to localize hMT+/V5 both at the group-level and in each subject individually (Huk et al., 2002). Visual motion and static conditions were generated using white random dot kinematograms (RDK) on a black background. Since the visual stimuli were presented at fixation, our localizer defines the whole hMT+/V5 complex including both MT and MST (Huk et al., 2002). We used dots moving in one of four possible translational motion directions [upward, downward, rightward, and leftward]. The visual motion localizer started with an initial 5 s of blank screen and ended with 13 s of blank screen. The run had 6 blocks of motion and static conditions. Blocks were separated by each other with an inter-block interval (IBI) of 8 s. Each block (~15.6 s) had 12 stimuli of 1.2 s each, and an inter-stimulus interval (ISI) of 0.1 s. Each motion block had 3 repetitions of the 4 motion directions. The order in which the motion directions were presented was randomized in each block and balanced across the different motion blocks. In the static condition, the location of the dots was randomized for each event (inducing 12 changes within one block). The fixation cross was presented during the whole duration of the visual localizer. To minimize eye movements and saccadic shifts (Corbetta et al., 1998; Petit & Haxby, 1999b), the participants were asked to detect a brief change (150 ms) in the fixation cross color. The number of targets (range: 0-2 in each block) was randomized and balanced across conditions. The participants performed the task while the fMRI data were acquired with an accuracy (mean ± SD) of 98.62% ± 2.36%.

Auditory motion localizer

A localizer was implemented to define regions responding preferentially to auditory motion sounds. Previous studies demonstrated that regions within the middle temporal cortex and PT are selectively recruited during auditory motion processing compared with static sounds (Alink et al., 2012; Griffiths & Green, 1999; Poirier et al., 2005; Saenz et al., 2008; von Saldern & Noppeney, 2013; Warren et al., 2002). We used an experimental design matching the one implemented for the visual motion localizer. The participants were blindfolded during the auditory motion localizer. The run started with an initial 5 s of silence and ended with 11 s of silence. The localizer run had 13 blocks of auditory motion and 13 blocks of auditory static conditions. Auditory blocks were

separated by an interval of 6 s. Each block had 12 events of 1.2 s, and an ISI of 0.1 s. In the motion blocks, auditory motion stimuli were presented in one of four directions [upward, downward, rightward, leftward] (Figure S2.2). Each motion block had 3 repetitions of each motion directions. The presentation order of the different auditory motion directions within each block was randomized and balanced across blocks. The static blocks had 12 stimuli of static events separated by the 0.1 s inter-trial interval. Participants were asked to detect target events that were faster in speed and shorter in duration (0.6 s; (Dormal et al., 2016). The number of targets ranged between 1 and 3 targets in each block and was balanced across conditions. The duration of each block varied depending on the number of targets present (range 14.4 - 15.6 s). Auditory stimuli were delivered through a SereneSound MR-compatible in-ear headphones inside the scanner. The participants performed the task while the fMRI data were acquired with an accuracy (mean ± SD) of 86.96% ± 14.71%.

Directional motion decoding experiment

The directional motion decoding experiment was composed of 12 runs, each run comprising 8 motion blocks (4 directions x 2 modalities). Each motion block had either visual or auditory stimuli moving in one of four possible directions [upward, downward, rightward, or leftward]. Each run started with an initial 5 s of blank screen and ended with 11 s of blank black screen. Each block had 10 events of a 1.2 s, all moving in the same direction. Events were separated by a 100 ms inter-trial interval resulting in a block duration of 13 s. To ensure fixation and to minimize eye movements during the motion blocks, the participants were asked to press a button whenever the fixation cross changed color (duration= 150ms). Performing a visual detection task during motion processing also decreases the possibility of visual imagery (Johnson, 1982; Schorr et al., 1978). Following each block, there was a response collection period of 5 s where the participants heard a voice saying “up”, “down”, “right”, and “left” in a pseudo-randomized order. The participants were instructed to press a button with their index finger when they heard the cue that matched the block’s motion direction in vision or in audition. The number and the order of the correct button presses were counterbalanced across the different conditions. The task was identical during the visual and the auditory motion blocks in the directional motion decoding experiment. After the response collection, there was a silent inter-block interval of 6 seconds. The order of the blocks was randomized for the motion direction and the presented modality in each run (Figure 2.4C).

MRI acquisition

Structural and functional data were acquired at the Center for Mind/Brain Sciences (CIMeC - University of Trento, Italy) using a Bruker MedSpec BioSpin 4-Tesla MR scanner with a standard eight-channel head coil. A whole-brain structural scan was acquired with a high-resolution T1-weighted MPRAGE sequence (176 sagittal slices, repetition time

(TR)= 2700 ms, echo time= 4.18 ms, voxel size= 1 x 1 x 1 mm, flip angle= 7°, field of view= 256 x 224 mm).

Functional data were acquired with a T2* weighted gradient echo-planar imaging sequence (EPI). A total of 39 slices were acquired in an ascending interleaved order. Acquisition parameters included a TR of 2500 ms, echo time of 26 ms, flip angle= 73°, field of view= 192 x 117 mm, gap= 0.3 mm, and voxel size of 3 x 3 x 3 mm. The number of volumes acquired in the visual motion localizer and the auditory motion localizer were 126 and 235 volumes, respectively. For the directional motion decoding experiment, 1068 functional volumes were acquired (89 volumes x 12 runs). The first four initial scans of each run were discarded to allow for equilibrium magnetization. To apply distortion correction to the acquired functional images, point spread function (PSF) runs were acquired (Zaitsev et al., 2004) before every three consecutive runs. Participants entered the scanner blindfolded for the MPRAGE and the auditory motion localizer. The blindfold was removed afterwards for the visual motion localizer and the directional motion decoding experiment.

fMRI preprocessing

fMRI data were preprocessed in statistical parametric mapping (SPM8 – Wellcome Department of Imaging Neuroscience, University College London, UK) implemented in Matlab R2012b (Mathworks, Inc.). Preprocessing steps included slice time correction, EPI alignment to the mean functional image with a 2nd degree B-spline interpolation, coregistration of the functional volumes to the structural image and normalization to the Montreal Neurological Institute (MNI) template using a resampling of the structural and functional data to an isotropic 2 mm resolution.

Eye tracker experiment

To investigate whether different auditory motion directions elicited systemic eye movement patterns, we tested 7 participants in an eye tracking experiment outside the fMRI scanner. We used an Eyelink 1000 eye tracker (SR Research, Mississauga, Canada) to record the gaze location. The eye tracker had a sampling rate of 1000 Hz, and gaze tracking range of 32° angle horizontally and 25° angle vertically. The eye tracker was calibrated using a built-in 9-point protocol. The participants performed 8 runs of the same experiment that was done inside the scanner for the auditory modality and performed the same task. We tested in each participant if the eye position was different when perceiving different auditory motion directions. First, we performed a within-subject per-timepoint analysis where we compared the gaze location in the horizontal and vertical plane at each timepoint (1 millisecond resolution) of the auditory motion blocks. Since the analysis was done within-subject, the variance of the gaze location for each motion direction was estimated

from the different runs. Additionally, we performed a within-subject analysis where we averaged the gaze position across time in each run for the horizontal and the vertical plane for each motion direction (See Figure S2.4A and S2.4B for the results).

Behavioral Analysis

The behavioral accuracy for discriminating the different motion directions in the directional motion decoding experiment was assessed using a 2 (modalities) x 4 (directions) repeated-measures ANOVA. A Greenhouse–Geisser correction was applied to the significance levels and degrees of freedom whenever the assumption of sphericity was violated. Further pairwise comparisons were performed and corrected for multiple comparisons using Family-wise error (FWE) correction. See Supplementary figure S1 for the behavioral data.

Univariate analysis

Functional data were spatially smoothed with a 6-mm full-width half-maximum (FWHM) smoothing kernel for the univariate analysis. For the visual motion localizer, a general linear model (GLM) was fitted for every voxel with the visual motion and the visual static conditions as regressors of interest. Each regressor was modeled with a boxcar function and convolved with the canonical hemodynamic response function (HRF). The 6 head motion parameters (3 translation and 3 rotation parameters) were included in the model as regressors of no interest. A high-pass filter of 128 s was used to remove low frequency signal drifts. The contrast [Motion > Static] was computed for every subject individually (Huk et al., 2002; Tootell, Reppas, Kwong, et al., 1995). A standard group-level analysis was performed. The individual contrasts were further smoothed with a 6-mm FWHM kernel and entered into a random effects model for the second-level analysis. A one-sample t-test was performed, and group-level statistical inferences were made at a voxel-level threshold of $p<0.05$, FWE-corrected. The group-level analysis revealed significant activations in V1, the inferior occipital gyrus, and the middle temporal gyrus (hMT+/V5) bilaterally [MNI peak coordinates: -42 -66 2 and 46 -62 6] (Figure 2.1A, table S1).

To define subject-specific ROIs that will be used for the MVPA on a separate dataset (directional motion decoding experiment), a lenient threshold of $p<0.01$ uncorrected was used to locate hMT+/V5 bilaterally. The individually-defined hMT+/V5 was identified in each subject as the area that responded significantly to motion more than static in the occipito-temporal cortex, and was constrained by the anatomical location of hMT+/V5 and an Euclidean distance not more than 12 mm away from the group-level hMT+/V5 peak coordinate. The peak coordinate of hMT+/V5 in each subject was used to create a 7-mm radius sphere to be used as individually-defined ROIs in the multivariate analysis. Out of

the 23 participants, the left hMT+/V5 was identified in 21 participants, and the right hMT+/V5 was identified in 22 participants (Figure 2.1B and 2.1C, see table S2 for hMT+/V5 MNI coordinates in each subject). For each ROI, the participants whose individually-defined regions couldn't be identified were not included in any analysis relying on individually-defined ROIs.

For the auditory motion localizer, the same procedure was applied to defined regions that show enhanced recruitment during processing auditory motion compared with auditory static stimuli. Previous studies demonstrated that the PT and regions within the middle temporal cortex are recruited during auditory motion processing (Krumbholz et al., 2005; Poirier et al., 2005; Saenz et al., 2008; Warren et al., 2002). PT and MTa were defined both at the individual-level as individually-defined ROIs for the MVPA, and at the group-level using the same procedure previously described for the visual motion localizer experiment. At the group-level, we observed an enhanced recruitment of the planum temporale (PT) (MNI peak coordinates: [-46 -30 8] and [62 -34 8]), the superior temporal gyri and the middle temporal gyrus (hereafter MTa, MNI coordinates: [-46 -64 6] and [48 -54 8]) bilaterally (Figure 2.1A, table S1). In addition to the group-level results, the peak coordinate for PT and MTa were individually-defined from the contrast [auditory motion > auditory static] which was constrained by anatomical location, and less than 12 mm away from the group-level PT and MTa peak coordinates. We were able to define bilateral MTa and PT in 22 out of the 23 participants (Figure 2.1C, table S2).

By overlaying the group-level maps from the visual and auditory motion localizer, we observed an overlap between the regions processing visual and auditory motion. However, regions preferential to auditory motion were more anterior and dorsal than the visually-defined hMT+/V5 (Figure 2.1A).

Beta parameter estimates

We used the unsmoothed data from the visual and the auditory motion localizer for the extraction of the beta parameter estimates. The use of the unsmoothed data prevents spill-over effects that may arise due to the close proximity between the visually-defined hMT+/V5 and the auditory-defined MTa. Beta extraction was performed on both individually-defined and group-level ROIs (Dormal et al., 2016; Jiang et al., 2014, 2015). For every ROI in each subject, we created a sphere of 3-mm radius around the subject-defined coordinates (and the group-level coordinates) and extracted the mean beta parameter estimates. To test if visually-defined hMT+/V5 showed enhanced recruitment during auditory motion processing, we extracted the beta parameter estimates from the individually-defined and the group-level hMT+/V5 for the auditory motion and static conditions in the auditory motion localizer. We implemented a paired-sample t-test to compare the beta parameter estimates of the auditory motion and auditory static conditions

in hMT+/V5 bilaterally. To test if auditory-defined ROIs (MTa and PT) showed enhanced recruitment during visual motion processing, the beta parameter estimates from the individually-defined and group-level MTa and PT were extracted for the visual motion and visual static conditions in the visual motion localizer. For each ROI in each hemisphere, a paired-sample t-test was implemented to compare the beta parameter estimates from the visual motion and the visual static condition. Results were corrected for multiple comparisons using Bonferroni correction. For illustration purposes only, the beta estimates for visual motion and visual static conditions were extracted from the individually and group-level defined hMT+/V5 in the visual motion localizer. Similarly, the beta estimates for the auditory motion and static conditions were extracted from the individually and group-level defined MTa and PT in the auditory motion localizer. These beta estimates were not analyzed statistically since there would be clear circularity between the ROI definition and beta extraction.

Functional connectivity analysis (PPI)

Psychophysiological Interaction (PPI) analysis (Friston et al., 1997; Gitelman et al., 2003) identifies voxels in which the activity is more related to the activity in a seed region of interest (seed ROI) in a given psychological context. In the present study, PPI analyses were performed in order to identify brain regions that were more functionally coupled with MTa or hMT+/V5 while processing moving vs. static auditory or visual information. The locations of the seed regions were defined from the group-level univariate analysis from the visual and auditory motion localizers. In each subject, the time series (first eigenvariate) from each seed region was extracted from a sphere (radius=8 mm) around the local peak: left hMT+/V5 [-42 -66 2], right hMT+/V5 [46 -62 6], left MTa [-46 -64 6], and right MTa [48 -54 8]. A first-level GLM analysis was performed in each subject where the model included the following regressors: [1] psychological regressor [motion>static], [2] the extracted activity from the seed region (physiological regressor), [3] and the interaction term (PPI) between the previous two regressors. The PPI term was estimated by first deconvolving the BOLD activity to estimate the neuronal response in the ROIs (Gitelman et al., 2003), then the interaction term was calculated as the element-wise product of the estimated neuronal activity and the psychological regressor. The interaction term was further convolved with the canonical HRF. The six motion parameters were included in the model as regressors of no interest. After estimating the PPI models for each subject, a random effects model was constructed and a one-sample t-test was performed. In the second level analysis, we tested for regions that showed enhanced (or decreased) coupling with each of the seed regions in the motion condition compared with the static condition in each of the visual and auditory motion localizers separately.

Multivariate pattern analysis (MVPA)

ROI definition for MVPA

Group-level ROIs: Group-level hMT+/V5 was defined by creating a 7mm sphere (179 voxels of 2 mm isotropic resolution- resampled voxels) around the peak coordinates from the contrast [visual motion > visual static] obtained from the group-level univariate analysis in the visual motion localizer. MTa and PT were defined from the peak coordinates from the contrast [auditory motion > auditory static] obtained from the group-level univariate analysis in the auditory motion localizer. The group-level ROIs were used only in the motion versus static decoding in experiment 1. Group-level ROIs were not used in the motion direction decoding in experiment 2.

Individually-defined ROIs: hMT+/V5 was defined in each subject by creating a 7mm sphere (179 voxels of 2 mm isotropic resolution- resampled voxels) around the peak coordinates from the first-level (individual) contrast [visual motion > visual static] obtained from the univariate analysis of the visual motion localizer. Similarly, MTa and PT was defined in each subject by creating a 7mm sphere around the peak coordinates from the first-level contrast [auditory motion > auditory static] obtained from the univariate analysis in the auditory motion localizer.

Experiment 1 (visual and auditory motion localizer)

Motion versus static decoding

For the visual and the auditory motion localizer separately, the preprocessing steps were similar to the ones implemented in the univariate analysis without applying smoothing to the functional data. A general linear model (GLM) analysis was performed to estimate the BOLD signal for every voxel. The GLM included a separate regressor for each motion and static block. The six head motion parameters (translation and rotation) were included in the model as regressors of no interest. A t-map was estimated for each motion and static block using the contrast [motion > baseline] and [static > baseline] respectively. The t-maps were used for further MVPA.

Multivariate analysis was performed using CoSMoMVPA (http://www.cosmomvpa.org; (Oosterhof et al., 2016) implemented in Matlab. Classification was performed using support vector machine (SVM) classifier as implemented in LIBSVM (Chang & Lin, 2011). To test if the representation of the motion condition was different from the representation of the static condition, a [motion vs static] decoding analysis was implemented in the group-level and the individually-defined ROIs (hMT+/V5, MTa, and PT bilaterally). Before running the decoding analysis in each ROI,

the patterns of each block and each condition (motion and static) was demeaned individually to minimize the univariate activation level differences and to mathematically equate the mean activity of each condition and each block. For each localizer, a linear SVM classifier (C parameter= 1) was trained and tested to discriminate the motion and the static blocks in each subject individually. A leave-one block out cross-validation scheme was implemented. In each cross-validation fold, the training data (5 blocks per condition for the visual motion localizer, 12 blocks per condition for the auditory localizer) were normalized (z-scored) across conditions and the classifier was trained to discriminate the motion and static conditions. An ANOVA-based feature selection was implemented on the training data in each cross-validation fold to identify the most informative 150 voxels. The normalization parameters from the training data were applied to the test data, and the performance of the SVM classifier was evaluated on the test data (1 block). The previous step was repeated n times (n=6 for the visual motion localizer, n=13 for the auditory motion localizer) where in each fold the classifier was tested on a different block. A single classification accuracy was obtained by averaging the classification accuracies for all the cross-validation folds. If the classifier could successfully discriminate the two conditions above chance (50%), this would indicate the presence of motion information in the tested modality that the classifier was able to learn during the training. No statistical analysis or inferences were made for the [visual motion versus visual static] decoding in hMT+/V5 to avoid circularity as this region was defined from the univariate analysis by contrasting visual motion vs visual static. Similarly, no statistical analysis was performed for the [auditory motion vs auditory static] decoding in MTa and PT for the same reason.

Statistical significance of the classification results was assessed using a non-parametric technique by combining permutations and bootstrapping (Stelzer et al., 2013). For each subject, the labels of the different conditions (motion and static) were permuted, and the same decoding analysis was performed. The previous step was repeated 100 times for each subject. A bootstrap procedure was applied in order to obtain a group-level null distribution that was representative of the whole group. From each subject's null distribution, one value was randomly chosen (with replacement) and averaged across all participants. This step was repeated 100,000 times resulting in a group-level null distribution of 100,000 values. The statistical significance of the MVPA results was estimated by comparing the observed result to the group-level null distribution. This was done by calculating the proportion of observations in the null distribution that had a classification accuracy higher than the one obtained in the real test. To account for the multiple comparisons, all p-values were corrected using false discovery rate (FDR) correction (Benjamini & Hochberg, 1995).

Experiment 2 (Directional motion decoding experiment)

For the directional motion decoding experiment, the preprocessing steps were similar to the ones implemented in the univariate analysis except no smoothing was applied to the functional data. A general linear model (GLM) analysis was performed to estimate the BOLD signal for every voxel. The GLM included a separate regressor for each direction in each modality in each run. Each regressor was convolved with the canonical HRF. The six head motion parameters (translation and rotation) for each run were included in the model as regressors of no interest. An additional regressor of no interest was included in each run to remove the effects related to the named directions after each block and the participants' responses. For each run, t-maps were estimated for each motion direction in each modality using the contrast [motion direction > baseline]. The t-maps were used for further MVPA.

Within-modality decoding

The MVPA was performed using SVM classifier as implemented in LIBSVM (Chang & Lin, 2011). To test for the presence of motion direction information, a within-modality decoding was implemented in each of the individually-defined ROIs (hMT+/V5, MTa, and PT bilaterally). For each modality, a linear SVM classifier (C parameter= 1) was trained and tested to discriminate the 4 motion directions in each subject individually. A leave-one run out cross-validation scheme was implemented. In each cross-validation fold, the training data (11 runs) were normalized (z-scored) across conditions and the classifier was trained to discriminate the patterns of the 4 motion directions. We implemented an ANOVA-based feature selection on the training data in each cross-validation fold to use the most informative 150 voxels in each subject and each ROI. The normalization parameters from the training data were applied to the test data, and the performance of the SVM classifier was evaluated on the test data (1 run). The previous step was repeated 12 times (N-fold cross-validation) where in each fold the classifier was tested on a different run. A single classification accuracy was obtained by averaging the classification accuracies for all the cross-validation folds. If the classifier could successfully discriminate the different motion directions above chance (25%), this would indicate the presence of motion direction information in the tested modality that the classifier was able to learn during the training. Statistical significance was assessed non-parametrically as previously described (Stelzer et al., 2013) in the motion versus static decoding section. To account for the multiple comparisons, all p-values were corrected using false discovery rate (FDR) correction (Benjamini & Hochberg, 1995).

In addition to the 4-way multi-class decoding, we performed a within-axis, and axis of motion direction decoding. In the within-axis binary decoding, we tried to discriminate motion patterns from the opposite directions within the same axis (upward vs

downward, and rightward vs leftward motion). In the axis of motion decoding, we tried to discriminate the horizontal and vertical axes of motion by treating rightward and leftward motion as horizontal motion, and upward and downward motion as vertical motion (chance level= 50%). The analysis procedure was identical to one described in the multi-class decoding.

Cross-modal decoding

To test whether there was shared motion direction information between the visual and auditory modalities, cross-modal classification was performed in regions that could successfully decode motion directions in both the visual and auditory modalities. Before the cross-modal decoding analysis in each ROI, the patterns of each direction in each modality were demeaned individually to mathematically equate the mean activity of the visual and the auditory modalities. The SVM classifier was trained on one modality (e.g. vision) and tested on the other modality (e.g. audition), and vice versa. This resulted in a cross-validation scheme of 24 folds. In every cross-validation fold, the classifier was trained on N-1 runs (11 runs) from one modality and tested on 1 run from the other modality. An ANOVA-based feature selection was implemented on the training data in each cross-validation fold to use the most informative 150 voxels. The cross-modal decoding accuracy was obtained by averaging the classifications of all the cross-validation folds. Successful classification above the chance level (25%) would suggest the presence of shared motion direction information across the different modalities. Statistical significance was assessed non-parametrically as previously described (Stelzer et al., 2013).

In addition to the cross-modal decoding in the ROIs, we implemented a whole-brain searchlight approach (Kriegeskorte et al., 2006) to test the regional specificity at the whole-brain level of the shared motion direction information across different modalities. A sphere of 3-voxels radius moved across the whole brain, where in each step, each voxel became the center of the searchlight sphere. Within each sphere, cross-modal decoding was implemented in the same manner described in the ROI analysis. The searchlight analysis results in a whole brain cross-modal decoding accuracy map for each subject. The individual accuracy maps were smoothed with 6 mm FWHM smoothing kernel and entered in a second-level model. A one-sample t-test was performed to test if the cross-modal decoding accuracy was above the chance level (25%). Statistical maps were corrected using a SVC of 10-mm radius at the location of hMT+/V5 that was defined independently from the visual motion localizer.

Previous studies suggested that MT in the macaques and hMT+/V5 in humans have an axis-of-motion organization (Albright, 1984; Albright et al., 1984a; Zimmermann et al., 2011). To test if the representation of auditory motion shows a similar axis-of-motion organization to the one in vision, we performed the same ROI decoding and searchlight

analysis to test if we can classify the horizontal and the vertical axes (chance level is 50%) in each of the visual and the auditory modality. We aggregated the rightward and leftward motion conditions to the horizontal axis, and the upward and downward motion to the vertical axis. In the ROI cross-modal decoding analysis, first we identified regions where we could classify the different axes of motion in both the visual and auditory modality. Then an SVM classifier was trained to discriminate the patterns from the horizontal and the vertical axes from one modality (vision) and tested on the other modality (audition), and vice versa. Additionally, the same analysis was done across the whole brain using a whole-brain searchlight approach (Kriegeskorte et al., 2006).

Modality decoding

To test whether the representation of motion directions across the visual and auditory modalities could be differentiated based on their activity patterns in each of the motion responsive areas, each motion direction pattern in each modality was demeaned separately to equate the mean activity of the visual and auditory modalities. For each direction separately, an SVM classifier was trained and tested to discriminate the two modalities (chance level=50%), and a decoding accuracy was obtained. The overall modality decoding accuracy was then obtained by averaging the results from the four directions. The decoding procedure and the non-parametric significance testing (Stelzer et al., 2013) were identical to the previously described ROI decoding analysis.

Representational similarity analysis (RSA)

Using representational similarity analysis (RSA) (Kriegeskorte, Mur, & Bandettini, 2008; Kriegeskorte, Mur, Ruff, et al., 2008), we further investigated the differences in the representational geometry of the four motion directions within and across modalities. The advantage of using RSA is that it captures the (dis)similarity structure between different categories (e.g. motion directions in this experiment) and different modalities (Kriegeskorte, Mur, & Bandettini, 2008). While cross-modal decoding analysis highlights the presence of common/shared information across modalities, it doesn't inform us about how (dis)similar the patterns are across directions and across modalities. Additionally, by using RSA we can construct different theoretical computational models and test which model best explains our observed data. By constructing a neural dissimilarity matrix from our fMRI data, we obtained an estimate of the (dis)similarity between the elicited patterns from the different motion directions and the different modalities in the right hMT+/V5. Pearson's correlation was used as a measure of dissimilarity (1- Pearson's correlation) resulting in an 8 x 8 dissimilarity matrix in each subject. To investigate the multi-modal or the modality-abstracted nature of hMT/V5, we created multiple theoretical models in the form of DSMs ranging from a pure modality-

invariant model to a pure multi-modal model with intermediate gradients in between them, and two unimodal (visual and auditory) models (Zabicki et al., 2017).

Theoretical models: In the modality-invariant model, the dissimilarity between the same motion direction across the different modalities were set to zero (hence, motion direction processing is abstracted from the input modality), and the dissimilarity between different motion directions was set to 1 regardless of the modality. Diagonal values were set to 0. On the other hand, the multi-modal model suggests that while motion directions within one modality are different from each other, they are more dissimilar than motion directions from other modalities. In the multi-modal model, the dissimilarity between the different motion directions within the same modality was set to 0.5, while the dissimilarity to motion directions from the different modality was set to 1. Diagonal values were set to 0.

In the intermediate models, we created a gradient from the modality-invariant to the multi-modal model. The dissimilarity between directions within the same modality was set to 0.5. The dissimilarity between the different directions across modalities was set to 1. While for the dissimilarity between the same directions across modalities were set to a gradient of values ranging from 0.1 to 0.9 with steps of 0.2.

In the unimodal visual and auditory models, the dissimilarity between the different motion directions within the dominant unimodal modality was set to 0.5. The dissimilarity between the different motion directions within the other non-dominant modality was set to 1 as this model assumes that there is no motion direction information in the non-dominant modality. The dissimilarity between the different directions across modalities was set to 1.

We correlated the neural DSM from the right hMT+/V5 with each of the theoretical models (Figure 2.5B). If hMT+/V5 is a multi-modal region, we would expect to see a low correlation with the modality-invariant model and a gradual increase in correlation as we progress in the direction of the multi-modal model. Oppositely, if hMT+/V5 is a supramodal region, we would expect to see a low correlation with the multi-modal model, and a gradual increase in correlation as we progress towards the modality-invariant model. If hMT+/V5 is a unimodal region, we would expect a higher correlation with one of the unimodal models than with the other models. We performed a 2-sided Wilcoxon signed rank test to investigate whether there was a difference between the correlation values of each two consecutive theoretical models and the neural DSM. Results were corrected for multiple comparisons using FWE-correction.

Split-half correlation analysis

In order to have a more in-depth understanding of the similarity between the motion directions' patterns within-modalities and across-modalities, we implemented a

split-half correlation analysis (Haxby et al., 2001) in the individually-defined ROIs. We first demeaned every pattern for every direction and for every modality separately to equate the mean activity of the visual and the auditory modality. For each condition in each modality, the t-maps of the odd and even runs were averaged separately resulting in 1 t-map per condition for the odd runs, and 1 t-map per condition for the even runs. Using Pearson's correlation as a measure of similarity, we estimated the within-modality split-half correlation of the pattern of each motion direction from the odd runs with the pattern of the same motion direction from the even runs (within the same modality). The correlations of the four directions within the same modality were averaged, resulting in one value which was considered to be the estimate of the within-modality split-half correlation. This was performed for both the visual and the auditory modalities separately. To estimate the cross-modal split-half correlation, we correlated the pattern of each motion direction from the odd runs in one modality (e.g. visual leftward motion pattern) with the pattern of the same motion direction from the even runs in the other modality (e.g. auditory leftward motion pattern), and the other way around. The correlation results from the four motion directions, and from both conditions ([odd: Vision - even: Audition] and [odd: Audition - even: Vision]) were averaged resulting in one value for each participant which was considered to be the estimate for the cross-modal split-half correlation (Figure 2.5C). The correlation values were Fisher-transformed and tested against zero using a one-sample t-test. Results were corrected for multiple comparisons using FWE-correction. To test whether there are differences in the correlation values across the three different conditions (within-modality visual, within-modality auditory, and crossmodal correlation) in each ROI, we implemented a repeated-measures ANOVA in each ROI separately. A Greenhouse–Geisser correction was applied to the significance levels and degrees of freedom whenever the assumption of sphericity was violated. Further pairwise comparisons were performed and corrected for multiple comparisons using FWE-correction.

Differential pattern correlation

To investigate how cross-modal decoding was successful in the right hMT+/V5 despite the negative correlation across modalities, we tested whether the relative relation between the different motion directions was similar across modalities. For instance, the relation between the pattern of the upward motion direction and that of the other three motion directions in vision was similar to that in audition. First, we demeaned the motion direction patterns across the different directions in each modality separately. Based on the obtained differential motion direction patterns from the mean, we correlated the differential pattern of each motion direction across the two modalities using Pearson's correlation (Figure 2.5E). We obtained four correlation values per subject in the left and the right hMT+/V5 which correspond to the four motion directions. The average of the four correlation values was used as an estimate of the differential pattern correlation in each ROI. Correlation values were Fisher-transformed and tested against zero using a one-

sample t-test to determine if there is a significant correlation of the differences between motion directions across modalities (Figure 2.5E). Results were corrected for multiple comparisons using FWE-correction.

Results

Experiment 1: Motion Localizers

We used separate visual and auditory motion localizers to functionally and individually define regions that are preferentially recruited during visual and auditory motion processing, and their connectivity with other brain regions. Lastly, we used MVPA to decode the motion and static conditions in each localizer.

Visual and auditory motion localizers

Description of the procedures used to define auditory (planum temporale (PT), and MTa) and visual (hMT+/V5) motion-selective regions individually is detailed in the methods section.

Beta parameter estimates in auditory and visual motion selective regions

Beta parameter estimates were extracted from 6 regions of interest (ROIs) (bilateral hMT+/V5, MTa, and PT) for the motion and static conditions in the visual and the auditory motion localizers. Due to the variability in the anatomical locations of the peak coordinates of hMT+/V5 (Dumoulin et al., 2000; Huk et al., 2002) and MTa across participants, and the possible illusionary overlap between the visual and auditory responsive regions arising from smoothing the functional data or using group-level averaging (Jiang et al., 2015), we extracted the beta parameter estimates from the individually-defined ROIs using unsmoothed data. The beta parameter extraction was performed in both group-level and individually-defined ROIs (Figure 2.1E). The beta parameter estimates from the visually-defined ROIs in the visual localizer, and the auditory-defined ROIs in the auditory localizer are for illustration purposes only. No statistical analyses were performed to avoid circularity as these ROIs were defined from contrasting the motion condition versus the static condition in their respective localizers.

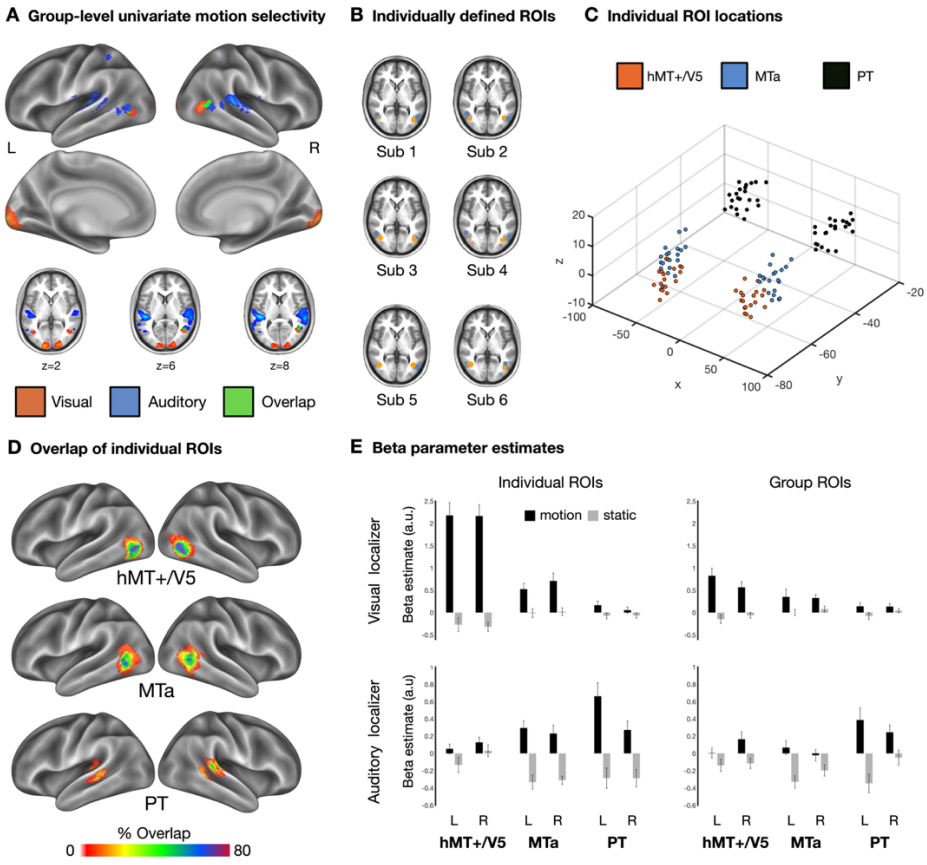


Figure 2.1 Univariate results from the visual and the auditory motion localizers.
[A] The univariate results of the contrast [visual motion > visual static] from the visual motion localizer (in warm colors) to functionally define hMT+/V5, and the contrast [auditory motion > auditory static] in the auditory motion localizer (in cold colors) to functionally define planum temporale (PT) and the auditory motion selective regions in the middle temporal cortex (MTa). The overlap between MTa and hMT+/V5 is highlighted in green. Results are FWE-corrected and are displayed on an inflated brain [62]. [B] Examples of the individually-defined ROIs in hMT+/V5 and MTa from 6 participants. [C] A 3D representation of the MNI coordinates of the individually-defined hMT+/V5 (orange), MTa (blue), and PT (black). [D] The overlap of each individually-defined ROI across participants. [E] Beta parameter estimates extracted from the group-level and individually-defined hMT+/V5, MTa, and PT in the visual and the auditory motion localizer. No statistical analyses were performed for the beta estimates from hMT+/V5 in the visual motion localizer, nor from MTa and PT in the auditory motion localizer (for illustration purposes only). Error bars represent the standard error of the mean. See table S1 and S2 for more details.

In hMT+/V5, we observed a significant difference between the auditory motion condition and the auditory static condition in the group-level defined right hMT+/V5 (p=0.0071), but not in the group-level defined left hMT+/V5 (p=0.1536), nor in the

individually-defined left (p=0.1819) or right hMT+/V5 (p=1). For the auditory-defined regions (MTa and PT) during visual motion processing in the visual motion localizer, we found enhanced recruitment during the visual motion condition in the individually-defined left (p= 0.0148) and right MTa (p= 0.0052), and in the group-level right MTa (p= 0.0074). In both individually-defined and group-level PT, there was no significant difference between the visual motion condition and the visual static condition (p>0.05).

Functional connectivity analysis

We ran psychophysiological interactions (PPI) analyses (Gitelman et al., 2003) to investigate the connectivity profile of hMT+/V5 and MTa during processing auditory and visual motion. In the visual motion localizer, visually-defined hMT+/V5 showed enhanced task-based connectivity with the bilateral middle occipito-temporal areas, the lingual gyrus, and the primary visual areas. Auditory-defined left MTa showed increased connectivity with the cuneus, and the lingual gyrus during visual motion processing (Figure 2.2A). In contrast, for the auditory motion localizer, hMT+/V5 did not show any connectivity with the primary visual cortex during motion processing (when compared to static). Similarly, MTa did not show enhanced connectivity with earlier visual areas, however, it showed enhanced task-based connectivity with the superior temporal gyrus and PT (Figure 2.2B, table S3).

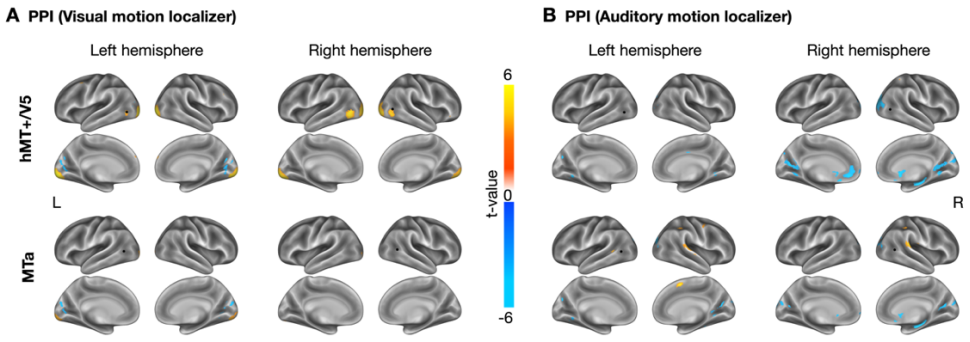


Figure 2.2 PPI analysis.
[A] PPI analysis in the visual motion localizer. Regions showing increased task-based functional connectivity with bilateral hMT+/V5 and MTa for the contrast (visual motion > visual static) in warm colors, and for the contrast (visual static > visual motion) in cold colors. [B] PPI analysis in the auditory motion localizer. Regions showing increased task-based functional connectivity with bilateral hMT+/V5 and MTa for the contrast (auditory motion > auditory static) in warm colors, and for the contrast (auditory static > auditory motion) in cold colors. PPI results are displayed at p<0.001, minimum cluster size of 20 voxels. See table S3 for more details. L: left hemisphere, R: right hemisphere. See table S3 for the PPI results.

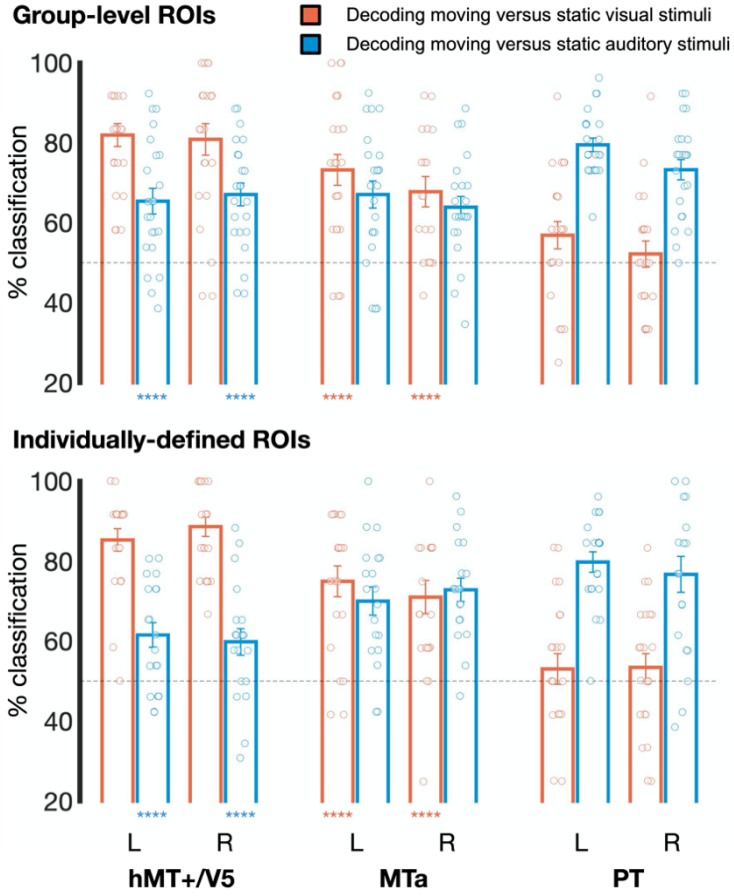


Figure 2.3 Motion versus static decoding.
*Decoding moving versus static stimuli from the visual and auditory motion localizers independently (chance level= 50%). Statistical analysis for decoding moving versus static sounds was implemented only in visually-defined ROIs to avoid any circularity. Similarly, statistical analysis for decoding moving versus static visual dots was implemented only in auditorily defined ROIs. Individual points represent individual subjects' data (****p<0.0001)*

Motion versus static decoding

The univariate analysis revealed a non-significant trend for preferential auditory motion processing, when compared to static, in individually-defined hMT+/V5. The lack of significant voxel-wise univariate activation does not constitute an evidence for the absence of auditory motion information in hMT+/V5. We relied on the higher sensitivity of MVPA to try to classify the motion and the static blocks in both the group-level and the individually-defined hMT+/V5, MTa, and PT in each motion localizer independently (See

methods section for analysis details). No statistical analysis was performed for the [visual motion vs visual static] decoding in hMT+/V5 to avoid circularity as this region was defined from the univariate analysis by contrasting visual motion vs visual static. Similarly, the [auditory motion vs auditory static] decoding was not tested in the auditorily defined ROIs (MTa and PT), and the statistical analysis was limited to hMT+/V5. The [auditory motion vs auditory static] decoding was significantly above chance (50%) in the group-level and in the individually-defined bilateral hMT+/V5 ($p<0.0001$). The [visual motion vs visual static] decoding was significant in the group-level and in the individually-defined bilateral MTa ($p<0.0001$), and not significant in PT (Figure 2.3).

Experiment 2: Directional motion decoding

The participants discriminated the direction of auditory and visual motion with high accuracy inside the scanner (see the supplementary methods S2.1 for the behavioral analysis).

Within-modality decoding

We tested whether the classification of the four motion directions in the individually-defined ROIs (hMT+/V5, MTa, and PT) was above chance level (25%; Figure 2.4D, table S4). Non-parametric significance testing (FDR-corrected) revealed that in vision, motion direction decoding was above chance in the left ($p=0.0041$) and the right hMT+/V5 ($p= 0.0048$), and in the left MTa ($p= 0.0401$). In the auditory modality, above chance classification was observed in right hMT+/V5 ($p=0.0086$), left MTa ($p=0.0002$), right MTa ($p=0.0004$), left PT ($p=0.00006$), and right PT ($p=0.00006$).

Interestingly, within-axis auditory decoding was less reliable than across axes auditory decoding in hMT+/V5 (Figure S2.1, 2.4D), which could be in line with the previously suggested large-scale axis-of-motion organization in hMT+/V5 (Zimmermann et al., 2011). Similarly, multi-dimensional scaling (MDS) (Abdi et al., 2005) showed that opposite directions within the same axis were clustered closer to each other when compared to motion directions in the different axis (Figure 2.4F).

Cross-modal decoding

To test if there was shared motion direction information across modalities in regions that contained both visual and auditory motion direction information, we performed a cross-modal decoding analysis where the classifier was trained on one modality and tested on the other modality (training in vision and testing in audition, and vice-versa; FDR-corrected). We found significant visual and auditory motion direction information in right hMT+/V5 and left MTa, therefore these two regions were considered candidates to

potentially contain shared representation of motion direction across modalities. Successful cross-modal decoding was observed in the right hMT+/V5 (p=0.0052) but not in left MTa (p=0.5432) (Figure 2.4E). In the binary within-modality axes decoding (vertical vs horizontal), visual and auditory motion information was found in hMT+/V5 bilaterally. When performing cross-modal decoding (Figure 2.4E), shared axis-of-motion direction information was again found in the right hMT+/V5 (p=0.0029) and not in the left hMT+/V5 (p= 0.0966).

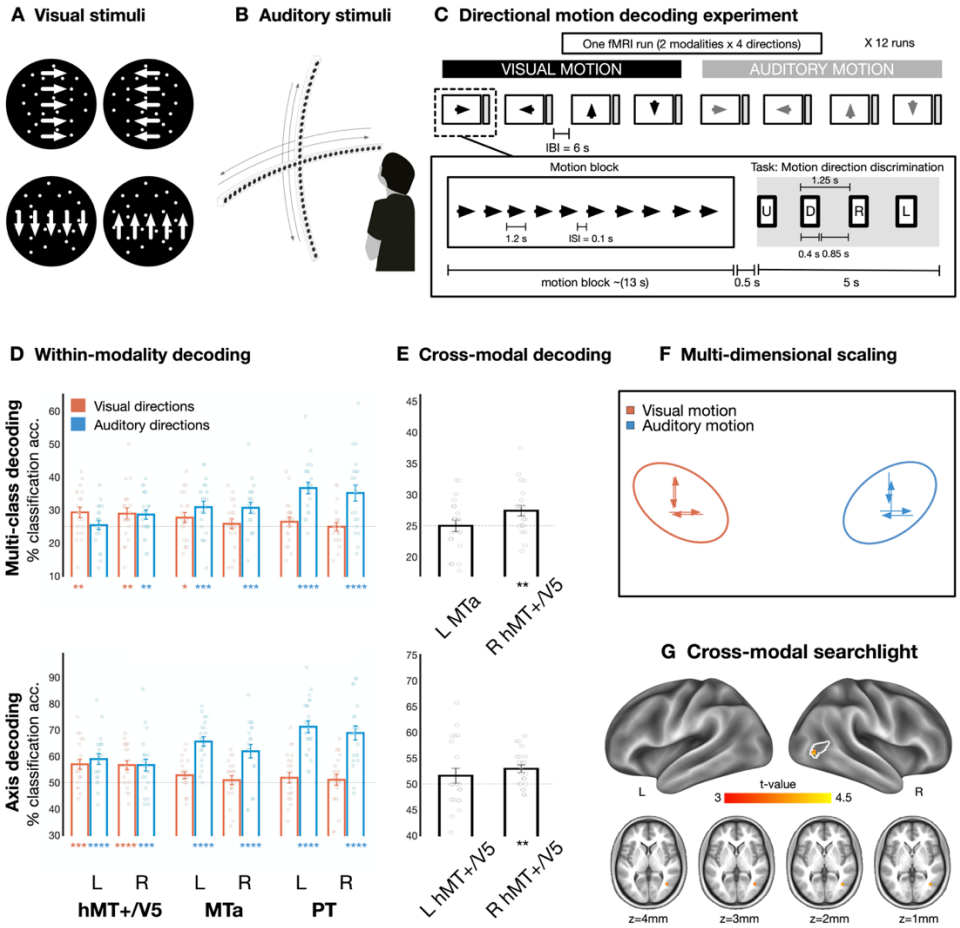


Figure 2.4 Directional motion decoding experiment.
[A] Exemplars from the visual stimuli using random dot kinematograms, and [B] the recorded auditory stimuli in 4 translational directions (upward, downward, rightward, and leftward motion). [C] Experimental design of the directional motion decoding experiment (1 run). Each run had 8 motion blocks (2 modalities x 4 directions). The participants performed a motion direction discrimination task following each block. The order of the blocks was randomized in each run. [D]

*Within modality multi-class classification of the 4 motion directions and the binary axis decoding (horizontal versus vertical) in the visual and auditory modality in individually-defined hMT+/V5, MTa, and PT. [E] Cross-modal decoding in regions that could successfully decode the motion directions (and axes) in both the auditory and the visual modality. Chance level (dotted line) is 25% for the multi-class direction decoding and 50% for the binary axis decoding. Error bars represent the standard error of the mean. Results are FDR-corrected (*p<0.05, **p<0.01, ***p<0.001, ****p<0.0001). Individual points reflect individual subjects' results. [F] Multi-dimensional scaling was used to visualize the distance between the patterns of the different motion directions in the visual and auditory modality using DISTATIS (Abdi et al., 2005). [G] Group-level searchlight analysis of the cross-modal axis of motion decoding. Only a region that overlapped with the right hMT+/V5 showed a successful cross-modal axis of motion decoding. L: left hemisphere, R: right hemisphere. See Figure S2.1 for the within-modality within-axis classification, Figure S2.2 for the control analysis for the cross-modal decoding, Figure S2.3 for the control analyses for eye movements. See table S4 for the within-modality decoding results.*

In addition to our ROI approach, we implemented a whole brain cross-modal searchlight analysis that revealed a single cluster in the vicinity of the right hMT+/V5 ($p=0.013$; corrected using a small volume correction (SVC)) where shared axis of motion information was present across modalities. This region overlapped with the posterior portion of the group-level visually-defined hMT+/V5 from the visual motion localizer (Figure 2.4G).

Modality decoding

Significant cross-modal decoding in right hMT+/V5 indicated the presence of shared motion direction representation across modalities. It, however, did not mean that the activity patterns were identical across the sensory modalities. We reasoned that if a region is purely abstracted from the input modality conveying the directional motion information, decoding the modality (visual or auditory) of the presented motion stimuli would be difficult. The modality decoding was highly significant in all ROIs ($p<0.0001$; see methods section for analysis procedure), suggesting that the neural patterns associated with each direction are highly dissimilar across the senses (Figure 2.5A)**.**

Representational similarity analysis

To further explore the differences in the representational format of auditory and visual motion directions in hMT+/V5, we tested the correlation between the neural dissimilarity matrix (DSM) of right hMT+/V5 in each subject with different theoretical models that included a pure modality-invariant model, a multimodal model, a series of intermediate gradients between them, a unimodal visual model, and a unimodal auditory model. The analysis revealed a negative correlation with the modality-invariant model (mean r ± SD= -0.3418 ± 0.0209) that increased gradually as the models progressed towards the multi-modal model. The model that correlated the most with our data was the multi-modal model (mean r ± SD= 0.9897 ± 0.0194), and this correlation was significantly

higher than all other models (Figure 2.5B, table S5). The gradual increase in correlation from the modality-invariant model to the multi-modal model added extra evidence that the representation of different motion directions in right hMT+/V5 was not abstracted from the input modality.

Pattern correlations

To better understand the relation of the pattern geometries for the different motion directions across the senses, we performed a split-half correlation (SHC) analysis (Haxby et al., 2001). We observed that the motion direction patterns were positively correlated in the odd and even runs in each individual modality (within-modality SHC) in each ROI (Figure 2.5C; Table S6). Yet, the cross-modal SHC showed a strong negative correlation in left ($p=1.877 \times 10^{-5}$) and right hMT+/V5 ($p=2.114 \times 10^{-6}$), no significant correlation in bilateral MTa ($p>0.05$), and a positive correlation in right PT ($p=8.945 \times 10^{-4}$).

To compare the correlation values across the three different conditions (within audition, within vision, and across modalities) in each ROI, a repeated-measure ANOVA was implemented. Results showed that the correlation values were significantly different ($p<0.001$) across the three conditions in each ROI. Post-hoc pairwise comparisons revealed that in hMT+/V5, the visual SHC was not different from the auditory SHC. The cross-modal SHC was significantly lower than both the visual and the auditory within-modality SHC in both hemispheres and all ROIs (table S6).

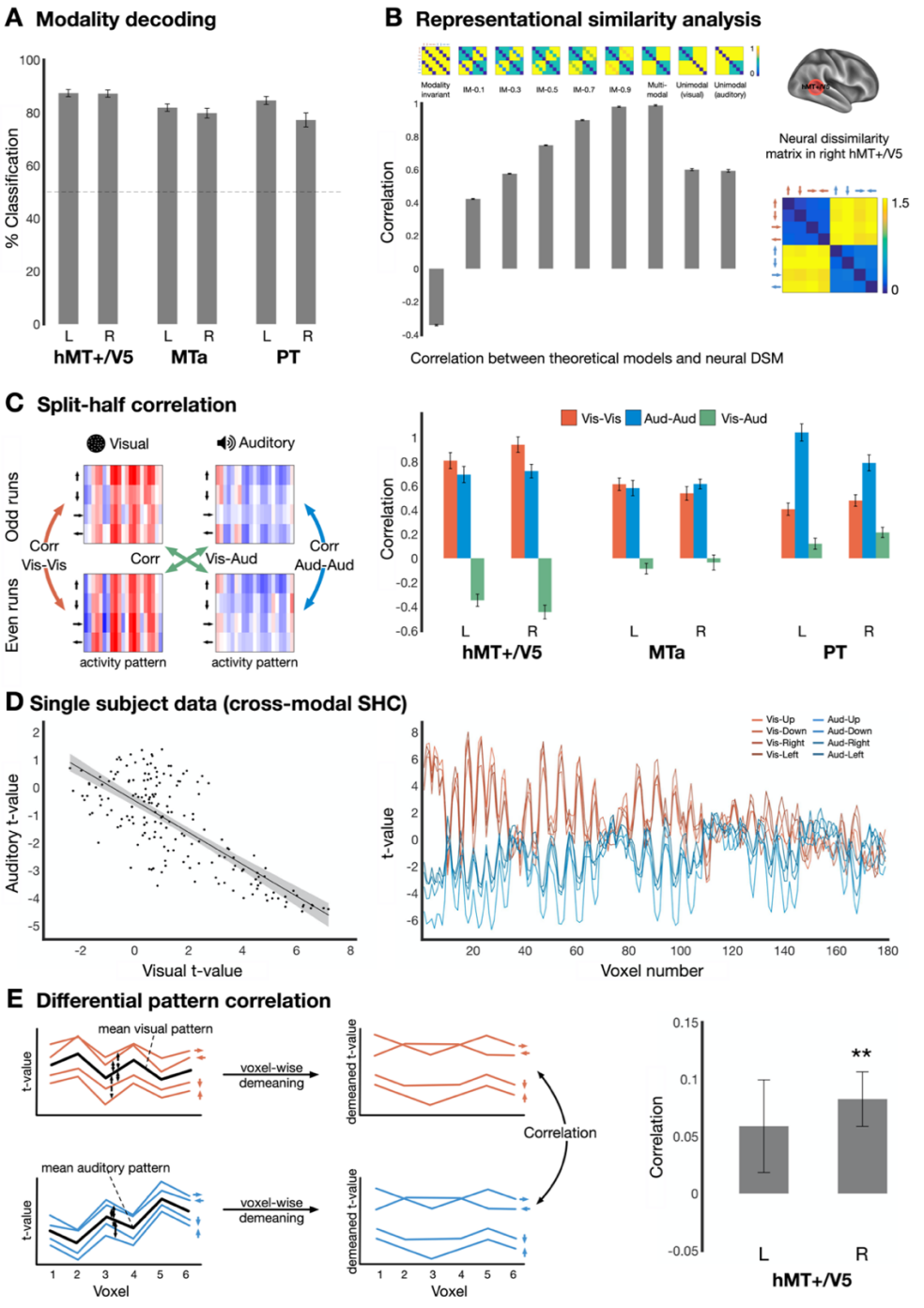


Figure 2.5 Multivariate analyses from the directional motion decoding experiment.

[A] Modality decoding results in hMT+/V5, MTa, and PT from the directional motion decoding experiment (chance level is 50%). [B] Representational similarity analysis in the right hMT+/V5: The theoretical models ranged from a modality-invariant model to a multi-modal model, the intermediate gradients between them, and the two unimodal visual and auditory models. The neural DSM from the right hMT+/V5 showed a gradient increase in correlation with the theoretical models as the models progressed towards the multi-modal model and was higher than the unimodal models. The right panel shows the average DSM in the right hMT+/V5 across participants. [C] Split-half correlation analysis (SHC) measured the correlation between the motion direction patterns in the odd and the even runs in the directional motion decoding experiment. The SHC analysis was performed within modality (visual modality in orange, and auditory modality in blue) and across-modalities (in green). The left-side panel is a graphical illustration of the SHC analysis. The right-side panel shows the results of the SHC in the individually-defined ROIs. [D] Single subject example: The visual motion patterns (averaged across directions) in the right hMT+/V5 of a representative subject shows a strong negative correlation with the auditory motion patterns. On the right panel, the plot shows the activity pattern of each motion direction in each modality in the right hMT+/V5 of the same subject. The single subject's raw data are for illustration purposes and are presented without demeaning. The Figure illustrates the high correlation between the different directions within each modality, the negative correlation between the visual and the auditory motion patterns, and the stronger activation of hMT+/V5 for the visual motion stimuli than for the auditory motion stimuli. [E] A graphical abstract illustrating the differential pattern correlation analysis. The analysis tested whether the relative differences between the different directions were similar across modalities. Note that the visual (in orange) and auditory motion patterns (in blue) are negatively correlated. The black line in each modality represents the mean pattern across the four directions. In each modality separately, the motion direction patterns were demeaned across the different directions. The differential patterns from each modality were then correlated with each other. The right panel shows the results of the analysis and that the relative differences between the four motion direction patterns were significantly correlated across modalities in the right hMT+/V5. Error bars represent the standard error of the mean. See table S5 and S6 for the results of the RSA and SHC analysis.

Differential pattern correlation

Despite the motion direction patterns being negatively correlated across the two modalities in hMT+/V5, cross-modal decoding was successful in the right hMT+/V5 (see cross-modal decoding section). While this might appear surprising, we reasoned that a successful cross-modal decoding would be possible if the relative relation between the patterns of the different motion directions in vision is similar to that in audition. In other words, if the representation of the different motion directions in vision is similar to that in audition (despite the global negative correlation between vision and audition) we would be able to cross-decode motion directions across modalities. We tested this hypothesis by calculating the differential pattern from the mean for each motion direction in each modality independently. The activity patterns of the different motion directions were demeaned across directions in each modality separately, resulting in four differential patterns for the four motion directions in each modality. We then tested whether there was a significant correlation between the differential patterns of the four-motion direction across the two modalities (Figure 2.5E). The differential direction patterns were positively correlated ($r=0.0827$, $p= 0.0047$, FWE-corrected) only in the right hMT+/V5. These results demonstrate that while the motion direction patterns are negatively correlated between

vision and audition in the right hMT+/V5 at a global scale (across all directions), the relative differences between the directions in each modality are however similar across the senses. These findings explain the successful cross-modal decoding in the right hMT+/V5 despite the global negative correlation between visual and auditory patterns.

Discussion

We demonstrate that a region that has long supported the idea of a "modular" visual system, hMT+/V5, is not impenetrable to information from the other senses and, in contrast, contain representation of auditory motion direction in a format that is partially aligned to the brain code this region uses to process the direction of visual motion. The presence of shared directional motion information across the senses in the right hMT+/V5 did not however indicate that motion processing is implemented using a fully abstracted response code since responses to visual and auditory motion were highly dissimilar at the global level. Our results therefore reveal a multidimensional representation of motion signals in hMT+/V5: while vision and audition overall produce opposite voxel-wise responses in this region, the relationship between motion directions are however aligned across the senses.

We used separate visual and auditory motion localizers to define, in each subject individually, regions that show preferential recruitment for visual and auditory motion processing. As expected, hMT+/V5 showed prominent preferential response to visual motion (Tootell, Reppas, Kwong, et al., 1995; J. D. G. Watson et al., 1993; Zeki et al., 1991), while PT showed the most prominent preferential response to auditory motion (Battal et al., 2019; Baumgart et al., 1999; Pavani et al., 2002; Poirier et al., 2017; Warren et al., 2002). Interestingly, we also found enhanced recruitment for auditory motion processing in the middle temporal cortex, in a region anterior to the visually-defined hMT+/V5 that we define here as MTa as it was more anterior to hMT+/V5 and responded to auditory motion (Figure 2.1C). Earlier human studies already suggested that auditory and tactile motion selectively activate a region anterior to the visually-defined hMT+/V5 cluster (Beauchamp et al., 2007; Jiang et al., 2015; Poirier et al., 2005; Saenz et al., 2008; Sani et al., 2010; Van Kemenade et al., 2014). Similarly, a recent study in the macaque demonstrated the presence of selective auditory motion responses in a region in the inferior bank of the superior temporal gyrus that was slightly anterior to the visual motion areas (Poirier et al., 2017). While we observed a degree of overlap between the visually and the auditory motion selective regions in the middle occipito-temporal cortex at the group-level (Battal et al., 2018; Poirier et al., 2005; Ricciardi et al., 2007; Van Kemenade et al., 2014), we did not observe a selective univariate preference for moving sounds in hMT+/V5 when avoiding smoothing and when using individual visual motion selective peaks to extract univariate beta parameters (Figure 2.1E), confirming previous univariate results (Beauchamp et al., 2007; Jiang et al., 2014, 2015). However, this did not constitute an

evidence for the absence of auditory motion information in hMT+/V5 since MVPA revealed robust decoding between auditory motion and static conditions in visually-defined hMT+/V5, highlighting that hMT+/V5 contained distributed information about the presence of motion information in sounds.

Using MVPA, we investigated the presence of motion direction information across the senses in hMT+/V5. We demonstrate that auditory and visual motion directions could be reliably decoded in the right hMT+/V5. Moreover, we observed that decoding opposite directions within the same axis of motion (up versus down; left versus right) was less reliable than decoding across axes of motion in both modalities (horizontal versus vertical). These results are reminiscent of animal studies showing that MT has an axis-of-motion columnar organization (Albright et al., 1984a; Diogo et al., 2003; Malonek et al., 1994; Shmuel & Grinvald, 1996), and high field fMRI studies suggesting a large-scale axis-of-motion organization in hMT+/V5 in humans (Zimmermann et al., 2011). The multi-dimensional scaling results clearly demonstrate the axis-of-motion organization for both the visual and the auditory modalities, and the shared representation of motion directions across modalities (Figure 2.4F). Interestingly, a similar auditory "axis-of-motion" organization was recently disclosed in the human Planum Temporale therefore suggesting that such representational structure for motion direction is shared across the senses and across brain regions (Battal et al., 2019).

Our cross-modal decoding results not only demonstrate that hMT+/V5 implements an axis-of-motion representational structure in both vision and audition, but further establish the presence of shared motion direction information across the senses (Figure 2.4E). Such shared motion direction information across the senses in the right hMT+/V5 might potentially relate to psychophysical studies showing cross-modal adaptation effects for motion directions (Berger & Ehrsson, 2016; Kitagawa & Ichihara, 2002; Konkle et al., 2009). Previous neuroimaging studies also highlighted the interaction between the visual and the auditory modalities in hMT+/V5 during multisensory processing (Alink et al., 2008; R. Lewis & Noppeney, 2010; Sadaghiani et al., 2009; Scheef et al., 2009). Our observation of shared motion direction information between vision and audition in hMT+/V5 provide evidence that hMT+/V5 may play a crucial role in providing a common representational structure between the two modalities to link auditory and visual motion direction information.

The successful cross-modal decoding in right hMT+V5 did not however indicate that the representation of motion direction was fully abstracted from sensory input. A series of complementary multivariate analyses demonstrated that the recorded activity in hMT+/V5 was highly dissimilar across the senses. For instance, motion direction patterns from the visual modality were negatively correlated with those from the auditory modality (Figure 2.5C, 2.5D). The negative correlation between the two modalities suggest that there

might exist different neural populations with a different level of preference for each modality in the voxels of hMT+/V5 and therefore voxels that have a higher density of visually responsive neurons have, de facto, a lower density of auditory responsive neurons. However, this hypothesis remains to be explored in future studies.

How does the presence of shared motion direction information across the two modalities (as inferred by significant cross-modal decoding) relate to the fact that patterns observed in hMT+/V5 in vision and audition negatively correlate? This was explained by our findings that, while the motion direction patterns were negatively correlated between vision and audition in right hMT+/V5 at a global scale (across all directions), the relation between the different motion directions in vision was similar to the one found in audition (see MDS, Figure 2.4F and 2.5E). These findings demonstrate that a successful cross-modal decoding indicates the presence of shared discriminating information between the different directions across modalities, but does not however indicate that the region is immune to the sensory input modality. Our results therefore serve as a timely reminder that cross-modal decoding is not a proxy for the presence of fully abstracted representations in a brain region.

Interestingly, we observed that motion directions could only be decoded in the auditory modality but not with visual stimuli in PT. These results suggest that whereas the right hMT+/V5 may contain information about auditory motion directions, the main auditory motion selective cluster (PT) does not reciprocally contain information about visual motion directions, at least in our dataset. Such difference in the presence of cross-modal information in regions typically preferring visual or auditory motion signals may relate to the fact that vision typically plays a dominant role in discriminating motion information (Alink et al., 2008; Berger & Ehrsson, 2016; Charbonneau et al., 2013; Hidaka et al., 2011). It may therefore be speculated that the regions typically providing the most reliable sensory signal for discriminating motion directions (i.e. vision) are more likely to also represents cross-modal signals for integration (Rohe & Noppeney, 2015; Ward et al., 2000).

It could be argued that the successful cross-modal decoding that we observed in right hMT+/V5 was attributed to the proximity to the MTa region. Our analyses demonstrate a clear anatomical and functional distinction between these two regions. The individually-defined hMT+/V5 and MTa were non-overlapping in almost all participants (Figure S2.2A). Even when excluding the overlapping voxels between the right hMT+/V5 and the right MTa ROIs, we still replicated the significant cross-modal decoding results in the right hMT+/V5 (Figure S2.2B).

Could the decoded auditory motion direction information in hMT+/V5 be related to eye movements? Unfortunately, we couldn’t track the gaze location inside the scanner

due to technical reasons. However, we tested additional participants outside the scanner and did not find any effect of the auditory motion direction on eye movements (Figure S2.3A, S2.3B). Eye movements can also be detected from the MRI signal from the eyes (Beauchamp, 2003). We tested whether the signal from the eyes varied across conditions and found no evidence for differences in eye movements profiles (Figure S2.3C). We are therefore convinced that the auditory moving information found in hMT+/V5 is unlikely to be explained by differences in eye movements.

Imagining visual motion can evoke a selective response in hMT+/V5 (Goebel et al., 1998; A. Kaas et al., 2010), and the direction of visual motion can be decoded from visual imagery (Emmerling et al., 2016). While the possibility of auditory-induced visual imagery cannot be fully excluded, we believe that it is very unlikely. Previous studies demonstrating the recruitment of hMT+/V5 during visual imagery of motion needed to train the participants on performing a precise mental imagery task (Emmerling et al., 2016; A. Kaas et al., 2010), which was not the case in our study. In addition, participants had to detect a change in color of the fixation cross during the auditory stimulation block in the directional motion decoding experiment, and performing this orthogonal visual task interferes with performing visual imagery (Johnson, 1982; Schorr et al., 1978). Maybe even more convincing is our functional connectivity analysis (Figure 2.2) revealing that while hMT+/V5 showed enhanced connectivity with early visual regions during visual motion processing, this was not the case during auditory motion processing, suggesting that auditory motion did not re-instantiate the network-level activity triggered by visual motion (Wolbers, Klatzky, et al., 2011). Finally, the split-half correlation analysis demonstrated that the patterns linked to visual directions were, globally, negatively correlated with the patterns evoked by auditory motion (Figure 2.5C). Overall, these results support the notion that the information about auditory motion directions in hMT+/V5 was not a simple byproduct of visual motion imagery.

In conclusion, our study demonstrates that the right hMT+/V5, a region typically considered as purely sensitive to visual motion, also contains information about auditory motion directions. The representation of auditory motion directions in hMT+/V5 is aligned to the brain code this region uses to process the direction of visual motion. Such aligned representation between auditory and visual motion directions may allow efficient interaction between the senses and support fast and optimal representation of multisensory signals. However, the presence of shared motion direction information did not indicate that hMT+/V5 was fully abstracted from the sensory input this region receives since the activity profile from the two modalities were highly distinguishable in this region. Altogether, our results have important implications for our understanding on how we classically consider the division of sensory labor between brain regions dedicated to a specific perceptual or cognitive function (here, motion). More precisely, our results suggest that regions classically considered exclusively visual may also contain information from the other

senses in a format that is partially aligned to the brain code these regions use to process vision.

References

Abdi, H., O'Toole, A. J., Valentin, D., & Edelman, B. (2005). DISTATIS: The analysis of multiple distance matrices. *Computer Vision and Pattern Recognition-Workshops, 2005. CVPR Workshops. IEEE Computer Society Conference On*, 42.

Albright, T. D. (1984). Direction and orientation selectivity of neurons in visual area MT of the macaque Direction and Orientation Selectivity of Neurons in Visual Area MT of the Macaque. *Journal of Neurophysiology*, *52*(6), 1106–1130. https://doi.org/10.1152/jn.1984.52.6.1106

Albright, T. D., Desimone, R., & Gross, C. G. (1984). Columnar organization of directionally selective cells in visual area MT of the macaque. *Journal of Neurophysiology*, *51*(1), 16–31. https://doi.org/10.1152/jn.1984.51.1.16

Alink, A., Euler, F., Kriegeskorte, N., Singer, W., & Kohler, A. (2012). Auditory motion direction encoding in auditory cortex and high-level visual cortex. *Human Brain Mapping*, *33*(4), 969–978. https://doi.org/10.1002/hbm.21263

Alink, A., Singer, W., & Muckli, L. (2008). Capture of Auditory Motion by Vision Is Represented by an Activation Shift from Auditory to Visual Motion Cortex. *Journal of Neuroscience*, *28*(11), 2690–2697. https://doi.org/10.1523/JNEUROSCI.2980-07.2008

Baker, J. F., Petersen, S. E., Newsome, W. T., & Allman, J. M. (1981). Visual response properties of neurons in four extrastriate visual areas of the owl monkey (Aotus trivirgatus): A quantitative comparison of medial, dorsomedial, dorsolateral, and middle temporal areas. *Journal of Neurophysiology*, *45*(3), 397–416. https://doi.org/10.1152/jn.1981.45.3.397

Battal, C., Rezk, M., Mattioni, S., Bottini, R., Bertonati, G., Occelli, V., Targher, S., & Collignon, O. (2018). Decoding auditory motion direction and location in hMT+/V5 and Planum Temporale of sighted and blind individuals. *Journal of Vision*, *18*(10), 436. https://doi.org/10.1167/18.10.436

Battal, C., Rezk, M., Mattioni, S., Vadlamudi, J., & Collignon, O. (2019). Representation of auditory motion directions and sound source locations in the human planum temporale. *The Journal of Neuroscience*, *39*(12), 2218–2289. https://doi.org/10.1523/JNEUROSCI.2289-18.2018

Baumgart, F., Gaschler-Markefski, B., Woldorff, M. G., Heinze, H.-J., & Scheich, H. (1999). A movement-sensitive area in auditory cortex. *Nature*, *400*(6746), 724–726. https://doi.org/10.1038/23390

Beauchamp, M. S. (2003). Detection of eye movements from fMRI data. *Magnetic*

Resonance in Medicine, *49*(2), 376–380. https://doi.org/10.1002/mrm.10345

Beauchamp, M. S., Yasar, N. E., Kishan, N., & Ro, T. (2007). Human MST But Not MT Responds to Tactile Stimulation. *Journal of Neuroscience*, *27*(31), 8261–8267. https://doi.org/10.1523/JNEUROSCI.0754-07.2007

Beckett, A., Peirce, J. W., Sanchez-Panchuelo, R. M., Francis, S., & Schluppeck, D. (2012). Contribution of large scale biases in decoding of direction-of-motion from high-resolution fMRI data in human early visual cortex. *NeuroImage*, *63*(3), 1623–1632. https://doi.org/10.1016/j.neuroimage.2012.07.066

Benjamini, Y., & Hochberg, Y. (1995). Controlling the False Discovery Rate: a Practical and Powerful Approach to Multiple Testing. *Journal of the Royal Statistical Society*, 289–300. https://doi.org/10.2307/2346101

Berger, C. C., & Ehrsson, H. H. (2016). Auditory Motion Elicits a Visual Motion Aftereffect. *Frontiers in Neuroscience*, *10*, 559. https://doi.org/10.3389/fnins.2016.00559

Bex, P. J., Dakin, S. C., & Simmers, A. J. (2003). The shape and size of crowding for moving targets. *Vision Research*, *43*(27), 2895–2904. https://doi.org/10.1016/S0042-6989(03)00460-7

Calvert, G. A., & Thesen, T. (2004). Multisensory integration: methodological approaches and emerging principles in the human brain. *Journal of Physiology-Paris*, *98*(1–3), 191–205. https://doi.org/10.1016/j.jphysparis.2004.03.018

Chang, C.-C., & Lin, C.-J. (2011). Libsvm. *ACM Transactions on Intelligent Systems and Technology*, *2*(3), 1–27. https://doi.org/10.1145/1961189.1961199

Chaplin, T. A., Allitt, B. J., Hagan, M. A., Rosa, M. G. P., Rajan, R., & Lui, L. L. (2018). Auditory motion does not modulate spiking activity in the middle temporal and medial superior temporal visual areas. *European Journal of Neuroscience*, *48*(4), 2013–2029. https://doi.org/10.1111/ejn.14071

Charbonneau, G., Veronneau, M., Boudrias-Fournier, C., Lepore, F., & Collignon, O. (2013). The ventriloquist in periphery: Impact of eccentricity-related reliability on audio-visual localization. *Journal of Vision*, *13*(12), 20–20. https://doi.org/10.1167/13.12.20

Corbetta, M., Akbudak, E., Conturo, T. E., Snyder, A. Z., Ollinger, J. M., Drury, H. A., Linenweber, M. R., Petersen, S. E., Raichle, M. E., Van Essen, D. C., & Shulman, G. L. (1998). A Common Network of Functional Areas for Attention and Eye Movements. *Neuron*, *21*(4), 761–773. https://doi.org/10.1016/S0896-6273(00)80593-0

Diogo, A. C. M., Soares, J. G. M., Koulakov, A., Albright, T. D., & Gattass, R. (2003). Electrophysiological imaging of functional architecture in the cortical middle temporal visual area of Cebus apella monkey. *The Journal of Neuroscience : The Official Journal of the Society for Neuroscience*, *23*(9), 3881–3898.

Dormal, G., Rezk, M., Yakobov, E., Lepore, F., & Collignon, O. (2016). Auditory motion in the sighted and blind: Early visual deprivation triggers a large-scale imbalance between auditory and "visual" brain regions. *NeuroImage*, *134*, 630–644. https://doi.org/10.1016/j.neuroimage.2016.04.027

Driver, J., & Spence, C. (2000). Multisensory perception: Beyond modularity and convergence. *Current Biology*, *10*(20), 10–12. https://doi.org/10.1016/S0960-9822(00)00740-5

Dumoulin, S. O., Bittar, R. G., Kabani, N. J., Baker, C. L., Le Goualher, G., Bruce Pike, G., & Evans, A. C. (2000). A new anatomical landmark for reliable identification of human area V5/MT: a quantitative analysis of sulcal patterning. *Cerebral Cortex*, *10*(5), 454–463. https://doi.org/10.1093/cercor/10.5.454

Emmerling, T. C., Zimmermann, J., Sorger, B., Frost, M. A., & Goebel, R. (2016). Decoding the direction of imagined visual motion using 7 T ultra-high field fMRI. *NeuroImage*, *125*, 61–73. https://doi.org/10.1016/j.neuroimage.2015.10.022

Friston, K. ., Buechel, C., Fink, G. ., Morris, J., Rolls, E., & Dolan, R. . (1997). Psychophysiological and Modulatory Interactions in Neuroimaging. *NeuroImage*, *6*(3), 218–229. https://doi.org/10.1006/nimg.1997.0291

Gitelman, D. R., Penny, W. D., Ashburner, J., & Friston, K. J. (2003). Modeling regional and psychophysiologic interactions in fMRI: the importance of hemodynamic deconvolution. *NeuroImage*, *19*(1), 200–207. https://doi.org/10.1016/S1053-8119(03)00058-2

Goebel, R., Khorram-Sefat, D., Muckli, L., Hacker, H., & Singer, W. (1998). The constructive nature of vision: Direct evidence from functional magnetic resonance imaging studies of apparent motion and motion imagery. *European Journal of Neuroscience*, *10*(5), 1563–1573. https://doi.org/10.1046/j.1460-9568.1998.00181.x

Griffiths, T. D., & Green, G. G. R. (1999). Cortical activation during perception of a rotating wide-field acoustic stimulus. *NeuroImage*, *10*(1), 84–90. https://doi.org/10.1006/nimg.1999.0464

Hagen, M. C., Franzén, O., McGlone, F., Essick, G., Dancer, C., & Pardo, J. V. (2002). Tactile motion activates the human middle temporal/V5 (MT/V5) complex. *European Journal of Neuroscience*, *16*(5), 957–964. https://doi.org/10.1046/j.1460-9568.2002.02139.x

Haxby, J. V., Gobbini, M. I., Furey, M. L., Ishai, A., Schouten, J. L., & Pietrini, P. (2001). Distrubuted and Overlapping Representations of Face and Objects in Ventral Temporal Cortex. *Science*, *293*(5539), 2425–2430. https://doi.org/10.1126/science.1063736

Hidaka, S., Teramoto, W., Sugita, Y., Manaka, Y., Sakamoto, S., & Suzuki, Y. (2011). Auditory motion information drives visual motion perception. *PLoS ONE*, *6*(3). https://doi.org/10.1371/journal.pone.0017499

Huk, A. C., Dougherty, R. F., & Heeger, D. J. (2002). Retinotopy and functional subdivision of human areas MT and MST. *The Journal of Neuroscience : The Official Journal of the Society for Neuroscience*, *22*(16), 7195–7205. https://doi.org/20026661

Jiang, F., Beauchamp, M. S., & Fine, I. (2015). Re-examining overlap between tactile and visual motion responses within hMT + and STS. *NeuroImage*, *119*, 187–196. https://doi.org/10.1016/j.neuroimage.2015.06.056

Jiang, F., Stecker, G. C., & Fine, I. (2014). Auditory motion processing after early blindness. *Journal of Vision*, *14*(13), 4–4. https://doi.org/10.1167/14.13.4

Johnson, P. (1982). The functional equivalence of imagery and movement. *The Quarterly Journal of Experimental Psychology Section A*, *34*(3), 349–365. https://doi.org/10.1080/14640748208400848

Kaas, A., Weigelt, S., Roebroeck, A., Kohler, A., & Muckli, L. (2010). Imagery of a moving object: The role of occipital cortex and human MT/V5+. *NeuroImage*, *49*(1), 794–804. https://doi.org/10.1016/j.neuroimage.2009.07.055

Kamitani, Y., & Tong, F. (2006). Decoding Seen and Attended Motion Directions from Activity in the Human Visual Cortex. *Current Biology*, *16*(11), 1096–1102. https://doi.org/10.1016/j.cub.2006.04.003

Kaplan, J. T., Man, K., & Greening, S. G. (2015). Multivariate cross-classification: applying machine learning techniques to characterize abstraction in neural representations. *Frontiers in Human Neuroscience*, *9*, 151. https://doi.org/10.3389/fnhum.2015.00151

Kitagawa, N., & Ichihara, S. (2002). *Hearing visual motion in depth*. *416*(March), 1–3.

Konkle, T., Wang, Q., Hayward, V., & Moore, C. I. (2009). Motion Aftereffects Transfer between Touch and Vision. *Current Biology*, *19*(9), 745–750. https://doi.org/10.1016/j.cub.2009.03.035

Kriegeskorte, N., Goebel, R., & Bandettini, P. (2006). Information-based functional brain mapping. *Proceedings of the National Academy of Sciences*, *103*(10), 3863–3868.

https://doi.org/10.1073/pnas.0600244103

Kriegeskorte, N., Mur, M., & Bandettini, P. (2008). Representational similarity analysis – connecting the branches of systems neuroscience. *Frontiers in Systems Neuroscience*, *2*, 4. https://doi.org/10.3389/neuro.06.004.2008

Kriegeskorte, N., Mur, M., Ruff, D. A., Kiani, R., Bodurka, J., Esteky, H., Tanaka, K., & Bandettini, P. A. (2008). Matching Categorical Object Representations in Inferior Temporal Cortex of Man and Monkey. *Neuron*, *60*(6), 1126–1141. https://doi.org/10.1016/j.neuron.2008.10.043

Krumbholz, K., Schönwiesner, M., Rübsamen, R., Zilles, K., Fink, G. R., & Von Cramon, D. Y. (2005). Hierarchical processing of sound location and motion in the human brainstem and planum temporale. *European Journal of Neuroscience*, *21*(1), 230–238.

Lewis, R., & Noppeney, U. (2010). Audiovisual Synchrony Improves Motion Discrimination via Enhanced Connectivity between Early Visual and Auditory Areas. *Journal of Neuroscience*, *30*(37), 12329–12339. https://doi.org/10.1523/JNEUROSCI.5745-09.2010

Malonek, D., Tootell, R., & Grinvald, A. (1994). Optical imaging reveals the functional architecture of neurons processing shape and motion in owl monkey area MT. *Proc. R. Soc. Lond. B*, *258*(1352), 109–119.

Møller, H. (1992). Fundamentals of binaural technology. *Applied Acoustics*, *36*(3–4), 171–218. https://doi.org/10.1016/0003-682X(92)90046-U

Oosterhof, N. N., Connolly, A. C., & Haxby, J. V. (2016). CoSMoMVPA: Multi-Modal Multivariate Pattern Analysis of Neuroimaging Data in Matlab/GNU Octave. *Frontiers in Neuroinformatics*, *10*. https://doi.org/10.3389/fninf.2016.00027

Pascual-Leone, A., & Hamilton, R. (2001). The metamodal organization of the brain. In *Progress in Brain Research* (pp. 427–445). https://doi.org/10.1016/S0079-6123(01)34028-1

Pavani, F., Macaluso, E., Warren, J. D., Driver, J., & Griffiths, T. D. (2002). A Common Cortical Substrate Activated by Horizontal and Vertical Sound Movement in the Human Brain. *Current Biology*, *12*(18), 1584–1590. https://doi.org/10.1016/S0960-9822(02)01143-0

Petit, L., & Haxby, J. V. (1999). Functional Anatomy of Pursuit Eye Movements in Humans as Revealed by fMRI. *Journal of Neurophysiology*, *82*(1), 463–471. https://doi.org/10.1152/jn.1999.82.1.463

Poirier, C., Baumann, S., Dheerendra, P., Joly, O., Hunter, D., Balezeau, F., Sun, L., Rees, A., Petkov, C., Thiele, A., & Griffiths, T. (2017). Auditory motion-specific mechanisms in the primate brain. *PLoS Biology*, *15*(5), e2001379. https://doi.org/10.1371/journal.pbio.2001379

Poirier, C., Collignon, O., DeVolder, A. G., Renier, L., Vanlierde, A., Tranduy, D., & Scheiber, C. (2005). Specific activation of the V5 brain area by auditory motion processing: An fMRI study. *Cognitive Brain Research*, *25*(3), 650–658. https://doi.org/10.1016/j.cogbrainres.2005.08.015

Ricciardi, E., Handjaras, G., Bonino, D., Vecchi, T., Fadiga, L., & Pietrini, P. (2013). Beyond Motor Scheme: A Supramodal Distributed Representation in the Action-Observation Network. *PLoS ONE*, *8*(3). https://doi.org/10.1371/journal.pone.0058632

Ricciardi, E., Vanello, N., Sani, L., Gentili, C., Scilingo, E. P., Landini, L., Guazzelli, M., Bicchi, A., Haxby, J. V., & Pietrini, P. (2007). The Effect of Visual Experience on the Development of Functional Architecture in hMT+. *Cerebral Cortex*, *17*(12), 2933–2939. https://doi.org/10.1093/cercor/bhm018

Rohe, T., & Noppeney, U. (2015). Cortical hierarchies perform Bayesian causal inference in multisensory perception. *PLoS Biology*, *13*(2), e1002073. https://doi.org/10.1371/journal.pbio.1002073

Sadaghiani, S., Maier, J. X., & Noppeney, U. (2009). Natural, Metaphoric, and Linguistic Auditory Direction Signals Have Distinct Influences on Visual Motion Processing. *Journal of Neuroscience*, *29*(20), 6490–6499. https://doi.org/10.1523/JNEUROSCI.5437-08.2009

Saenz, M., Lewis, L. B., Huth, A. G., Fine, I., & Koch, C. (2008). Visual Motion Area MT+/V5 Responds to Auditory Motion in Human Sight-Recovery Subjects. *Journal of Neuroscience*, *28*(20), 5141–5148. https://doi.org/10.1523/JNEUROSCI.0803-08.2008

Sani, L., Ricciardi, E., Gentili, C., Vanello, N., Haxby, J. V., & Pietrini, P. (2010). Effects of Visual Experience on the Human MT+ Functional Connectivity Networks: An fMRI Study of Motion Perception in Sighted and Congenitally Blind Individuals. *Frontiers in Systems Neuroscience*, *4*, 159. https://doi.org/10.3389/fnsys.2010.00159

Scheef, L., Boecker, H., Daamen, M., Fehse, U., Landsberg, M. W., Granath, D. O., Mechling, H., & Effenberg, A. O. (2009). Multimodal motion processing in area V5/MT: Evidence from an artificial class of audio-visual events. *Brain Research*, *1252*, 94–104. https://doi.org/10.1016/j.brainres.2008.10.067

Schorr, D., Balzano, G., & Smith, E. E. (1978). Selective interference between imagery and perception: Is it modality specific or relation specific? *Bulletin of the Psychonomic*

Society, *12*(6), 419–422. https://doi.org/10.3758/BF03329725

Schroeder, C. E., & Foxe, J. (2005). Multisensory contributions to low-level, 'unisensory' processing. *Current Opinion in Neurobiology*, *15*(4), 454–458. https://doi.org/10.1016/j.conb.2005.06.008

Shmuel, A., & Grinvald, A. (1996). Functional organization for direction of motion and its relationship to orientation maps in cat area 18. *Journal of Neuroscience*, *16*(21), 6945–6964.

Stelzer, J., Chen, Y., & Turner, R. (2013). Statistical inference and multiple testing correction in classification-based multi-voxel pattern analysis (MVPA): Random permutations and cluster size control. *NeuroImage*, *65*, 69–82. https://doi.org/10.1016/j.neuroimage.2012.09.063

Tootell, R. B. H., Reppas, J. B., Dale, A. M., Look, R. B., Sereno, M. I., Malach, R., Brady, T. J., & Rosen, B. R. (1995). Visual motion aftereffect in human cortical area MT revealed by functional magnetic resonance imaging. *Nature*, *375*(6527), 139–141. https://doi.org/10.1038/375139a0

Tootell, R. B. H., Reppas, J., Kwong, K., Malach, R., Born, R., Brady, T., Rosen, B., & Belliveau, J. (1995). Functional analysis of human MT and related visual cortical areas using magnetic resonance imaging. *The Journal of Neuroscience*, *15*(4), 3215–3230. https://doi.org/10.1523/JNEUROSCI.15-04-03215.1995

Van Kemenade, B. M., Seymour, K., Wacker, E., Spitzer, B., Blankenburg, F., & Sterzer, P. (2014). Tactile and visual motion direction processing in hMT+/V5. *NeuroImage*, *84*, 420–427. https://doi.org/10.1016/j.neuroimage.2013.09.004

von Saldern, S., & Noppeney, U. (2013). Sensory and Striatal Areas Integrate Auditory and Visual Signals into Behavioral Benefits during Motion Discrimination. *Journal of Neuroscience*, *33*(20), 8841–8849. https://doi.org/10.1523/JNEUROSCI.3020-12.2013

Wacker, E., Spitzer, B., Lützkendorf, R., Bernarding, J., & Blankenburg, F. (2011). Tactile motion and pattern processing assessed with high-field fmRi. *PLoS ONE*, *6*(9). https://doi.org/10.1371/journal.pone.0024860

Ward, L. M., Mcdonald, J. J., & Lin, D. (2000). On asymmetries in cross-modal spatial attention orienting. *Perception & Psychophysics*, *62*(6), 1258–1264. https://doi.org/10.3758/BF03212127

Warren, J. D., Zielinski, B. A., Green, G. G. R., Rauschecker, J. P., & Griffiths, T. D. (2002). Perception of Sound-Source Motion by the Human Brain. *Neuron*, *34*(1), 139–148. https://doi.org/10.1016/S0896-6273(02)00637-2

Watson, J. D. G., Myers, R., Frackowiak, R. S. J., Hajnal, J. V., Woods, R. P., Mazziotta, J. C., Shipp, S., & Zeki, S. (1993). Area V5 of the Human Brain: Evidence from a Combined Study Using Positron Emission Tomography and Magnetic Resonance Imaging. *Cerebral Cortex*, *3*(2), 79–94. https://doi.org/10.1093/cercor/3.2.79

Wolbers, T., Klatzky, R. L., Loomis, J. M., Wutte, M. G., & Giudice, N. A. (2011). Modality-independent coding of spatial layout in the human brain. *Current Biology*, *21*(11), 984–989. https://doi.org/10.1016/j.cub.2011.04.038

Zabicki, A., De Haas, B., Zentgraf, K., Stark, R., Munzert, J., & Krüger, B. (2017). Imagined and executed actions in the human motor system: Testing neural similarity between execution and imagery of actions with a multivariate approach. *Cerebral Cortex*, *27*(9), 4523–4536. https://doi.org/10.1093/cercor/bhw257

Zaitsev, M., Hennig, J., & Speck, O. (2004). Point spread function mapping with parallel imaging techniques and high acceleration factors: Fast, robust, and flexible method for echo-planar imaging distortion correction. *Magnetic Resonance in Medicine*, *52*(5), 1156–1166. https://doi.org/10.1002/mrm.20261

Zeki, S. (1974). Functional organization of a visual area in the posterior bank of the superior temporal sulcus of the rhesus monkey. *The Journal of Physiology*, *236*(3), 549–573. https://doi.org/10.1113/jphysiol.1974.sp010452

Zeki, S. (1980). The response properties of cells in the middle temporal area (area MT) of owl monkey visual cortex. *Proc. R. Soc. Lond. B*, *207*(1167), 239–248.

Zeki, S., Watson, J. D. G., Lueck, C., Friston, K., Kennard, C., & Frackowiak, R. (1991). A direct demonstration of functional specialization in human visual cortex. *The Journal of Neuroscience*, *11*(3), 641–649. https://doi.org/10.1523/JNEUROSCI.11-03-00641.1991

Zimmermann, J., Goebel, R., de Martino, F., van de Moortele, P. F., Feinberg, D., Adriany, G., Chaimow, D., Shmuel, A., Uğurbil, K., & Yacoub, E. (2011). Mapping the organization of axis of motion selective features in human area mt using high-field fmri. *PLoS ONE*, *6*(12), 1–10. https://doi.org/10.1371/journal.pone.0028716

Supplementary materials

Methods S2.1 Behavioral data from the directional motion decoding experiment.

During the visual and the auditory motion blocks, the participants detected a brief change in the color of the fixation cross to ensure that they maintained fixation. The participants performed the task with high accuracy (mean accuracy ± SD = 96.2% ± 5.43%). Moreover, after each motion block, the participants had to indicate the direction that was just presented. The repeated-measures ANOVA revealed a main effect of modality ($F(1,22)= 26.210$, $p<0.001$), indicating that the behavioral accuracy of motion direction discrimination (collapsed across different directions) was higher in the visual modality (mean ± SD = 98.46% ± 2.45%) than that in the auditory modality (mean ± SD = 86.32% ± 11.97%). The analysis also revealed a main effect of motion directions ($F(3,66)= 10.048$, $p<0.001$) and a significant [modality x direction] interaction ($F(3,66)= 11.243$, $p<0.001$). Post-hoc pair-wise comparisons showed no difference between motion direction discrimination in the visual modality ($p>0.05$). In the auditory modality, there was no difference between the discrimination of motion directions within the same axis ($p>0.05$). However, the behavioral accuracy was significantly higher in the horizontal axis compared to the vertical axis. The discrimination of rightward auditory motion (mean ± SD = 96.38% ± 9.67%) was significantly higher than the discrimination of upward (mean ± SD = 74.28% ± 27.74%, $t(22)=3.52$,$p= 0.012$) and downward auditory motion (mean ± SD = 78.26% ± 23.27%, $t(22)=3.38$,$p=0.016$). Leftward auditory motion discrimination (mean ± SD = 96.38% ± 4.91%) was higher than upward (mean ± SD = 74.28% ± 27.74%, $t(22)=3.71$ $p=0.007$) and downward auditory motion discrimination (mean ± SD = 78.26% ± 23.27% , $t(22)= 3.67$, $p=0.008$).

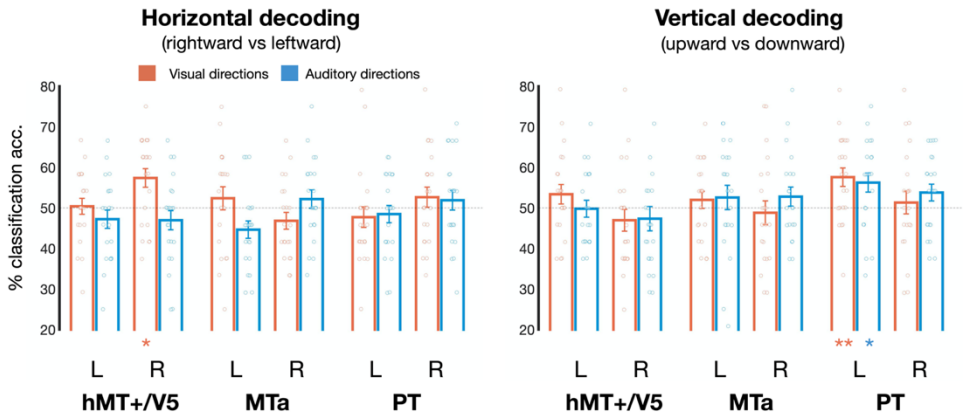


Figure S2.1 Within-modality Within-axis classification.

*Within-modality within-axis classification in the individually defined hMT+/V5, MTa, and PT. Classification results of the two opposing directions within the same axis (rightward vs leftward motion in the horizontal axis, and upward vs downward motion in the vertical axis) in the visual and the auditory modality separately. Individual points reflect individual subjects' results. Results are corrected for multiple comparisons using FDR-correction (*p<0.05, **p<0.01).*

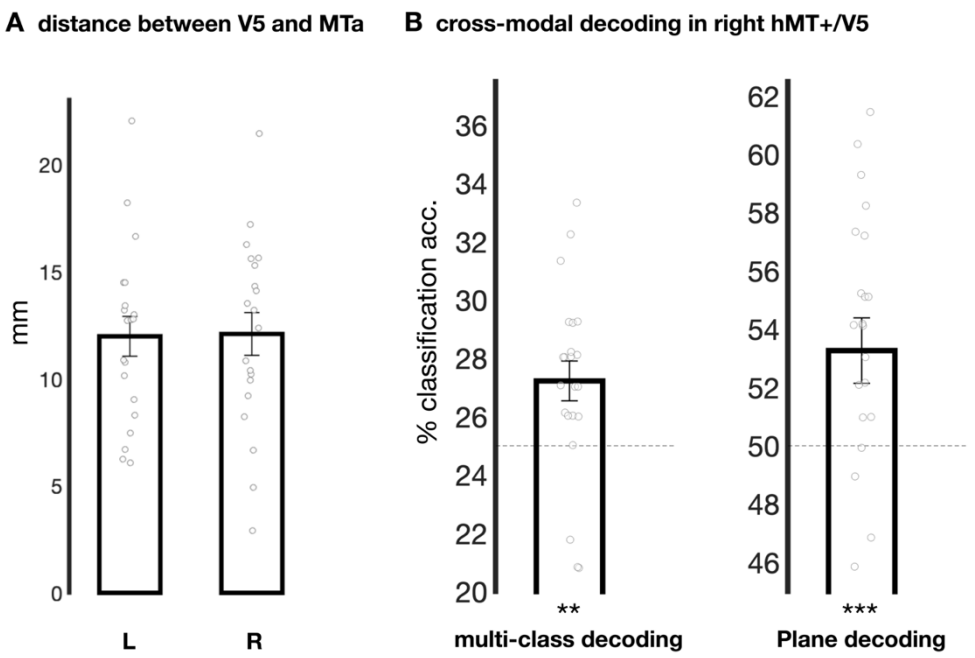
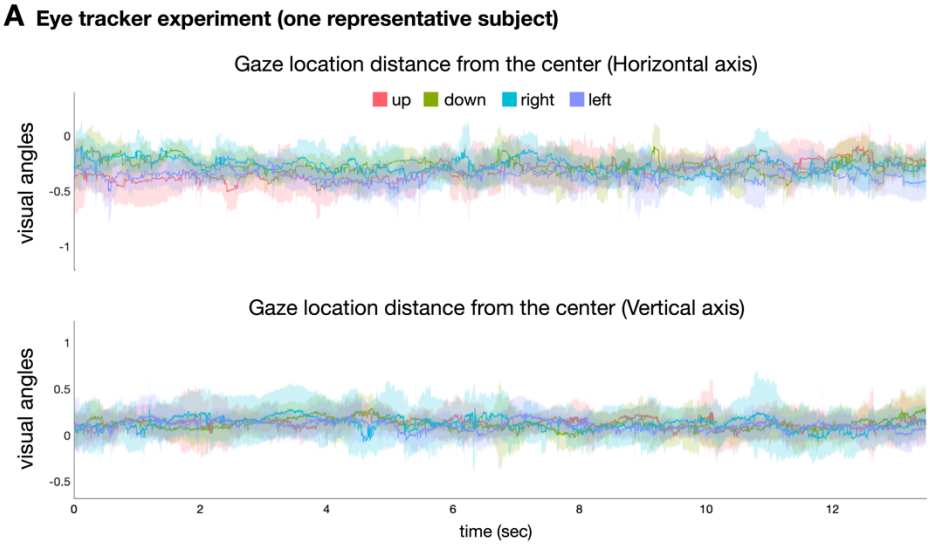
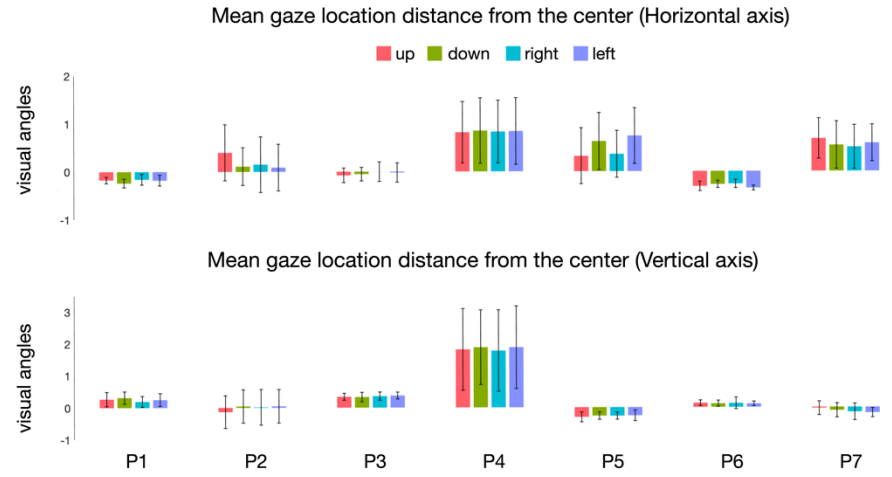


Figure S2.2 Control analysis for the cross-modal decoding.
*[A] The mean Euclidean distance between the MNI peak coordinates of the individually defined hMT+/V5 and MTa in both hemispheres. Each dot represents the distance between hMT+/V5 and MTa in a single subject. The distance (mean ± SD) between hMT+/V5 and MTa was 11.98 mm ± 4.1582 mm in the left hemisphere, and was 12.09 mm ± 4.47 mm in the right hemisphere (Figure S2.3a). The distance between hMT+/V5 and MTa was significantly different from zero both in the left (t(19)= 12.89, p= 3.85x10-11), and in the right hemisphere (t(19)= 12.09, p= 1.13x10-10). L: Left hemisphere, R: Right hemisphere. [B] The cross-modal motion direction and axis of motion decoding in individually defined right hMT+/V5 ROIs after excluding voxels that overlapped with the right MTa, and voxels that had a t-value <1.5 when comparing the visual motion with the visual static condition from the visual motion localizer. The cross-modal multiclass (27.23% ± 0.68%, p = 0.0034) and plane decoding (53.27% ± 1.12%, p = 0.0008) were significantly above chance. Error bars represent the standard error of the mean. Individual points reflect individual subjects' results. (**p<0.01, ***p<0.001).*


A Eye tracker experiment (one representative subject)
Gaze location distance from the center (Horizontal axis)
up
down
right
left
visual angles
0
-0.5
-1
Gaze location distance from the center (Vertical axis)
visual angles
1
0.5
0
-0.5
0
2
4
6
8
10
12
time (sec)


B Average gaze location for each participant
Mean gaze location distance from the center (Horizontal axis)
up
down
right
left
visual angles
2
1
0
-1
Mean gaze location distance from the center (Vertical axis)
visual angles
3
2
1
0
-1
P1
P2
P3
P4
P5
P6
P7

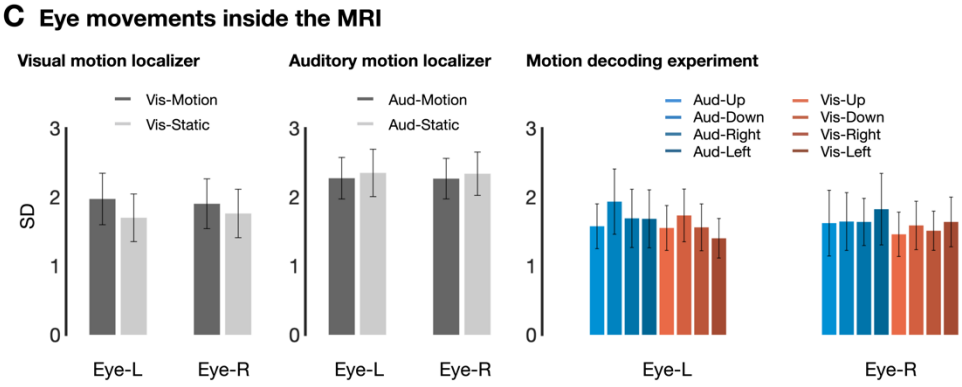

C Eye movements inside the MRI
Visual motion localizer
Vis-Motion
Vis-Static
SD
3
2
1
0
Eye-L
Eye-R
Auditory motion localizer
Aud-Motion
Aud-Static
3
2
1
0
Eye-L
Eye-R
Motion decoding experiment
Aud-Up
Aud-Down
Aud-Right
Aud-Left
Vis-Up
Vis-Down
Vis-Right
Vis-Left
3
2
1
0
Eye-L
Eye-R

Figure S2.3 Eye movements.

[A] Eye tracker experiment: The Gaze location from the fixation cross during the auditory motion stimulation blocks from one representative participant. Different colors represent the gaze location for each auditory motion direction. Lighter colors represent the standard error of the mean. There was no difference between the gaze position in both the horizontal and the vertical plane for the four auditory motion directions in all participants. [B] The bar graphs represent the average gaze location from the fixation for each auditory motion direction in each participant from the eye tracker experiment. The gaze location in each stimulation block for each motion direction is averaged across time. Error bars represent the standard error of the mean. There was no difference between the eye position in the horizontal ($p>0.05$) or the vertical plane ($p>0.05$) for all participants [C] Eye movements inside the MRI: We tested if eye movements could be detected from the MRI signal from the eyes. We performed the same analysis in our three fMRI experiments where the eyes of the participants were defined as a 7mm sphere at the center of each eye. The fMRI signal from each eye was extracted, and the standard deviation of the signal during each stimulation block of each condition was measured. In the visual and auditory motion localizers, we found no effect of condition, ROI, or an interaction between the two. We repeated the same analysis in the motion decoding experiment, and found no effect of ROI, modality, direction, or any interaction. Error bars represent the standard error of the mean.

Area	Cluster size	x (mm)	y (mm)	z (mm)	peak t-value	p-value (FWE-corr)
Visual Motion Localizer [Visual motion > Visual static]						
L Inferior occipital gyrus	1887	-14	-100	-2	11.71	0
R Inferior occipital gyrus		20	-96	0	10.49	0
		-8	-90	-12	9.21	0
R Middle temporal gyrus	163	46	-62	6	8.8	0
		50	-52	8	6.87	0.013
L Middle temporal gyrus	39	-42	-66	2	7.12	0.008
Auditory Motion Localizer [Auditory motion > Auditory static]						
L Superior temporal gyrus	1131	-46	-30	8	13.24	0
		-54	-40	10	8.4	0.001
		-62	-16	10	7.83	0.002
R Superior temporal gyrus	1203	62	-34	8	10.63	0
		52	-24	6	9.05	0
		52	-16	10	8.93	0
R Middle temporal gyrus	115	48	-54	8	7.96	0.002
L Middle temporal gyrus	37	-46	-64	6	7.6	0.004
L Postcentral gyrus	70	-38	-44	64	7.09	0.009
		-30	-44	50	6.98	0.011
	14	34	-44	46	6.66	0.019

Table S2.1 Results of the univariate analysis from the visual and the auditory motion localizers. *Results are corrected for multiple comparisons using family-wise error correction (FWE) across the whole brain at a significance level of $p<0.05$. Coordinates are reported in MNI space.*

	hMT+/V5						MTa						PT					
	LH			RH			LH			RH			LH			RH		
	x	y	z	x	y	z	x	y	z	x	y	z	x	y	z	x	y	z
S1	-40	-66	-2	44	-68	-2	-52	-68	2	52	-56	4	-46	-32	10	60	-28	10
S2	-40	-72	-2	46	-66	-4	-52	-64	0	50	-58	-2	-52	-20	6	58	-26	8
S3	-36	-74	6	44	-72	8	-54	-64	-2	54	-56	-2	-56	-28	8	62	-42	10
S4	-44	-72	4	42	-68	2	-50	-68	-4	52	-58	0	-54	-36	10	62	-34	12
S5	-38	-64	2	40	-68	2	-50	-68	4	50	-62	8	-40	-34	14	64	-38	6
S6	-38	-74	-4	44	-60	0	-52	-68	6	46	-58	0	-52	-24	2	56	-28	10
S7	-42	-70	-2	42	-62	2	-44	-60	6	54	-58	8	-48	-34	14	62	-40	8
S8	-42	-66	2	44	-62	6	-50	-66	6	56	-56	8	-44	-30	12	58	-32	2
S9	--	--	--	44	-68	0	--	--	--	--	--	--	--	--	--	--	--	--
S10	--	--	--	--	--	--	-52	-66	8	42	-54	4	-46	-30	6	52	-32	10
S11	-40	-64	0	44	-64	2	-52	-68	4	48	-58	10	-52	-32	10	62	-38	12
S12	-42	-72	0	46	-68	-2	-52	-68	2	46	-62	6	-54	-38	6	60	-42	10
S13	-40	-64	2	50	-70	2	-42	-68	6	--	--	--	-52	-36	6	54	-40	14
S14	-40	-76	2	46	-60	2	-52	-68	2	48	-56	0	-56	-32	8	54	-40	12
S15	-42	-72	-2	44	-68	10	-38	-70	10	46	-62	8	-44	-32	4	56	-34	14
S16	-44	-62	6	46	-66	0	-46	-62	12	46	-56	12	-46	-36	6	62	-26	10
S17	-40	-64	0	52	-62	-2	-48	-62	6	46	-60	6	-42	-34	2	62	-26	6
S18	-38	-72	2	46	-66	0	-44	-60	12	52	-60	6	-46	-38	10	60	-26	12
S19	-44	-68	6	50	-72	8	-48	-62	2	52	-60	6	-42	-36	10	60	-42	8
S20	-46	-68	6	44	-64	2	-48	-62	4	52	-50	8	-40	-38	6	52	-30	8
S21	-42	-72	-2	42	-68	4	--	--	--	48	-54	2	-54	-24	8	62	-34	14
S22	-44	-70	2	44	-60	0	-46	-64	-2	48	-54	-4	-44	-36	10	64	-30	10
S23	-40	-70	-4	46	-64	0	-44	-62	6	56	-54	8	-46	-26	2	56	-36	10

Table S2.2 Peak coordinates of the individually defined regions of interest.
coordinates of hMT+/V5 were defined in each subject from the contrast [visual motion > visual static] in the visual motion localizer. Peak coordinates from MTa and PT were defined individually from the contrast [auditory motion > auditory static] in the auditory motion localizer. Coordinates are in MNI space.

Seed	ROI	K	t-value	p-value	MNI Coordinates		
Visual motion localizer							
Left hMT+/V5							
	L middle temporal G	37	4.96	0.002	-40	-66	2
	L lingual G	234	6.02	p<0.001	-14	-94	-6
	L middle Temporal G		5.90	p<0.001	-14	-96	-2
	L lingual Gyrus		5.24	0.001	-16	-90	-2
	R Lingual G	244	5.22	0.001	20	-94	2
	R Lingual G		5.19	0.001	18	-98	-2
	R Lingual G		4.91	0.002	10	-94	-8
			4.68	0.003	6	-98	-6
Right hMT+/V5							
	L middle temporal G	210	5.71	p<0.001	-38	-68	2
	R inferior temporal G	92	5.03	0.001	44	-66	0
	L lingual G	217	5.04	0.001	-10	-94	-10
	L lingual G		5.02	0.001	-12	-90	-10
	L lingual G		4.87	0.002	-6	-90	-12
	L Middle Occipital G		4.73	0.003	-14	-96	-2
	L lingual G		4.24	0.006	-16	-90	-2
	R Calcarine G	240	4.61	0.003	18	-98	0
	R Lingual G		4.60	0.003	20	-94	2
	Calcarine G (BA17)		3.98	0.011	4	-94	-6
	Calcarine G (BA17)		3.81	0.015	2	-98	-2
Left MTa							
	L lingual G	23	3.81	0.016	-10	-94	-10
	R lingual G	118	3.79	0.016	12	-90	-6
	R lingual G		3.70	0.019	20	-94	2
	R Cuneus		3.64	0.021	8	-102	-2
	R Calcarine G		3.63	0.022	10	-98	0
Auditory motion localizer							
Left MTa							
	R Superior Temporal G	184	4.39	0.006	60	-26	10
Right MTa							
	R Superior Temporal G	165	5.64	p<0.001	60	-24	16
	R Superior Temporal G		5.33	0.001	60	-34	18

Table S2.3 Psychophysiological interactions (PPI) from the visual and the auditory motion localizers.

Results of the task based functional connectivity (PPI) in the visual motion localizer for the contrast (visual motion > visual static), and in the auditory motion localizer for the contrast (auditory motion > auditory static). The seed regions included bilateral hMT+/V5 and MTa that were defined from the group-level analysis of the visual and auditory motion localizers. Reported results are significant (p<0.05 FWE) after applying a SVC. The coordinates for V1, hMT+/V5, and planum temporale used for the SVC were extracted using the meta-analysis tool neurosynth (Yarkoni et al., 2011). Bilateral V1 [MNI coordinates: -6 -90 -2 and 10 -94 2] was defined from a set of 101 studies. Left and right hMT+/V5 [MNI coordinates: -46 -70 2 and 48 -66 4] were defined from 106 studies. Bilateral planum temporale [MNI coordinates: -60 -32 14 and 58 -30 10] was defined from a set of 97 studies. K represents the number of voxels when displayed at p<0.001 (uncorrected). L: left, R: right, G: gyrus.

	left hMT+/V5	right hMT+/V5	left MTa	right MTa	left PT	right PT
[a] mutli-class decoding (4-way decoding)						
Visual	29.27% ± 7.17%	28.88% ± 8.04%	27.68% ± 7.16%	25.79% ± 6.92%	26.42% ± 6.57%	24.91% ± 5.77%
Auditory	25.40% ± 6.41%	28.60% ± 6.59%	30.85% ± 8.17%	30.65% ± 7.60%	36.65% ± 8.17%	35.13% ± 11.23%
[b] axis of motion decoding (horizontal vs vertical)						
Visual	56.94% ± 8.57%	56.63% ± 7.97%	52.78% ± 6.19%	50.89% ± 7.87%	51.80% ± 9.28%	51.04% ± 9.85%
Auditory	58.93% ± 9.37%	56.63% ± 10.64%	65.58% ± 8.27%	61.90% ± 11.84%	71.21% ± 10.71%	68.84% ± 12.59%
[c] horizontal decoding (rightward vs leftward motion)						
Visual	50.40%±9.02 %	57.39%± 10.75%	52.38%± 13.02%	46.83% ± 9.49%	47.73% ± 11.84%	52.65% ± 11.61%
Auditory	47.22% ± 10.40%	46.97% ± 11.07%	44.64% ± 9.78%	52.18%± 10.34%	48.48%± 10.01%	51.89% ± 11.26%
[d] vertical decoding (upward vs downward motion)						
Visual	53.37% ± 10.99%	46.97% ± 12.61%	51.98%±9. 65%	48.81%± 13.45%	57.58%± 10.65%	51.33%± 13.14%
Auditory	49.80% ± 9.54%	47.35% ± 14.00%	52.58% ± 13.72%	52.78%± 10.81%	56.25%± 11.04%	53.79%± 9.70%

Table S2.4 Within-modality classification results.

Classification results of the different motion directions (mean accuracy ± standard deviation) in each ROI for each modality separately. The multi-class decoding shows the results of classifying the 4 motion directions in each modality (chance level = 25%). The axis of motion decoding shows the results for classifying the horizontal versus the vertical axis (chance level = 50%). The horizontal and vertical decoding shows the results for classifying the two opposite directions that lie in the same axis (chance level = 50%).

Theoretical models	mean r	Standard deviation
Modality-invariant model	-0.3418	0.020
IM-0.1	0.4229	0.0131
IM-0.3	0.5757	0.0122
IM-0.5	0.7480	0.0125
IM-0.7	0.9004	0.0148
IM-0.9	0.9814	0.0180
Multi-modal model	0.9897	0.0194
Unimodal model (visual)	0.6006	0.0294
Unimodal model (auditory)	0.5931	0.0379
Model comparisons	**z-score**	**p-value**
Modality-Invariant – IM-0.1	-41.069	0.000321
IM-0.1 – IM-0.3	-41.069	0.000321
IM-0.3 – IM-0.5	-41.069	0.000321
IM-0.5 – IM-0.7	-41.069	0.000321
IM-0.7 – IM-0.9	-41.069	0.000321
IM-0.9 – Multimodal	-40.744	0.000369
Multimodal – Unimodal (visual)	41.069	0.000321
Unimodal (visual) – Unimodal (auditory)	0.0162	1

Table S2.5 RSA analysis and the comparison of the RSA models' correlation.

The first section of the table illustrates the correlation of each of the theoretical models with the neural DSM from the right hMT+/V5 (mean ± SD). The second section of the table illustrates the statistical comparison between the correlation of the different theoretical dissimilarity models and the neural dissimilarity matrix of right hMT+/V5 using a 2-sided Wilcoxon signed-rank test. The multimodal model had the highest correlation value with the neural DSM of hMT+/V5 than all the other theoretical models. Results were controlled for multiple comparisons using FWE-correction.

Split-half correlation results						
	Left hemisphere			Right hemisphere		
	Vis-Vis	Aud-Aud	Vis-Aud	Vis-Vis	Aud-Aud	Vis-Aud
hMT+/V5						
t-stat	12.308	10.292	-6.907	14.693	12.944	-7.824
p-value	1.562×10^{-9}	3.504×10^{-8}	1.877×10^{-5}	2.885×10^{-11}	3.202×10^{-10}	2.114×10^{-6}
MTa						
t-stat	11.936	9.23	-1.975	9.522	15.291	-0.556
p-value	2.69×10^{-9}	2.152×10^{-7}	1	1.29×10^{-7}	3.038×10^{-11}	1
PT						
t-stat	7.971	14.592	2.673	10.092	11.881	5.079
p-value	1.571×10^{-6}	3.294×10^{-11}	0.256	2.967×10^{-8}	1.575×10^{-9}	8.945×10^{-4}
Comparison between the split-half correlation values in the different conditions						
ROI	Visual - Auditory		Visual - Cross-modal		Auditory - Cross-modal	
	t-value	p-value	t-value	p-value	t-value	p-value
L hMT+/V5	1.21	1	11.38	6.198×10^{-09}	12.38	1.405×10^{-9}
R hMT+/V5	2.79	0.2	13.78	2.056×10^{-10}	14.53	7.764×10^{-11}
L MTa	0.48	1	12.62	1.976×10^{-09}	10.69	3.19×10^{-8}
R MTa	-1.14	1	11.22	1.449×10^{-08}	13.67	4.995×10^{-10}
L PT	-7.82	2.141×10^{-06}	9.97	6.009×10^{-08}	12.79	7.828×10^{-10}
R PT	-3.86	0.017	11.6	4.425×10^{-09}	12.67	9.273×10^{-10}

Table S2.6 Split-half correlation results and the comparison between the SHC values in the different conditions.

The first section of the table illustrates the correlation of the motion direction patterns in the odd and even runs within and across-modalities in each region of interest in the motion decoding experiment. The within-modality split half correlation measures the correlation between the odd and even runs in the visual modality (Vis-Vis), and in the auditory modality (Aud-Aud). The cross-modal split-half correlation measures the correlation of the motion direction patterns between the visual and auditory modality (Vis-Aud). Correlation values were Fisher-transformed and tested against zero. The second section of the table presents the results for the repeated-measures t-test that was performed to compare the split-half correlation values of the visual and the auditory condition, the visual and the cross-modal condition, and the auditory and the cross-modal condition. All p-values were FWE-corrected.

Chapter 3

A brief period of postnatal visual deprivation permanently alters visual motion processing in V1 but not in V5

Mohamed Rezk[1], Stefania Mattioni[1], Xiaoqing Gao[4], Junghyun Nam[2], Zhong-Xu Liu[3], Terri Lewis[5], Daphne Maurer [5], & Olivier Collignon[1,6]

[1] Institut de Recherche en Sciences Psychologiques (IPSY) and Institute of Neuroscience (IoNS), Louvain Bionics, Crossmodal Perception and Plasticity Lab, Université catholique de Louvain (UCL), 1348 Louvain-la-Neuve, Belgium [2] University of Toronto, Canada [3] University of Michigan-Dearborn, USA [4] Zhejiang University, China [5] McMaster University, Canada [6] University of Trento, Italy

---

How does early visual experience shape the development of the visual motion network? To address this question, we used functional magnetic resonance imaging to characterize the brain responses elicited by visual motion in adults born with dense bilateral cataracts that were treated early in life. Our results demonstrate reduced motion selective recruitment of the early visual areas in early cataract-reversal patients (CAT) when compared to matched controls with typical visual development. The reduced recruitment in the early visual cortex in CAT correlated with the duration of visual deprivation. Interestingly, no alterations were observed in the higher order visual motion area hMT+/V5. Psychophysiological interaction analyses however revealed reduced connectivity between hMT+/V5 and V1 during visual motion processing in CAT. Moreover, multivariate pattern analyses indicated reduced motion direction information in V1, but not in hMT+/V5, in the cataract-reversal patients. Altogether these results suggest that a brief and transient period of visual deprivation early in life has a region-specific impact on the visual motion network with V1 being permanently affected while hMT+/V5 showing resilience to deprivation.

Chapter 3

A brief period of postnatal visual deprivation permanently alters visual motion processing in V1 but not in V5

Introduction

Early animal studies highlighted the importance of early visual experience for the development of the visual system (Wiesel & Hubel, 1963a, 1965a). For instance, visual deprivation in one eye in cats even for a few days during the sensitive period early in life can lead to a strong and permanent shift in the ocular dominance to the non-deprived eye (Hubel & Wiesel, 1970). These results compellingly indicated that early visual experience is necessary for the typical development of the visual system.

In humans, the study of congenital bilateral cataract-reversal patients provides a unique "natural" model to test the role early visual experience plays in shaping the development of visual functions. Studies involving congenital bilateral cataract-reversal patients have documented the existence of different sensitive periods during which visual inputs are necessary, or not, for the normal development of different aspects of vision (Maurer et al., 2005). While some aspects of vision do not seem affected by a brief period of visual deprivation early in life like low-frequency discrimination, face discrimination based on the shape of internal features, facial expression discrimination, eye gaze, and lip reading perception (Geldart et al., 2002; Le Grand et al., 2001; Maurer et al., 2006) other aspects of vision like the processing of high-spatial frequencies (Maurer et al., 2006) or the holistic processing of faces (Le Grand et al., 2004) do not develop normally in cataract-reversal patients.

Arguably the most striking impaired visual function in early cataract-reversal patients is the processing of global motion information (Ellemberg et al., 2002; Hadad et al., 2012; T. L. Lewis & Maurer, 2009; Maurer et al., 2005, 2007). For instance, Ellemberg and colleagues tested global motion perception abilities in a group of bilateral cataract-reversal patients that had been visually deprived at birth and for a period lasting from 3 to 8 months (i.e., congenital group) or in a separate group that had been visually deprived between 8 and 57 months of age, after a period of normal visual experience (i.e., developmental group). The congenital group was found to be strongly impaired compared to the developmental group. In the latter group, all participants performed within normal limits, even in cases where vision had been lost as young as 8 months of age and for a period lasting up to 6 months (Ellemberg et al., 2002). These observations suggest that visual deprivation during the first months of life is sufficient to permanently alter global motion perception abilities, whereas visual experience before the age of approximately 8

months may be necessary and sufficient for the normal development of sensitivity to global motion in humans. Consistent with these findings, kittens raised in the dark up to 4 to 12 weeks of age, showed profound and long-lasting deficits in global motion perception following the period of deprivation, provided that it started before 6 weeks of age (Mitchell et al., 2009). Few weeks of early visual deprivation can lead to permanent deficits in global motion processing.

The neurophysiological correlate of such impairment in global motion processing remains unknown. Global motion perception is a visual function associated with the dorsal visual stream (Sunaert et al., 1999; Tootell et al., 1995; Watson et al., 1993). hMT+/V5 is known to process global motion information, and its recruitment during global motion processing increases with increasing the global coherence of motion (Braddick et al., 2001; Rees et al., 2000). Therefore, it was speculated that deficits in global motion processing in cataract-reversal patients originate from impaired functioning of hMT+/V5. In this study, we comprehensively investigated the impact of an early and brief period of visual deprivation on the visual motion processing network and demonstrated a selective alteration in the response properties of V1 but not of hMT+/V5. Additionally, we demonstrate the presence of long-lasting functional connectivity changes within the early visual cortex in the cataract-reversal patients as a result of brief early visual deprivation.

Materials and methods

Participants

Fifteen cataract-reversal patients (7 males, mean age ± SD= 28.26 ± 6.32 years, age range= 18 - 39 years, see Table S3.1) and seventeen matched controls (11 males, mean age ± SD= 29.12 ± 5.71 years, age range= 21 – 39 years) participated in the experiment. Two participants from the cataract-reversal group and one from the control group had a history of depression. All participants were naive to the purpose of the experiment. The protocol was approved by the research ethics committee in the University of Toronto and McMaster University. A written consent was acquired from all participants. Participants were monetarily compensated for their participation. Prior to testing, participants underwent a training session where they were familiarized with the experiments and the required tasks.

Visual tests

Assessment of visual acuity

Visual acuity was assessed using the Freiburg Visual Acuity Test (FrACT; Bach, 1996, 2006). Participants were tested at a distance of 210 cm from the stimulation monitor (CRT monitor of screen width of 53.5 cm, and screen resolution of 800 x 600 pixels). The test run compromised 30 Landolt-C trials that were presented in a random orientation. The size of the stimuli was adjusted on each trial based on the previous responses to estimate the most probable visual acuity threshold by using a maximum-likelihood staircase procedure (Best PEST; Lieberman & Pentland, 1982). The participants performed a forced choice task where they indicated the orientation of the C-stimulus gap (up, down, right, left). The Logarithm of the Minimum Angle of Resolution (logMar) was used as a measure of visual acuity. The visual acuity of the two groups were compared using a two-sample t-test.

Assessment of contrast sensitivity

Contrast is modulated by the difference between the luminance of a stimulus in the foreground and the luminance of the background. The Weber contrast was estimated using the FrACT software (Bach, 1996, 2006) by calculating the luminance difference between the stimulus and the background divided by the maximum luminance [CWeber = (Luminance max – Luminance min) / Luminance max]. The test run compromised 30 trials of a letter "C" with a fixed diameter of 30 arc minutes with varying contrast at the center of the screen that changed its orientation randomly on each trial. The participants performed a forced choice task where they indicated the orientation of the stimulus. The difference in luminance between the stimulus and the background was adjusted on each trial using a maximum-likelihood staircase procedure (Best PEST; Lieberman & Pentland, 1982) that relied on the subject's responses in the previous trials. The logarithm of the inverse Weber contrast (logCS Weber) was used as a measure of contrast sensitivity. The contrast sensitivity of the two groups were compared using a two-sample t-test.

Assessment of motion sensitivity

Stimuli: Visual stimuli were presented on a CRT monitor (screen width: 53.5 cm, screen resolution: 800 x 600 pixels). The visual stimuli consisted of random dot kinematograms (RDK) within an invisible circular aperture of 25 visual degrees centered around a white fixation cross. Each visual event was composed of 100 white dots (diameter= 1°) on a black background. Motion dots had a speed of 4°/s and a limited dot lifetime of 200 ms. Dots moved in one of four possible motion directions [upward, downward, rightward, and leftward] depending on the performed experiment.

To assess the behavioral performance in global motion direction discrimination, we ran three behavioral experiments using a two-forced choice paradigm. In the first experiment, the participants performed a motion direction discrimination task within the horizontal plane where the participants indicated whether the RDKs moved rightward or leftward. In the second experiment, the participants indicated whether the RDKs moved upwards or downwards (vertical plane). In the third experiment, the participants indicated whether the RDKs moved in the horizontal (alternating between rightward and leftward motion) or the vertical plane (alternating between upward and downward motion). In each of these experiments, we used an adaptive QUEST staircase procedure (Watson & Pelli, 1983) to determine the coherence level of the presented RDKs in the different trials. The experiments estimated the necessary coherence threshold to achieve 75% behavioral performance. Each experiment had 60 trials where each event lasted 1.2 s. Events were separated by an inter-trial interval of 5 s. The participant's head was stabilized on a chin-rest while they performed the experiment (distance from monitor= 60 cm).

The statistical analysis included a mixed ANOVA with the three motion discrimination conditions as within-subject factors, and the group as a between-subject factor. A Greenhouse-Geisser correction was applied whenever the assumption of sphericity was violated. Post-hoc pairwise t-tests were performed to compare the two groups, and to compare the different motion discrimination conditions combined across the two groups. Results were corrected for multiple comparisons using Bonferroni correction.

Additionally, we tested whether the estimated behavioral thresholds in the cataract-reversal patients correlated with the duration of visual deprivation. In each experiment, we tested whether the estimated coherence thresholds, to achieve 75% behavioral accuracy, were correlated with the duration of visual deprivation in the cataract reversal patients.

fMRI experiments

Stimuli: Visual stimuli were projected on a screen (frame rate: 60 Hz; screen resolution 1920 x 1080 pixels) behind the scanner. Participants viewed the screen (distance from head= 45 cm) through a mirror mounted on the MRI head coil. Participants performed a task in each experiment by responding with an MR-compatible response button. Visual stimuli consisted of RDKs within an invisible circular aperture of 25 visual degrees centered around a white fixation cross. Each visual event was composed of 120 white dots (diameter= 1°) on a black background. Motion dots had a speed of 12°/s and a limited dot lifetime of 200 ms. The use of the limited lifetime ensures that motion direction discrimination could be achieved by relying on the global motion perception rather than focusing on a single dot (Bex et al., 2003). Dots moved in one of four possible motion directions [upward, downward, rightward, and leftward] with 100% coherence level. Each

visual motion event lasted 1.2 s. In the visual static condition, each static event had RDKs of 120 dots that remained static. The location of the dots was randomized in each event.

Experimental design (Experiment I): Motion selectivity Experiment

We implemented a motion selectivity experiment to localize regions showing enhanced recruitment during visual motion processing. Visual motion and static conditions were generated using white RDKs on a black background. Dots moved in one of four possible motion directions [upward, downward, rightward, and leftward]. The motion selectivity experiment started with an initial 2 s of blank screen and ended with 13 s of blank screen. The run had 6 blocks of motion and static conditions. Blocks were separated from each other with an inter-block interval (IBI) of 8 s. Each block had 12 events (1.2 s for normal events, and 0.6 s for target events), and an inter-stimulus interval (ISI) of 0.1 s. Each motion block had 3 repetitions of the 4 motion directions presented in random order. In the static condition, the location of the dots was randomly changed for each event (inducing 12 changes within one block). The fixation cross was presented during the whole duration of the visual localizer. To minimize eye movements and saccadic shifts (Corbetta et al., 1998; Petit & Haxby, 1999a), the participants were asked to detect a brief change (150 ms) in the fixation cross color. Moreover, the participant was additionally asked to detect the presence, within a block, stimuli with faster speed (24°/s) and shorter duration (0.6 s). The number of targets (range: 1-2 in each block) was randomized and balanced across conditions.

Experimental design (Experiment II): Directional motion decoding experiment

The directional motion decoding experiment was composed of 10 runs, each run comprising 4 motion blocks. Each motion block had stimuli moving in one of four possible directions [upward, downward, rightward, or leftward]. Each run started with an initial 5 s of black screen and ended with 11 s of blank black screen. Each block had 10 events of a 1.2 s, all moving in the same direction. Events were separated by a 100 ms inter-trial interval resulting in a block duration of 13 s. Blocks were separated from each other with an inter-block interval (IBI) of 6 s. To ensure fixation and to minimize eye movements during the motion blocks, the participants were asked to press a button whenever the fixation cross changed color (duration= 150ms). Moreover, the participant was additionally asked to detect the presence, within a block, stimuli with faster speed (24°/s) and shorter duration (0.6 s). The order of the blocks was randomized in each run.

MRI acquisition

Structural and functional data were acquired at the Sherman Health Science Research Centre (University of York, Toronto, Canada) using a Siemens MAGNETOM 3T PrismaFit MRI scanner with a standard 64 channel head coil. Structural high-resolution T1-weighted MPRAGE scans were acquired using parallel imaging (GRAPPA factor = 2). The acquisition parameters for the T1 images included a repetition time (TR) of 2300 ms, echo time (TE) = 2.62 ms, voxel size = 1 mm isotropic voxels, number of slices=192, and a flip angle of 9°. Functional scans were acquired using T2*-weighted echoplanar BOLD imaging for the visual motion selectivity experiment and the motion decoding experiment. The acquisition parameters included simultaneous interleaved multi-slice acquisition using parallel imaging with multiband acceleration = 2, phase encoding acceleration = 3, TR = 1170 ms, TE = 30ms, voxel-size = 2 mm isotropic voxels, number of slices = 51, flip angle = 66°, and echo-spacing 0.68 ms. The first four initial scans of each run were discarded to allow for equilibrium magnetization.

fMRI preprocessing

fMRI data was preprocessed in statistical parametric mapping software (SPM12 – Wellcome Department of Imaging Neuroscience, University College London, UK) implemented in Matlab R2017b (Mathworks, Inc.). Preprocessing steps included slice time correction, EPI alignment to the mean functional image with a 2nd degree B-spline interpolation, co-registration of the functional volumes to the structural image and normalization to the Montreal Neurological Institute (MNI) template.

Experiment 1 (Motion selectivity experiment)

Univariate analysis

Functional data were spatially smoothed with a 6-mm full-width half-maximum (FWHM) smoothing kernel for the univariate analysis. For the motion selectivity experiment, a general linear model (GLM) was fitted for every voxel with the visual motion and the visual static conditions as regressors of interest. Each regressor was modeled with a boxcar function and convolved with the canonical hemodynamic response function (HRF). The 6 head motion parameters (3 translation and 3 rotation parameters) were included in the model as regressors of no interest. A high-pass filter of 128 s was used to remove low frequency signal drifts. The contrast [Motion > Static] was computed for every subject individually (Huk et al., 2002; Tootell, Reppas, Kwong, et al., 1995). Then a standard group-level analysis was performed. The individual contrasts were further smoothed with a 6-mm FWHM kernel and entered into a random effects model for the second-level analysis. A one-sample t-test was performed, and group-level statistical inferences were made at a

voxel-level threshold of $p<0.05$, Family-wise error (FWE)-corrected. Additionally, we performed a conjunction analysis to define regions that were activated more in the motion condition than the static condition in both groups at a statistical threshold of $p<0.05$ FWE-corrected. To compare the two groups, a two-sample two-sided t-test was implemented. Results were corrected for multiple comparisons using threshold-free cluster enhancement (TFCE) (S. M. Smith & Nichols, 2009).

In a complementary analysis, we investigated whether the differences between the cataract-reversal patients and controls could be attributed to a general lower level of recruitment of the visual cortex in the cataract-reversal patients when processing visual stimuli, and not motion processing per se. Therefore, we tested whether the visual static stimuli [Contrast: Static > Baseline] elicited lower responses in the visual cortex in the cataract reversal patients. The same analysis was applied for the motion condition [Contrast: Motion > Baseline] (Fig S3.1).

Correlation

We tested whether the changes in motion selectivity in the cataract-reversal patients were correlated with their behavioral performance in motion direction discrimination from the behavioral experiment that was done outside the MRI. To have one measure from the three different behavioral experiments, we calculated the average coherence level across the three experiments that was estimated to give a 75% behavioral performance in each subject. The average behavioral thresholds were entered in a regression model which was fitted in every voxel in the brain. We tested whether the behavioral thresholds correlated with the motion selectivity [Motion > Static] in the cataract-reversal patients.

Additionally, we tested whether the duration of visual deprivation in the cataract-reversal patients correlated with the motion selectivity. The duration of visual deprivation was estimated as the period until the first cataract removal surgery was performed. A regression model was fitted in each voxel in the brain to identify regions showing a correlation between motion selectivity and the duration of visual deprivation. Results were Family-wise error corrected using a small volume correction (SVC) centered on regions of interest (Worsley et al., 1996).

We also investigated whether the reduced motion selectivity in the cataract-reversal patients was correlated with visual acuity or contrast sensitivity. We used the estimated logMar and logCS values obtained from the acuity and the contrast sensitivity testing in the cataract-reversal patients. We performed a whole-brain voxel-wise analysis where we fitted a regression model in each voxel to test for a correlation between motion selectivity and visual acuity or contrast sensitivity in the cataract-reversal patients.

Functional connectivity analysis (PPI)

Psychophysiological Interaction (PPI) analysis (Friston et al., 1997; Gitelman et al., 2003) identifies voxels in which the activity is more related to the activity in a seed region of interest (seed ROI) in a given psychological context. In the present study, PPI analyses were performed to test if the task-based functional connectivity profile of the motion selective region hMT+/V5 differed across the two groups when processing motion versus static. We defined the hMT+/V5 seed regions from the conjunction analysis between the two groups of the Motion>Static contrast. In each subject in each group, we extracted the time series (first eigenvariate) from a sphere (5 mm radius) around the peak of the left [-38 -76 4] and the right hMT+/V5 [44 -66 2].

A first-level GLM analysis was performed in each subject where the model included the following regressors: [1] psychological regressor [motion>static], [2] the extracted activity from the seed region (physiological regressor), [3] and the interaction term (PPI) between the previous two regressors. The PPI term was estimated by first deconvolving the BOLD activity to estimate the neuronal response in the ROIs (Gitelman et al., 2003). The interaction term was calculated as the element-wise product of the estimated neuronal activity and the psychological regressor. The interaction term was further convolved with the canonical HRF. The six head motion parameters were included in the model as regressors of no interest. After estimating the PPI models for each subject, a random effects model was constructed and a one-sample t-test was performed in each group to test for regions that showed enhanced task-based correlation with hMT+/V5 when processing motion. Additionally, a two-sample t-test was performed to compare the hMT+/V5 connectivity profile from the two groups. Additionally, we tested the connectivity profile of the early visual cortex where we observed a difference between the two groups. We defined seed regions in the left and [-14 -98 2] right early visual cortex [16 -92 2] and performed the same analysis PPI analysis.

Retinotopic motion selectivity

The results from the univariate analysis demonstrated that deficits in visual motion processing were prominent in the early visual cortex. To further investigate the impairments in visual motion processing in V1, we tested whether the impairments in visual motion processing were limited to specific retinotopic regions in V1. To do so, we used a technique that performs retinotopic mapping in the early visual areas based on anatomy and surface topology. This technique fits a group and anatomically-defined template to each participant's anatomical image while correcting for distortions caused by cortical folding (Benson et al., 2012, 2014). Retinotopic eccentricity maps in the native subject's space are produced. The eccentricity maps reflect the preference of each voxel to a specific location in the visual field measured in the distance (in degrees) from the fovea. In each subject, we

masked the generated retinotopic maps with the subject-specific V1 mask (in the native volumetric space). We then divided the subject-specific V1 into four sub-modules. A foveal-V1 ROI comprising bilateral V1 voxels that have an eccentricity preference less than 12.5 visual angles, a para-foveal V1 ROI with bilateral V1 voxels that have an eccentricity preference in the range of 12.5 - 25 visual angles, a peripheral V1 ROI with bilateral V1 voxels that have an eccentricity preference in the range of 25 - 50 visual angles, and a far-peripheral V1 ROI with bilateral V1 voxels that have an eccentricity preference in the range of 50 - 75 visual angles.

To test if motion selectivity and the recruitment of V1 is modulated by eccentricity, condition, or group [cataract-reversal patients/controls], we extracted the beta parameter estimates from the eccentricity-based V1 ROIs (n=4), in each condition [motion and static], in the native space of each subject in each group [cataract-reversal patients/controls]. To compare the beta estimates, we ran a 3-way ANOVA [eccentricity ROIs x condition x Group]. Post-hoc pairwise comparisons were performed and corrected for multiple comparisons using FWE-correction.

Experiment 2 (Directional motion decoding experiment)

For the directional motion decoding experiment, the preprocessing steps were similar to the ones implemented in the univariate analysis except that we applied minimal smoothing (2 mm) to the functional data to improve the signal-to-noise ratio while still maintaining a fine-grained multivariate response profile for each motion direction within a ROI. A general linear model (GLM) analysis was performed to estimate the BOLD signal for every voxel. The GLM included a separate regressor for each motion in each run. Each regressor was convolved with the canonical HRF. The six head motion parameters (3 translation and 3 rotation) for each run were included in the model as regressors of no interest. For each run, t-maps were estimated for each motion direction using the contrast [motion direction > baseline]. The t-maps were used for further MVPA.

ROI definition for MVPA

The motion selectivity experiment (Experiment I) indicated that while hMT+/V5 was recruited in both groups with no statistical difference, the early visual cortex was significantly less recruited in the cataract-reversal patients. To test the differences between V1 and V5, we used a probabilistic atlas (L. Wang et al., 2015) to define V1 [by combining both dorsal (V1d) and ventral V1 (V1v) ROIs from the probabilistic atlas into one ROI] and the motion selective area (MT) in each hemisphere. MT is a part of the hMT+/V5 complex that does not include the MST or FST regions that also process visual motion information. We tested whether we could predict the perceived motion direction from the elicited activity patterns in these ROIs.

Control analysis ROI

The size of the MT ROI in the probabilistic atlas was smaller (compared to the V1 ROIs), therefore, the lower decoding in MT or the absence of difference between the two groups could be possibly attributed to the lower number of features. To control for this possible confound, we performed 2 control analyses. In the first control analysis, we used the group-level functionally-defined hMT+/V5 from the conjunction analysis from the motion selectivity experiment. The hMT+/V5 complex includes an agglomeration of motion sensitive structures notably composed of multiple sub-regions as MT, MST, and FST (Huk et al., 2002; Morrone et al., 2000; Smith et al., 2006). In each hemisphere, we created a sphere of 10 mm radius centered around the peak coordinate of the group-level hMT+/V5 from the conjunction analysis. These ROIs had a larger number of features that was comparable to those from the V1 ROIs from the probabilistic atlas. Additionally, we tested whether there were group differences in decoding the motion directions in the hMT+/V5 ROIs when varying the number of features by changing the radius of the sphere from 4 mm to 10 mm.

In the second control analysis, we used individually defined hMT+/V5 using the data of the first experiment to test if we can predict the perceived motion directions in the two groups. The choice for using individually defined ROIs is motivated by hMT+/V5 having high variability in anatomical location across individuals (Dumoulin et al., 2000; Huk et al., 2002; Large et al., 2016). The individually-defined hMT+/V5 was identified functionally in each subject as the area that responded significantly to motion more than static in the occipito-temporal cortex and passed a statistical threshold [t-value > 2]. It was constrained by the anatomical location of hMT+/V5 where the peak coordinate had an Euclidean distance not more than 10-mm away from the group-level hMT+/V5 peak coordinate defined from the conjunction analysis. The peak coordinate of hMT+/V5 in each subject was used to create a 10-mm radius sphere to be used as individually-defined ROIs in the multivariate analysis (See Table S3.2 for the hMT+/V5 MNI coordinates in each subject). Additionally, we tested whether there are group differences in hMT+/V5 when using ROIs with different sphere sizes (from 4 mm to 10 mm radius).

Multivariate pattern analysis

The Multivariate pattern analysis (MVPA) was performed using CoSMoMVPA (http://www.cosmomvpa.org; (Oosterhof et al., 2016)) implemented in Matlab. The MVPA was performed using a linear discriminant analysis (LDA) classifier. A classifier was trained and tested to discriminate the four motion directions in each subject individually in V1 and MT (defined from the probabilistic atlas), as well as the group-level and the individually-defined hMT+/V5. A leave-one run out cross-validation scheme was implemented. In each cross-validation fold, the training data (9 runs) were normalized (z-

scored) across directions and the classifier was trained to discriminate the patterns from the four motion directions. The normalization parameters from the training data were applied to the test data, and the performance of the LDA classifier was evaluated on the test data (1 run). The previous step was repeated 10 times (N-fold cross-validation) where in each fold the classifier was tested on a different run. A single classification accuracy was obtained by averaging the classification accuracies for all the cross-validation folds. If the classifier could successfully discriminate the different motion directions above chance (25%), this would indicate the presence of motion direction information in the tested ROI that the classifier was able to learn during the training.

Due to the very large size of the V1 ROIs (number of voxels > 1000), we used a feature selection approach when performing the classification analysis in the V1 ROIs. In each cross-validation fold, an ANOVA-based feature selection was implemented on the training data to identify the most informative 500 voxels on which the classifier was trained and tested. Additionally, in a supplementary analysis, we investigated the effect of varying the number of V1 features (n= 200- 600) on the classification analysis (See Figure S3.2).

To assess the statistical significance of the classification in each group and each ROI, the classification results were assessed using a non-parametric technique by combining permutations and bootstrapping (Stelzer et al., 2013). For each subject in each group, the labels of the different motion directions were permuted, and the same decoding analysis was performed. The previous step was repeated 100 times for each subject. A bootstrap procedure was applied in order to obtain a group-level null distribution that was representative of the whole group. From each subject's null distribution, one value was randomly chosen (with replacement) and averaged across all participants. This step was repeated 100,000 times resulting in a group-level null distribution of 100,000 values. The statistical significance of the MVPA results was estimated by comparing the observed result to the group-level null distribution. This was done by calculating the proportion of observations in the null distribution that had a classification accuracy higher than the one obtained in the real test. To account for the multiple comparisons, all p-values were corrected using Bonferroni correction. To compare the classification results across groups in V1, we ran a 3-way ANOVA [ROI (dorsal/ventral), Group (control/cataract-reversal), Hemisphere (left/right)]. Similarly, in hMT+/V5, we ran a 2-way ANOVA [group x hemisphere] to test for differences across groups or hemispheres.

Correlation

We tested whether the motion direction classification results in the cataract-reversal patients were correlated with their behavioral performance in motion direction discrimination from the behavioral experiments that were done outside the MRI. To have one estimate from all the behavioral experiments, we calculated the average coherence level

across the three experiments that was estimated to give a 75% behavioral performance in each subject. The average coherence thresholds were then correlated with the classification results in bilateral V1 and MT as defined from the probabilistic atlas (L. Wang et al., 2015), functionally defined group-level hMT+/V5, and individually defined hMT+/V5 ROIs. Additionally, we tested whether the duration of visual deprivation, or visual acuity, or contrast sensitivity correlated with the motion direction classification results in any of the ROIs. The results were corrected for multiple comparisons using Bonferroni correction.

Bayesian analysis

Using parametric statistical analysis, our results demonstrated no difference between motion direction classification in hMT+/V5. To further evaluate the similarities/differences between the two groups, we used Bayesian statistical analysis to evaluate the evidence for the null hypothesis (no differences between the cataract-reversal patients and the controls) and the alternative hypothesis (the presence of difference between the two groups) in MT (as defined from the probabilistic atlas (L. Wang et al., 2015), the functionally defined group-level, and individually-defined hMT+/V5 ROIs in each hemisphere. The Bayes factor (BF) values obtained from the analysis represent a measure of how strongly the data supports either the null hypothesis or the alternative hypothesis. A BF less than 1 provides moderate evidence for the null hypothesis, while a high BF (more than 3) provides strong evidence for the alternative hypothesis (Wagenmakers et al., 2010; Wetzels et al., 2011). The Bayesian analysis was performed using JASP (JASP Team, 2020).

Split-half correlation analysis

In addition to the pattern classification, we investigated how stable is the representation of individual motion directions in the visual motion network. To test for the stability of the elicited activity patterns in the early visual area (V1) and the higher order visual area MT, we used the ROIs defined from the probabilistic atlas (L. Wang et al., 2015) to perform a split-half correlation analysis (Haxby et al., 2001). The t-maps of the odd and even runs were averaged separately resulting in one t-map per motion direction for the odd runs, and one t-map per direction for the even runs. We used Pearson's correlation as a measure of similarity. In each participant, we correlated the activity patterns of each motion direction in the odd runs with the patterns from the even runs. The correlation of the four motion directions was then averaged resulting in one correlation value which was indicative of the pattern stability in each ROI and in each subject in each group. The correlation values were Fisher-transformed to fulfil the assumption of normality to perform parametric statistical tests on the correlation data. For each group, the Fisher-transformed correlation values were tested against zero using a one-sample t-test. Results were corrected for multiple comparisons using FWE-correction. For each ROI, V1 and MT, a 2-way

ANOVA was implemented with hemisphere (left/right), and group (cataract-reversal patients/controls) as factors. The same analysis was also performed in the individually-defined hMT+/V5 ROIs.

Structural analysis

We investigated whether there were morphometric differences (surface area, cortical thickness or cortical volume) between the cataract-reversal patients and the matched controls in V1 and MT (as defined in freesurfer (Fischl et al., 2008; Hinds et al., 2008)). Structural morphometric analysis was performed in freesurfer (www.surfer.nmr.mgh.harvard.edu). The automated reconstruction of the structural T1-weighted images included the removal of non-brain structures, intensity normalization (Sled et al., 1998), segmentation of white and gray matter tissue (Fischl et al., 2004a, 2004b), topology correction (Fischl et al., 2001), and cortical surface reconstruction. The cortical thickness was calculated as the average shortest distance between the Grey matter/white matter boundary and pial surface across the cortical mantle. The cortical volume was obtained by multiplying the surface area by cortical thickness (Fischl & Dale, 2000). To compare the two groups in V1 and MT for each of the morphometric measures, a 2-way ANOVA was implemented with hemisphere and group as factors.

Experiment III (Resting-State)

Participants

Eleven cataract-reversal patients (7 males, mean age ± SD= 26.82 ± 6.08 years, age range= 19 – 35 years; 9 of the 11 cataract-reversal patients participated in experiment I and II) and fifteen matched controls (7 males, mean age ± SD= 25.47 ± 4.36 years, age range= 17 – 36 years) participated in the experiment.

MRI acquisition

Structural high-resolution T1-weighted MPRAGE scans were acquired using parallel imaging (GRAPPA factor = 2). The acquisition parameters for the T1 images included a TR of 2300 ms, TE = 2.62 ms, voxel size = 1 mm isotropic voxels, number of slices=192, and a flip angle of 9°. Functional scans included 240 T2*-weighted echoplanar BOLD images for the resting state experiment. Acquisition parameters included simultaneous interleaved multi-slice acquisition using parallel imaging (GRAPPA factor = 2), TR=2250 ms, TE=30ms, voxel-size = 3 x 3 x 3.5 mm, number of slices=37, flip angle= 90°, and echo-spacing 0.72 ms. The first four initial scans were discarded to allow for equilibrium magnetization.

Regions of interest: ROIs were defined from the results of experiment I. The ROIs included hMT+/V5 defined from the conjunction analysis, and the early visual cortex where differences between the groups were observed. The ROIs in each hemisphere were defined by creating a 10-mm sphere centered around the peak coordinates of these regions as defined from experiment I. Additionally, we included the lateral geniculate nucleus (LGN) as a possible alternative sub-cortical route for information to reach hMT+/V5. The LGN ROI was defined from the Jülich brain atlas (Eickhoff et al., 2005).

Resting-state functional connectivity analysis

The preprocessing steps were identical to the performed steps in experiment 1. However, since functional connectivity measures are highly sensitive to motion (Power et al., 2012; Satterthwaite et al., 2012; Van Dijk et al., 2012), we implemented a scrubbing approach using Artifact detection tools (ART; www.nitrc.org/projects/ artifact_detect) to identify outlier volumes that had a difference in scan-to-scan global intensity more than 9 standard deviations away from the mean global brain signal, or volumes that had more than 2 mm of scan-to-scan composite motion.

A component-based noise correction (Compcorr) (Behzadi et al., 2007) strategy was implemented to control for nuisance effects and physiological noise. Motion parameters and their first derivatives, and outlier time points that were defined from the scrubbing approach were included as first level covariates to remove the variance related to head motion. Linear detrending and a band-pass filter of 0.008-0.09 Hz was applied to the functional data. First level analysis was performed in the CONN functional connectivity toolbox (Whitfield-Gabrieli & Nieto-Castanon, 2012) to investigate functional connectivity changes within-subject. Pearson's correlation coefficient was used as a measure of functional connectivity. Age was added as a second-level covariate of no interest in all analyses to rule out the effect of age on the connectivity changes between groups

ROI-to-ROI functional connectivity

The ROIs included in the analyses were the early visual cortex, hMT+/V5, and the LGN in each hemisphere (total number of ROIs= 6). The bold time series from each ROI was extracted by averaging the unsmoothed functional time series from all the voxels within the ROI. The time series from the seed region was correlated with the rest of the ROIs. The correlation coefficients were fisher transformed to fulfill the assumption of normality of the data and to be used for parametric statistical testing. Two-sided two-samples t-test was performed to assess differences in the functional connectivity between the two groups. Results were corrected for multiple comparisons using FWE-correction for the number of all possible pairwise connections (n= 15).

Seed-to-voxel functional connectivity

We also tested the resting-state functional connectivity of the LGN with the rest of the brain. It has been suggested that in the case of the damage of the early visual cortex, visual information can reach hMT+/V5 through subcortical routes from the LGN (Ajina, Pestilli, et al., 2015; Ajina & Bridge, 2018, 2019). The time series from the left and right LGN was extracted by averaging the signal from all the voxels in the seed ROI. The time series from each seed was then correlated with each voxel in the rest of the brain. The correlation coefficients were fisher transformed to perform second-level statistical analysis. A one-sample t-test was implemented to test the resting-state connectivity of the LGN in each group. The two groups were compared using a two-sample t-test. The statistical threshold was set at $p<0.001$ at the voxel level and FDR-corrected $p<0.05$ at the cluster level.

Results

Visual tests

Assessment of visual acuity

We investigated the visual acuity of cataract-reversal patients and their matched controls using the FrACT software (Table S3.1; Bach, 1996, 2006). The logMar was used as a measure of visual acuity. The results demonstrated a significant difference between the two groups ($t(30) = 4.56$, $p = 0.0001$), where the logMar values of the cataract-reversal patients (mean ± SD = 0.22 ± 0.17) were higher than that of the controls (mean ± SD = 0.01 ± 0.07), indicating lower acuity in the cataract-reversal patients.

Assessment of contrast sensitivity

We also investigated the contrast sensitivity in the cataract-reversal patients and their controls using FrACT (Table S3.1; Bach, 1996, 2006). The logarithm of the inverse Weber contrast (logCS Weber) was used as a measure of contrast sensitivity. The analysis demonstrated that the contrast sensitivity in the cataract-reversal patients (mean ± SD = 1.57 ± 0.15) was lower than that in the controls (mean ± SD = 1.72 ± 0.09, $t(30) = -3.26$, $p = 0.0028$).

Behavioral results:

To assess the behavioral performance of the cataract-reversal patients in motion processing, we estimated the necessary coherence level to achieve 75% behavioral

performance in the horizontal, vertical, and plane motion discrimination. In the controls, the estimated thresholds were 17.93% ± 7.70% for horizontal motion discrimination, 17.14% ± 6.37% for vertical motion discrimination, and 16.43% ± 3.97% for plane motion discrimination. For the cataract-reversal group, the estimated thresholds were 42.99% ± 21.27% for horizontal motion discrimination, 39.43% ± 14.41% for vertical motion discrimination, and 30.99% ± 11.08% for plane motion discrimination. The mixed ANOVA indicated a main-effect of condition ($F(2,60)= 4.83$, $p=0.021$), a main effect of group ($F(1,30)= 37.69$, $p<0.001$), and no interaction ($F(2,60)= 3.014$, $p=0.075$). The post-hoc analyses indicated that the coherence thresholds for the plane discrimination (mean ± SD = 23.25% ±10.86%) was significantly lower than the horizontal discrimination (mean ± SD = 29.67% ± 19.91%; $t(31)= -3.04$, $p= 0.0143$; FWE-corrected). When comparing the two groups across the combined motion discrimination conditions, the coherence thresholds necessary to achieve 75% behavioral performance in the cataract-reversal group (mean ± SD = 37.8% ± 16.58%) was significantly higher than the control group (mean ± SD = 17.17% ± 6.11%; $t(94)= 8.28$, $p= 8.33x10^{-13}$).

Additionally, we tested whether the estimated coherence thresholds in each experiment correlated with the duration of visual deprivation in the cataract-reversal patients. We found no correlation between the duration of the visual deprivation in the cataract-reversal patients and the behavioral performance in the horizontal motion ($R^2= 0.029$, adjusted-$R^2= -0.045$, $p= 0.541$), vertical motion ($R^2= 0.024$, adjusted-$R^2= -0.051$, $p= 0.581$), or the plane motion experiment ($R^2= 0.128$, adjusted-$R^2= 0.061$, $p= 0.190$).

Experiment I: Motion selectivity

Inside the MRI, the participants detected a brief change in the fixation cross color and events that were faster and shorter in duration. The controls (mean ± SD= 93.06% ± 5.53%) and the cataract-reversal patients (mean ± SD= 85.63% ± 15.01%) performed the task with high accuracy. No significant difference was observed between the two groups ($t(30)= 1.904$, $p = 0.07$).

We investigated which regions were recruited during global motion processing in the two groups. The group-level analysis indicated that both groups recruited the calcarine gyrus (V1), the middle temporal gyrus (hMT+/V5) bilaterally [MNI peak coordinates: -38 -76 4 and 44 -66 2] (Figure 3.1, Table S3.3) and intraparietal regions. When comparing both groups, the early visual areas within the visual motion network showed reduced recruitment in the cataract reversal group compared with the control group. No differences were observed between the two groups in the higher order visual area hMT+/V5 even at lenient thresholds.

In a supplementary analysis, we also investigated whether the differences between the two groups could be a result of a reduced recruitment of the visual cortex in the cataract-reversal patients when processing any visual stimuli. When comparing the two groups when processing visual static stimuli, no differences were observed in the early visual cortex even at lenient thresholds. Differences between the two groups in the early visual cortex only appeared when processing visual motion stimuli demonstrating that the differences between the two groups are related to motion processing (Fig S3.1).

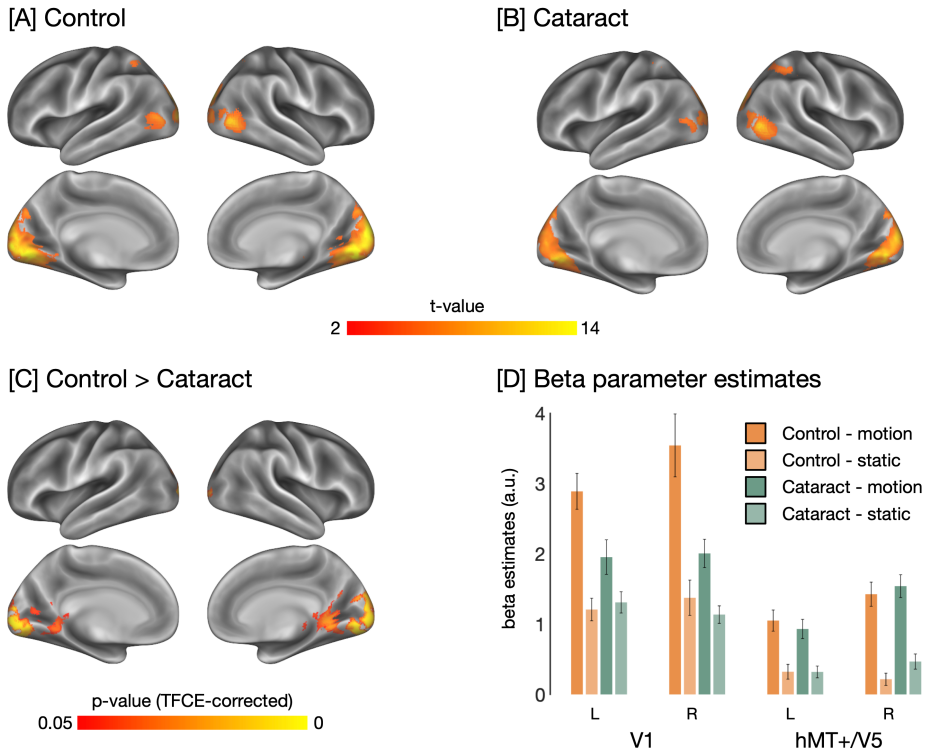


Figure 3.1 Univariate results from the motion selectivity experiment.

The univariate results for the contrast [motion > static] in [A] the control and [B] the cataract-reversal group showing the recruitment of the visual motion network including the early visual areas and the higher-order visual area hMT+/V5. Results are FWE corrected at statistical threshold of $p<0.05$ and displayed on an inflated brain (Marcus et al., 2013). [C] The comparison between the two groups demonstrated reduced recruitment of the early visual cortex in the cataract-reversal patients. Results are corrected for multiple comparisons using threshold free cluster enhancement (TFCE) at a statistical level of $p<0.05$ (FWE-corrected). [D] Beta parameter extraction was performed in the early visual cortex (V1), where a significant difference between the two groups was observed, and in hMT+/V5 as defined from the group-level conjunction analysis. A sphere of 5-mm radius was created around the group-level coordinates and the mean beta parameter estimates were extracted. The beta parameter estimates are for illustration purposes. No statistical analysis was performed to avoid circularity as these regions were defined from the univariate analysis.

Correlation

We tested whether there was a correlation between the motion selectivity and the duration of visual deprivation. The whole-brain regression analysis indicated that there was a significant negative correlation in the early visual cortex between the motion selectivity and the duration of visual deprivation (Figure 3.2A; Table S3.4). As the duration of visual deprivation increased, the motion selectivity decreased in the early visual cortex. In our data, we did not observe any significant correlation in the higher order visual regions (or hMT+/V5) even at lenient thresholds. We also tested whether there was a correlation between the behavioral performance in the behavioral experiment outside the scanner and the motion selectivity in the cataract-reversal patients. We do observe a strong trend for a negative correlation in the early visual cortex, but not statistically significant (Fig. 3.2B). This trend suggested that when the behavioral performance was worse (higher coherence thresholds) in the cataract reversal patients, the motion selectivity was lower in the early visual cortex (Figure 3.2). We also investigated whether there was a correlation between motion selectivity and visual acuity or contrast sensitivity in the cataract-reversal patients, however, we did not observe any correlation between motion selectivity and any of the visual measures.

Functional connectivity analysis (PPI)

The PPI analyses (Friston et al., 1997; Gitelman et al., 2003) investigated the connectivity profile of hMT+/V5 during processing motion compared to static in the cataract-reversal patients and the control group. As expected, hMT+/V5 showed enhanced connectivity with the visual motion network including the contralateral hMT+/V5 as well as the early visual areas in both groups. When comparing the two groups, hMT+/V5 showed reduced connectivity with the early visual cortex in the cataract-reversal group (Figure 3.3, Table S3.5). V1 showed a non-significant trend for reduced contralateral V1 connectivity (Figure 3.3, Table S3.5).

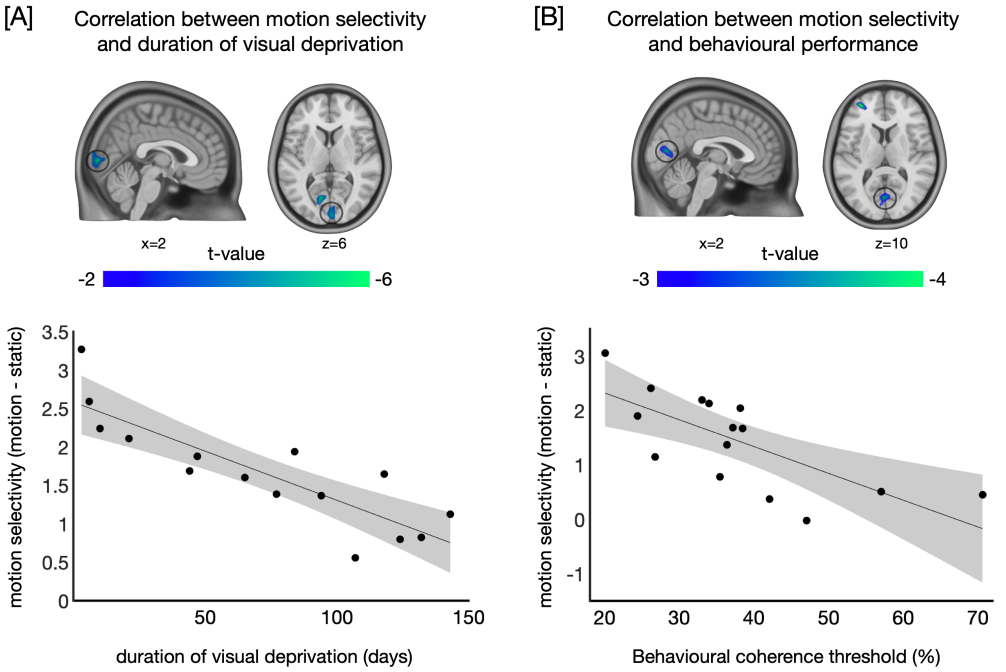


Figure 3.2 Correlation analysis in the cataract-reversal patients.
The correlation results between the motion selectivity [motion > static] and the duration of visual deprivation was statistically significant in the early visual cortex. The correlation in the significant cluster in the early visual cortex is visualized in the lower panel (no statistical analysis was applied). [B] The correlation between the motion selectivity [motion > static] and the behavioral performance was not significant, however, a trend was observed in the early visual cortex. The visualization of this trend is presented in the lower panel. The results are displayed at p<0.005 uncorrected.

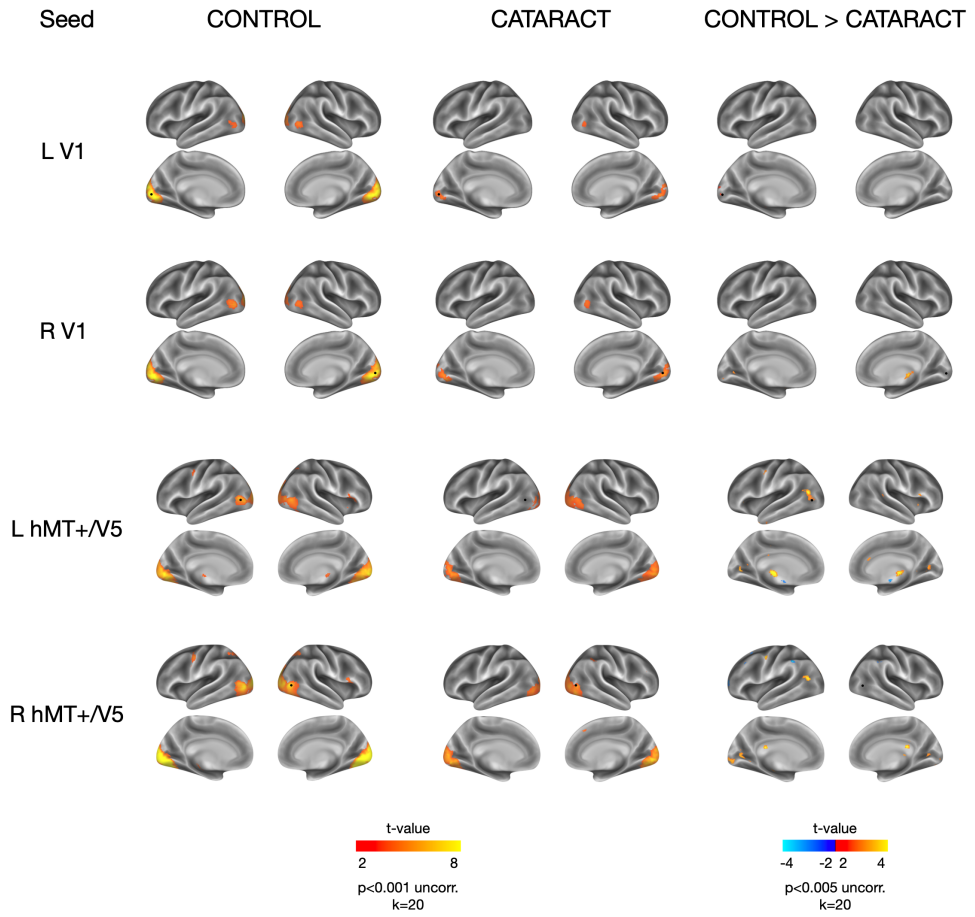


Figure 3.3 PPI Analysis in the motion selectivity experiment.
The PPI analysis was performed using the early visual cortex (V1), hMT+/V5, and LGN as seed regions. Regions showing increased task-based functional connectivity with the seed region for the contrast [motion > static] in the controls and the cataract-reversal patients are displayed in warm colors. Results are displayed at p<0.001 uncorrected (minimum cluster size = 20). The third column displays the group comparison with the contrast [control > cataract] in warm colors, and the contrast [cataract > controls] in cold colors. Results are displayed at p<0.005 uncorrected (minimum cluster size = 20). L, left hemisphere; R, right hemisphere.

Retinotopic motion selectivity

We tested whether the deficits in visual motion processing in V1 in the cataract-reversal patients were retinotopically-specific. We divided V1 into four sub-modules (foveal, para-foveal, peripheral, far-peripheral V1 ROIs), and extracted the beta parameter estimates for the different conditions and groups (Figure 3.4). The ANOVA results showed significant main effects of group ($F(3,240)=6.332$, $p=0.013$), condition ($F(3,240)=130.268$,

p<0.001), and eccentricity (F(3,240)= 141.305, p<0.001). There was also significant group x condition (F(1,240)=10.345, p=0.001), and condition x eccentricity (F(3,240)= 11.080, p<0.001) interactions. However, the group x eccentricity (F(3,240)=0.031, p=0.993) and the group x condition x eccentricity interactions (F(3,240)=0.471, p=0.703) were not significant. Post-hoc analysis demonstrated the beta estimates for the static condition (collapsed across different eccentricities) were not significantly different in the cataract-reversal patients and the controls (P>0.05). The beta estimates (collapsed across different eccentricities) for the motion condition were significantly higher than the static condition in both groups (p<0.001, FWE corrected). More importantly, the beta estimates from the motion condition (collapsed across different eccentricities) were significantly higher in the controls than in the cataract-reversal patients (p<0.001, FWE corrected). These results altogether, highlight that the deficits in visual motion processing are attributed to motion per se, and not to visual stimuli (as demonstrated by the absence of difference in the static condition) or eccentricity.

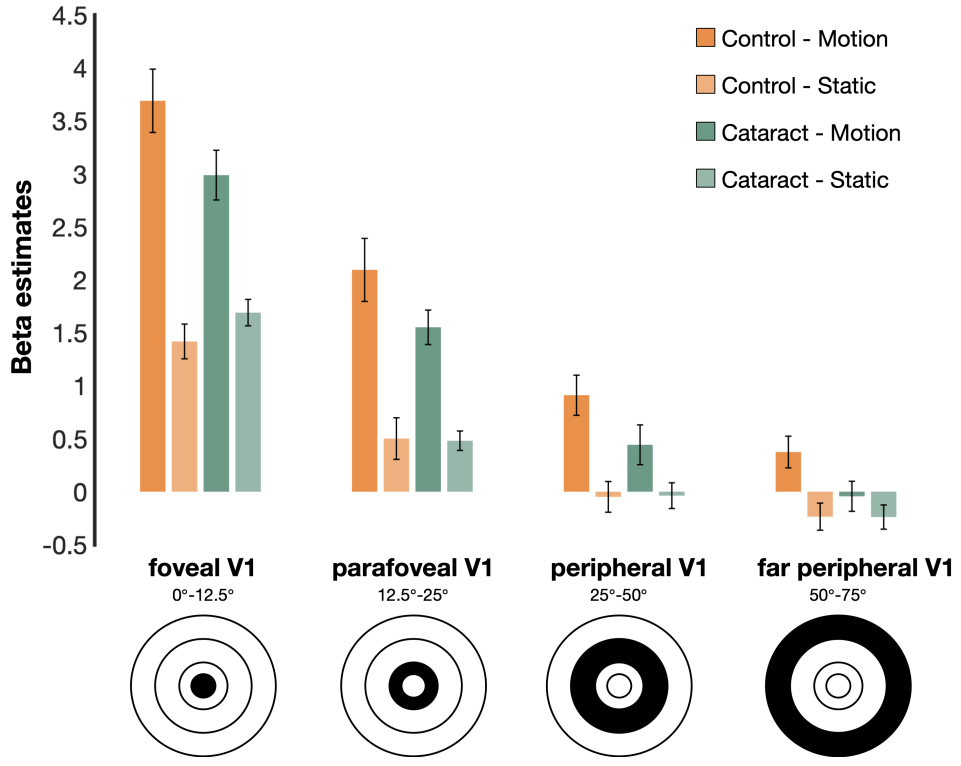


Figure 3.4 Beta parameter estimates for different retinotopic regions in V1.
An illustration of the extracted beta parameter estimates for the motion and static conditions in the cataract-reversal patients and the controls from different retinotopic (foveal, parafoveal, peripheral, far peripheral) regions in V1.

Experiment II: Directional motion decoding experiment

In the directional motion decoding experiment, the participants detected a brief change in the fixation cross color, and events that were faster and shorter in duration than the normal events. The controls (mean ± SD= 93.74% ± 11.50%) and the cataract-reversal patients (mean ± SD= 88.13% ± 14.55%) performed the task with high accuracy. No difference was observed between the two groups (t(30)= 1.217, p = 0.233).

We tested whether we can predict the perceived motion direction from the activity patterns in V1 and the higher-order visual region MT using ROIs defined from an independent probabilistic atlas (L. Wang et al., 2015). Motion direction classification was significantly above chance in V1 in both hemispheres and in both groups. For the left MT, motion direction decoding was significantly above chance in both groups. In the right MT, it was significant only in controls (Table S3.6, Figure 3.5). The ANOVA results in V1 indicated a main effect of group (F(1,60)= 5.341, p= 0.024), and no effect of hemisphere (F(1,60)= 0.107, p=0.744) or group x hemisphere interaction (F(1,60)= 0.032, p= 0.859). Post-hoc analysis indicated that the motion direction classification in V1 (collapsed across hemispheres) in the cataract-reversal group (mean ± SD = 33.08% ± 9.84%) was significantly lower than in the control group (mean ± SD = 39.93% ± 13.02%; t(62)=-2.35, p= 0.022). For MT, the ANOVA revealed no effect of group (F(1,60)= 0.15,p=0.697), hemisphere (F(1,60)= 2.16, p= 0.147), or an interaction (F(1,60)=0.25,p=0.621).

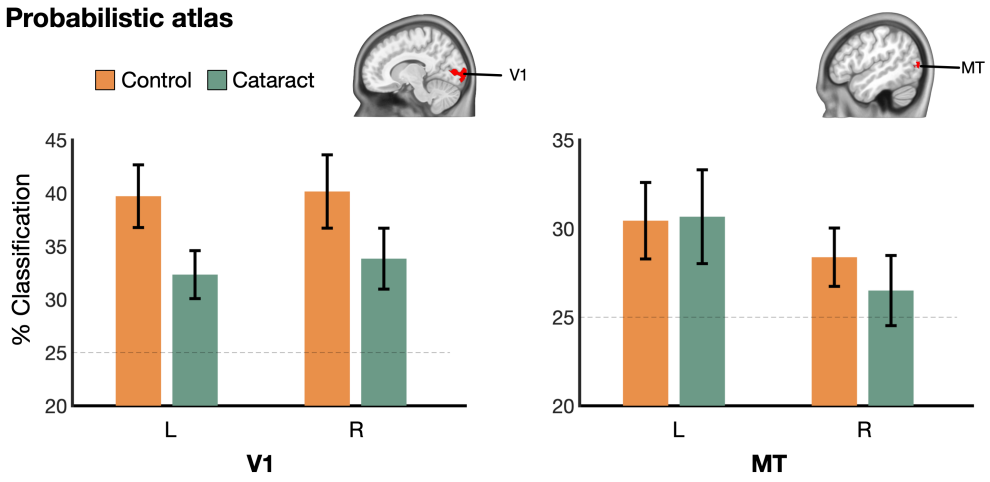


Figure 3.5 MVPA results from the directional motion experiment in V1 and MT.
The multi-class classification results in the cataract-reversal patients and the controls in V1 and MT as defined from the probabilistic atlas (L. Wang et al., 2015)*. The classification results were higher in V1 (collapsed across regions and hemispheres) in the controls than in the cataract-reversal patients. No differences were observed in MT. Chance level is 25%. L: Left, R: Right.*

Control Analysis 1: Group-level hMT+/V5 ROI

The MVPA analysis indicated that reduced motion information was present in the cataract-reversal patients only in V1 and not MT. It could be argued that no difference was observed in MT due to lower power as a result of the lower number of features (voxels) in the left (n=57) and right MT (n=29) ROIs compared with the V1 ROIs. To control for the number of features, we functionally defined the higher-order motion area hMT+/V5 from the group-level analysis from the motion selectivity experiment. The number of features in the 10-mm spherical hMT+/V5 ROIs (n=515) was comparable to the number of features (n=500) used in the motion direction classification in V1. The classification results in the group-level defined hMT+/V5 were significantly above chance in both groups ($p<0.001$, FWE-corrected). The ANOVA revealed no effect of group ($F(1,60)=0.46$, $p=0.5$), hemisphere ($F(1,60)=1.63$, $p=0.206$), or an interaction ($F(1,60)=0.74$, $p=0.394$). We also varied the number of voxels of the hMT+/V5 ROIs by changing the size of the ROI spheres from 4 mm to 10 mm radius. No differences were observed between the two groups (Figure 3.6A).

Control Analysis 2: Individual-level hMT+/V5 ROI

Due to the variability in the anatomical location of hMT+/V5 (Dumoulin et al., 2000; Huk et al., 2002), we also performed another control analysis where we defined hMT+/V5 in each subject individually. The classification results in the individually-defined hMT+V5 in both hemispheres were significantly above chance in both groups ($p<0.001$, FWE-corrected). The ANOVA revealed no effect of group ($F(1,60)=0.01$, $p= 0.919$), hemisphere ($F(1,60)=0.63$,$p=0.432$), or an interaction ($F(1,60)=0$,$p=0.964$). Also, when testing different sizes (from 4 mm to 10 mm radius) of individually-defined hMT+/V5 ROIs, no differences were observed between the two groups (Figure 3.6B).

Correlation

We tested whether, in the cataract-reversal patients, the duration of visual deprivation, or the motion direction discrimination threshold, or visual acuity or contrast sensitivity correlated with the motion direction classification results in V1 and MT (defined from the probabilistic atlas (L. Wang et al., 2015)), the functionally-defined group-level hMT+/V5, and the individually-defined hMT+/V5 ROIs. We did not observe a significant correlation between any of these factors and the motion direction classification results in any of the ROIs ($p>0.05$; Figure S3.3- S3.6).

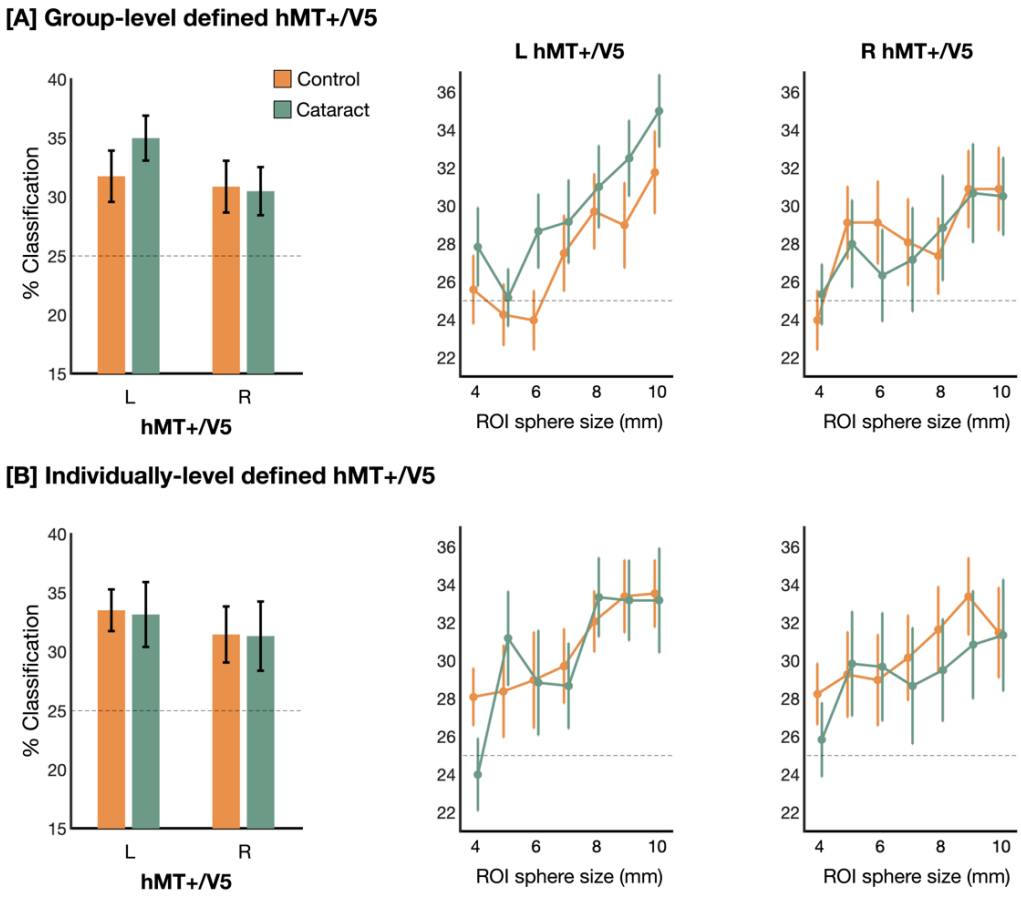


Figure 3.6 MVPA results from the directional motion experiment in the functionally-defined hMT+/V5.

The multi-class classification results in the cataract-reversal patients and the controls in [A] hMT+/V5 that was defined on the group-level and in [B] individually-defined hMT+/V5. We also performed the analysis using spherical ROIs with different sizes (4 mm to 10 mm radius), and therefore different number of features. No differences between the two groups were observed. Chance level is 25%. L: Left, R: Right.

Bayesian analysis

The previous results using parametric statistical methods found no difference between the cataract-reversal patients and the controls in hMT+/V5. To investigate whether the data provides evidence for similar decoding accuracy in hMT+/V5 in the cataract-reversal patients and the controls, we used Bayesian statistics to compare the two groups. The analysis was performed in MT (as defined from the probabilistic atlas (L. Wang et al.,

2015), the functionally defined group-level, and individually-defined hMT+/V5 ROIs in each hemisphere. The BF from the left (BF= 0.335) and right MT (BF= 0.415), as defined from the probabilistic atlas, provided evidence for the null hypothesis (no difference between the two groups). Similarly, the BF from the left (BF= 0.536) and right group-level hMT+/V5 (BF= 0.339), and the left (BF= 0.338) and right individually-defined hMT+/V5 (BF= 0.337) were in favor of the null hypothesis demonstrating evidence for similar motion direction decoding accuracy in the two groups.

Split-half correlation

We tested the stability of the elicited activity patterns in the early visual area (V1) and the higher-order visual motion area (MT), defined from the probabilistic atlas (L. Wang et al., 2015), in the controls and the cataract-reversal patients using split-half correlation (Haxby et al., 2001). The SHC was highly significant in all ROIs and in all groups ($p<0.001$; FWE-corrected; Figure 3.7A, B). The ANOVA in the V1 ROIs revealed a main effect of group ($F(1,60)= 5.05$, $p= 0.028$), and no effect of hemisphere ($F(1,60)= 0.01$, $p= 0.921$), or and interaction between the two ($F(1,60)= 0.3$, $p= 0.589$). Post-hoc analysis indicated that the split-half correlation (collapsed across hemispheres) in the control group (mean ± SD= 1.81 ± 0.29) was higher than in the cataract-reversal patients (mean ± SD= 1.63 ± 0.34, $t(62)= 2.28$, $p= 0.026$). The ANOVA in MT indicated no effect of group ($F(1,60)= 0$, $p= 0.994$), hemisphere ($F(1,60)= 3.56$, $p= 0.064$), or an interaction ($F(1,60)= 0.03$, $p= 0.869$).

We also tested the stability of the elicited patterns in the individually defined hMT+/V5 ROIs (Figure 3.7C). The SHC was highly significant in the left and right individually defined hMT+/V5 ROIs in both groups ($p<0.001$; FWE-corrected). The ANOVA in the individually-defined hMT+/V5 ROIs revealed no effect of group ($F(1,60)= 0$, $p= 0.967$), hemisphere ($F(1,60)= 0.44$, $p= 0.508$), or an interaction ($F(1,60)= 1.28$, $p= 0.262$).

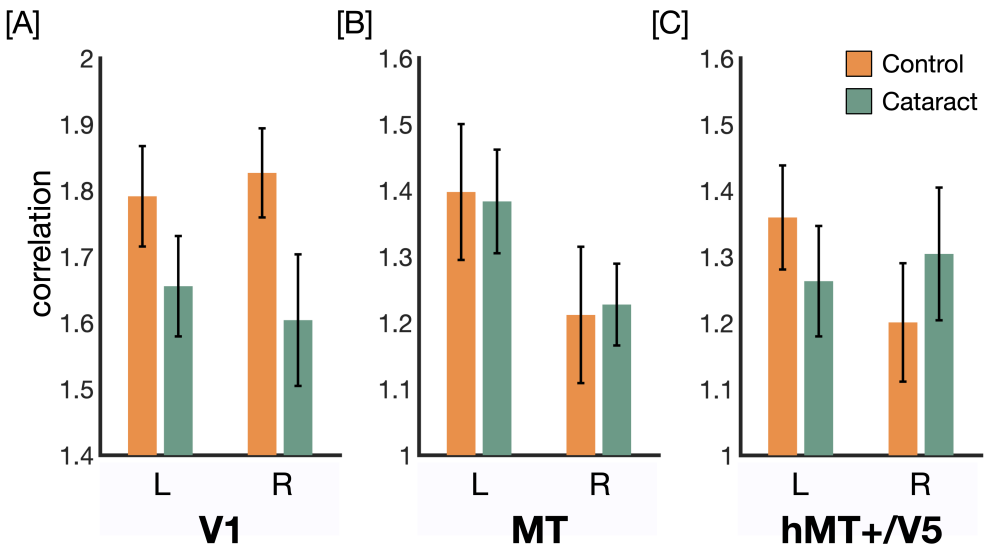


Figure 3.7 Split-half correlation results.
The split-half correlation measured the stability of the patterns across the odd and the even runs in the controls and the cataract-reversal patients. The Fisher-transformed correlation values are plotted in each group in V1 and MT as defined from the probabilistic atlas (L. Wang et al., 2015)*, and from the individually and functionally defined hMT+/V5.*

Structural analysis

We investigated whether there were structural differences between the cataract-reversal patients and their matched controls in V1 and MT. We tested whether there were differences between the two groups in cortical thickness, surface area, and gray matter volume (Figure 3.8). In V1, the cortical thickness analysis found no effect of group ($F(1,60)= 1.018$, $p=0.317$), hemisphere ($F(1,60)= 1.472$, $p=0.230$), or an interaction between the two factors ($F(1,60)= 0.048$, $p=0.828$). Similarly, for the surface area, no effect of group ($F(1,60)=0.013$, $p=0.909$), hemisphere ($F(1,60)=1.885$, $p=0.175$), or an interaction ($F(1,60)= 0.357$, $p=0.553$) was observed. For the gray matter volume, there was no effect of group ($F(1,60)= 0.032$, $p=0.859$), hemisphere ($F(1,60)=3.235$, $p=0.077$), or an interaction ($F(1,60)= 0.550$, $p=0.461$). In MT, the cortical thickness analysis found no effect of group ($F(1,60)= 2.420$, $p=0.125$), hemisphere ($F(1,60)= 0.669$, $p=0.417$), or an interaction ($F(1,60)= 1.939 \times 10^{-4}$, $p=0.989$). For the surface area, no effect of group ($F(1,60)= 0.002$, $p=0.964$), hemisphere ($F(1,60)= 0.851$, $p=0.360$), or an interaction ($F(1,60)= 0.011$, $p=0.915$) was observed. For the gray matter volume, there was no effect of group ($F(1,60)= 0.569$, $p=0.454$), hemisphere ($F(1,60)=0.049$, $p=0.825$), or an interaction ($F(1,60)= 0.007$, $p=0.933$). In summary, no structural differences between the two groups were observed in any of the morphometric measures in V1 or MT.

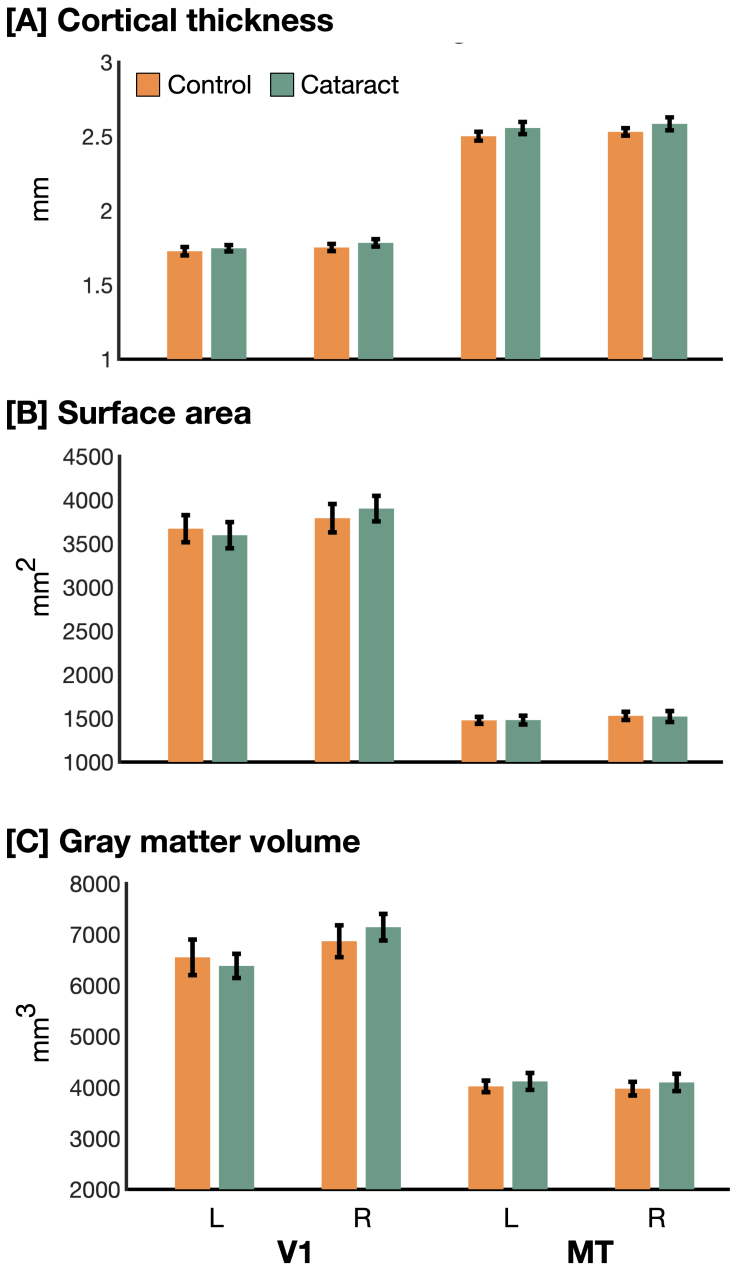


Figure 3.8 Structural analysis results

The structural morphometric analysis investigated differences between the cataract-reversal patients and their controls in [A] cortical thickness, [B] surface area, or [C] gray matter volume in V1 and MT. No differences between the two groups were observed in any of the structural measures in V1 and MT. L: left, R: right.

Experiment III: Resting-state

In this experiment, we investigated the resting-state functional connectivity (Biswal et al., 1995) between different regions within the visual network. We used an ROI-to-ROI approach to test for changes in the functional connectivity between the early visual cortex, hMT+/V5, and the LGN. The LGN was included in the analysis as it was suggested that visual information reaches hMT+/V5 in the case of V1 damage through the LGN (Ajina, Pestilli, et al., 2015; Ajina & Bridge, 2018, 2019). The ROI-to-ROI functional connectivity results demonstrated that the cataract-reversal group showed reduced inter-hemispheric connectivity in the early visual cortex compared with the matched controls ($t(24)=-3.41$, $p= 0.035$, FWE-corrected, Figure 3.9).

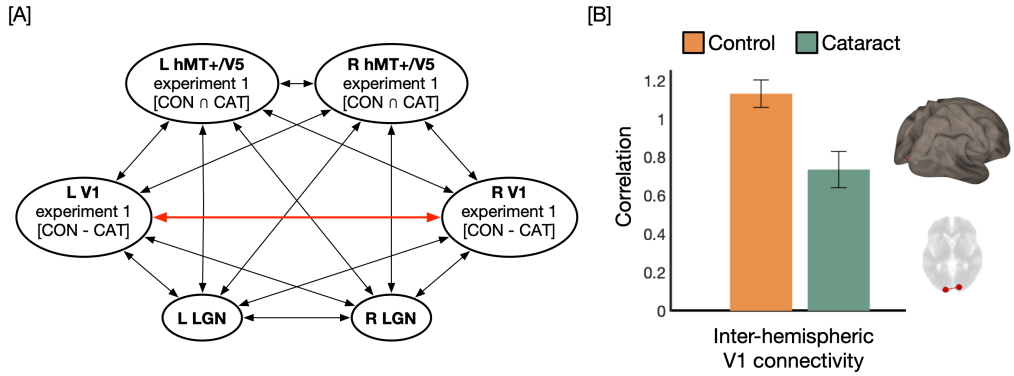


Figure 3.9 Resting-state functional connectivity analysis.
[A] The ROI-to-ROI analysis included V1, hMT+/V5, and the LGN in each hemisphere. The arrows represent all possible pairwise correlations between each pair of ROIs. The resting-state functional connectivity analysis indicated that when comparing the cataract-reversal patients with their matched controls, the cataract-reversal patients showed reduced connectivity between the left and right V1 (highlighted in red). [B] A bar plot of the average correlation values between the left and right V1 in the cataract-reversal patients and their matched controls. L: Left, R: Right.

Additionally, the seed-to-voxel analysis in the left LGN demonstrated a strong significant correlation with the early visual cortex. Oppositely, no significant correlation was observed between the LGN and the early visual cortex in the cataract-reversal patients (Figure 3.10). However, no significant differences were observed between the two groups. These results are in line to that obtained from the task-based functional connectivity during processing motion information.

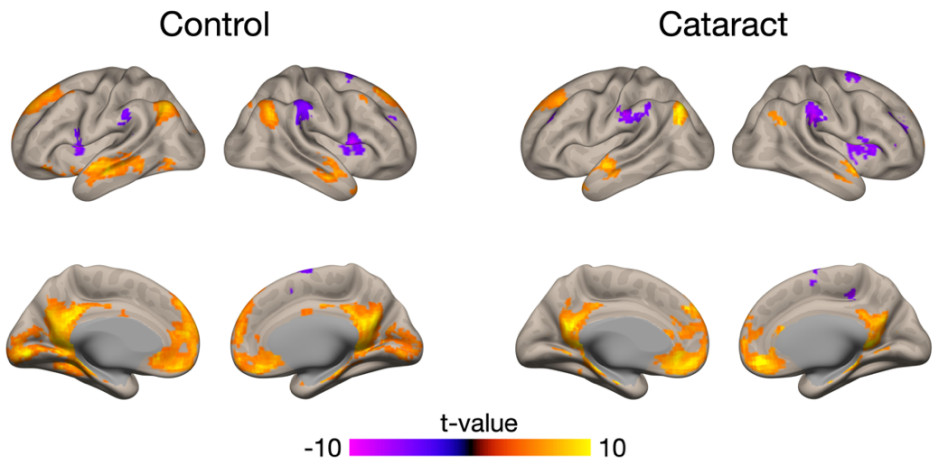


Figure 3.10 Resting-state seed-to-voxel functional connectivity.
The seed-to-voxel analysis results indicated that the left LGN was connected to the early visual cortex in the controls but not in the cataract-reversal patients. Results are displayed at $p<0.001$ at the voxel level and FDR-corrected $p<0.05$ at the cluster level.

Discussion

In this study we aimed to investigate the impact of a brief period of visual deprivation early in life on the development of the visual motion network. Our results demonstrated reduced preferential responses to moving information in the early visual cortex in the cataract-reversal patients compared with controls that negatively correlated with the period of visual deprivation. No differences were observed in the higher-order visual motion area hMT+/V5. Similarly, our MVPA results revealed reduced motion direction information in the early visual cortex in the cataract-reversal patients with no difference between the two groups in hMT+/V5.

Animal studies in kittens suggested that a brief visual deprivation during the first six weeks of life leads to permanent deficits in the perception of global motion (Mitchell et al., 2009). Studies with humans who had a history of transient congenital bilateral cataract also demonstrated that visual deprivation during the first year in life led to deficits in global visual motion processing (Ellemberg et al., 2002; Hadad et al., 2012). Our results replicated these findings and showed that the lack of visual experience during the first year of life had a strong influence on the behavioral performance in motion processing despite having a long period of visual experience following the cataract-removal. The previously mentioned studies hypothesized that the deficits in global motion processing are most likely attributed to the extra-striate motion area hMT+/V5 (Ellemberg et al., 2002; Hadad et al., 2012; Mitchell et al., 2009). The authors concluded that visual experience very early in life is

necessary for the typical development of hMT+/V5 to process global motion information. Additionally, they hypothesized that, similar to the early visual cortex, there is a sensitive period early in life in which visual deprivation, even for a short period, could negatively impact the development of hMT+/V5 (Mitchell et al., 2009),

We investigated the impact of brief early visual deprivation in cataract-reversal patients on the visual motion network. Our data suggests that early and brief visual deprivation has a more pronounced effect on the early visual areas (V1), with hMT+/V5 showing resilience to visual deprivation. In the motion selectivity experiment (Experiment 1), when processing visual motion stimuli compared with visual static stimuli, the cataract-reversal patients showed reduced recruitment of the early visual cortex compared with their matched controls. The reduced recruitment of the early visual cortex in the cataract-reversal patients correlated negatively with the duration of the visual deprivation. Interestingly, no differences between the two groups were observed in hMT+/V5. In the directional motion experiment (Experiment 2), we investigated the representation of individual motion directions in V1 and hMT+/V5 in the cataract-reversal patients and their matched controls. Using sensitive techniques as MVPA could potentially allow us to capture subtle differences between the two groups that might be inaccessible using univariate analysis. Our results demonstrated that while the perceived motion direction could be predicted from the activity patterns from V1 and hMT+/V5, there was reduced motion direction information in the cataract-reversal patients compared with controls only in V1. No differences were observed between the two groups in hMT+/V5. Additionally, using split-half correlations, we looked at the stability of elicited activity patterns in V1 and hMT+/V5 when processing motion directions. Our results demonstrated that while there was no difference between the pattern stability in the two groups in hMT+/V5, the elicited activity patterns in V1 were less stable in the cataract-reversal patients compared with the controls. Contrary to previous suggestions (Mitchell et al., 2009), these results altogether demonstrate that early brief visual deprivation has a more pronounced effect on the early visual areas than on hMT+/V5.

Could the observed differences in the early visual cortex be attributed to acuity (T. L. Lewis et al., 1995; Maurer & Lewis, 2001) or other visual properties not related to motion? Our beta parameter estimates in the early visual cortex demonstrated that there was no difference between the two groups in the static condition (Figure 3.1D and Figure 3.4). Moreover, when comparing the two groups when processing visual static stimuli, no differences were observed in the early visual cortex. Differences between the groups were only observed when processing motion information (Figure 3.4 and Figure S3.1). Therefore, these results eliminate the possibility that the differences in the early visual cortex could be due to reduced recruitment to visual stimulation or lower acuity in the cataract-reversal patients.

When does direction selectivity emerge in the early visual cortex? It was suggested that visual experience is needed for ferrets in order to develop direction selective responses in the early visual cortex. This was unique to direction selectivity but not to orientation or ocular dominance (Y. Li et al., 2006). In humans, infants up to two months are not sensitive to changes in motion direction on the behavioral level (Wattam-Bell, 1996) or with neurophysiological recordings (Braddick et al., 2005). This suggests that visual experience early in life is most likely necessary for the development of motion direction selective neurons in the early visual cortex. Our results go in line with these suggestions as a brief period of early visual deprivation impacted the processing and the representation of motion direction information in the early visual cortex.

These results raise an important question. Most of the input arriving to hMT+/V5 comes from highly myelinated direct feed-forward connections from V1 (Felleman & Van Essen, 1991; Maunsell & van Essen, 1983; Rockland, 1989, 1995). How does hMT+/V5 show a similar response profile in the two groups despite having major deficits in the early visual cortex in the cataract-reversal patients. Moreover, our results demonstrated that when processing motion information, the cataract-reversal patients, compared to the controls, showed reduced functional connectivity between hMT+/V5 and the early visual cortex. We speculate that motion information arrives to hMT+/V5 through alternative pathways bypassing V1. Even in the case of V1 damage, hMT+/V5 can still respond to visual information (Ajina, Kennard, et al., 2015), which could be mediated through sub-cortical routes (Lin et al., 1974; Maunsell & van Essen, 1983; Rodman et al., 1989; Sincich et al., 2004). Individuals with blindsight who had severe damage in their primary visual cortex can perceive visual information in their blind hemifield (Stoerig & Cowey, 1997; Weiskrantz et al., 1974). It has been demonstrated that blindsight is attributed to intact connections between the lateral geniculate nucleus and hMT+/V5 (Ajina, Pestilli, et al., 2015; Ajina & Bridge, 2018, 2019). In our results, we did not observe a statistically significant difference between the two groups in the LGN-hMT+/V5 connectivity. Future studies with more appropriate methodological techniques should address the possible reorganization in sub-cortical routes for motion processing in the cataract-reversal patients.

The maladaptive consequences of brief early visual deprivation on the early visual cortex were not limited to performing a visual motion task. Even during rest and without performing any visual task, the resting-state connectivity of the early visual cortex was reduced across hemispheres in the cataract-reversal patients adding more evidence for the permanent plastic changes in the early visual cortex following brief early visual deprivation. We also investigated whether there were structural changes in the early visual cortex as suggested in a previous study (Guerreiro, Erfort, et al., 2015), however, in our data, we did not observe structural differences between the groups.

What drives the plastic changes in the early visual cortex following early visual deprivation? It was suggested that early visual deprivation affects the synaptic pruning occurring in the occipital cortex early in life (Bourgeois et al., 1989) leading to changes in the organization and the development of the occipital cortex (Amedi et al., 2003; Bedny et al., 2011; Büchel et al., 1998; Pietrini et al., 2004; Sadato et al., 1996). Due to early visual deprivation, the occipital cortex in the early blind is recruited during auditory processing (Bedny et al., 2010; Collignon et al., 2007; Dormal et al., 2016; Weeks et al., 2000). Similarly, the cataract-reversal patients showed enhanced recruitment in the cuneus compared to controls when processing auditory information (Collignon et al., 2015). However, in contrast to the massive reorganization of the visual motion system in the early blind including low-level and high-level visual motion areas, the reorganization in the cataract-reversal patients to process auditory information was limited to the early visual areas and not hMT+/V5 (Collignon et al., 2015). This is in line with our findings where the functional recruitment of the visual motion network was reduced only in the early visual areas and not the higher-order motion area hMT+/V5. The functional recruitment of the early visual cortex in the cataract-reversal patients correlated negatively with the duration of visual deprivation. This suggests that the reduced efficiency of visual processing in early visual areas could potentially relate to enhanced auditory processing (Bottari et al., 2018) and cross-modal reorganization of the visual system (Collignon et al., 2015).

One limitation in our study is that we could not record the eye position inside the fMRI scanner. However, the analysis of the MRI signal from the eyes (Beauchamp, 2003) in the motion selectivity experiment showed no difference between the two groups (See supplementary materials). In the directional motion decoding experiment, the cataract-reversal patients had more variability in the MRI signal from the eyes compared with controls (Figure S3.7). However, it is unlikely that our results from the directional motion decoding experiment could be explained by eye movements. The variability of the signal from the eyes was not different across different motion directions. Therefore, a decoder wouldn't benefit from this information to discriminate different motion directions. Additionally the signal/activity in submodules of hMT+/V5 (as MT and MST) is modulated by eye movements (Chukoskie & Movshon, 2009; Komatsu & Wurtz, 1988; Petit & Haxby, 1999a). If more variable eye movements in the cataract-reversal patients will impact the classification of motion directions, then we should observe differences between the two groups in the motion direction classification in hMT+/V5, however, this was not the case. Additionally, we tested whether we can predict the perceived motion directions from the recorded signals from the eyes, however, it was not significant (See supplementary materials, Figure S3.8).

The reduced functional recruitment, and the reduced motion direction information in the early visual cortex in the cataract-reversal patients indicated that the most pronounced effects are in the early visual areas rather than hMT+/V5. Does that mean that

the function of hMT+/V5 is not affected at all? In our fMRI experiments, we used RDKs with 100% coherence to provide an optimum condition for the classifier to discriminate the motion directions with no noise. It is possible that if the same task was performed at different difficulty levels with lower motion coherence, we might observe reduced motion information in hMT+/V5 in the cataract-reversal patients. However, this hypothesis remains to be tested.

In summary, our data suggests that brief and early visual deprivation has a region-specific impact on the functional development of the early visual cortex while hMT+/V5 shows resilience.

References

Ajina, S., & Bridge, H. (2018). Blindsight relies on a functional connection between hMT+ and the lateral geniculate nucleus, not the pulvinar. *PLOS Biology*, *16*(7), e2005769. https://doi.org/10.1371/journal.pbio.2005769

Ajina, S., & Bridge, H. (2019). Subcortical pathways to extrastriate visual cortex underlie residual vision following bilateral damage to V1. *Neuropsychologia*, *128*(January 2018), 140–149. https://doi.org/10.1016/j.neuropsychologia.2018.01.007

Ajina, S., Kennard, C., Rees, G., & Bridge, H. (2015). Motion area V5/MT+ response to global motion in the absence of V1 resembles early visual cortex. *Brain*, *138*(1), 164–178. https://doi.org/10.1093/brain/awu328

Ajina, S., Pestilli, F., Rokem, A., Kennard, C., & Bridge, H. (2015). Human blindsight is mediated by an intact geniculo-extrastriate pathway. *ELife*, *4*(OCTOBER2015), 1–23. https://doi.org/10.7554/eLife.08935

Amedi, A., Raz, N., Pianka, P., Malach, R., & Zohary, E. (2003). Early "visual" cortex activation correlates with superior verbal memory performance in the blind. *Nat. Neurosci.*, *6*(7), 758–766. https://doi.org/10.1038/nn1072

Bach, M. (1996). The Freiburg Visual Acuity Test - Automatic Measurement of Visual Acuity. *Optometry and Vision Science*. https://doi.org/10.1097/00006324-199601000-00008

Bach, M. (2006). The Freiburg Visual Acuity Test-Variability unchanged by post-hoc re-analysis. *Graefe's Archive for Clinical and Experimental Ophthalmology*. https://doi.org/10.1007/s00417-006-0474-4

Beauchamp, M. S. (2003). Detection of eye movements from fMRI data. *Magnetic Resonance in Medicine*, *49*(2), 376–380. https://doi.org/10.1002/mrm.10345

Bedny, M., Konkle, T., Pelphrey, K., Saxe, R., & Pascual-Leone, A. (2010). Sensitive period for a multimodal response in human visual motion area MT/MST. *Current Biology*, *20*(21), 1900–1906. https://doi.org/10.1016/j.cub.2010.09.044

Bedny, M., Pascual-Leone, A., Dodell-Feder, D., Fedorenko, E., & Saxe, R. (2011). Language processing in the occipital cortex of congenitally blind adults. *Proceedings of the National Academy of Sciences*, *108*(11), 4429–4434. https://doi.org/10.1073/pnas.1014818108

Behzadi, Y., Restom, K., Liau, J., & Liu, T. T. (2007). A component based noise correction method (CompCor) for BOLD and perfusion based fMRI. *NeuroImage*, *37*(1), 90–101. https://doi.org/10.1016/j.neuroimage.2007.04.042

Benson, N. C., Butt, O. H., Brainard, D. H., & Aguirre, G. K. (2014). Correction of Distortion in Flattened Representations of the Cortical Surface Allows Prediction of V1-V3 Functional Organization from Anatomy. *PLoS Computational Biology*, *10*(3). https://doi.org/10.1371/journal.pcbi.1003538

Benson, N. C., Butt, O. H., Datta, R., Radoeva, P. D., Brainard, D. H., & Aguirre, G. K. (2012). The retinotopic organization of striate cortex is well predicted by surface topology. *Current Biology*, *22*(21), 2081–2085. https://doi.org/10.1016/j.cub.2012.09.014

Bex, P. J., Dakin, S. C., & Simmers, A. J. (2003). The shape and size of crowding for moving targets. *Vision Research*, *43*(27), 2895–2904. https://doi.org/10.1016/S0042-6989(03)00460-7

Biswal, B., Zerrin Yetkin, F., Haughton, V. M., & Hyde, J. S. (1995). Functional connectivity in the motor cortex of resting human brain using echo-planar mri. *Magnetic Resonance in Medicine*, *34*(4), 537–541. https://doi.org/10.1002/mrm.1910340409

Bottari, D., Kekunnaya, R., Hense, M., Troje, N. F., Sourav, S., & Röder, B. (2018). Motion processing after sight restoration: No competition between visual recovery and auditory compensation. *NeuroImage*, *167*(October 2017), 284–296. https://doi.org/10.1016/j.neuroimage.2017.11.050

Bourgeois, J. P., Jastreboff, P. J., & Rakic, P. (1989). Synaptogenesis in visual cortex of normal and preterm monkeys: Evidence for intrinsic regulation of synaptic overproduction. *Proceedings of the National Academy of Sciences of the United States of America*, *86*(11), 4297–4301. https://doi.org/10.1073/pnas.86.11.4297

Braddick, O. J., Birtles, D., Wattam-Bell, J., & Atkinson, J. (2005). Motion- and orientation-specific cortical responses in infancy. *Vision Research*, *45*(25–26), 3169–3179. https://doi.org/10.1016/j.visres.2005.07.021

Braddick, O. J., O'Brien, J. M. D., Wattam-Bell, J., Atkinson, J., Hartley, T., & Turner, R. (2001). Brain areas sensitive to coherent visual motion. *Perception*, *30*(1), 61–72. https://doi.org/10.1068/p3048

Büchel, C., Price, C. J., Frackowiak, R. S. J., & Friston, K. (1998). Different activation patterns in the visual cortex of late and congentially blind subjects. *Brain*, *121*, 409–419.

Chukoskie, L., & Movshon, J. A. (2009). Modulation of visual signals in macaque MT and MST neurons during pursuit eye movement. *Journal of Neurophysiology*. https://doi.org/10.1152/jn.90692.2008

Collignon, O., Dormal, G., De Heering, A., Lepore, F., Lewis, T. L., & Maurer, D. (2015). Long-Lasting Crossmodal Cortical Reorganization Triggered by Brief Postnatal Visual Deprivation. *Current Biology*, *25*(18), 2379–2383. https://doi.org/10.1016/j.cub.2015.07.036

Collignon, O., Lassonde, M., Lepore, F., Bastien, D., & Veraart, C. (2007). Functional cerebral reorganization for auditory spatial processing and auditory substitution of vision in early blind subjects. *Cerebral Cortex*, *17*(2), 457–465. https://doi.org/10.1093/cercor/bhj162

Corbetta, M., Akbudak, E., Conturo, T. E., Snyder, A. Z., Ollinger, J. M., Drury, H. A., Linenweber, M. R., Petersen, S. E., Raichle, M. E., Van Essen, D. C., & Shulman, G. L. (1998). A Common Network of Functional Areas for Attention and Eye Movements. *Neuron*, *21*(4), 761–773. https://doi.org/10.1016/S0896-6273(00)80593-0

Dormal, G., Rezk, M., Yakobov, E., Lepore, F., & Collignon, O. (2016). Auditory motion in the sighted and blind: Early visual deprivation triggers a large-scale imbalance between auditory and "visual" brain regions. *NeuroImage*, *134*, 630–644. https://doi.org/10.1016/j.neuroimage.2016.04.027

Dumoulin, S. O., Bittar, R. G., Kabani, N. J., Baker, C. L., Le Goualher, G., Bruce Pike, G., & Evans, A. C. (2000). A new anatomical landmark for reliable identification of human area V5/MT: a quantitative analysis of sulcal patterning. *Cerebral Cortex*, *10*(5), 454–463. https://doi.org/10.1093/cercor/10.5.454

Eickhoff, S. B., Stephan, K. E., Mohlberg, H., Grefkes, C., Fink, G. R., Amunts, K., & Zilles, K. (2005). A new SPM toolbox for combining probabilistic cytoarchitectonic maps and functional imaging data. *NeuroImage*, *25*(4), 1325–1335. https://doi.org/10.1016/j.neuroimage.2004.12.034

Ellemberg, D., Lewis, T. L., Maurer, D., Brar, S., & Brent, H. P. (2002). Better perception of global motion after monocular than after binocular deprivation. *Vision Research*, *42*(2), 169–179. https://doi.org/10.1016/S0042-6989(01)00278-4

Felleman, D. J., & Van Essen, D. C. (1991). Distributed Hierarchical Processing in the Primate Cerebral Cortex. *Cerebral Cortex*, *1*(1), 1–47. https://doi.org/10.1093/cercor/1.1.1

Fischl, B., & Dale, A. M. (2000). Measuring the thickness of the human cerebral cortex from magnetic resonance images. *Proceedings of the National Academy of Sciences*, *97*(20), 11050–11055.

Fischl, B., Liu, A., & Dale, A. M. (2001). Automated manifold surgery: constructing geometrically accurate and topologically correct models of the human cerebral

cortex. *IEEE Transactions on Medical Imaging*, *20*(1), 70–80. https://doi.org/10.1109/42.906426

Fischl, B., Rajendran, N., Busa, E., Augustinack, J., Hinds, O., Yeo, B. T. T., Mohlberg, H., Amunts, K., & Zilles, K. (2008). Cortical Folding Patterns and Predicting Cytoarchitecture. *Cerebral Cortex*, *18*(8), 1973–1980. https://doi.org/10.1093/cercor/bhm225

Fischl, B., van der Kouwe, A., Destrieux, C., Halgren, E., Ségonne, F., Salat, D. H., Busa, E., Seidman, L. J., Goldstein, J., Kennedy, D., Caviness, V., Makris, N., Rosen, B., & Dale, A. M. (2004). Automatically Parcellating the Human Cerebral Cortex. *Cerebral Cortex*, *14*(1), 11–22. https://doi.org/10.1093/cercor/bhg087

Friston, K. ., Buechel, C., Fink, G. ., Morris, J., Rolls, E., & Dolan, R. . (1997). Psychophysiological and Modulatory Interactions in Neuroimaging. *NeuroImage*, *6*(3), 218–229. https://doi.org/10.1006/nimg.1997.0291

Geldart, S., Mondloch, C. J., Maurer, D., de Schonen, S., & Brent, H. P. (2002). The effect of early visual deprivation on the development of face processing. *Developmental Science*, *5*(4), 490–501. https://doi.org/10.1111/1467-7687.00242

Gitelman, D. R., Penny, W. D., Ashburner, J., & Friston, K. J. (2003). Modeling regional and psychophysiologic interactions in fMRI: the importance of hemodynamic deconvolution. *NeuroImage*, *19*(1), 200–207. https://doi.org/10.1016/S1053-8119(03)00058-2

Guerreiro, M. J. S., Erfort, M. V., Henssler, J., Putzar, L., & Röder, B. (2015). Increased visual cortical thickness in sight-recovery individuals. *Human Brain Mapping*, *36*(12), 5265–5274. https://doi.org/10.1002/hbm.23009

Hadad, B., Maurer, D., & Lewis, T. L. (2012). Sparing of sensitivity to biological motion but not of global motion after early visual deprivation. *Developmental Science*, *15*(4), 474–481. https://doi.org/10.1111/j.1467-7687.2012.01145.x

Haxby, J. V., Gobbini, M. I., Furey, M. L., Ishai, A., Schouten, J. L., & Pietrini, P. (2001). Distrubuted and Overlapping Representations of Face and Objects in Ventral Temporal Cortex. *Science*, *293*(5539), 2425–2430. https://doi.org/10.1126/science.1063736

Hinds, O. P., Rajendran, N., Polimeni, J. R., Augustinack, J. C., Wiggins, G., Wald, L. L., Diana Rosas, H., Potthast, A., Schwartz, E. L., & Fischl, B. (2008). Accurate prediction of V1 location from cortical folds in a surface coordinate system. *NeuroImage*. https://doi.org/10.1016/j.neuroimage.2007.10.033

Hubel, D. H., & Wiesel, T. N. (1970). The period of susceptibility to the physiological

effects of unilateral eye closure in kittens. *The Journal of Physiology*, *206*(2), 419–436. http://www.ncbi.nlm.nih.gov/pubmed/5498493

Huk, A. C., Dougherty, R. F., & Heeger, D. J. (2002). Retinotopy and functional subdivision of human areas MT and MST. *The Journal of Neuroscience : The Official Journal of the Society for Neuroscience*, *22*(16), 7195–7205. https://doi.org/20026661

JASP Team. (2020). JASP. In *[Computer software]*.

Komatsu, H., & Wurtz, R. H. (1988). Relation of cortical areas MT and MST to pursuit eye movements. I. Localization and visual properties of neurons. *Journal of Neurophysiology*, *60*(2), 580–603. https://doi.org/10.1152/jn.1988.60.2.580

Large, I., Bridge, H., Ahmed, B., Clare, S., Kolasinski, J., Lam, W. W., Miller, K. L., Dyrby, T. B., Parker, A. J., Smith, J. E. T., Daubney, G., Sallet, J., Bell, A. H., & Krug, K. (2016). Individual Differences in the Alignment of Structural and Functional Markers of the V5/MT Complex in Primates. *Cerebral Cortex*, *26*(10), 3928–3944. https://doi.org/10.1093/cercor/bhw180

Le Grand, R., Mondloch, C. J., Maurer, D., & Brent, H. P. (2001). Early visual experience and face processing. *Nature*, *410*(6831), 890–890. https://doi.org/10.1038/35073749

Le Grand, R., Mondloch, C. J., Maurer, D., & Brent, H. P. (2004). Impairment in Holistic Face Processing Following Early Visual Deprivation. *Psychological Science*, *15*(11), 762–768. https://doi.org/10.1111/j.0956-7976.2004.00753.x

Lewis, T. L., & Maurer, D. (2009). Effects of early pattern deprivation on visual development. *Optometry and Vision Science*, *86*(6), 640–646. https://doi.org/10.1097/OPX.0b013e3181a7296b

Lewis, T. L., Maurer, D., & Brent, H. P. (1995). Development of grating acuity in children treated for unilateral or bilateral congenital cataract. *Investigative Ophthalmology & Visual Science*, *36*(10), 2080–2095. http://www.ncbi.nlm.nih.gov/pubmed/7657547

Li, Y., Fitzpatrick, D., & White, L. E. (2006). The development of direction selectivity in ferret visual cortex requires early visual experience. *Nature Neuroscience*, *9*(5), 676–681. https://doi.org/10.1038/nn1684

Lieberman, H. R., & Pentland, A. P. (1982). Microcomputer-based estimation of psychophysical thresholds: the best PEST. *Behavior Research Methods & Instrumentation*, *14*(1), 21–25.

Lin, C. S., Wagor, E., & Kaas, J. H. (1974). Projections from the pulvinar to the middle temporal visual area (MT) in the owl monkey,Aotus trivirgatus. *Brain Research*, *76*(1), 145–149. https://doi.org/10.1016/0006-8993(74)90520-4

Marcus, D. S., Harms, M. P., Snyder, A. Z., Jenkinson, M., Wilson, J. A., Glasser, M. F., Barch, D. M., Archie, K. A., Burgess, G. C., Ramaratnam, M., Hodge, M., Horton, W., Herrick, R., Olsen, T., McKay, M., House, M., Hileman, M., Reid, E., Harwell, J., … Van Essen, D. C. (2013). Human Connectome Project informatics: Quality control, database services, and data visualization. *NeuroImage*, *80*, 202–219. https://doi.org/10.1016/j.neuroimage.2013.05.077

Maunsell, J. H., & van Essen, D. C. (1983). The connections of the middle temporal visual area (MT) and their relationship to a cortical hierarchy in the macaque monkey. *The Journal of Neuroscience : The Official Journal of the Society for Neuroscience*, *3*(12), 2563–2586.

Maurer, D., Ellemberg, D., & Lewis, T. L. (2006). Repeated measurements of contrast sensitivity reveal limits to visual plasticity after early binocular deprivation in humans. *Neuropsychologia*, *44*(11), 2104–2112. https://doi.org/10.1016/j.neuropsychologia.2005.10.008

Maurer, D., & Lewis, T. L. (2001). Visual acuity: The role of visual input in inducing postnatal change. *Clinical Neuroscience Research*. https://doi.org/10.1016/S1566-2772(01)00010-X

Maurer, D., Lewis, T. L., & Mondloch, C. J. (2005). Missing sights: Consequences for visual cognitive development. *Trends in Cognitive Sciences*, *9*(3 SPEC. ISS.), 144–151. https://doi.org/10.1016/j.tics.2005.01.006

Maurer, D., Mondloch, C. J., & Lewis, T. L. (2007). Sleeper effects. *Developmental Science*, *10*(1), 40–47. https://doi.org/10.1111/j.1467-7687.2007.00562.x

Mitchell, D. E., Kennie, J., & Kung, D. (2009). Development of Global Motion Perception Requires Early Postnatal Exposure to Patterned Light. *Current Biology*, *19*(8), 645–649. https://doi.org/10.1016/j.cub.2009.02.038

Morrone, M. C., Tosetti, M., Montanaro, D., Fiorentini, A., Cioni, G., & Burr, D. C. (2000). A cortical area that responds specifically to optic flow, revealed by fMRI. *Nature Neuroscience*, *3*(12), 1322–1328. https://doi.org/10.1038/81860

Oosterhof, N. N., Connolly, A. C., & Haxby, J. V. (2016). CoSMoMVPA: Multi-Modal Multivariate Pattern Analysis of Neuroimaging Data in Matlab/GNU Octave. *Frontiers in Neuroinformatics*, *10*. https://doi.org/10.3389/fninf.2016.00027

Petit, L., & Haxby, J. V. (1999). Functional Anatomy of Pursuit Eye Movements in Humans as Revealed by fMRI. *Journal of Neurophysiology*, *82*(1), 463–471. https://doi.org/10.1152/jn.1999.82.1.463

Pietrini, P., Furey, M. L., Ricciardi, E., Gobbini, M. I., Wu, W.-H. C., Cohen, L., Guazzelli,

M., & Haxby, J. V. (2004). Beyond sensory images: Object-based representation in the human ventral pathway. *Proceedings of the National Academy of Sciences*, *101*(15), 5658–5663. https://doi.org/10.1073/pnas.0400707101

Power, J. D., Barnes, K. A., Snyder, A. Z., Schlaggar, B. L., & Petersen, S. E. (2012). Spurious but systematic correlations in functional connectivity MRI networks arise from subject motion. *NeuroImage*, *59*(3), 2142–2154. https://doi.org/10.1016/j.neuroimage.2011.10.018

Rees, G., Friston, K., & Koch, C. (2000). A direct quantitative relationship between the functional properties of human and macaque V5. *Nature Neuroscience*, *3*(7), 716–723. https://doi.org/10.1038/76673

Rockland, K. S. (1989). Bistratified Distribution Of Terminal Arbors Of Individual Axons Projecting From Area Vi To Middle Temporal Area (Mt) In The Macaque Monkey. *Visual Neuroscience*. https://doi.org/10.1017/S0952523800004466

Rockland, K. S. (1995). Morphology of individual axons projecting from area V2 to MT in the macaque. *Journal of Comparative Neurology*. https://doi.org/10.1002/cne.903550105

Rodman, H. R., Gross, C. G., & Albright, T. D. (1989). Afferent basis of visual response properties in area MT of the macaque. I. Effects of striate cortex removal. *Journal of Neuroscience*, *9*(6), 2033–2050. https://doi.org/10.1523/jneurosci.09-06-02033.1989

Sadato, N., Pascual-Leone, A., Grafman, J., Ibañez, V., Deiber, M.-P., Dold, G., & Hallett, M. (1996). Activation of the primary visual cortex by Braille reading in blind subjects. *Nature*, *380*(6574), 526–528. https://doi.org/10.1038/380526a0

Salat, D. H., van der Kouwe, A. J. W., Makris, N., Ségonne, F., Quinn, B. T., & Dale, A. M. (2004). Sequence-independent segmentation of magnetic resonance images. *NeuroImage*, *23*, S69–S84. https://doi.org/https://doi.org/10.1016/j.neuroimage.2004.07.016

Satterthwaite, T. D., Wolf, D. H., Loughead, J., Ruparel, K., Elliott, M. A., Hakonarson, H., Gur, R. C., & Gur, R. E. (2012). NeuroImage Impact of in-scanner head motion on multiple measures of functional connectivity : Relevance for studies of neurodevelopment in youth ☆. *NeuroImage*, *60*(1), 623–632. https://doi.org/10.1016/j.neuroimage.2011.12.063

Sincich, L. C., Park, K. F., Wohlgemuth, M. J., & Horton, J. C. (2004). Bypassing V1: a direct geniculate input to area MT. *Nature Neuroscience*, *7*(10), 1123–1128. https://doi.org/10.1038/nn1318

Sled, J. G., Zijdenbos, A. P., & Evans, A. C. (1998). A nonparametric method for automatic

correction of intensity nonuniformity in MRI data. *IEEE Transactions on Medical Imaging*, *17*(1), 87–97.

Smith, A. T., Wall, M. B., Williams, A. L., & Singh, K. D. (2006). Sensitivity to optic flow in human cortical areas MT and MST. *European Journal of Neuroscience*, *23*(2), 561–569. https://doi.org/10.1111/j.1460-9568.2005.04526.x

Smith, S. M., & Nichols, T. E. (2009). Threshold-free cluster enhancement: Addressing problems of smoothing, threshold dependence and localisation in cluster inference. *NeuroImage*, *44*(1), 83–98. https://doi.org/10.1016/j.neuroimage.2008.03.061

Stelzer, J., Chen, Y., & Turner, R. (2013). Statistical inference and multiple testing correction in classification-based multi-voxel pattern analysis (MVPA): Random permutations and cluster size control. *NeuroImage*, *65*, 69–82. https://doi.org/10.1016/j.neuroimage.2012.09.063

Stoerig, P., & Cowey, A. (1997). Blindsight in man and monkey. *Brain*, *120*(3), 535–559. https://doi.org/10.1093/brain/120.3.535

Sunaert, S., Van Hecke, P., Marchal, G., & Orban, G. A. (1999). Motion-responsive regions of the human brain. *Experimental Brain Research*. https://doi.org/10.1007/s002210050804

Tootell, R. B. H., Reppas, J., Kwong, K., Malach, R., Born, R., Brady, T., Rosen, B., & Belliveau, J. (1995). Functional analysis of human MT and related visual cortical areas using magnetic resonance imaging. *The Journal of Neuroscience*, *15*(4), 3215–3230. https://doi.org/10.1523/JNEUROSCI.15-04-03215.1995

Van Dijk, K. R. A., Sabuncu, M. R., & Buckner, R. L. (2012). The influence of head motion on intrinsic functional connectivity MRI. *NeuroImage*, *59*(1), 431–438. https://doi.org/10.1016/j.neuroimage.2011.07.044

Wagenmakers, E. J., Lodewyckx, T., Kuriyal, H., & Grasman, R. (2010). Bayesian hypothesis testing for psychologists: A tutorial on the Savage-Dickey method. *Cognitive Psychology*. https://doi.org/10.1016/j.cogpsych.2009.12.001

Wang, L., Mruczek, R. E. B. B., Arcaro, M. J., & Kastner, S. (2015). Probabilistic maps of visual topography in human cortex. *Cerebral Cortex*, *25*(10), 3911–3931. https://doi.org/10.1093/cercor/bhu277

Watson, A. B., & Pelli, D. G. (1983). QUEST: A Bayesian adaptive psychometric method. *Perception & Psychophysics*, *33*(2), 113–120.

Watson, J. D. G., Myers, R., Frackowiak, R. S. J., Hajnal, J. V., Woods, R. P., Mazziotta, J. C., Shipp, S., & Zeki, S. (1993). Area V5 of the Human Brain: Evidence from a

Combined Study Using Positron Emission Tomography and Magnetic Resonance Imaging. *Cerebral Cortex*, *3*(2), 79–94. https://doi.org/10.1093/cercor/3.2.79

Wattam-Bell, J. (1996). Visual motion processing in one-month-old infants: Habituation experiments. *Vision Research*, *36*(11), 1679–1685. https://doi.org/10.1016/0042-6989(95)00237-5

Weeks, R., Horwitz, B., Aziz-Sultan, A., Tian, B., Wessinger, C. M., Cohen, L. G., Hallett, M., & Rauschecker, J. P. (2000). A Positron Emission Tomographic Study of Auditory Localization in the Congenitally Blind. *The Journal of Neuroscience*, *20*(7), 2664–2672. https://doi.org/10.1523/JNEUROSCI.20-07-02664.2000

Weiskrantz, L., Warrington, E. K., Sanders, M. D., & Marshall, J. (1974). Visual Capacity in the Hemianopic Field Following a Restricted Occipital Ablation. *Brain*, *97*(4), 709–728. https://doi.org/10.1093/brain/97.4.709

Wetzels, R., Matzke, D., Lee, M. D., Rouder, J. N., Iverson, G. J., & Wagenmakers, E. J. (2011). Statistical evidence in experimental psychology: An empirical comparison using 855 t tests. *Perspectives on Psychological Science*. https://doi.org/10.1177/1745691611406923

Whitfield-Gabrieli, S., & Nieto-Castanon, A. (2012). *Conn* : A Functional Connectivity Toolbox for Correlated and Anticorrelated Brain Networks. *Brain Connectivity*, *2*(3), 125–141. https://doi.org/10.1089/brain.2012.0073

Wiesel, T. N., & Hubel, D. H. (1963). Responses in Striate Deprived of Vision Cortex of One Eye. *Journal of Neurophysiology*, *26*(6), 1003–1017.

Wiesel, T. N., & Hubel, D. H. (1965). Comparison of the effects of unilateral and bilateral eye closure on cortical unit responses in kittens. *Journal of Neurophysiology*, *28*(6), 1029–1040. https://doi.org/10.1152/jn.1965.28.6.1029

Worsley, K. J., Marrett, S., Neelin, P., Vandal, a C., Friston, K. J., & Evans, a C. (1996). A unified statistical approach for determining significant voxels in images of cerebral activation. *Human Brain Mapping*, *4*, 58–73. https://doi.org/10.1162/NECO_a_00006-Arleo

Supplementary materials

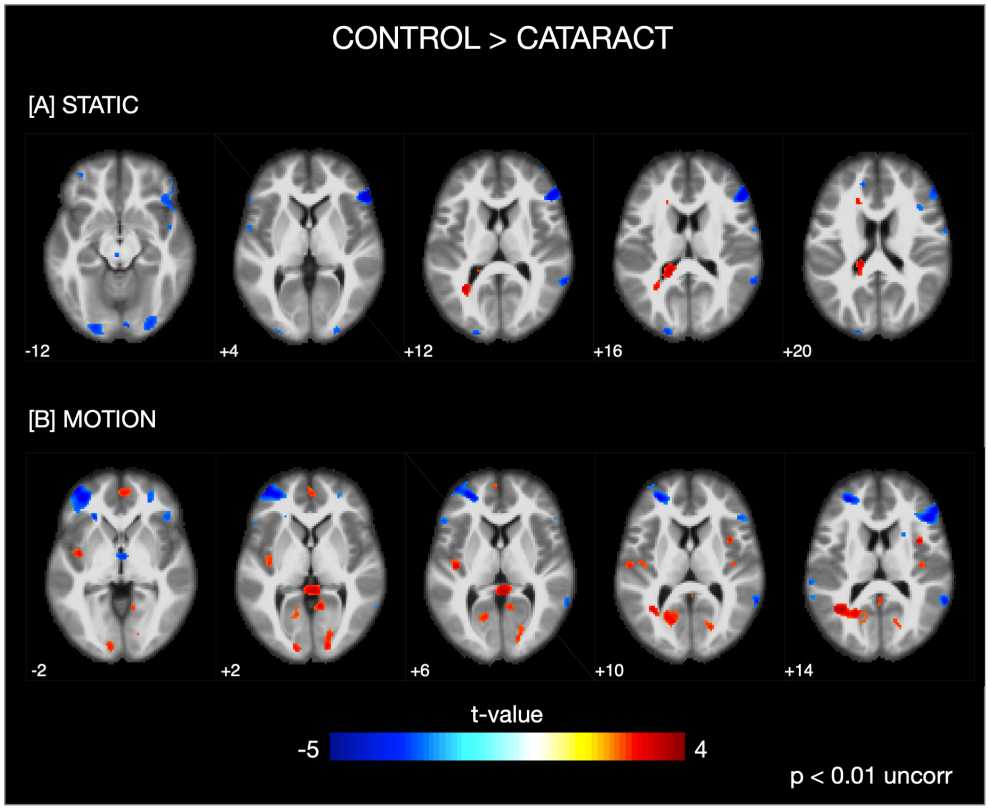


Figure S3.1 Supplementary analysis for the motion selectivity experiment.
The univariate results for [A] the contrast [static > baseline] and [B] the contrast [motion > baseline] when comparing the control group and the cataract-reversal patients. Warm colors indicate reduced recruitment in the control group and cold colors indicate enhanced recruitment in the cataract-reversal patients. Results are displayed at a lenient threshold of p<0.01 uncorrected. The results demonstrate no differences between the two groups in the early visual cortex when processing static stimuli. Reduced recruitment of the early visual cortex in the cataract reversal patients is observed when processing motion stimuli.

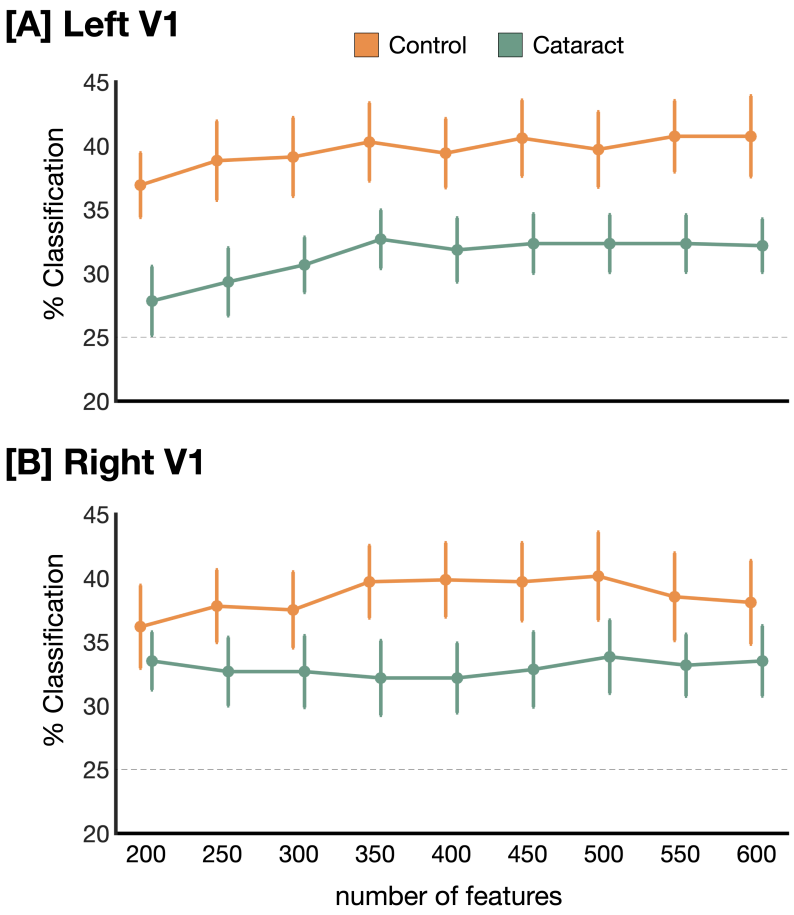


Figure S3.2 Effect of varying the number of features on motion direction decoding in V1
In the directional motion decoding experiment, we investigated the effect of varying the number of the features (from 200 to 600 voxels) on the motion direction decoding in the [a] left and [b] the right V1. The results demonstrate that while the motion direction classification was significantly above chance in V1 in both groups and both hemispheres, the motion direction classification was consistently higher in the controls than in the cataract-reversal patients.

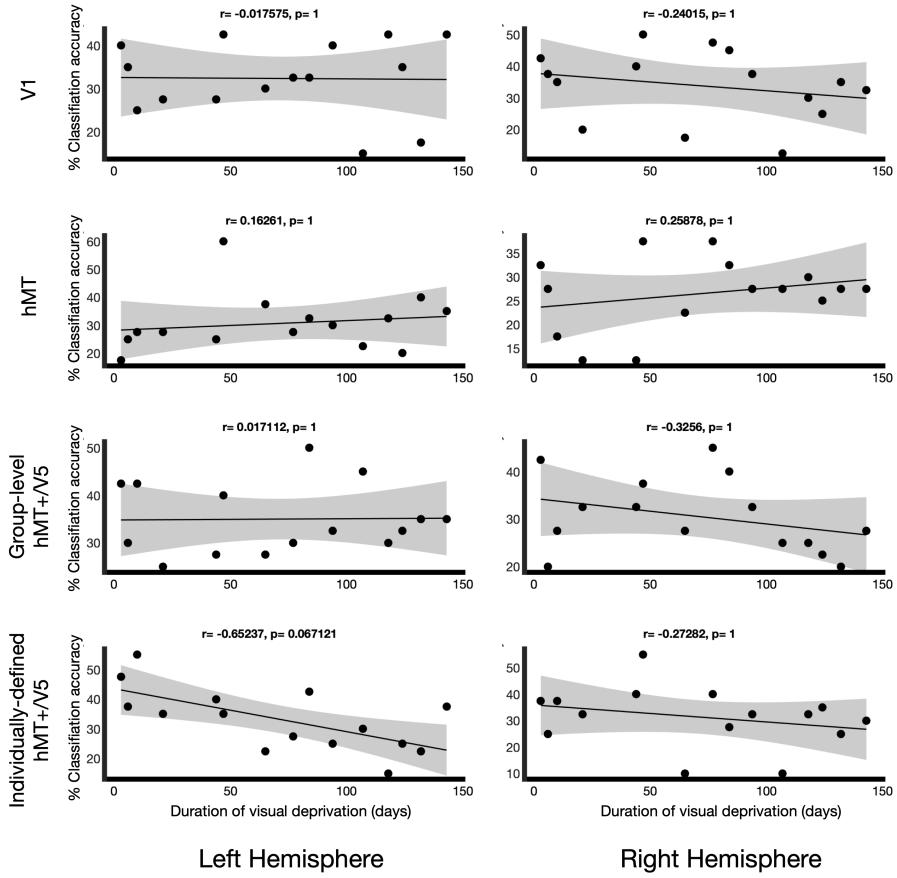


Figure S3.3 Correlation between the duration of visual deprivation and motion direction classification.

The correlation results between the duration of visual deprivation and the motion direction classification in bilateral V1, MT (as defined from the probabilistic atlas), the functionally-defined group-level hMT+/V5, and the functionally individually-defined hMT+/V5. Results are corrected for multiple comparisons using FWE-correction.

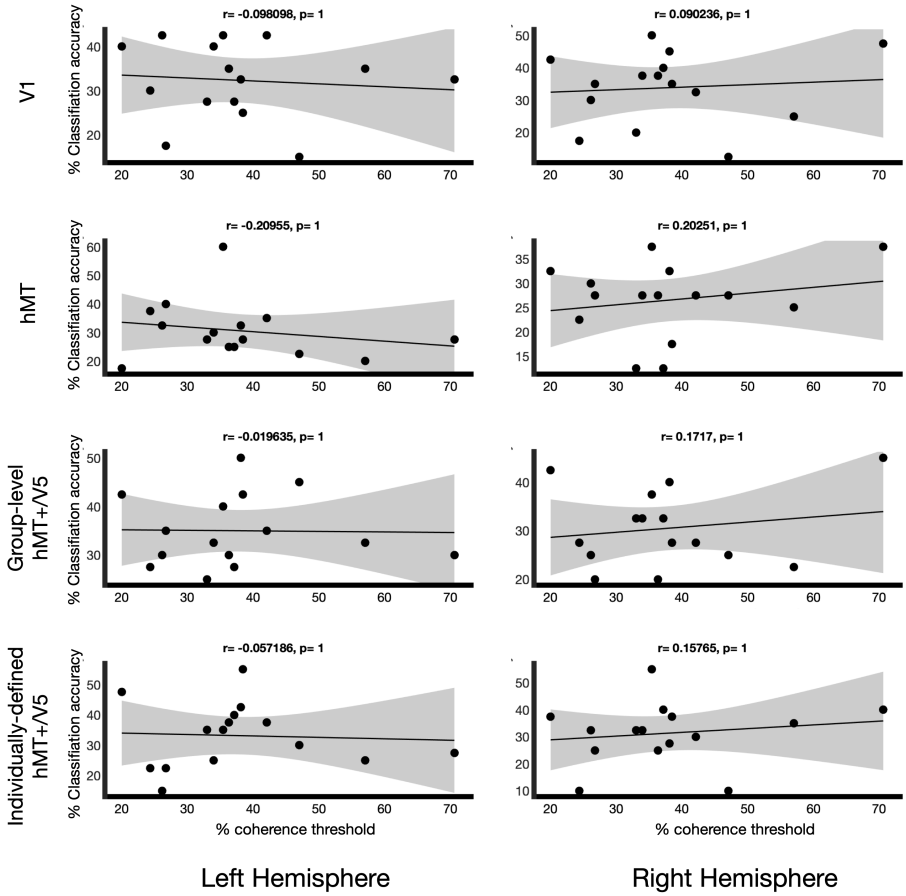


Figure S3.4 **Correlation between the behavioral motion direction discrimination threshold and motion direction classification.**

The correlation results between the behavioral motion direction discrimination threshold and the motion direction classification in bilateral V1, MT (as defined from the probabilistic atlas), the functionally-defined group-level hMT+/V5, and the functionally individually-defined hMT+/V5. Results are corrected for multiple comparisons using FWE-correction.

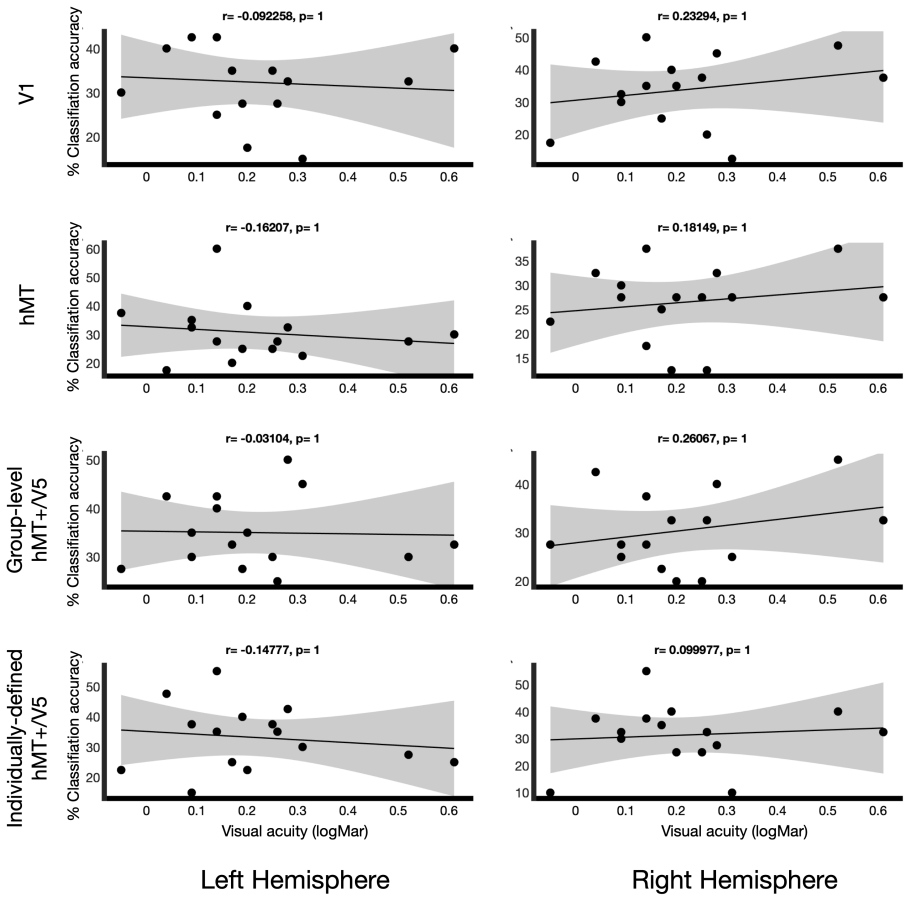


Figure S3.5 **Correlation between visual acuity and motion direction classification.**
The correlation results between the visual acuity and the motion direction classification in bilateral V1, MT (as defined from the probabilistic atlas), the functionally-defined group-level hMT+/V5, and the functionally individually-defined hMT+/V5. Results are corrected for multiple comparisons using FWE-correction.

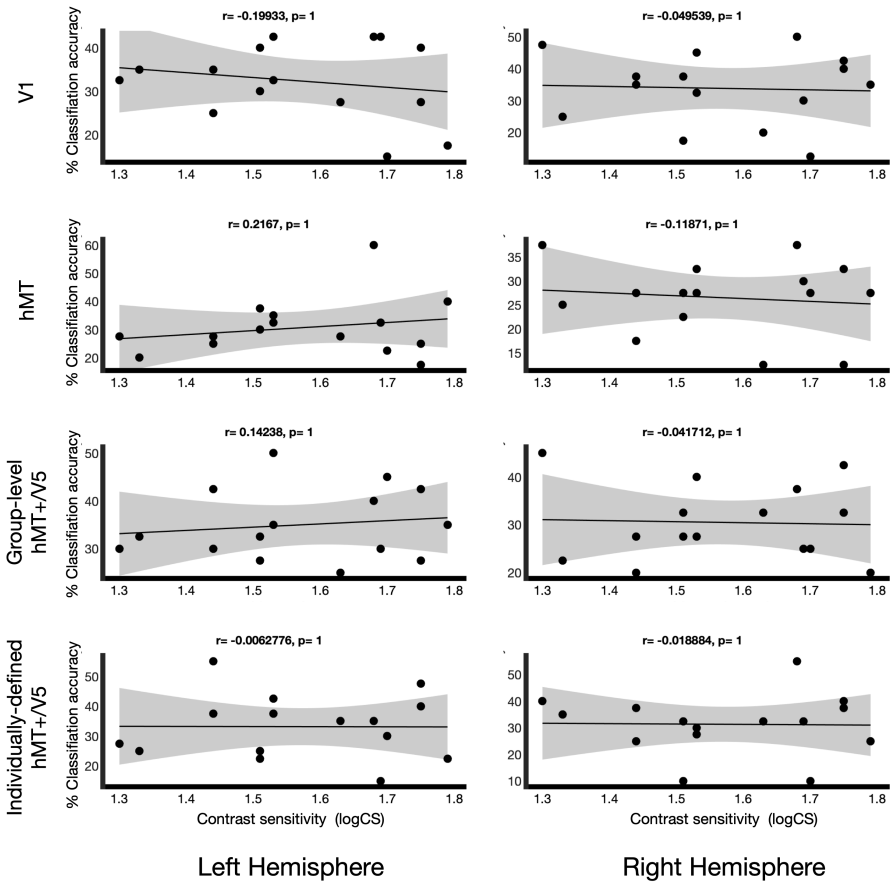


Figure S3.6 **Correlation between contrast sensitivity and motion direction classification.**
The correlation results between contrast sensitivity and the motion direction classification in bilateral V1, MT (as defined from the probabilistic atlas), the functionally-defined group-level hMT+/V5, and the functionally individually-defined hMT+/V5. Results are corrected for multiple comparisons using FWE-correction.

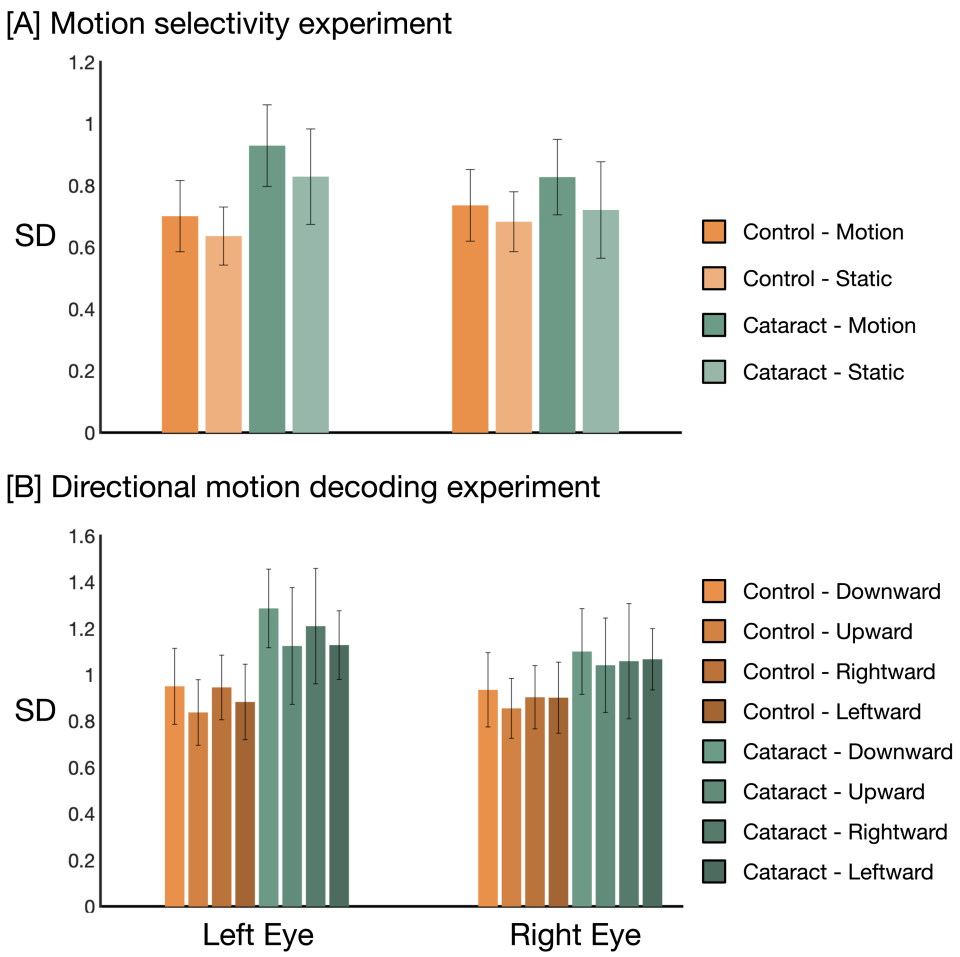


Figure S3.7 Variability of the MRI signal from the eyes.

The MRI signal from the eyes becomes more variable during performing eye movements (Beauchamp, 2003). To test for eye movements, we extracted the signal from the left and right eye during the stimulation blocks in each subject. [A] In the motion selectivity experiment, we extracted the signal from the eyes during the motion and the static blocks. The ANOVA revealed no effect of group ($F(1,120)= 2.48$, $p= 0.118$), ROI ($F(1,120)= 0.14$, $p= 0.714$), condition ($F(1,120)=0.86$, $p=0.355$) , or any significant interaction ($p>0.05$). [B] In the directional motion decoding experiment, the signals from the eyes were extracted for each motion block in each direction, run, and subject. The ANOVA revealed only a significant effect of group ($F(1,240)= 6.61$, $p= 0.011$), and no effect ROI ($F(1,240)=0.51$, $p= 0.474$), condition ($F(3,240)=0.26$, $p=0.855$), or any significant interaction ($p>0.05$). The standard deviation of the signal from the eyes (collapsed across directions and hemispheres) was significantly lower in the controls (mean ± SD= 0.9023 ± 0.5996) than the cataract-reversal patients (mean ± SD= 1.1281 ± 0.7691, $t(254)= -2.63$, $p = 0.0089$).

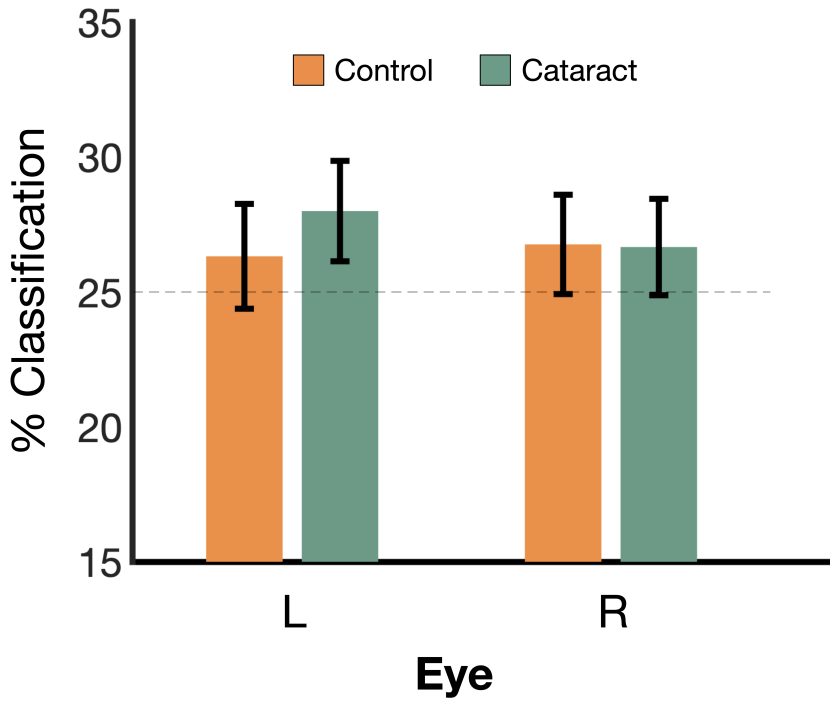


Figure S3.8 Motion direction decoding from the eyes.
We tested whether we could predict the perceived motion direction from the recorded activity from eyes. A 10 mm sphere was created for the left [MNI coordinates: -31 52 -44] and right eye [MNI coordinates: 34 50 -44]. The analysis procedure is identical to that described in the methods section for the multivariate pattern classification analysis in the directional motion decoding experiment. The motion direction classification analysis was not significant in any of the groups or the ROIs (all p>0.05). L: left, R: right.

	Age	Gender	Hand dominance	Age at diagnosis (days)	Duration of deprivation (days)	Acuity (logMar)	Contrast sensitivity (logCS)
cat-01	38	F	R	0	44	0,17	1,33
cat-02	27	F	L	124	132	0,14	1,68
cat-03	22	F	R	82	84	0,28	1,53
cat-04	23	M	R	0	3	0,2	1,79
cat-05	32	M	R	n/a	94	0,19	1,75
cat-06	25	F	R	61	65	0,31	1,7
cat-07	26	M	R	0	77	0,25	1,44
cat-08	34	F	R	~35	47	0,61	1,51
cat-09	37	M	R	142	143	0,52	1,3
cat-10	27	F	R	~90	107	0,09	1,53
cat-11	18	F	R	0	10	0,14	1,44
cat-12	26	M	R	12	21	-0,05	1,51
cat-13	27	M	R	113	118	0,26	1,63
cat-14	23	F	R	1	6	0,09	1,69
cat-15	39	M	R	122	124	0,04	1,75

Table S3.1 Cataract-reversal patients' information.

	Left hMT+/V5			Right hMT+/V5		
	x	y	z	x	y	z
con-01	-42	-70	6	40	-66	8
con-02	-44	-74	0	50	-74	2
con-03	-46	-72	4	46	-72	2
con-04	-46	-72	8	48	-60	4
con-05	-38	-84	10	48	-68	2
con-06	-42	-76	12	42	-68	6
con-07	-46	-74	2	44	-60	2
con-08	-42	-74	12	44	-72	6
con-09	-46	-72	4	42	-68	0
con-10	-44	-82	4	42	-68	6
con-11	-40	-70	4	50	-66	6
con-12	-44	-68	4	40	-60	6
con-13	-46	-72	4	48	-66	6
con-14	-46	-70	4	52	-62	0
con-15	-44	-72	-2	50	-64	0
con-16	-42	-72	12	52	-66	-2
con-17	-46	-72	4	52	-64	6
cat-01	-42	-80	6	44	-58	8
cat-02	-46	-74	8	52	-68	0
cat-03	-40	-78	0	46	-74	4
cat-04	-44	-72	10	48	-66	6
cat-05	-44	-74	0	50	-64	4
cat-06	-42	-76	4	40	-66	6
cat-07	-46	-80	4	46	-64	8
cat-08	-42	-72	-4	42	-64	-2
cat-09	-44	-70	2	46	-60	4
cat-10	-42	-78	12	52	-62	0
cat-11	-48	-76	4	50	-66	10
cat-12	-40	-80	10	46	-68	0
cat-13	-44	-80	10	46	-74	6
cat-14	-38	-80	6	46	-66	0
cat-15	-42	-72	-2	44	-70	-4

Table S3.2 Peak coordinates of the individually defined hMT+/V5.
Peak coordinates were defined in each subject from the contrast [motion > static] in motion selectivity experiment. Coordinates are in MNI space.

	cluster size	peak t-value	p(FWE-corr)	x	y	z
CONTROL						
R Lingual G	12701	17.33	0	4	-80	-4
L V2		16.8	0	-6	-76	-6
R Lingual G		16.53	0	12	-78	-10
L hMT+/V5	311	8.35	0	-44	-72	8
R Thalamus	61	7.36	0.001	22	-28	0
L inf. Parietal C	121	6.81	0.003	-24	-52	50
R Sup. Parietal C	69	6.51	0.007	24	-52	54
R Postcentral C	1	5.68	0.045	38	-40	58
	1	5.66	0.047	-22	-28	0
CATARACT						
R Sup. Occipital C	9550	14.55	0	20	-88	28
L V2		13.95	0	-6	-76	-6
R Lingual G		13.06	0	4	-80	-4
R Inf Parietal	329	7.43	0.001	30	-48	52
R Postcentral C		6.14	0.016	34	-36	38
L Sup Parietal	16	6.14	0.016	-32	-46	56
R Thalamus	5	6.09	0.018	26	-28	0
CONJUNCTION						
R Sup. Occipital C	7620	14.55	0	20	-88	28
L V2		13.95	0	-6	-76	-6
R Lingual G		13.06	0	4	-80	-4
R hMT+/V5	601	11.65	0	44	-66	2
L hMT+/V5	143	7.13	0.002	-38	-76	4
R Parietal C		6.84	0.003	-44	-70	10
R Parietal C	55	6.49	0.007	26	-50	52
L Sup Parietal	12	6.09	0.018	-32	-48	54
CONTROL > CATARACT (TFCE)						
L Middle Occip. C	3951	2266.84	0.002	-14	-98	2
R V2		2030.68	0.004	12	-80	-10
L Lingual G		2007.33	0.004	-16	-90	-16
R Calcarine C	1216	1338.89	0.023	20	-48	2
L Lingual G		1207.5	0.032	-16	-48	-4
R Lingual G		1172.35	0.035	16	-60	-6

Table S3.3 Results of the univariate analysis from the motion selectivity experiment.

For the control and the cataract-reversal groups, the results are corrected for multiple comparisons using family-wise error correction (FWE) across the whole brain at a significance level of $p<0.05$. For the contrast [Control > Cataract], the results are reported using threshold-free cluster enhancement (TFCE) at a significance level of $p<0.05$ (FWE-corrected). Coordinates are reported in MNI space. C: Cortex, G: Gyrus, L: Left, R: Right.

name	cluster size	peak T	p(FWE-corr)	x	y	z	SVC
Calcarine Gyrus	37	4.63	0.018	2	-92	2	*

Table S3.4 Correlation between motion selectivity and duration of visual deprivation.
*Results of the correlation analysis between the duration of visual deprivation in the cataract-reversal patients and motion selectivity [motion>static]. The MNI coordinate [-6 -90 -2] for V1 that was used for the SVC was extracted using the meta-analysis tool neurosynth (Yarkoni et al., 2011). It was defined from a set of 101 studies. K represents the number of voxels when displayed at p<0.005 (uncorrected). * SVC corrected.*

name	cluster size	peak T	p(FWE-corr)	x	y	z {mm}	SVC
Seed: L V1							
CONTROL							
L Lingual G	2753	10.6	0	-12	-96	4	
L Calcarine G		9.76	0	0	-90	-4	
R V1		8.67	0	14	-88	0	
L hMT+/V5	91	4.09	0.01	-46	-74	4	*
		3.8	0.019	-38	-66	6	*
R hMT+/V5	142	4.61	0.003	40	-62	2	*
		4.54	0.004	44	-66	4	*
CATARACT							
R Calcarine G	209	4.9	0.002	10	-88	0	*
L Calcarine G		4.84	0.002	2	-90	-2	*
R Calcarine G		4.41	0.005	10	-94	12	*
R hMT+/V5	52	3.93	0.015	46	-68	4	*
Seed: R V1							
CONTROL							
L Lingual G	2624	9.21	0	-8	-86	-6	
R Calcarine G		8.56	0	14	-90	2	
L Cuneus		7.31	0.001	-12	-94	16	
L hMT+/V5	231	6.07	0	-46	-72	4	*
R hMT+/V5	144	4.46	0.005	40	-62	4	*
		4.34	0.006	44	-68	4	*
CATARACT							
L Lingual G	318	5.41	0.001	-8	-84	-6	*
R Calcarine G	235	5.52	0	12	-88	0	*
		5	0.001	12	-92	10	*
R hMT+/V5	137	4.28	0.007	48	-70	4	*
		4.09	0.011	40	-66	4	*
Seed: L hMT+/V5							
CONTROLS							
L Lingual G	2059	7.98	0	-8	-84	-4	
R V1		7.93	0	14	-92	0	
L Cuneus		7.22	0.002	-18	-86	2	
L Sup. Occipital C	161	7.57	0.001	-18	-90	26	
L hMT+/V5	14	6.21	0.019	-46	-74	6	
R hMT+/V5	283	5.4	0.001	44	-74	6	*
		5.36	0.001	44	-66	4	*
CATARACT							
Calcarine G	401	5.58	0	2	-92	-2	*
L Lingual G		5.13	0.001	-8	-82	-4	*
L Calcarine G		5.06	0.001	-6	-88	2	*
R V1	480	5.58	0	12	-90	-2	*
L V1		5.58	0	2	-92	-2	*
R Calcarine		5.05	0.001	12	-90	10	*
R hMT+/V5	229	4.56	0.004	46	-66	2	*
		4.43	0.005	44	-74	6	*

		4.3	0.007	42	-62	-2	*
Seed: R hMT+/V5							
CONTROL							
L Sup. Occipital C	7996	11.93	0	-20	-90	24	
R Calcarine G		11.93	0	14	-86	-2	
L Lingual G		11.35	0	-10	-88	-6	
L hMT+/V5	384	7.81	0	-46	-74	4	*
CATARACT							
L Calcarine G	570	7.8	0.001	2	-90	-4	
R Calcarine G		7.41	0.001	12	-88	-2	
R Lingual G		6.62	0.008	8	-74	-4	
L Sup. Occipital C	180	6.97	0.003	-18	-92	24	
L Mid. Occipital C		6.87	0.004	-18	-94	16	
R Calcarine G	47	6.59	0.008	12	-92	12	
R Fusiform G	8	6.2	0.02	26	-68	-8	
R hMT+/V5	2	5.99	0.033	46	-68	2	
R Lingual G	3	5.9	0.04	24	-86	-4	
L Lingual G	3	5.86	0.043	-6	-76	-4	
L hMT+/V5	76	4.97	0.002	-42	-78	-2	*
CONTROL > CATARACT							
L V1	126	3.4	0.049	-14	-94	0	*
		3.38	0.05	-8	-94	-4	*
		3.34	0.054	-12	-90	-2	*

Table S3.5 Psychophysiological interactions (PPI) from the motion selectivity experiment.

*Results of the task based functional connectivity for the contrast [motion > static]. The seed regions included the early visual cortex where we observed a reduced recruitment in the cataract reversal patients, hMT+/V5 as defined from the conjunction analysis. The coordinates for V1 and hMT+/V5 used for the SVC were extracted using the meta-analysis tool neurosynth (Yarkoni et al., 2011). Bilateral V1 [MNI coordinates: -6 -90 -2 and 10 -94 2] was defined from a set of 101 studies. Left and right hMT+/V5 [MNI coordinates: -46 -70 2 and 48 -66 4] were defined from 106 studies. K represents the number of voxels when displayed at p<0.001 (uncorrected). * SVC corrected, L: left, R: right, G: gyrus, C: cortex.*

Motion direction decoding			
V1 defined from the Probabilistic atlas			
		L V1	R V1
Con	Mean accuracy ± SD	39.71% ± 12.15%	40.15% ± 14.21%
	p-value	0.0001	0.0001
Cat	Mean accuracy ± SD	32.33% ± 8.74 %	33.83% ± 11.1%
	p-value	0.0001	0.0001
MT defined from the Probabilistic atlas			
		L MT	R MT
Con	Mean accuracy ± SD	30.44% ± 8.89%	28.38% ± 6.79%
	p-value	0.0002	0.047
Cat	Mean accuracy ± SD	30.67% ± 10.24%	26.5% ± 7.66%
	p-value	0.0002	0.98
Group-level defined hMT+/V5 (Control analysis I)			
		L hMT+/V5	R hMT+/V5
Con	Mean accuracy ± SD	31.77% ± 8.96%	30.88% ± 9.06%
	p-value	4×10^{-5}	8×10^{-5}
Cat	Mean accuracy ± SD	35% ± 7.38%	30.5% ± 7.92%
	p-value	4×10^{-5}	12×10^{-5}
Individually defined hMT+/V5 (Control analysis II)			
		L hMT+/V5	R hMT+/V5
Con	Mean accuracy ± SD	33.53% ± 7.29%	31.47% ± 9.81%
	p-value	4×10^{-5}	8×10^{-5}
Cat	Mean accuracy ± SD	33.17% ± 10.67%	31.33% ± 11.37%
	p-value	4×10^{-5}	4×10^{-5}

Table S3.6 Directional motion classification results.

Classification results of the different motion directions (mean accuracy ± standard deviation) in each ROI for the control (Con) and the cataract-reversal group (Cat). Chance level is 25%. The classification analysis was done in V1 and MT as defined from the probabilistic atlas (L. Wang et al., 2015)*. Additionally, the analysis was performed in the functionally-defined hMT+/V5 that was defined both at the group-level and the individual-level.*

Chapter 4

Impact of blindness onset on the connectivity profile of hMT+/V5

Mohamed Rezk[1] & Olivier Collignon[1,2]

[1]Institut de Recherche en Sciences Psychologiques (IPSY) and Institute of Neuroscience (IoNS), Louvain Bionics, Crossmodal Perception and Plasticity Lab, Universite catholique de Louvain (UCL), 1348 Louvain-la-Neuve, Belgium [2]Center for Mind/Brain Sciences (CIMeC), University of Trento, 38068 Rovereto, Italy

---

Previous studies demonstrated that hMT+/V5, a region known to code for visual motion in the sighted, enhances its response to auditory and tactile moving information in case of congenital blindness. In this study, we aimed to investigate the impact of blindness onset on the resting connectivity profile of hMT+/V5 with different regions within the visual motion network and with non-visual auditory and tactile networks. Our results demonstrated that the resting connectivity architecture of hMT+/V5 within the visual motion system is similar across groups and is therefore independent from visual experience. In striking contrast, the connectivity profile of hMT+/V5 with the non-visual networks was altered in the EB, showing reduced connectivity between hMT+/V5 and the tactile sensory network, but not in the LB. These results suggest that there is an organization within the visual motion system that develops regardless of visual experience, while the connectivity of hMT+/V5 with non-visual networks is instead influenced by the onset of visual deprivation.

Chapter 4

Impact of blindness onset on the connectivity profile of hMT+/V5

Introduction

Early studies in animals used visual deprivation as a tool to understand the development of the visual cortex (Le Vay et al., 1980; Wiesel & Hubel, 1963b, 1965a). In humans, early blindness provides a natural unique model to investigate the organization and the development of the "visual" system in the absence of visual input.

Studies in the early blind (EB) demonstrated that in the case of early visual deprivation, the "visual" system is reorganized to process non-visual information while preserving the functional specialization of different functional regions (Collignon et al., 2011; Dormal & Collignon, 2011). For instance, the visual word fusiform area (VWFA), which is specialized in processing visual words in the sighted (Cohen et al., 2000; McCandliss et al., 2003), is reorganized in the EB to process Braille words (Reich et al., 2011). The multimodal motion area, hMT+/V5, that shows preferential recruitment for processing visual motion (J. D. G. Watson et al., 1993; Zeki et al., 1991), is reorganized in the EB to enhance its processing of motion information from the auditory and tactile modalities (Bedny et al., 2010; Dormal et al., 2016; Jiang et al., 2014; Poirier et al., 2006; Ricciardi et al., 2007). It has been suggested that the cross-modal reorganization of these functional regions, and others, could be driven by their connectivity architecture (Hannagan et al., 2015; Op de Beeck et al., 2019). For instance, in individuals with typical visual development, the VWFA is connected to the language network (Bouhali et al., 2014; Stevens et al., 2017), and therefore, is driven to perform the same function even in the absence of vision. The multi-modal motion area hMT+/V5, despite being dominantly visual, processes motion information from different sensory modalities (Poirier et al., 2005; Rezk et al., 2020; Van Kemenade et al., 2014), and has direct structural connections with the auditory motion processing regions (Gurtubay-Antolin et al., 2021). Therefore, following visual deprivation, hMT+/V5 is reorganized to enhance its processing of non-visual motion (Bedny et al., 2010; Dormal et al., 2016; Poirier et al., 2006). These findings emphasize the importance of mapping the connectivity architecture of different functionally-specialized regions in the case of visual deprivation.

In this study, we focus on the multi-modal motion processing area hMT+/V5, and its connectivity architecture in the visually deprived. We use resting-state functional connectivity as a proxy to investigate the communication between different brain regions at

rest (Biswal et al., 1995; Biswal, Van Kylen, et al., 1997). The resting connectivity profile of a brain region is suggested to reflect its functional role and organization (Fox et al., 2005). Moreover, resting-state connectivity has been widely used to investigate the connectivity architecture of the occipital cortex in the visually deprived (for a review, see Bock & Fine, 2014).

While many studies investigated the connectivity architecture of the occipital cortex in the EB (Burton et al., 2014; Liu et al., 2007; Qin et al., 2013), almost no study comprehensively investigated the connectivity architecture of hMT+/V5. Most of the connectivity studies either focused on the early visual cortex (Striem-amit et al., 2015), or looked at the connectivity organization between large-scale networks (Burton et al., 2014; Liu et al., 2007). These studies demonstrated that early visual deprivation results in connectivity changes between the occipital cortex and different brain networks, as well as connectivity changes within the visual network (Bedny et al., 2011; Burton et al., 2014; Liu et al., 2007; Qin et al., 2013). Oppositely, other studies suggested that the connectivity architecture of the early visual cortex in the EB follows a similar topographic organization to that in the sighted, and that the connectivity of the early visual cortex with other visual regions is indistinguishable between groups. These findings suggested that there is an innate connectivity architecture within the early visual cortex that develops regardless of visual experience (Bock et al., 2015; Striem-amit et al., 2015). However, whether these findings apply to hMT+/V5 remains unexplored.

To fill this gap in the literature, we investigate the connectivity architecture of hMT+/V5 at three different scales. At a fine-grained scale, we investigate the connectivity profile of hMT+/V5 within the visual motion network with regions that are a part of the visual motion processing hierarchy. At the intermediate scale, we investigate the connectivity profile of hMT+/V5 with early sensory networks (visual, auditory, and tactile) due to its functional role in processing motion information from these modalities in the sighted (Poirier et al., 2005; Rezk et al., 2020; Van Kemenade et al., 2014; Zeki et al., 1991), and its enhanced processing of auditory and tactile motion information in the visually deprived (Bedny et al., 2010; Dormal et al., 2016; Poirier et al., 2006; Ricciardi et al., 2007). At the large-scale, we investigate the connectivity profile of hMT+/V5 with the rest of the brain. We hypothesize that hMT+/V5 has an innate connectivity profile within the visual system that is developed regardless of visual experience as observed in V1 (Bock et al., 2015; Striem-amit et al., 2015). However, the connectivity architecture of hMT+/V5 with non-sensory visual networks will be reorganized as consequence of visual deprivation and the multisensory organization of hMT+/V5 (Dormal et al., 2016; Poirier et al., 2005; Rezk et al., 2020; Ricciardi et al., 2007; Van Kemenade et al., 2014).

Additionally, we investigate the impact of blindness onset on the reorganization of the resting connectivity architecture of hMT+/V5. Some studies suggested that in the case

of late visual deprivation, hMT+/V5 is reorganized to process auditory information, however such reorganization is not as functionally selective, or as strong as that observed in the EB (Collignon et al., 2013). Other studies suggested that in the late blind (LB), cross-modal plasticity is not observed in hMT+/V5, and that visual deprivation early in life is necessary for the cross-modal reorganization of hMT+/V5 (Bedny et al., 2010). Surprisingly, few studies investigated the connectivity architecture in the LB during rest (Ortiz-Terán et al., 2016; Qin et al., 2015). Therefore, we will investigate the impact of the onset of visual deprivation on the connectivity organization of hMT+/V5 within the visual motion system, with other sensory networks, and across the whole brain. We hypothesize that the onset of visual deprivation will have a strong impact on the connectivity profile of hMT+/V5, with the LB having less reorganization as consequence of late visual deprivation, and due to the development and the stabilization of the connectivity architecture of hMT+/V5 in a typical fashion as in sighted individuals.

Materials & Methods

Participants

We recruited participants that were divided into 4 groups. An early blind group of 14 subjects (9 males, age range= 26-59 years, mean age ± SD= 44 ± 11.19 years), a late blind group of 11 subjects (3 males, age range= 42-61 years, mean age ± SD= 52 ± 5.3 years), a sighted control group for the early blind (SCEB) of 14 subjects (7 males, age range= 23-60 years, mean age ± SD= 41 ± 13.65 years), and a sighted control group for the late blind (SCLB) of 11 subjects (3 males, age range= 25-60 years, mean age ± SD= 46.5 ± 13.28 years). Both control groups were matched with their respective blind groups for age, gender, and handedness. Early blind participants never had functional vision nor pattern recognition abilities. On the other hand, late blind participants had experienced normal vision (mean age of blindness onset ± SD = 23 ± 15 years). During testing, all blind participants were totally blind or had no pattern vision with a rudimentary sensitivity to brightness differences. No neurological impairment was found in any of the blind participants. All participants were blindfolded during the experiment. A written consent was obtained from all participants, and all the procedures were approved by the research ethic and scientific boards of the Centre for Interdisciplinary Research in Rehabilitation of Greater Montreal (CRIR) and the Quebec Bio-Imaging Network (QBIN).

fMRI Acquisition

All subjects participated in one functional MRI run. The run lasted 5 minutes (136 volumes). All subjects were instructed to keep their eyes closed, and to relax and not think about anything in particular. Functional time series were acquired using a 3-T TRIO TIM system (Siemens) equipped with a 12-channel head coil. Multi-slice T2*- weighted fMRI

images were obtained with a gradient echo-planar sequence using axial slice orientation [repetition time (TR) 2,200 ms; echo time (TE) 30 ms; functional anisotropy (FA) 90°; 35 transverse slices; 3.2 mm slice thickness; 0.8 mm inter-slices gap; field of view (FoV) 192×192 mm^2; matrix size 64×64×35; voxel size 3×3×3.2 mm^3. A structural T1-weighted 3D magnetization prepared rapid gradient echo sequence (voxel size 1×1×1.2 mm^3; matrix size 240×256; TR 2,300 ms; TE 2.91 ms; TI 900 ms; FoV 256; 160 slices) was also acquired for all subjects.

fMRI data preprocessing

Data were analyzed in SPM8 (http://www.fil.ion.ucl.ac.uk/spm) implemented in Matlab2012b (The MathWorks, Inc.). Slice-timing correction was performed, and the functional images were realigned to the mean functional image using a second-degree B-Spline interpolation. Functional images were then co-registered to the structural T1 volume. The structural volume was segmented to produce the grey matter, white matter, and cerebrospinal fluid (CSF) for each subject. Functional and anatomical volumes were then normalized to the standard Montreal Neurological Institute (MNI) template with resampling the functional volumes at a 3-mm isotropic resolution.

To control for possible motion artifacts, we implemented a scrubbing approach using Artifact detection tools (ART; www.nitrc.org/projects/artifact_detect) to identify outlier volumes that had a difference in scan-to-scan global intensity more than 9 standard deviations away from the mean global brain signal, or volumes that had more than 2 mm of scan-to-scan composite motion. The outlier time points were used as a first level covariate. Afterwards, the functional volumes were spatially smoothed using a 4-mm full-width half-maximum (FWHM) Gaussian kernel to be used for the seed-to-voxel connectivity analysis. To rule out the possibility that any connectivity changes could be attributed to motion (Power et al., 2012; Satterthwaite et al., 2012; Van Dijk et al., 2012), we compared the mean composite motion between groups using a one-way ANOVA, and found no significant difference between the 4 groups ($F(3,46)=2.389$, $p=0.081$).

Functional connectivity

Functional connectivity analysis was performed in CONN functional connectivity toolbox (Whitfield-Gabrieli & Nieto-Castanon, 2012); www.nitrc.org/projects/conn). A component-based noise correction (Compcorr) (Behzadi et al., 2007) strategy was implemented to control for nuisance effects and physiological noise. Motion parameters and their first derivatives, and outlier time points from ART toolbox were included as first level covariates to remove the variance related to head motion. Linear detrending and a band-pass filter of 0.008-0.09 Hz was applied to the functional data. First level analysis was performed in the CONN framework to investigate functional connectivity changes within-

subject. Pearson's correlation coefficient was used as a measure of functional connectivity. Age was added as a second-level covariate of no interest in all analyses to rule out the effect of age on the connectivity changes between groups.

Connectivity within-visual system

ROIs Definition

To define regions of interest (ROIs) within the visual motion system and to respect the visual hierarchy, we relied on the widely accepted proposed pathway for visual information to reach hMT/V5 according to Felleman & Van Essen (Born & Bradley, 2005; Felleman & Van Essen, 1991). We used a probabilistic atlas that has a fine-grained definition of the different regions within the visual system (Wang et al., 2015; Figure 4.1A). Using this atlas, we extracted V1d, V1v, V2d, V2v, V3a, V3b, V3d, V3v, and hMT as our ROIs. Additionally, we included the lateral geniculate nucleus, as defined from the FSL atlas, which is a subcortical region that has been suggested to be a part of the visual motion processing pathway (Born & Bradley, 2005; Sincich et al., 2004).

ROI-to-ROI functional connectivity

The bold time series from each ROI was extracted by averaging the unsmoothed functional time series from all the voxels within the ROI. The time series from each seed region was then correlated with each of the rest ROIs. The correlation coefficients were Fisher-transformed to fulfill the assumption normality of the data to be used for parametric testing in the second-level general linear model (GLM) analysis. Two-sided two-samples t-test was performed to assess differences in the functional connectivity between groups. Results were thresholded at $p<0.05$ (FDR-corrected).

Similarities of average fingerprints across groups

To evaluate the similarity of the connectivity profile of each seed region between the different groups, we tested how the average connectivity fingerprint of each seed region in one group is similar to that from another group. For each seed region, we averaged (across subjects) the connectivity vector with the rest of the visual motion network resulting in one connectivity fingerprint of 19 values (number of total ROIs [20] – the seed region [1]) per group. Then for each seed region, the average connectivity fingerprint was correlated across groups. Results were thresholded at $p<0.05$ (FDR-corrected).

Connectivity across different sensory systems

ROIs Definition

We investigated the connectivity between hMT+/V5 and the different sensory networks (visual, auditory, and tactile). Our interest in these specific networks is because hMT+/V5, in addition to being a part of the visual system, is reorganized in the case of visual deprivation, to process auditory (Battal et al., 2018; Dormal et al., 2016; Jiang et al., 2014; Poirier et al., 2006) and tactile motion information (Ricciardi et al., 2007). Moreover, when processing auditory (or tactile) motion information, hMT+/V5 shows enhanced connectivity with the auditory (or tactile) network (Battal et al., 2018; Dormal et al., 2016; Sani et al., 2010). Therefore, we look at the large-scale connectivity between hMT+/V5 and the early visual, auditory, and tactile networks. To define the seed regions, we used an independent study (Rezk et al., 2020) to functionally define bilateral hMT+/V5 ROIs. A 10-mm sphere was created around the peak MNI coordinate of the left [-42 -66 2] and the right hMT+/V5 [46 62 6]. The choice of using a moderately large ROI (radius = 10mm) is to account for the variability in the spatial location of hMT+/V5 across individuals (Dumoulin et al., 2000; Huk et al., 2002). To define the target ROIs from different sensory networks, we used the Schaefer atlas (200 parcels) which is one of the latest cortical parcellations of the human brain. These parcellations, derived from a huge dataset (n=1489 participants), agreed with the boundaries of cortical areas that were defined using histology and task-based fMRI studies demonstrating its high precision and its reflection of the brain's functional organization (Schaefer et al., 2018). To define the early visual cortex, we used the parcels located within the striate and the calcarine cortex (n=4). Similarly, for the auditory and the tactile networks, we extracted the parcels that overlapped with the auditory cortex (n=5) and the somatosensory cortex (n=19). Therefore, we have two seed regions (bilateral hMT+/V5) and 28 target regions from the different sensory modalities (the early visual cortex, the auditory cortex, and the somatosensory cortex).

ROI-to-ROI functional connectivity

The procedure for the ROI-to-ROI connectivity analysis is similar to that implemented in the within-visual system connectivity.

Similarities of average fingerprints across groups

We tested how similar was the connectivity profile of hMT+/V5 with the different sensory networks across the different groups. For each of the right and the left hMT+/V5 seed ROI, we calculated the average connectivity fingerprint (across subjects) with the different sensory networks resulting in an average connectivity fingerprint of 28 values.

Then the average connectivity fingerprints were correlated across groups. Results were thresholded at $p<0.05$ (FWE-corrected).

Connectivity across the whole brain

Seed-to-voxel functional connectivity

To explore the connectivity profile of hMT+/V5 and its reorganization at a large scale, and not only limited to specific regions of interest, a seed-based voxel-wise correlation analysis was performed. The defined seed regions were bilateral hMT+/V5 as defined functionally from an independent study (Rezk et al., 2020). A 10-mm sphere was created around the peak MNI coordinate of the left [-42 -66 2] and the right hMT+/V5 [46 62 6]. The time series from each seed region were extracted by averaging the signal from all the voxels in the seed ROI. The average time series from each seed was then correlated with each voxel in the rest of the brain. The correlation coefficients were Fisher-transformed to perform second-level statistical comparison across groups. Two-sided two-samples t-test was performed to assess differences in the functional connectivity between groups. Results were thresholded at $p<0.001$ at the voxel level and $p<0.05$ FDR-corrected at the cluster level.

Group Classification

We investigated whether the connectivity profile of hMT+/V5 with the rest of the brain was unique and distinguishable across groups. We used a machine learning classifier to test if we can predict the groups that the subjects belonged to, based on the whole-brain connectivity profile of hMT+/V5[1]. We used the previously defined 10-mm spherical hMT+/V5 ROIs as our seed regions. To define our whole-brain ROIs, we used the cortical parcels from the previously described Schaefer atlas (n=200 parcels; Schaefer et al., 2018). This resulted in a connectivity matrix of dimensions 2 (number of seeds [left and right hMT+/V5]) x 200 (number of whole-brain ROIs) in each subject. For each seed region, the connectivity fingerprint with the rest of the brain was represented as a vector of 200 correlation values. The connectivity fingerprints were then used in the classification

[1] We aimed to perform the same group classification analysis in the "connectivity within-visual system" and "Connectivity across-sensory networks", however, it was not possible due to the low number of samples (in this case, number of subjects) and the low number of features [connectivity pattern in the connectivity within-visual system (n=19), and the connectivity across-sensory networks (n=28)]. The low number of features and samples is not suitable for MVPA analysis and would result in unreliable and false negative results.

analysis (Figure 4.8A). We trained a binary support vector machine (SVM) classifier with a linear kernel with a fixed regularization parameter of C=1 to discriminate the connectivity pattern of each seed region across the different groups. The multivariate pattern analysis (MVPA) was performed in CoSMoMVPA (Oosterhof, Connolly, & Haxby, 2016; http://www.cosmomvpa.org/) implemented in MATLAB. A leave-one subject out cross-validation scheme was implemented. The binary classifier was trained to discriminate the connectivity pattern from all subjects minus one from each of the two groups, then it was tested on the left-out subject from each group (Figure 4.8A). To evaluate the performance of the classifier and its generalization across all the data, the previous step was implemented n-times (n= number of subjects that was being tested in both groups). In each cross-validation fold a different subject was used as the test subject, and the rest of the data were used as the training data. For each seed region, the classification accuracy was obtained by averaging the accuracies from all cross-validation folds.

To assess the statistical significance of our result for each seed region, we used a non-parametric permutation approach (Nichols & Holmes, 2002) to test if the classification accuracy was above chance level (50%). The label of the group to which the subjects belonged to were randomly shuffled, and the classification analysis was performed to the newly shuffled dataset in a similar manner to that of the original dataset. This permutation step was repeated 10,000 times, thus allowing us to generate a null distribution of classification accuracies of 10,000 values. A non-parametric p-value was obtained by comparing the classification accuracy from the original dataset to the classification accuracies obtained from the null distribution. The multivariate analysis was performed by classifying the subjects in the EB and the SCEB group (n=14 in each group) based on the connectivity profile of each seed region with the rest of the visual motion network. The same analysis was performed to discriminate the LB and the SCLB (n=11 in each group), and the EB and the LB (n=11 in each group). In the classification of the EB and the LB, 11 random subjects were selected from the EB group to achieve an equal number of subjects in both groups, thus having equal training and testing of both groups. This to avoid any bias in the classification due to unequal training in the different cross-validation folds. Results were corrected for multiple comparisons using FDR-correction.

Results

Connectivity within the visual system

ROI-to-ROI connectivity

We investigated the resting-state functional connectivity between cortical regions (V1d, V1v, V2d, V2v, V3a, V3b, V3d, V3v, and hMT) that are a part of the motion processing pathway, as well as the LGN in the EB, LB, and their matched control groups.

Our results demonstrated a strong intra- and inter-hemispheric connectivity between the different visual regions in all groups. Additionally, we observed significant subcortico-cortical connectivity between the LGN and the different cortical regions within the visual motion processing pathway (Figure 4.1B).

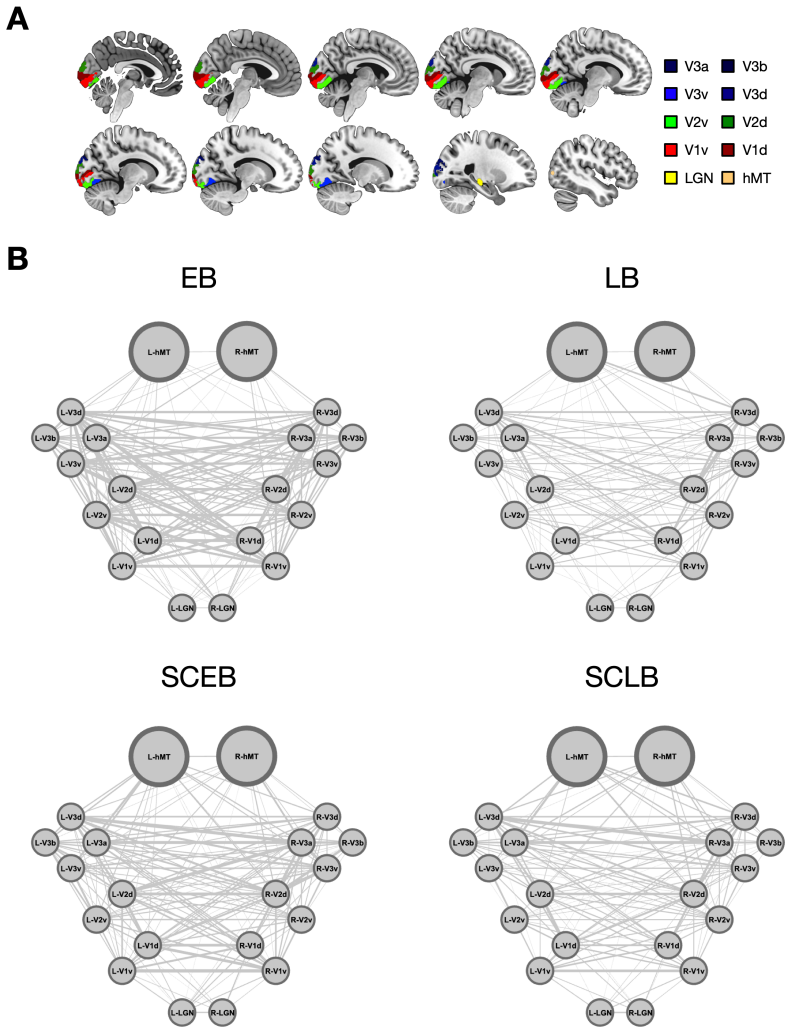


Figure 4.1 ROI-to-ROI functional connectivity in the visual motion system.
[A] ROIs used in the connectivity analysis included the LGN (defined from FSL), V1,V2,V3 (dorsal and ventral), V3a, V3b, and hMT as defined from the a probabilistic atlas (L. Wang et al., 2015) *displayed on an MNI template brain. [B] The ROI-to-ROI connectivity results in the early blind (EB), late blind (LB), controls for the early blind (SCEB), controls for the late blind (SCLB). Lines between two regions indicate the presence of a statistically significant connectivity between the two regions. The connection width is proportional to the t-value.*

When comparing the EB with their matched controls, and the LB with their matched sighted group, we observed no connectivity differences between the visually deprived and the sighted controls. When comparing the EB and the LB, we only found enhanced connectivity ($t(23) = 4.34$, $p=0.0458$, FDR-corrected) between the right V1v and the right V3b ROIs in the EB (Figure 4.2).

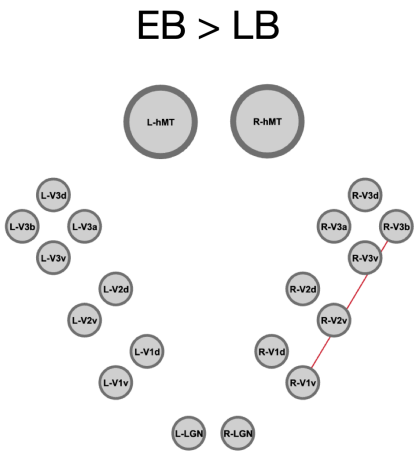


Figure 4.2 Functional connectivity differences between the EB and the LB within the visual motion network.
When comparing the pairwise connectivity between the different regions in the EB and the LB, the EB showed enhanced connectivity between the right V1v and the right V3b.

Similarities of average fingerprints across groups

To directly test the similarity of the connectivity fingerprint of hMT (and other visual regions) with the rest of the visual motion network, we calculated the average connectivity fingerprint across participants in each group (Figure 4.3). The connectivity fingerprint of hMT was highly similar across groups ($p<0.01$, FDR-corrected for all comparisons across all visual ROIs). The high similarity of the connectivity fingerprints was not limited to hMT. All the cortical regions and the LGN showed a very high similarity in their connectivity fingerprints across all the tested groups (Figure S4.1-S4.6, $p<0.001$, FDR-corrected).

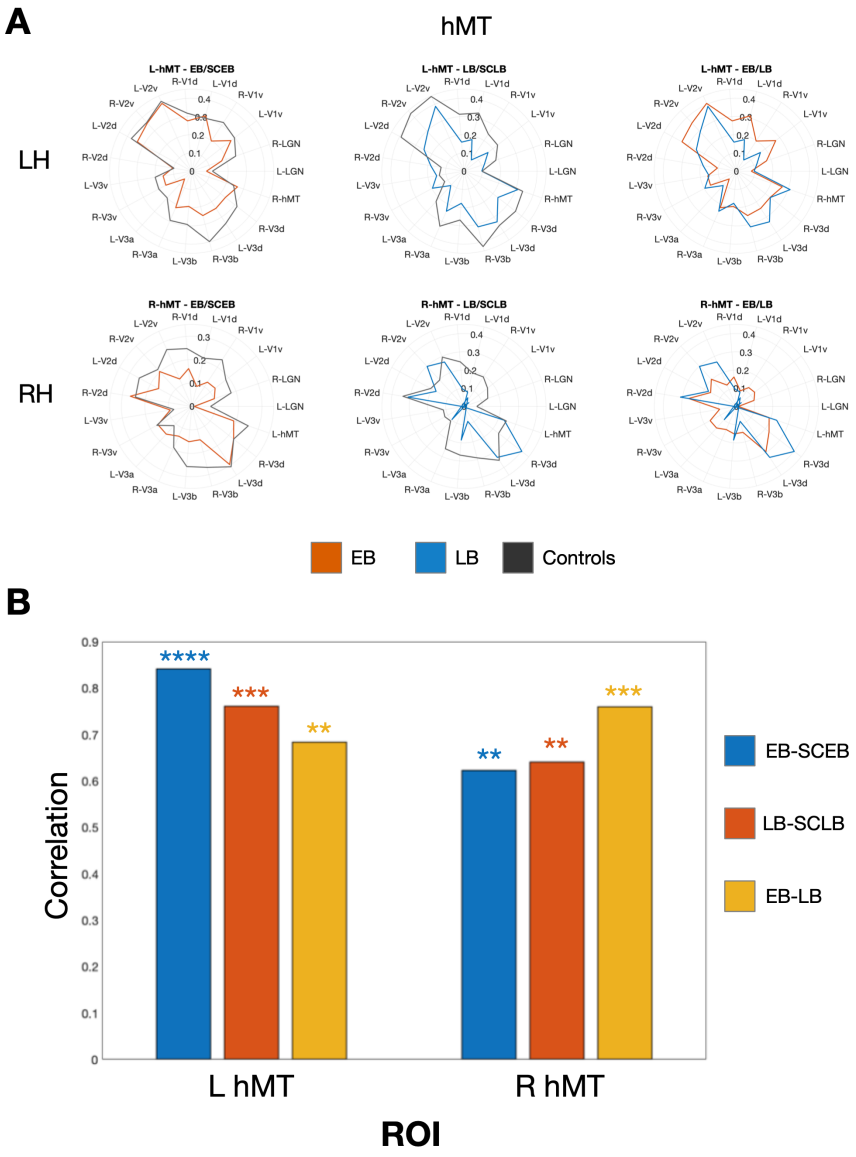


Figure 4.3 Connectivity fingerprint of hMT within the visual motion system.
*[A] A polar plot representation of the average connectivity fingerprint of the left and right hMT with other regions within the visual motion system. The figure illustrates the high similarity of the hMT connectivity fingerprint across groups. [B] The correlation analysis indicated that the average connectivity fingerprint of hMT with the visual motion system was highly correlated across the different groups. (** p<0.01, *** p<0.001, **** p<0.0001 FDR-corrected for all the visual ROIs and all pairwise group correlations)*

Connectivity across sensory systems

ROI-to-ROI connectivity

We investigated the resting-state functional connectivity between hMT+/V5 and the early visual, auditory, and tactile networks. The results demonstrated that hMT+/V5 was connected to all sensory networks in all groups during rest (Figure 4.4). When comparing the EB with their matched controls, hMT+/V5 showed reduced connectivity with the tactile network, and no significant changes with the auditory network (Figure 4.5, Table S4.1). When comparing the LB with their matched controls, or the EB with the LB, no significant differences were observed.

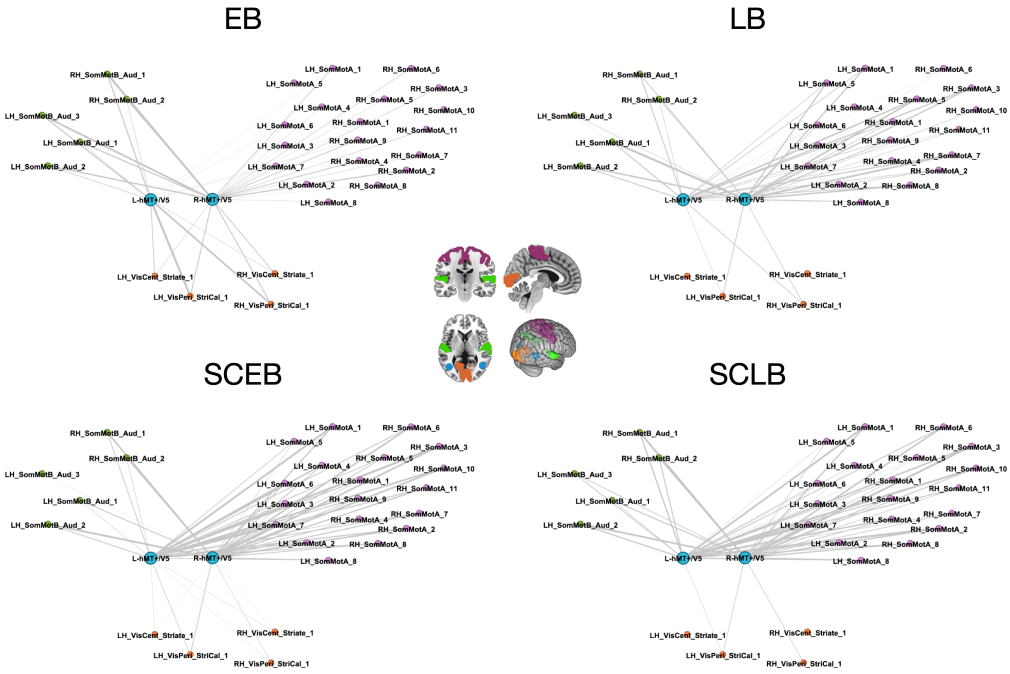


Figure 4.4 ROI-to-ROI functional connectivity of hMT+/V5 with different sensory networks
hMT+/V5 seed regions (in blue) are functionally-defined spheres from an independent study (Rezk et al., 2020). Target ROIs were defined from the Schaefer atlas (Schaefer et al., 2018) where we included parcels that belonged to the early visual (in orange), auditory (in green), and tactile networks (in purple). The figure displays the connectivity results in the early blind (EB), late blind (LB), controls for the early blind (SCEB), controls for the late blind (SCLB). Lines between two regions indicate the presence of a statistically significant connectivity between the two regions. The connection width is proportional to the t-value.

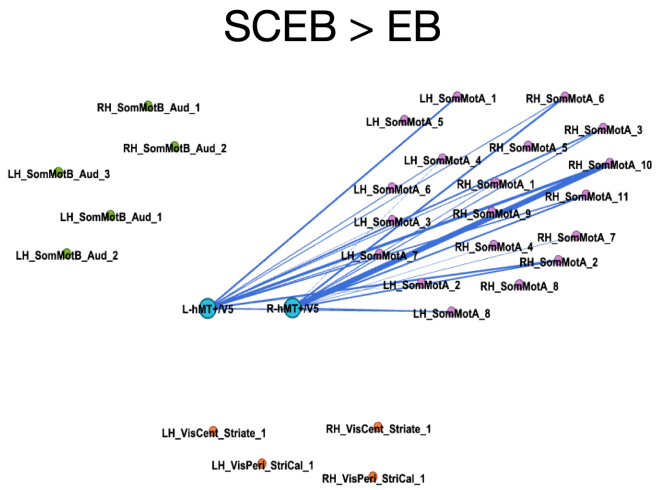


Figure 4.5 Connectivity changes of hMT+/V5 with the different sensory networks due to early visual deprivation.

When comparing the connectivity of hMT+/V5 with different regions within the different sensory networks, we observed a strong reduced connectivity of hMT+/V5 (in blue) with the tactile network (in purple), and no differences with the visual (in orange) or the auditory network (in green). The connection width is proportional to the t-value.

Similarities of average fingerprints across groups

We investigated how similar were the connectivity fingerprints of hMT+/V5 with the different sensory networks across the different groups (Figure 4.6). The average connectivity fingerprint of hMT+/V5 was not correlated in the EB and the SCEB in the left (r=-0.35, p=0.405) or the right hemisphere (r=0.005, p=1). There was also no correlation between the EB and the LB in the left (r=0.136, p=1) or right hemisphere (r=0.454, p=0.091). Only the LB showed a significant correlation of the hMT+/V5 connectivity fingerprint with the SCLB in the left (r=0.497, p=0.043) and the right hemisphere (r=0.704, p= 0.0002).

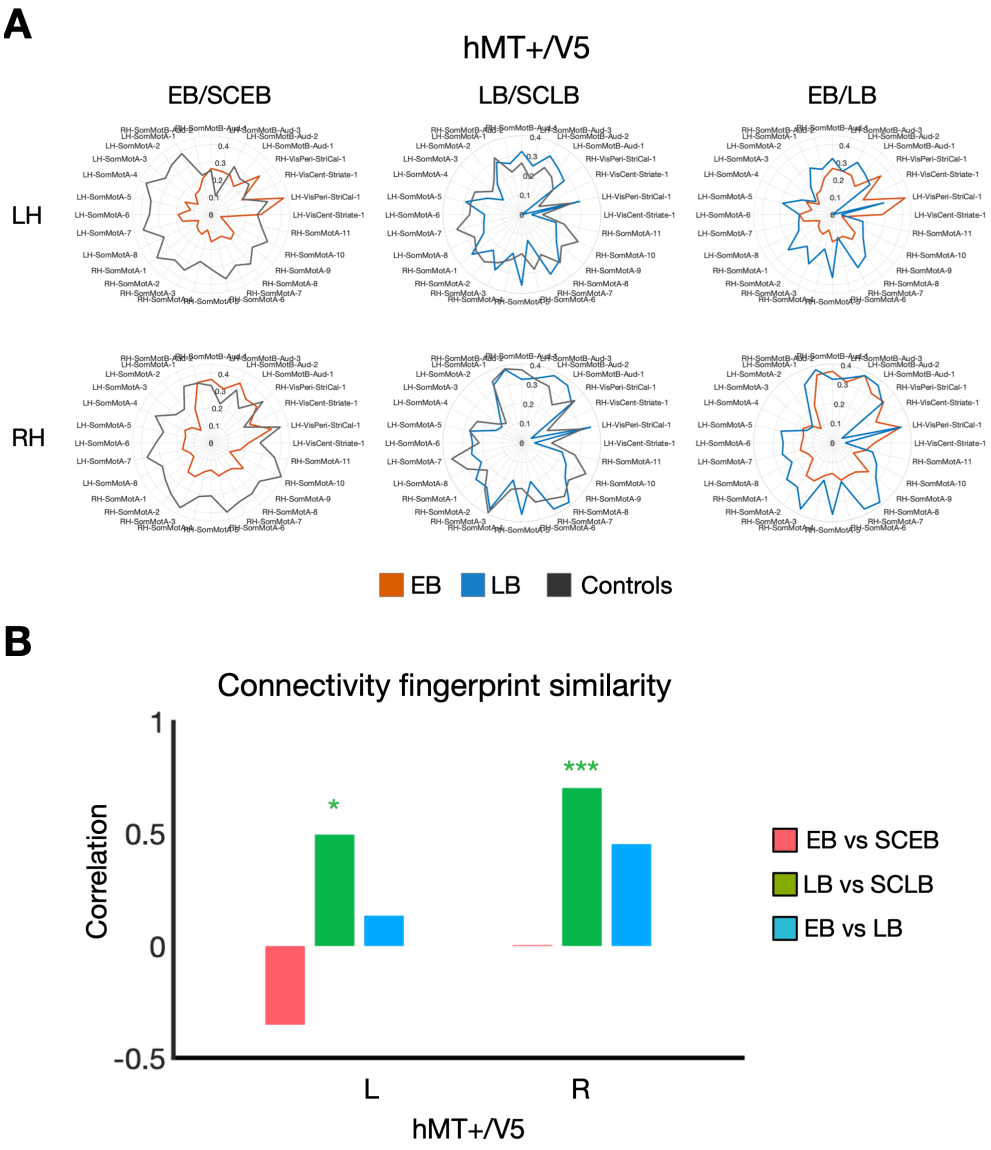


Figure 4.6 Multisensory connectivity fingerprint of hMT+/V5.
*[A] Representation of the connectivity fingerprint of hMT+/V5 with the visual, the auditory, and the tactile network in the EB (in orange), LB (in blue), SCEB and SCLB (in black). [B] The correlation analysis of the average connectivity fingerprint of hMT/V5 with the different sensory networks was only significant between the LB and the SCLB. There was no significant correlation between the EB and the SCEB, or the EB and the LB. (LH: Left hemisphere, RH: Right hemisphere, * p<0.05, ** p<0.01, *** p<0.001, **** p<0.0001)*

Seed-to-voxel analysis

To investigate the connectivity architecture of hMT+/V5 in a hypothesis-free manner, we conducted a whole brain seed-to-voxel functional connectivity analysis. We correlated the activity pattern from hMT+/V5 with each voxel in the brain. Our results demonstrated that in all groups, hMT+/V5 was connected to the early visual cortex, the visual motion network, the parietal cortex, the auditory cortex, the somatosensory, and the motor cortex (Figure 4.7A, B). When comparing the visually deprived groups with their matched controls, the right hMT+/V5 in the EB showed enhanced connectivity with the superior parietal lobule, and reduced connectivity with the precentral gyrus when compared with sighted controls which confirms the results from the ROI analysis. In the LB, the right hMT+/V5 showed enhanced recruitment with the supramarginal gyrus, and the inferior frontal gyrus (Figure 4.7C, table S4.2). No differences were observed between the EB and the LB.

Group Classification

We tested whether we could predict the group that the subjects belonged to, based on the connectivity profile of hMT+/V5 with the rest of the brain (Figure 4.8A). The group classification analysis demonstrated that we could discriminate the EB and their matched controls based on the connectivity fingerprint of the left ($p=0.007$) and right hMT+/V5 ($p=0.035$). We could also discriminate the LB and their matched controls from the connectivity patterns from the right hMT+/V5 ($p=0.035$). However, the discrimination of the EB and the LB was not significant (Figure 4.8B).

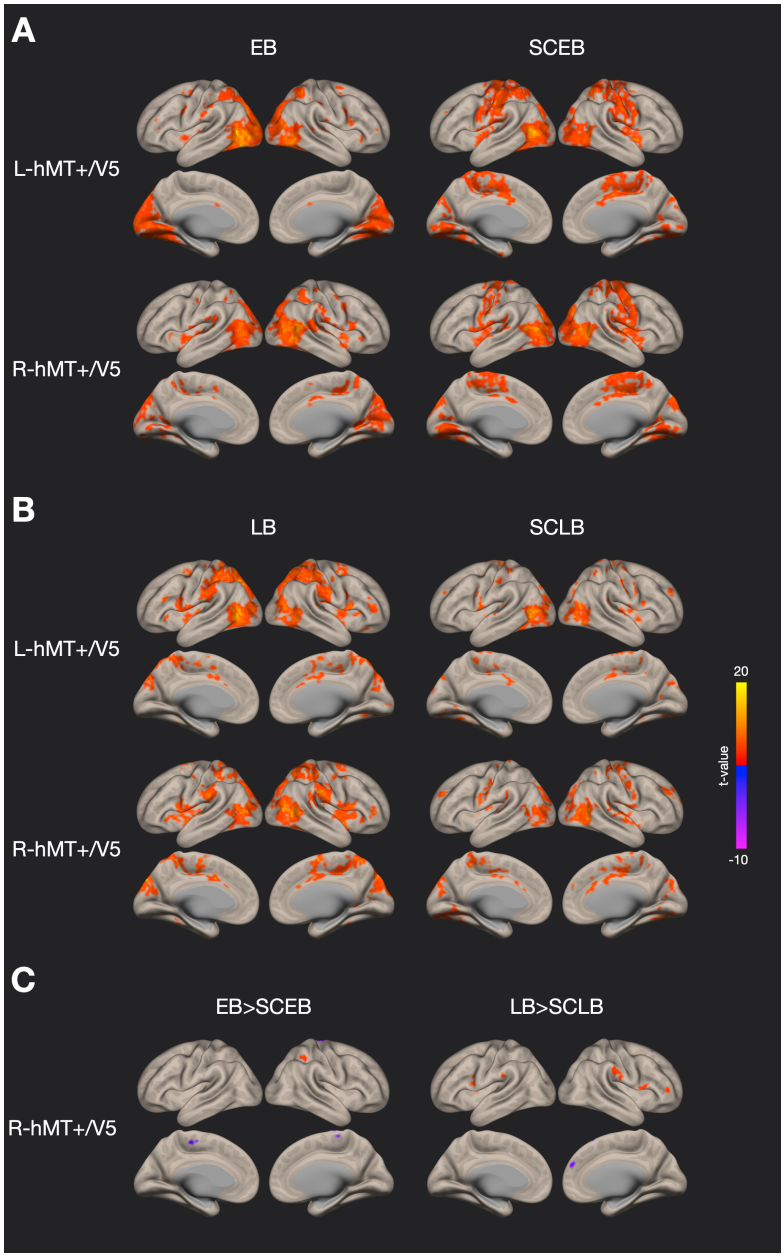


Figure 4.7 Seed-to-voxel analysis
The results of the seed-to-voxel connectivity analysis of the left and right hMT+/V5 in [A] the EB and the SCEB, and [B] the LB and the SCLB. [C] Differences in the voxel-wise connectivity of the right hMT+/V5 between the EB and the SCEB, and the LB and the SCLB. Results are displayed at $p<0.001$ at the voxel-level, and $p<0.05$ FDR-corrected at the cluster-level.

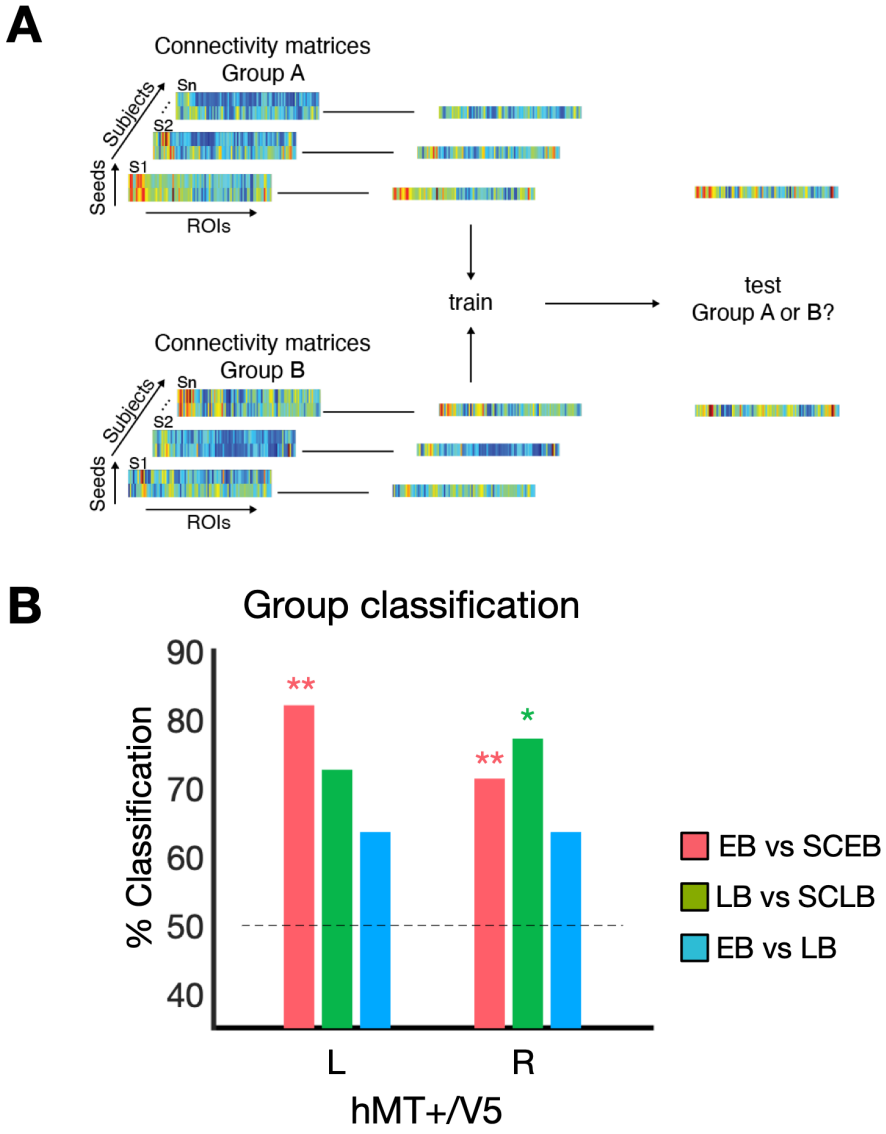


Figure 4.8 Group Classification based on the hMT+/V5 connectivity fingerprint

*[A] Group Classification: For each hMT+/V5 seed region, the connectivity fingerprint was defined by extracting the correlation values with the whole-brain ROIs (n=200). A support vector machine classifier was trained to discriminate the connectivity fingerprint of the subjects from the two groups, and then it was tested on other subjects that were not included in the training phase. [B] Group classification results when using the connectivity fingerprint of the left and the right hMT+/V5 to discriminate the EB and the SCEB, the LB and the SCLB, and the EB and the LB. * p<0.05, ** p<0.01 FDR-corrected.*

Discussion

In this study, we comprehensively investigated the connectivity architecture of hMT+/V5 within the visual motion system, and across sensory and whole-brain networks in the EB and the LB. Our results demonstrated that there is a maintenance of the connectivity profile of hMT+/V5 within the visual motion network even in the absence of any visual experience. Oppositely, the connectivity of hMT+/V5 with different sensory networks was only altered in the case of early visual deprivation. These results highlight the impact of blindness onset on the development of the connectivity architecture of hMT+/V5.

We focused in this study on the connectivity organization of hMT+/V5 at different scales. First investigated the resting connectivity profile of the different cortical and subcortical regions within the visual motion network starting from LGN and V1 to hMT. One proposed view is that the connectivity architecture within the occipital cortex is reorganized as a result of visual deprivation (Burton et al., 2014; Liu et al., 2007; Qin et al., 2013). Interestingly, we did not observe any changes in the functional connectivity between the different visual regions. This might be surprising considering previous studies suggesting changes in the connectivity of the occipital cortex following early visual deprivation (Bedny et al., 2010, 2012; Qin et al., 2013; Watkins et al., 2012). However, it is important to highlight that these connectivity changes are not all agreed upon. For instance, some studies found reduced intra-hemispheric connectivity in the occipital cortex in the EB (Bedny et al., 2010), while other studies reported increased intra-hemispheric connectivity between the early visual cortex and the lateral occipital cortex (Qin et al., 2013).

Another view suggests that there is an innate connectivity architecture within the occipital cortex that develops regardless of visual experience (Bock et al., 2015; Striem-amit et al., 2015). We investigated this hypothesis, and our findings are in line with these suggestions. Our results demonstrated that there was a very high similarity in the connectivity profile of all the visual regions within the visual motion network including the early visual cortex as well as the higher-order visual motion area hMT. This suggests that early visual experience is not necessary for this connectivity architecture to develop. Studies have shown that there is a strong similarity between the EB and the sighted in the retinotopic connectivity profile of the early visual cortex (Bock et al., 2015; Striem-amit et al., 2015). In other words, regions in the early visual cortex that show strong connectivity to other regions that have a certain retinotopic preference (as elevation, eccentricity, or laterality) share a similar connectivity profile in the EB and the sighted. Even with no visual experience since birth, the retinotopic connectivity maps are highly similar to the sighted individuals (Bock et al., 2015; Striem-amit et al., 2015). This suggests that there is an innate connectivity architecture within the visual system that develops regardless of visual experience, which is also confirmed by our findings.

We also investigated the connectivity of hMT+/V5 with different sensory networks. The motivation for investigating the connectivity of hMT+/V5 with the auditory and tactile networks is that in the case of visual deprivation, hMT+/V5 is reorganized to enhance its processing of auditory (Battal et al., 2018; Dormal et al., 2016; Jiang et al., 2014; Poirier et al., 2006) and tactile motion information (Ricciardi et al., 2007). It has also been demonstrated that there is an enhanced connectivity in the EB between hMT+/V5 and the auditory/tactile network when processing auditory/tactile motion information (Battal et al., 2018; Dormal et al., 2016; Sani et al., 2010). We investigated the resting-state connectivity of hMT+/V5 with the different sensory networks, and our results demonstrated that there was significant connectivity between hMT+/V5 and the auditory and the tactile networks in the EB, LB, and the sighted. However, in the case of early blindness, the connectivity between hMT+/V5 and the tactile network was strongly reduced. This is in line with previous studies demonstrating reduced connectivity between the occipital cortex and the somatosensory cortex in the EB (Bedny et al., 2010; Burton et al., 2014; Liu et al., 2007; Qin et al., 2013; Yu et al., 2008).

Some studies suggested that there is a reduced resting-state connectivity between the occipital cortex and the auditory cortex in the EB (Burton et al., 2014). However, we did not observe reduced connectivity between hMT+/V5 and the auditory cortex. It is trickier to investigate the resting-state correlations with the auditory cortex in the blind. hMT+/V5 and the auditory cortex are both recruited during processing auditory stimuli in the EB (Collignon et al., 2011; Dormal et al., 2016; Poirier et al., 2006). Therefore, the observed correlation between hMT+/V5 and the auditory cortex might be enhanced due to the continuous auditory stimulation from the scanner noise during the acquisition (Bedny et al., 2010; Bock & Fine, 2014).

It might be counter-intuitive that hMT+/V5 in the EB shows reduced connectivity with the tactile network (Liu et al., 2007; Qin et al., 2013) despite being massively recruited during tactile motion processing (Ricciardi et al., 2007). This was indeed puzzling with the first resting-state studies investigating the connectivity of the occipital cortex in the blind. However, these findings have been replicated across different studies (Burton et al., 2014; Liu et al., 2007; Qin et al., 2013). There is no definite explanation yet of why the connectivity with the non-visual sensory networks in the EB is reduced during rest and enhanced during a performing a related non-visual task, however, two suggestions have been proposed.

The first suggestion is that the occipital cortex in the EB acts as a multiple demand system (Duncan & Owen, 2000) where it is recruited in different cognitive tasks. Therefore, during rest, the visual cortex in the EB switches its connectivity to different regions leading to more variability of the connectivity profile across time. While during performing a non-visual task, the occipital cortex will be dedicated to performing a specific task leading to

reduced variability of the connectivity profile and enhanced connectivity with the recruited non-sensory network (Pelland et al., 2017).

The second suggestion proposed a *mixture-of-experts model* (Bock & Fine, 2014; Jacobs et al., 1991) to explain the reorganization and the connectivity changes in the case of visual deprivation. According to this model, there are different expert networks that are specializing in performing different computations. There is also a gating network that receives the output from the different expert networks and then assigns different weights to the different expert networks. This allows the system as a whole to perform more efficient computations when performing a specific task (Figure 4.9). According to this theory, in the case of early blindness, the gating network diminishes the weight of visual input while maximizing the weight of non-visual sensory inputs arriving to hMT+/V5 leading to the observed enhancement in non-visual motion processing. According to the proposed theory, it was suggested that the reduced resting-state functional connectivity between hMT+/V5 and the somatosensory cortex is a result of the reorganization of hMT+/V5 to process tactile motion information. This leads to the presence of two expert networks, one in hMT+/V5 and one in the somatosensory cortex. The gating network will try to orthogonalize the output from these two expert networks leading to a reduced correlation/connectivity between the two (Bock & Fine, 2014).

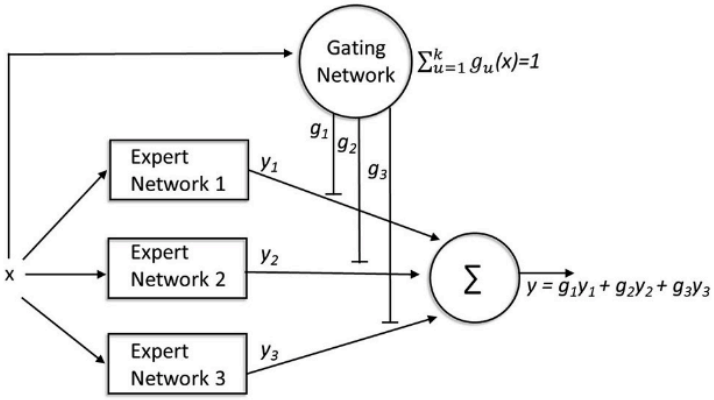


Figure 4.9 Mixture-of-experts model.
This model suggests that there are different expert networks that are dedicated to performing certain computations with the presence of a gating network the mediates the influence of the different expert networks. The gating network receives the output from the different expert networks, and assigns weights to the different networks to perform a certain task. For example, when processing visual motion in hMT+/V5, the visual sensory input will be assigned a high weight, and auditory sensory inputs will be assigned a low weight. Therefore, hMT+/V5 will be strongly recruited during visual motion processing. In the case of visual deprivation, the gating network will assign a low weight to visual expert networks as a consequence of early visual deprivation, and will assign a high weight to non-visual expert networks leading to the enhanced cross-modal responses observed in the blind. Figure adapted from (Bock & Fine, 2014).

We also investigated the connectivity profile of hMT+/V5 at a global scale with all the brain networks. The results in the EB demonstrated that hMT+/V5 had reduced functional connectivity with the tactile network, which confirms our previous results from the ROI-to-ROI connectivity analysis. Additionally, we investigated whether the whole brain connectivity profile of hMT+/V5 was stable and could be used as a marker to predict whether an individual belonged to the EB group or not. The significant classification results suggest that following early visual deprivation, there is a stable and unique hMT+/V5 connectivity profile that is distinguishable across groups.

We also investigated the impact of blindness onset on the connectivity architecture of hMT+/V5. Previous studies showed that late visual deprivation might lead to changes in the connectivity between visual and non-visual regions (Bedny et al., 2010; Sabbah et al., 2016). However, the EB showed a stronger reorganization of the occipital's connectivity architecture (Bedny et al., 2010; Qin et al., 2015). Our data supports these findings. While we did not observe connectivity changes within the visual motion network or with the auditory and tactile networks, the whole brain seed-to-voxel analysis in the LB demonstrated enhanced connectivity with the supramarginal gyrus and the inferior frontal cortex. Additionally, the group classification analysis demonstrated that the LB could be discriminated from the sighted based on the whole-brain connectivity fingerprint of the right hMT+/V5. This suggests that even in the case of late visual deprivation, hMT+/V5 still reorganizes its connectivity with other brain regions, however, it is less extensive than that observed in the EB. This is similar to what was observed in task-based studies. hMT+/V5 was recruited during auditory motion processing only in the EB, and not the LB (Bedny et al., 2010). One explanation is that having typical visual experience during the early years of life strongly shapes and sediments the structural and the functional organization of the visual system and makes it less susceptible to massive plastic reorganization as that observed in the EB (Noppeney, 2007; Ptito et al., 2008). This was also evident in our results where the connectivity fingerprint of hMT+/V5 with the different sensory networks in the LB was highly correlated with that in the sighted. Oppositely, there was no correlation between the hMT+/V5 connectivity fingerprint between the EB and their matched controls. The results suggest that while early visual deprivation reshaped the connectivity profile of hMT+/V5 with the different sensory networks, the presence of early visual experience in the LB developed the hMT+/V5 connectivity profile with the non-visual sensory networks in a similar manner to that in the sighted.

In summary, we investigated the connectivity architecture of hMT+/V5 within the visual motion network and across different sensory networks. The connectivity profile of hMT+/V5 within the visual motion system developed in a similar fashion regardless of visual experience suggesting the presence of an innate connectivity organization within the visual motion system. Oppositely, the connectivity of hMT+/V5 with non-visual networks

was reorganized as a consequence of visual deprivation, and this reorganization was modulated by the onset of visual deprivation.

References

Battal, C., Rezk, M., Mattioni, S., Bottini, R., Bertonati, G., Occelli, V., Targher, S., & Collignon, O. (2018). Decoding auditory motion direction and location in hMT+/V5 and Planum Temporale of sighted and blind individuals. *Journal of Vision*, *18*(10), 436. https://doi.org/10.1167/18.10.436

Bedny, M., Konkle, T., Pelphrey, K., Saxe, R., & Pascual-Leone, A. (2010). Sensitive period for a multimodal response in human visual motion area MT/MST. *Current Biology*, *20*(21), 1900–1906. https://doi.org/10.1016/j.cub.2010.09.044

Bedny, M., Pascual-Leone, A., Dodell-Feder, D., Fedorenko, E., & Saxe, R. (2011). Language processing in the occipital cortex of congenitally blind adults. *Proceedings of the National Academy of Sciences*, *108*(11), 4429–4434. https://doi.org/10.1073/pnas.1014818108

Bedny, M., Pascual-Leone, A., Dravida, S., & Saxe, R. (2012). A sensitive period for language in the visual cortex: Distinct patterns of plasticity in congenitally versus late blind adults. *Brain and Language*, *122*(3), 162–170. https://doi.org/10.1016/j.bandl.2011.10.005

Behzadi, Y., Restom, K., Liau, J., & Liu, T. T. (2007). A component based noise correction method (CompCor) for BOLD and perfusion based fMRI. *NeuroImage*, *37*(1), 90–101. https://doi.org/10.1016/j.neuroimage.2007.04.042

Biswal, B., Van Kylen, J., & Hyde, J. S. (1997). Simultaneous assessment of flow and BOLD signals in resting-state functional connectivity maps. *NMR in Biomedicine*, *10*(4–5), 165–170. https://doi.org/10.1002/(SICI)1099-1492(199706/08)10:4/5<165::AID-NBM454>3.0.CO;2-7

Biswal, B., Zerrin Yetkin, F., Haughton, V. M., & Hyde, J. S. (1995). Functional connectivity in the motor cortex of resting human brain using echo-planar mri. *Magnetic Resonance in Medicine*, *34*(4), 537–541. https://doi.org/10.1002/mrm.1910340409

Bock, A. S., Binda, P., Benson, N. C., Bridge, H., Watkins, K. E., & Fine, I. (2015). Resting-State Retinotopic Organization in the Absence of Retinal Input and Visual Experience. *Journal of Neuroscience*, *35*(36), 12366–12382. https://doi.org/10.1523/JNEUROSCI.4715-14.2015

Bock, A. S., & Fine, I. (2014). Anatomical and functional plasticity in early blind individuals and the mixture of experts architecture. *Frontiers in Human Neuroscience*, *8*(December), 1–13. https://doi.org/10.3389/fnhum.2014.00971

Born, R. T., & Bradley, D. C. (2005). Structure and Function of Visual Area MT. *Annual Review of Neuroscience*, *28*(March), 157–189. https://doi.org/10.1146/annurev.neuro.26.041002.131052

Bouhali, F., Schotten, M. T. De, Pinel, P., Poupon, C., Universite, S., Atomique, E., Bm, I., & Yvette, G. (2014). *Anatomical Connections of the Visual Word Form Area*. *34*(46), 15402–15414. https://doi.org/10.1523/JNEUROSCI.4918-13.2014

Burton, H., Snyder, A. Z., & Raichle, M. E. (2014). Resting state functional connectivity in early blind humans. *Frontiers in Systems Neuroscience*, *8*(April), 1–13. https://doi.org/10.3389/fnsys.2014.00051

Cohen, L., Dehaene, S., Naccache, L., Lehéricy, S., Dehaene-Lambertz, G., Hénaff, M.-A., & Michel, F. (2000). The visual word form area: Spatial and temporal characterization of an initial stage of reading in normal subjects and posterior split-brain patients. *Brain*, *123*(2), 291–307. https://doi.org/10.1093/brain/123.2.291

Collignon, O., Dormal, G., Albouy, G., Vandewalle, G., Voss, P., Phillips, C., & Lepore, F. (2013). Impact of blindness onset on the functional organization and the connectivity of the occipital cortex. *Brain*, *136*(9), 2769–2783. https://doi.org/10.1093/brain/awt176

Collignon, O., Vandewalle, G., Voss, P., Albouy, G., Charbonneau, G., Lassonde, M., & Lepore, F. (2011). Functional specialization for auditory-spatial processing in the occipital cortex of congenitally blind humans. *Proceedings of the National Academy of Sciences*, *108*(11), 4435–4440. https://doi.org/10.1073/pnas.1013928108

Dormal, G., & Collignon, O. (2011). Functional selectivity in sensory-deprived cortices. *Journal of Neurophysiology*, *105*(6), 2627–2630. https://doi.org/10.1152/jn.00109.2011

Dormal, G., Rezk, M., Yakobov, E., Lepore, F., & Collignon, O. (2016). Auditory motion in the sighted and blind: Early visual deprivation triggers a large-scale imbalance between auditory and "visual" brain regions. *NeuroImage*, *134*, 630–644. https://doi.org/10.1016/j.neuroimage.2016.04.027

Dumoulin, S. O., Bittar, R. G., Kabani, N. J., Baker, C. L., Le Goualher, G., Bruce Pike, G., & Evans, A. C. (2000). A new anatomical landmark for reliable identification of human area V5/MT: a quantitative analysis of sulcal patterning. *Cerebral Cortex*, *10*(5), 454–463. https://doi.org/10.1093/cercor/10.5.454

Duncan, J., & Owen, A. M. (2000). Common regions of the human frontal lobe recruited by diverse cognitive demands. In *Trends in Neurosciences*. https://doi.org/10.1016/S0166-2236(00)01633-7

Felleman, D. J., & Van Essen, D. C. (1991). Distributed Hierarchical Processing in the Primate Cerebral Cortex. *Cerebral Cortex*, *1*(1), 1–47. https://doi.org/10.1093/cercor/1.1.1

Fox, M. D., Snyder, A. Z., Vincent, J. L., Corbetta, M., Van Essen, D. C., & Raichle, M. E. (2005). The human brain is intrinsically organized into dynamic, anticorrelated functional networks. *Proceedings of the National Academy of Sciences of the United States of America*. https://doi.org/10.1073/pnas.0504136102

Gurtubay-Antolin, A., Battal, C., Maffei, C., Rezk, M., Mattioni, S., Jovicich, J., & Collignon, O. (2021). Direct structural connections between auditory and visual motion selective regions in humans. *The Journal of Neuroscience*. https://doi.org/10.1523/jneurosci.1552-20.2021

Hannagan, T., Amedi, A., Cohen, L., Dehaene-lambertz, G., & Dehaene, S. (2015). Origins of the specialization for letters and numbers in ventral occipitotemporal cortex. *Trends in Cognitive Sciences*, *19*(7), 374–382. https://doi.org/10.1016/j.tics.2015.05.006

Huk, A. C., Dougherty, R. F., & Heeger, D. J. (2002). Retinotopy and functional subdivision of human areas MT and MST. *The Journal of Neuroscience : The Official Journal of the Society for Neuroscience*, *22*(16), 7195–7205. https://doi.org/20026661

Jacobs, R. A., Jordan, M. I., Nowlan, S. J., & Hinton, G. E. (1991). Adaptive Mixtures of Local Experts. *Neural Computation*. https://doi.org/10.1162/neco.1991.3.1.79

Jiang, F., Stecker, G. C., & Fine, I. (2014). Auditory motion processing after early blindness. *Journal of Vision*, *14*(13), 4–4. https://doi.org/10.1167/14.13.4

Le Vay, S., Wiesel, T. N., & Hubel, D. H. (1980). The development of ocular dominance columns in normal and visually deprived monkeys. *Journal of Comparative Neurology*, *191*(1), 1–51. https://doi.org/10.1002/cne.901910102

Liu, Y., Yu, C., Liang, M., Li, J., Tian, L., Zhou, Y., Qin, W., Li, K., & Jiang, T. (2007). Whole brain functional connectivity in the early blind. *Brain*, *130*(8), 2085–2096. https://doi.org/10.1093/brain/awm121

McCandliss, B. D., Cohen, L., & Dehaene, S. (2003). The visual word form area: Expertise for reading in the fusiform gyrus. *Trends in Cognitive Sciences*. https://doi.org/10.1016/S1364-6613(03)00134-7

Nichols, T. E., & Holmes, A. P. (2002). Nonparametric permutation tests for functional neuroimaging: A primer with examples. *Human Brain Mapping*, *15*(1), 1–25. https://doi.org/10.1002/hbm.1058

Noppeney, U. (2007). The effects of visual deprivation on functional and structural organization of the human brain. *Neuroscience and Biobehavioral Reviews*, *31*(8), 1169–1180. https://doi.org/10.1016/j.neubiorev.2007.04.012

Oosterhof, N. N., Connolly, A. C., & Haxby, J. V. (2016). CoSMoMVPA: Multi-Modal Multivariate Pattern Analysis of Neuroimaging Data in Matlab/GNU Octave. *Frontiers in Neuroinformatics*, *10*. https://doi.org/10.3389/fninf.2016.00027

Op de Beeck, H. P., Pillet, I., & Ritchie, J. B. (2019). Factors Determining Where Category-Selective Areas Emerge in Visual Cortex. *Trends in Cognitive Sciences*, 1–14. https://doi.org/10.1016/j.tics.2019.06.006

Ortiz-Terán, L., Ortiz, T., Perez, D. L., Aragón, J. I., Diez, I., Pascual-Leone, A., & Sepulcre, J. (2016). Brain Plasticity in Blind Subjects Centralizes Beyond the Modal Cortices. *Frontiers in Systems Neuroscience*, *10*(July). https://doi.org/10.3389/fnsys.2016.00061

Pelland, M., Orban, P., Dansereau, C., Lepore, F., Bellec, P., & Collignon, O. (2017). State-dependent modulation of functional connectivity in early blind individuals. *NeuroImage*, *147*(June 2016), 532–541. https://doi.org/10.1016/j.neuroimage.2016.12.053

Poirier, C., Collignon, O., DeVolder, A. G., Renier, L., Vanlierde, A., Tranduy, D., & Scheiber, C. (2005). Specific activation of the V5 brain area by auditory motion processing: An fMRI study. *Cognitive Brain Research*, *25*(3), 650–658. https://doi.org/10.1016/j.cogbrainres.2005.08.015

Poirier, C., Collignon, O., Scheiber, C., Renier, L., Vanlierde, A., Tranduy, D., Veraart, C., & De Volder, A. G. (2006). Auditory motion perception activates visual motion areas in early blind subjects. *NeuroImage*, *31*(1), 279–285. https://doi.org/10.1016/j.neuroimage.2005.11.036

Power, J. D., Barnes, K. A., Snyder, A. Z., Schlaggar, B. L., & Petersen, S. E. (2012). Spurious but systematic correlations in functional connectivity MRI networks arise from subject motion. *NeuroImage*, *59*(3), 2142–2154. https://doi.org/10.1016/j.neuroimage.2011.10.018

Ptito, M., Schneider, F. C. G. G., Paulson, O. B., & Kupers, R. (2008). Alterations of the visual pathways in congenital blindness. *Experimental Brain Research*, *187*(1), 41–49. https://doi.org/10.1007/s00221-008-1273-4

Qin, W., Liu, Y., Jiang, T., & Yu, C. (2013). The Development of Visual Areas Depends Differently on Visual Experience. *PLoS ONE*, *8*(1), 1–10. https://doi.org/10.1371/journal.pone.0053784

Qin, W., Xuan, Y., Liu, Y., Jiang, T., & Yu, C. (2015). Functional connectivity density in congenitally and late blind subjects. *Cerebral Cortex*, *25*(9), 2507–2516. https://doi.org/10.1093/cercor/bhu051

Reich, L., Szwed, M., Cohen, L., & Amedi, A. (2011). A ventral visual stream reading center independent of visual experience. *Current Biology*, *21*(5), 363–368. https://doi.org/10.1016/j.cub.2011.01.040

Rezk, M., Cattoir, S., Battal, C., Occelli, V., Mattioni, S., & Collignon, O. (2020). Shared Representation of Visual and Auditory Motion Directions in the Human Middle-Temporal Cortex. *Current Biology*, *30*(12), 2289-2299.e8. https://doi.org/10.1016/j.cub.2020.04.039

Ricciardi, E., Vanello, N., Sani, L., Gentili, C., Scilingo, E. P., Landini, L., Guazzelli, M., Bicchi, A., Haxby, J. V., & Pietrini, P. (2007). The Effect of Visual Experience on the Development of Functional Architecture in hMT+. *Cerebral Cortex*, *17*(12), 2933–2939. https://doi.org/10.1093/cercor/bhm018

Sabbah, N., Authié, C. N., Sanda, N., Mohand-Saïd, S., Sahel, J.-A. A., Safran, A. B., Habas, C., & Amedi, A. (2016). Increased functional connectivity between language and visually deprived areas in late and partial blindness. *NeuroImage*, *136*, 162–173. https://doi.org/10.1016/j.neuroimage.2016.04.056

Sani, L., Ricciardi, E., Gentili, C., Vanello, N., Haxby, J. V., & Pietrini, P. (2010). Effects of Visual Experience on the Human MT+ Functional Connectivity Networks: An fMRI Study of Motion Perception in Sighted and Congenitally Blind Individuals. *Frontiers in Systems Neuroscience*, *4*, 159. https://doi.org/10.3389/fnsys.2010.00159

Satterthwaite, T. D., Wolf, D. H., Loughead, J., Ruparel, K., Elliott, M. A., Hakonarson, H., Gur, R. C., & Gur, R. E. (2012). NeuroImage Impact of in-scanner head motion on multiple measures of functional connectivity : Relevance for studies of neurodevelopment in youth ☆. *NeuroImage*, *60*(1), 623–632. https://doi.org/10.1016/j.neuroimage.2011.12.063

Schaefer, A., Kong, R., Gordon, E. M., Laumann, T. O., Zuo, X.-N., Holmes, A. J., Eickhoff, S. B., & Yeo, B. T. T. (2018). Local-Global Parcellation of the Human Cerebral Cortex from Intrinsic Functional Connectivity MRI. *Cerebral Cortex*, *28*(9), 3095–3114. https://doi.org/10.1093/cercor/bhx179

Sincich, L. C., Park, K. F., Wohlgemuth, M. J., & Horton, J. C. (2004). Bypassing V1: a direct geniculate input to area MT. *Nature Neuroscience*, *7*(10), 1123–1128. https://doi.org/10.1038/nn1318

Stevens, W. D., Kravitz, D. J., Peng, C. S., Tessler, M. H., & Martin, A. (2017). Privileged functional connectivity between the visual word form area and the language system.

Journal of Neuroscience. https://doi.org/10.1523/JNEUROSCI.0138-17.2017

Striem-amit, E., Ovadia-caro, S., Caramazza, A., Margulies, S., Villringer, A., & Amedi, A. (2015). *Functional connectivity of visual cortex in the blind follows retinotopic organization principles*. 1–17. https://doi.org/10.1093/brain/awv083

Van Dijk, K. R. A., Sabuncu, M. R., & Buckner, R. L. (2012). The influence of head motion on intrinsic functional connectivity MRI. *NeuroImage*, *59*(1), 431–438. https://doi.org/10.1016/j.neuroimage.2011.07.044

Van Kemenade, B. M., Seymour, K., Wacker, E., Spitzer, B., Blankenburg, F., & Sterzer, P. (2014). Tactile and visual motion direction processing in hMT+/V5. *NeuroImage*, *84*, 420–427. https://doi.org/10.1016/j.neuroimage.2013.09.004

Wang, L., Mruczek, R. E. B. B., Arcaro, M. J., & Kastner, S. (2015). Probabilistic maps of visual topography in human cortex. *Cerebral Cortex*, *25*(10), 3911–3931. https://doi.org/10.1093/cercor/bhu277

Watkins, K. E., Cowey, A., Alexander, I., Filippini, N., Kennedy, J. M., Smith, S. M., Ragge, N., & Bridge, H. (2012). Language networks in anophthalmia: Maintained hierarchy of processing in "visual" cortex. *Brain*, *135*(5), 1566–1577. https://doi.org/10.1093/brain/aws067

Watson, J. D. G., Myers, R., Frackowiak, R. S. J., Hajnal, J. V., Woods, R. P., Mazziotta, J. C., Shipp, S., & Zeki, S. (1993). Area V5 of the Human Brain: Evidence from a Combined Study Using Positron Emission Tomography and Magnetic Resonance Imaging. *Cerebral Cortex*, *3*(2), 79–94. https://doi.org/10.1093/cercor/3.2.79

Whitfield-Gabrieli, S., & Nieto-Castanon, A. (2012). *Conn* : A Functional Connectivity Toolbox for Correlated and Anticorrelated Brain Networks. *Brain Connectivity*, *2*(3), 125–141. https://doi.org/10.1089/brain.2012.0073

Wiesel, T. N., & Hubel, D. H. (1963). Responses in Striate Deprived of Vision Cortex of One Eye. *Journal of Neurophysiology*, *26*(6), 1003–1017. https://doi.org/10.1152/jn.1963.26.6.1003

Wiesel, T. N., & Hubel, D. H. (1965). Comparison of the effects of unilateral and bilateral eye closure on cortical unit responses in kittens. *Journal of Neurophysiology*, *28*(6), 1029–1040. https://doi.org/10.1152/jn.1965.28.6.1029

Yu, C., Liu, Y., Li, J., Zhou, Y., Wang, K., Tian, L., Qin, W., Jiang, T., & Li, K. (2008). Altered functional connectivity of primary visual cortex in early blindness. *Human Brain Mapping*, *29*(5), 533–543. https://doi.org/10.1002/hbm.20420

Zeki, S., Watson, J. D. G., Lueck, C., Friston, K., Kennard, C., & Frackowiak, R. (1991). A

direct demonstration of functional specialization in human visual cortex. *The Journal of Neuroscience*, *11*(3), 641–649. https://doi.org/10.1523/JNEUROSCI.11-03-00641.1991

Supplementary materials

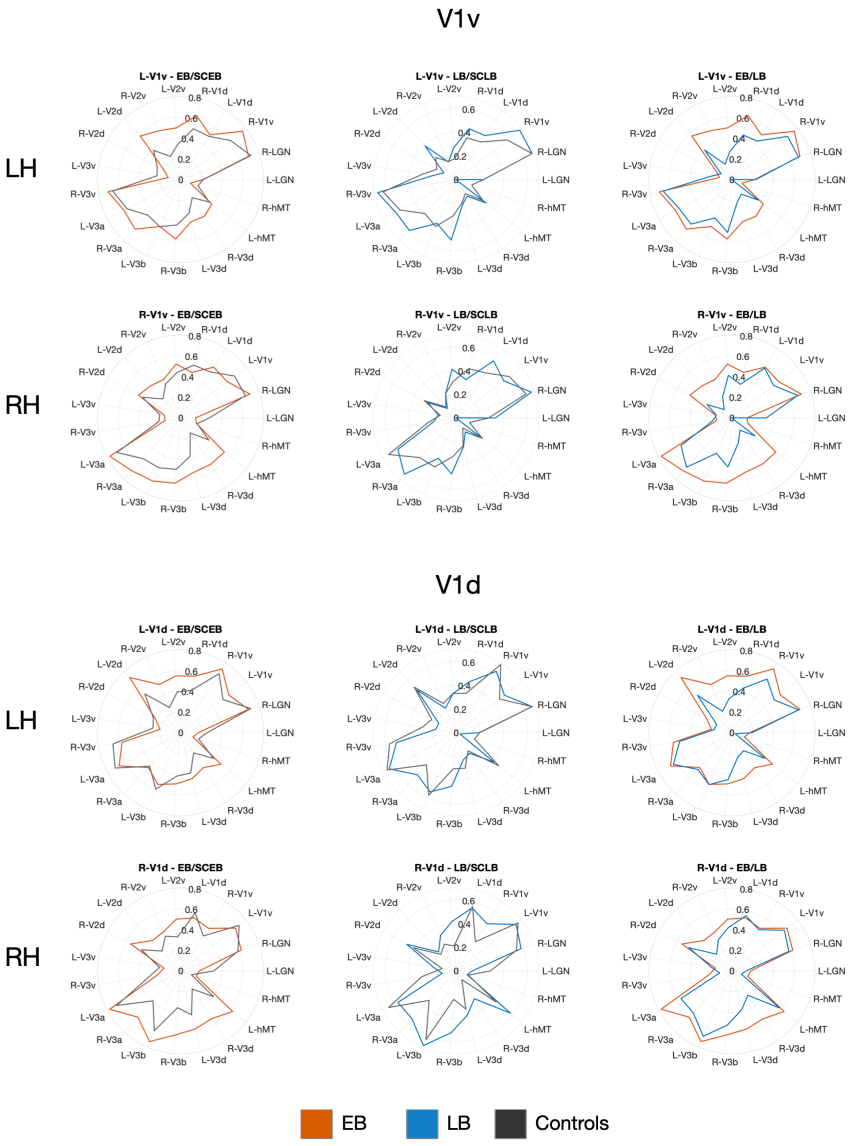


Figure S4.1 Connectivity fingerprint of V1 within the visual motion system.

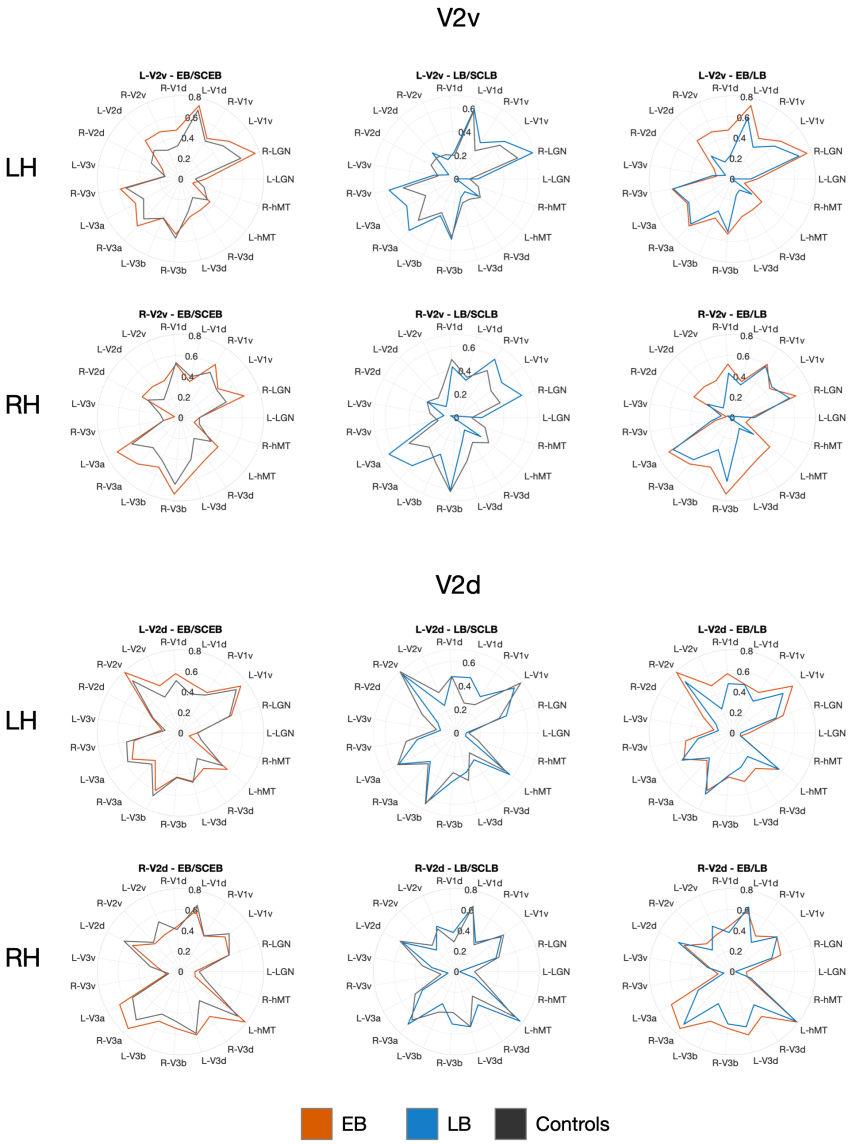


Figure S4.2 Connectivity fingerprint of V2 within the visual motion system.

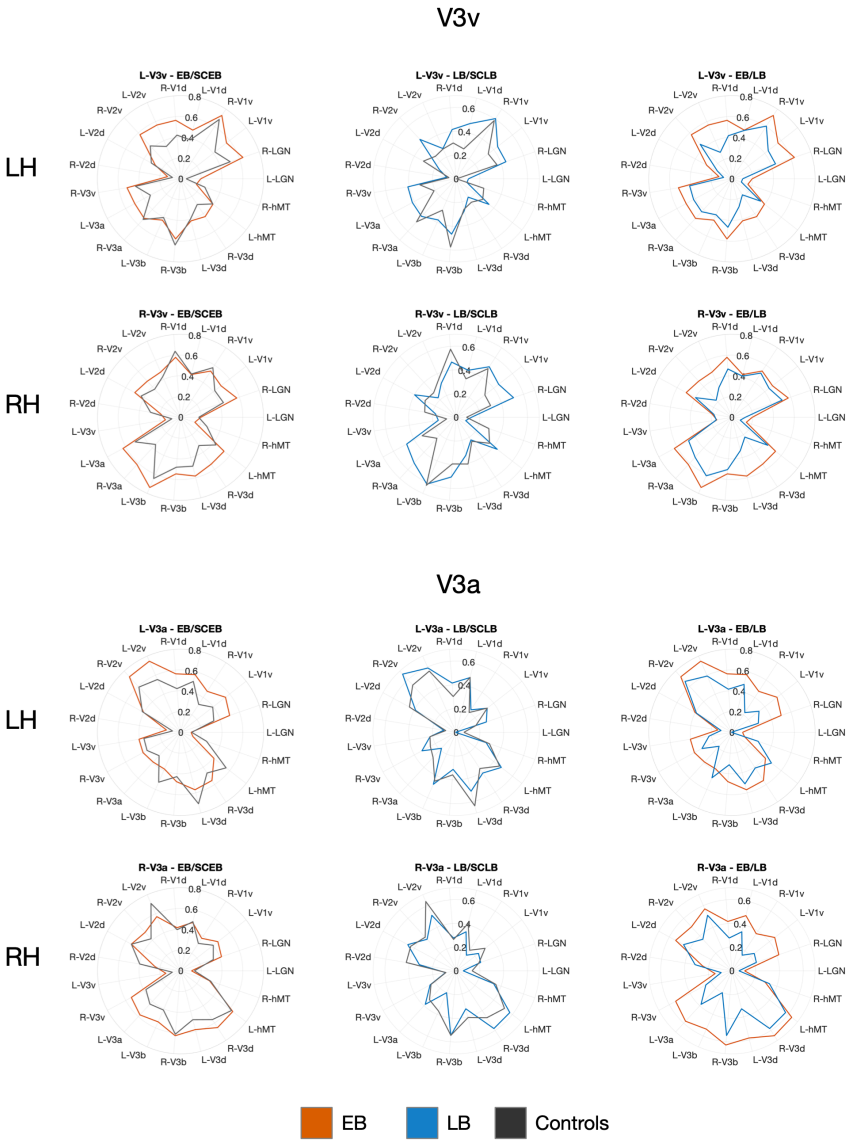


Figure S4.3 Connectivity fingerprint of V3v and V3a within the visual motion system.

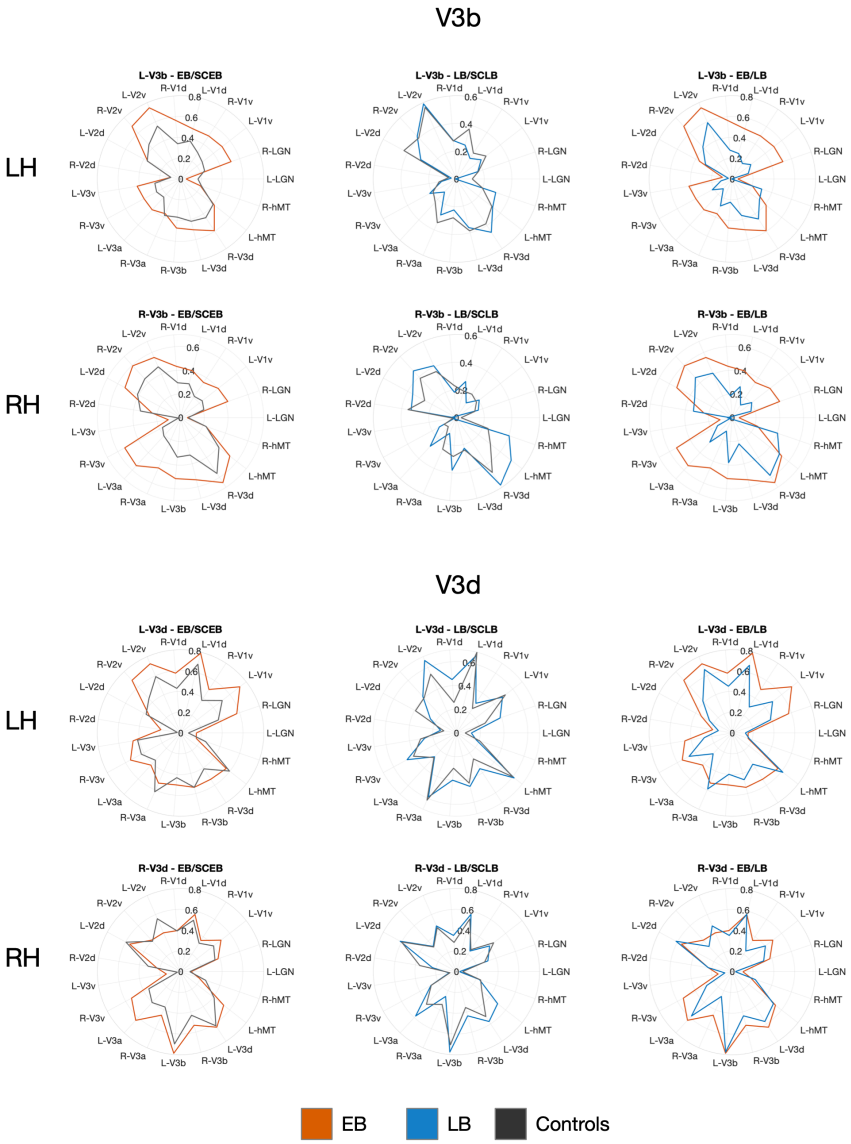


Figure S4.4 Connectivity fingerprint of V3b and V3d within the visual motion system.

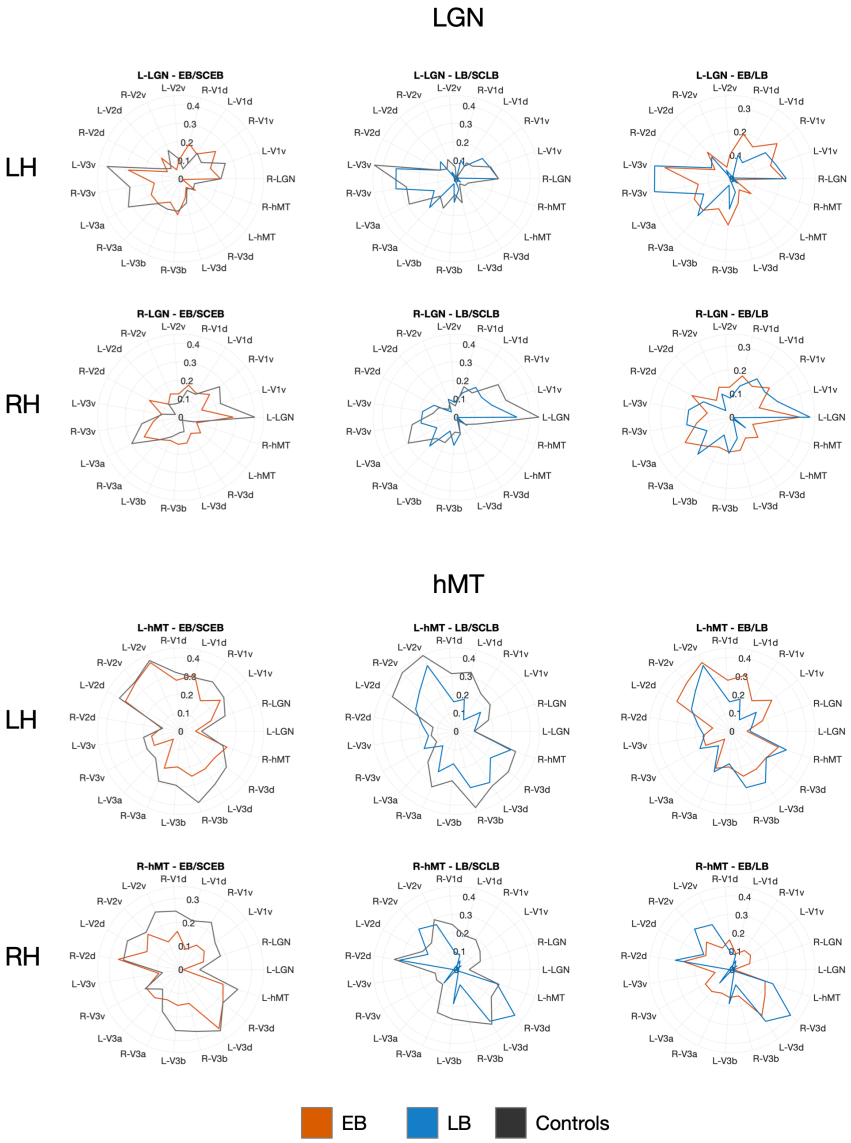


Figure S4.5 Connectivity fingerprint of LGN and hMT within the visual motion system.

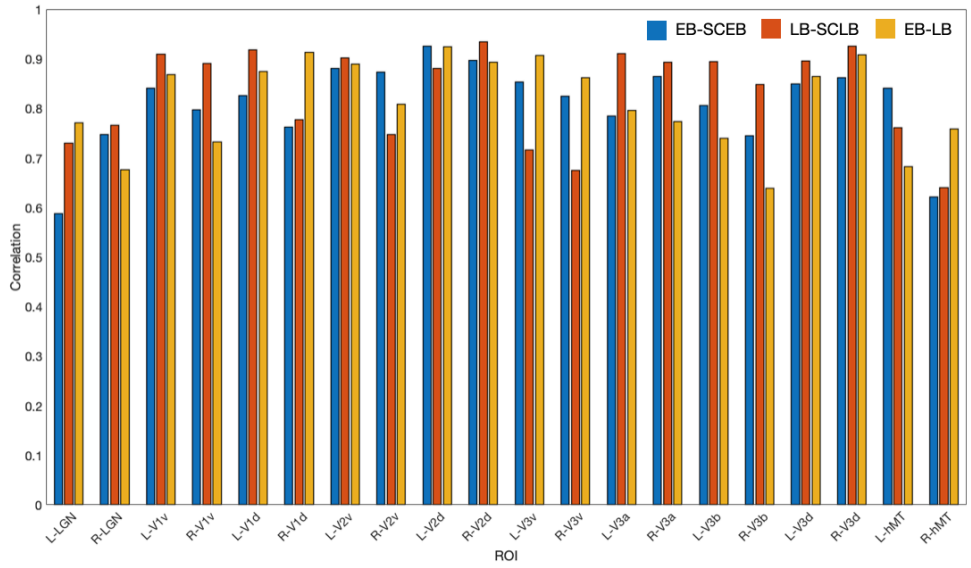


Figure S4.6 The correlation analysis of the average connectivity fingerprint of the different visual regions within the visual motion system.

Seed ROI	Target ROI	pValue (FDR-corrected)	t-value
L hMT+/V5	LH_SomMotA_1	0.0309	-3.300
L hMT+/V5	LH_SomMotA_2	0.0498	-2.468
L hMT+/V5	LH_SomMotA_3	0.0479	-2.544
L hMT+/V5	LH_SomMotA_4	0.0334	-2.827
R hMT+/V5	LH_SomMotA_4	0.0481	-2.504
L hMT+/V5	LH_SomMotA_7	0.0334	-2.799
R hMT+/V5	LH_SomMotA_7	0.0334	-2.860
L hMT+/V5	LH_SomMotA_8	0.0325	-3.012
R hMT+/V5	LH_SomMotA_8	0.0334	-2.805
L hMT+/V5	RH_SomMotA_1	0.0340	-2.765
R hMT+/V5	RH_SomMotA_1	0.0359	-2.718
L hMT+/V5	RH_SomMotA_2	0.0309	-3.270
R hMT+/V5	RH_SomMotA_2	0.0321	-3.103
L hMT+/V5	RH_SomMotA_3	0.0309	-3.173
R hMT+/V5	RH_SomMotA_3	0.0334	-2.867
R hMT+/V5	RH_SomMotA_4	0.0479	-2.526
L hMT+/V5	RH_SomMotA_6	0.0334	-2.805
R hMT+/V5	RH_SomMotA_6	0.0309	-3.332
R hMT+/V5	RH_SomMotA_7	0.0433	-2.614
L hMT+/V5	RH_SomMotA_10	0.0264	-3.729
R hMT+/V5	RH_SomMotA_10	0.0017	-5.047
L hMT+/V5	RH_SomMotA_11	0.0325	-3.006
R hMT+/V5	RH_SomMotA_11	0.0309	-3.172

Table S4.1 Connectivity changes of hMT+/V5 with the different sensory networks due to early visual deprivation.

Region	cluster size	x	y	z	size p-FDR	peak-uncorr
EB > SCEB						
R Superior parietal lobule	16	33	-46	46	0.0376	0.037564
SCEB > EB						
Precentrral Gyrus	35	9	-25	73	0.0015	0.001490
LB > SCLB						
R Supramarginal G	29	63	-22	28	0.0027	0.000052
R Inferior frontal G	29	60	17	19	0.0027	0.000007
R Frontal Pole	19	42	41	4	0.0137	0.000056
L Insular Cortex	14	-36	2	13	0.026	0.000108
L Inferior frontal G	13	-51	8	13	0.026	0.000009
L Frontal Pole	13	-48	41	7	0.026	0.000045
L Supramarginal G	10	-57	-31	25	0.0482	0.000289
SCLB > LB						
R Superior frontal G	13	12	23	64	0.026	0.000042
R Superior frontal G	12	6	53	25	0.03	0.000050

Table S4.2 Seed-to-voxel analysis.
This table displays the connectivity changes of the right hMT+/V5 across the whole brain when compared in the EB and the SCEB, as well as when compared in the LB and the SCLB.

Chapter 5

Discussion

The aim of the thesis

The aim of the present thesis was to address three main questions: [1] Is there a unimodal, or multi-modal, or abstracted representation of motion direction information in hMT+/V5? [2] What is the effect of brief and early visual deprivation on the development of the visual motion network? [3] Does blindness onset impact the resting-state connectivity architecture of hMT+/V5 within the visual motion network and with non-visual sensory networks?

The nature of motion processing in hMT+/V5

In the first study of the present thesis, we investigated how hMT+/V5 represents motion direction information. hMT+/V5 has long been known to be a dedicated region for processing visual motion (Baker et al., 1981; J. D. G. Watson et al., 1993; Zeki, 1974, 1980; Zeki et al., 1991). When disrupting the activity of hMT+/V5 by applying transcranial magnetic stimulation (TMS) during visual motion processing, the behavioral performance is impaired (Beckers & Zeki, 1995). Similarly, when hMT+/V5 is damaged due to a bilateral lesion, the perception of visual motion is strongly impaired, with apparently no impairment in auditory motion processing (Zihl et al., 1983, 1991). These findings together highlighted the important role of hMT+/V5 in processing visual motion. In the last decade, studies suggested that hMT+/V5 could be implicated in auditory (Battal et al., 2018; Dormal et al., 2016; Poirier et al., 2005; Strnad et al., 2013) and tactile motion processing (Hagen et al., 2002; Ricciardi et al., 2007; Van Kemenade et al., 2014). These findings opened a new door to question the nature of motion processing in hMT+/V5. Is hMT+/V5 a unisensory visual motion area as previously believed, or whether it is involved in processing motion information from different sensory modalities? Many studies using univariate or multivariate analysis debated this question with some studies supporting the presence of non-visual motion information in hMT+/V5 (or sub-regions of hMT+/V5) (Battal et al., 2018; Dormal et al., 2016; Hagen et al., 2002; Poirier et al., 2005; Ricciardi et al., 2007; Strnad et al., 2013; Van Kemenade et al., 2014). Oppositely, other studies advocated for a unisensory visual hMT+/V5, and suggested that if hMT+/V5 was properly defined, and if proper methodological approaches were implemented, non-visual motion information would not be detected in hMT+/V5 (Jiang et al., 2014, 2015).

To resolve this long-standing debate, we investigated how motion information is represented in hMT+/V5 using a combination of univariate and multivariate analyses while controlling for the suggested methodological confounds. Our results indicated that visual and auditory motion direction information were present in hMT+/V5. Our univariate analyses demonstrated that the activation level of hMT+/V5 for auditory motion was low and even not statistically significant if hMT+/V5 was individually defined, and when data smoothing was avoided. This was in line with the studies that did not find univariate activation in hMT+/V5 for non-visual motion processing (Jiang et al., 2015; Saenz et al., 2008). However, the absence of significant activation was not a proof of lack of auditory motion information. Using multivariate pattern analysis (MVPA), we demonstrated that hMT+/V5 can discriminate motion and static conditions based on the activity patterns. This indicated that despite the low level of univariate activity, there was auditory motion information in hMT+/V5 (Battal et al., 2018; Dormal et al., 2016; Strnad et al., 2013). Additionally, we investigated how auditory individual motion directions are represented in hMT+/V5. It is well-established that MT/V5 has a columnar axis-of-motion organization (Albright et al., 1984a; Dubner & Zeki, 1971; Malonek et al., 1994). This organization was also demonstrated in humans (Zimmermann et al., 2011) using high-field functional magnetic resonance imaging (fMRI). However, no previous evidence has been provided to indicate how auditory motion directions are represented in hMT+/V5. Our results demonstrated that hMT+/V5 has an axis-of-motion organization for visual and auditory motion directions. The similar axis-of-motion organization is most likely the reason we had a significant cross-modal decoding in hMT+/V5, and we could predict the perceived motion direction in one modality (e.g., vision) by using the information from the other modality (e.g., audition). The axis-of-motion organization of auditory motion directions in hMT+/V5 is reminiscent of the recently suggested axis-of-motion organization of auditory motion directions in *planum temporale* (PT) (Battal et al., 2019). The similar organization for motion direction preference in hMT+/V5 (for visual and auditory motion), and PT (for auditory motion) could provide an efficient way of communication and transferring information between different sensory modalities. Recent studies demonstrated the presence of direct connections between hMT+/V5 and PT (Gurtubay-Antolin et al., 2021). The direct structural connections between PT and hMT+/V5 is likely to be the main route of auditory motion information to reach hMT+/V5 either for additional non-visual motion processing or multisensory integration (Alink et al., 2008; Scheef et al., 2009).

Format of representation

There is now a lot of evidence, including our results, indicating the presence of non-visual motion information in hMT+/V5 (Battal et al., 2018; Dormal et al., 2016; Hagen et al., 2002; Poirier et al., 2005; Ricciardi et al., 2007; Van Kemenade et al., 2014), however, the presence of non-visual motion information cannot be a proxy to indicate abstraction of motion processing. Just because one region is recruited in two different tasks

does not guarantee that the underlying computations or representations are similar (Bulthé et al., 2014). Some studies used cross-modal decoding to infer supra-modality or abstracted brain representations (Fairhall & Caramazza, 2013; Kaplan et al., 2015). However, a successful cross-modal decoding only indicates that the necessary information to discriminate different conditions is useful to discriminate the similar conditions from another modality. It does not indicate that the representation across modalities is identical. We highlighted this point in our results, and demonstrated that despite the shared motion direction information from the different modalities in hMT+/V5, motion stimuli from the different modalities elicited opposite responses in hMT+/V5. hMT+/V5 voxels showing the highest responses for visual motion elicited the lowest responses for auditory motion, and vice versa. Therefore, the representation of motion information in hMT+/V5 is not abstracted from the sensory modality, and is in fact modulated by the sensory input modality. The significant cross-modal decoding merely indicates the presence of shared discriminating information, but it does not indicate abstraction. To infer abstraction, a series of multivariate analyses should be implemented to ensure similar representations across modalities. Our results demonstrated that hMT+/V5 is a multi-modal motion processing region that has shared information across modalities, while maintaining a unique response code for each modality.

Multisensory motion processing in hMT+/V5

The multi-modal nature of motion processing in hMT+/V5 does not indicate that hMT+/V5 processes the two modalities separately, or that there is no interplay between the two modalities. On the behavioral level, there is an interplay between the processing of motion information from different sensory modalities. Adapting participants to tactile motion in one direction leads to a motion aftereffect in the visual modality, and vice versa. The cross-modal aftereffects suggested that there is a level of shared representation and information transfer between the two modalities in hMT+/V5 (Konkle et al., 2009). Moreover, integrating motion information from different sensory modalities modulates the activity of hMT+/V5 (Alink et al., 2008; Scheef et al., 2009). Therefore, the multisensory processing and integration of motion information in hMT+/V5 to one coherent percept is advantageous in terms of neural processing, and beneficial on the behavioral level in the perception of our multisensory environment (Soto-Faraco et al., 2003).

Development of the visual motion system in the early blind

Despite the mentioned debate regarding the recruitment of hMT+/V5 during non-visual motion processing in the sighted (Battal et al., 2018; Dormal et al., 2016; Jiang et al., 2014, 2015; Poirier et al., 2005; Ricciardi et al., 2007; Saenz et al., 2008; Van Kemenade et al., 2014), there is an agreement on the recruitment of the visual cortex during non-visual processing in the visually-deprived individuals (Büchel et al., 1998; Pietrini et al., 2004;

Sadato et al., 1996; Weeks et al., 2000). During my PhD, I was also involved in multiple projects investigating the cross-modal reorganization of the "visual" motion system during auditory motion processing, as well as investigating the structural connections between the visual motion area hMT+/V5 and the auditory motion area PT. These projects provided a unique opportunity to work with more data to understand the organization and the development of hMT+/V5 in the absence of visual input. Using machine learning techniques (as that presented in chapter 2), the analysis demonstrated that different planes of auditory motion could be decoded in both the sighted and the early blind (EB). However, more auditory motion information was present in hMT+/V5 in the EB due to cross-modal plasticity (Figure 5.1). This was compensated by reduced auditory motion information in PT in the EB, suggesting a re-allocation of the computational load from PT to hMT+/V5 (Dormal et al., 2016).

These results were later replicated in a second project in our lab where different auditory motion directions were decoded from hMT+/V5 in both groups, and with higher auditory motion information in hMT+/V5, and lower auditory motion information in PT in the EB (Figure 5.2; Battal et al., 2018). We then investigated how auditory motion could reach hMT+/V5 in the sighted and the EB by looking at the structural connectivity between hMT+/V5 and PT. Our results demonstrated that direct connections exist between the two motion processing regions. These results were also replicated when using an independent large-scale dataset from the human connectome project (Figure 5.3). These findings provide strong evidence for direct connections between PT and hMT+/V5. These results potentially explain how auditory motion information reaches hMT+/V5, and why PT redistributes its computational load to hMT+/V5 in the case of early visual deprivation (Gurtubay-Antolin et al., 2021).

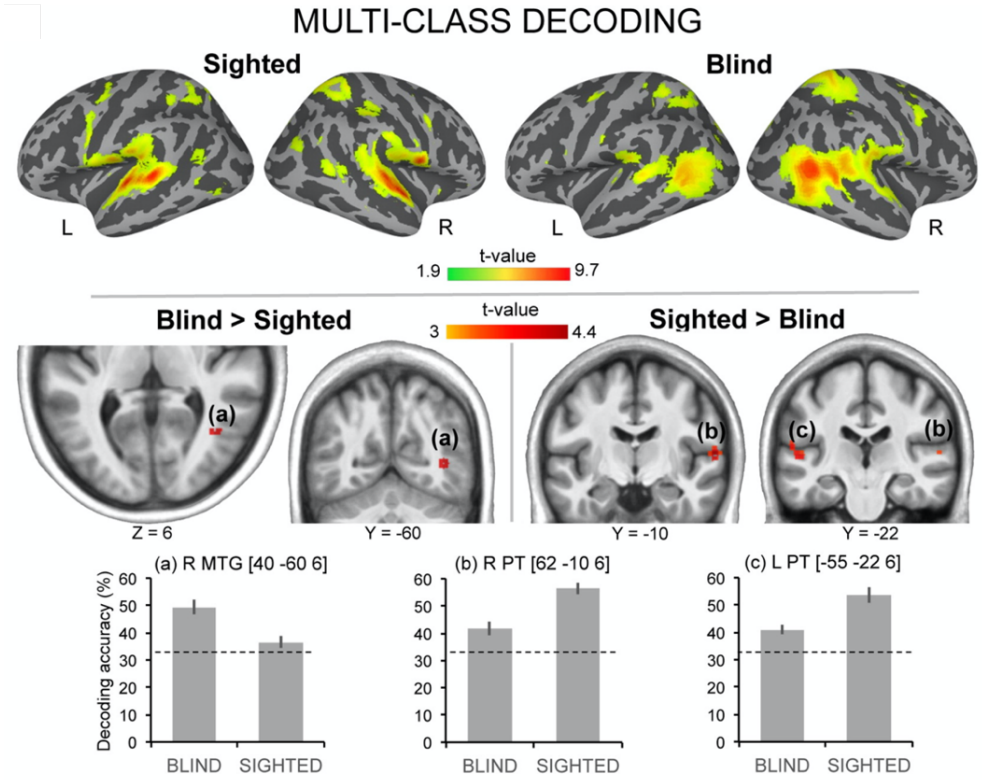


Figure 5.1 Auditory motion plane decoding in the early blind

Multi-class decoding of different auditory motion stimuli (in-depth motion, lateral motion, static): The top panel depicts regions showing above chance level (33.33%) decoding in the sighted and the early blind group (p-uncorrected < 0.001). The bottom panel depicts regions showing significantly higher decoding accuracy in the early blind compared to the sighted group and in the sighted compared to blind group (p-uncorrected < 0.001). The results demonstrate the presence of more auditory motion information in hMT+/V5, and reduced auditory motion information in PT in the early blind. For illustration purposes, the mean decoding accuracy (± SEM) of the 3 auditory conditions (in-depth motion, lateral motion, and static) is plotted for the early blind and the sighted in hMT+/V5 and PT. The figure is adapted from (Dormal et al., 2016).

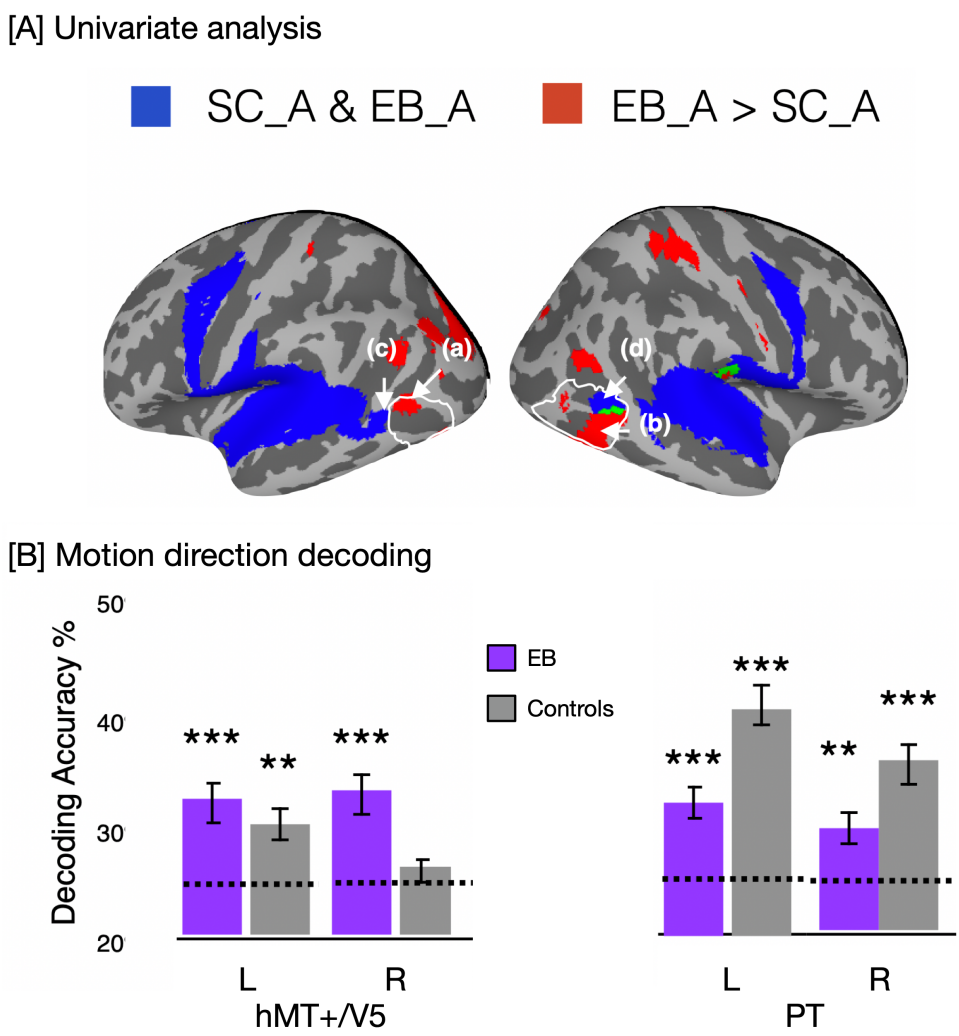


Figure 5.2 Auditory motion direction decoding in the early blind

[A] The univariate results demonstrate that while PT and hMT+/V5 (or subregions of hMT+/V5) are recruited in the early blind and the sighted controls during auditory motion processing, hMT+/V5 shows enhanced recruitment in the early blind. [B] Auditory Motion directions could be predicted above chance (25%) from the activity patterns from hMT+/V5 and PT in both groups. However, more auditory motion direction information was present in hMT+/V5, and less auditory motion direction information was present in PT in the early blind. The figure is adapted from (Battal et al., 2018).

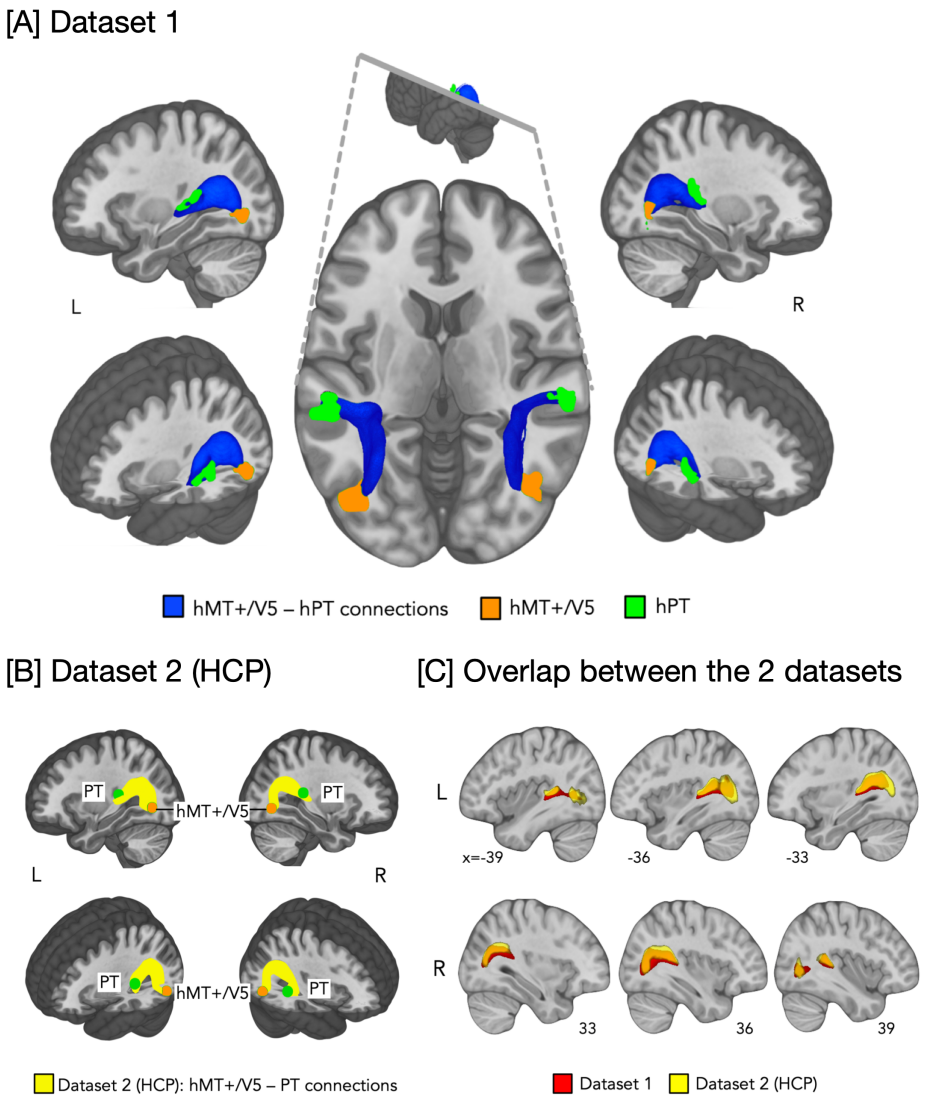


Figure 5.3 Structural connectivity between hMT+/V5 and PT

[A] Dataset 1: Group-averaged structural pathways between hMT+/V5 and PT (in blue) are determined using diffusion tensor imaging (DTI). hMT+/V5 and PT are shown in orange and green respectively. [B] Results from Dataset 2 obtained from the human connectome project (HCP): Group-averaged structural pathways between hMT+/V5 and PT (in yellow). [C] Overlap of the hMT+/V5 – PT connections (from group-level ROIs) derived from Dataset 1 (red) and Dataset 2 (yellow). The results from the two datasets are highly overlapping advocating for the integrity and the robustness of the structural connection between hMT+/V5 and PT. Results are depicted on a T1 MNI template. L: left, R: right. The figure is adapted from (Gurtubay-Antolin et al., 2021).

In addition to the enhanced recruitment of hMT+/V5 in the EB during auditory motion processing (Battal et al., 2018; Bedny et al., 2010; Dormal et al., 2016; Jiang et al., 2014; Poirier et al., 2006; Ricciardi et al., 2007; Strnad et al., 2013; Wolbers, Zahorik, et al., 2011), it is also recruited during processing tactile motion information (Ricciardi et al., 2007). This led researchers to suggest that cross-modal plasticity occurs in a way that respects the functional organization of the brain, where regions typically dedicated to processing visual motion information enhance their processing of non-visual motion information. Therefore, there is a preservation of function while switching preference for the spared modalities (Collignon et al., 2007; Dormal et al., 2016; Pascual-Leone & Hamilton, 2001). The interesting question is what drives a region to perform a specific function following reorganization? What drives hMT+/V5 to process non-visual motion information rather than performing a different cognitive function?

As previously discussed in the introduction of the present thesis, recent theories suggested that functional specialization could develop due to the preference of a certain region to process specific visual features, or due to its connectivity architecture (Op de Beeck et al., 2019). Visual features cannot explain the functional organization of the occipital cortex in the EB as they did not have any visual experience. The biased connectivity hypothesis is a strong candidate to explain the functional role of the different reorganized visual regions. We already demonstrated that hMT+/V5 is a multimodal motion processing region (Rezk et al., 2020) that has direct structural connections with PT (Gurtubay-Antolin et al., 2021). These direct structural connections between PT and hMT+/V5 potentially allows for the transfer of auditory motion information from PT to hMT+/V5. In the absence of visual input, these connections would drive hMT+/V5 to process more auditory motion information while relieving the computational load on PT (Battal et al., 2018; Dormal et al., 2016). Even during rest and without performing any specific task, our resting-state connectivity results demonstrated the presence of functional connectivity between hMT+/V5 and the auditory network in the EB and the sighted. Therefore, we claim that the multisensory nature of motion processing in hMT+/V5, and its connectivity with other motion processing regions from a different sensory network is what drives its functional role in processing non-visual motion following early visual deprivation.

Development of the visual motion system in the late blind

We briefly discussed the effect of early and permanent visual deprivation on the reorganization of the visual motion system (Battal et al., 2018; Bedny et al., 2010; Dormal et al., 2016; Poirier et al., 2006). We also proposed that the cross-modal reorganization observed in hMT+/V5 might link to its intrinsic multi-modal nature (Rezk et al., 2020) and its potentially innate connectivity with the auditory motion network (Gurtubay-Antolin et al., 2021). However, what is the critical/sensitive period for hMT+/V5 to reorganize to have

an enhanced preference for non-visual motion? Studies investigating the effect of early visual experience used the late blind (LB) as a model of late visual deprivation. LB individuals had years of visual experience which was followed by late and permanent visual deprivation. Studies demonstrated that the reorganization of the dorsal stream in the LB was either absent (Bedny et al., 2010) or reduced when compared with the EB (Collignon et al., 2013). This suggested that early visual experience shaped the architecture of the visual system making it less malleable to cross-modal reorganization. That is not to say that the visual system is immune to cross-modal reorganization in the LB (Voss et al., 2006). The visual system can reorganize following visual deprivation to process non-visual information, however, it will not be as extended or as strong as in the case of early blindness (Bedny et al., 2012; Collignon et al., 2013; Voss et al., 2008). Even blindfolding sighted individuals for a few days can lead to the recruitment of the visual cortex during tactile processing, however, following the restoration of visual input, the activity of the visual cortex returns to its normal state before deprivation (Merabet et al., 2008).

Development of the visual motion system in the cataract-reversal patients

In addition to our studies in permanently blind people, we investigated how critical is visual experience during the sensitive period early in life for the development of the visual motion system. Cataract-reversal patients who had their cataract removed early in life represent a unique model of brief and early visual deprivation followed by a long period of visual experience. How does a temporary absence of visual input influence the development of the visual motion system? Some studies investigated whether the brief visual deprivation will trigger a reorganization of hMT+/V5 to process non-visual information, however, the cross-modal reorganization was observed in the early visual cortex rather than in hMT+/V5 (Collignon et al., 2015). This was a bit surprising considering that previous studies demonstrated an impairment in global motion processing in the visual modality (Ellemberg et al., 2002; Hadad et al., 2012) and an enhancement in auditory motion direction discrimination (Bottari et al., 2018) in the cataract-reversal patients. Similarly, animal studies in kittens highlighted that bilateral visual deprivation for a few days in the first weeks in life can lead to permanent deficits in global motion processing (Mitchell et al., 2009). Due to the role of hMT+/V5 in processing global motion (Braddick et al., 2001; Rees et al., 2000), it was speculated that such impairments in global motion processing in the cataract-reversal patients are arising from altered functioning of hMT+/V5 (Ellemberg et al., 2002; Hadad et al., 2012; Mitchell et al., 2009). However, the development of the early and higher-order visual regions following brief early visual deprivation has not been properly tested.

In chapter 3 of the present thesis, we investigated the development of the visual motion system following brief early visual deprivation due to congenital bilateral cataract.

Our results demonstrated that the brief and early visual deprivation had an effect on the early visual cortex, and not on hMT+/V5 (Mitchell et al., 2009). The early visual cortex in the cataract-reversal patients showed reduced recruitment during visual motion processing, and reduced interhemispheric resting-state connectivity. Moreover, the motion selectivity in the early visual cortex correlated negatively with the duration of visual deprivation, and also showed a trend of negative correlation with their behavioral performance in a motion direction discrimination task. Additionally, predicting the perceived motion direction from the activity patterns from V1 was lower in the cataract-reversal patients than in the controls. No univariate and multivariate alterations were found in the response profile of hMT+/V5 in the cataract-reversal patients. These results altogether indicate that the deficits were limited to the early visual cortex while sparing hMT+/V5. This would indicate that V1 is more sensitive to the presence/absence of visual experience to develop in a typical fashion.

Is hMT+/V5 immune to change

Our results in the cataract-reversal patients indicated no changes in the functional recruitment or in the motion direction information in hMT+/V5. However, we are not implying that early brief visual deprivation has no impact at all on hMT+/V5. Studies have already demonstrated that there are impairments in multisensory integration in higher-order visual regions in the occipito-temporal junction, as well as in higher order auditory regions in the superior temporal gyrus in individuals with a history of congenital bilateral cataract (Guerreiro, Putzar, et al., 2015). The responses in hMT+/V5 are modulated by different factors as motion direction, speed, and coherence levels (Braddick et al., 2001; Chawla et al., 1998; Maunsell & Van Essen, 1983; Rees et al., 2000). In our experiment, we used 100% coherence stimuli that are optimal for MVPA and for predicting the perceived motion direction. However, if the coherence level or the speed of motion are modulated, we might observe differences between the groups in the recruitment level of hMT+/V5, however, this remains to be investigated. What we can conclude with confidence is that with salient visual motion stimuli (100% coherence), no differences were observed between the two groups in hMT+/V5. This would indicate that the maladaptive changes due to brief early visual deprivation are more prominent in the early visual cortex, and not in hMT+/V5 as previously suggested (Ellemberg et al., 2002; Hadad et al., 2015; Mitchell et al., 2009).

Cross-modal reorganization in the cataract-reversal patients

Our experiment in chapter 3 focused on the maladaptive plasticity of the visual motion system in the cataract-reversal patients as a result of brief and early visual deprivation. We focused on motion and the visual motion system, however, there are other long-lasting maladaptive consequences in others domains as visual acuity (Lewis et al., 1995; Lewis & Maurer, 2009; Maurer, 2017; Maurer & Lewis, 2001) or face processing

(De Heering & Maurer, 2014; Le Grand et al., 2001; Maurer, 2017). There are also impairments in multisensory integration that could be due to the brain relying less on the noisy signal from the visual input, and relying more on the stable auditory input (de Heering et al., 2016; Guerreiro, Putzar, et al., 2015). But are the maladaptive changes in visual processing compensated with cross-modal plastic changes in the visual system? Recently, it has been demonstrated that the occipital cortex in the cataract-reversal patients showed enhanced recruitment during auditory processing. Interestingly, the regions that showed enhanced recruitment in the cataract-reversal patients during auditory processing were limited to the early visual cortex, and did not include the higher order motion area hMT+/V5 (Collignon et al., 2015). As our findings showed that the highest impairment in visual motion processing was in the early visual cortex, this would suggest that the maladaptive changes in the visual domain were compensated in the auditory domain. We can infer that the absence of visual input early in life is what impaired the early visual cortex to process visual information, and at the same time initiated its reorganization to allow it to perform auditory computations. On the other hand, hMT+/V5 in the cataract-reversal patients and the controls showed enhanced recruitment during processing auditory motion, and no differences between the two groups were observed (Collignon et al., 2015). We speculate that the multisensory nature of hMT+/V5 is what makes it more resilient to a brief period of visual deprivation, and allows it to maintain its role in processing visual and auditory motion.

Connectivity architecture of the visual motion system in the cataract-reversal patients

Since most of the feedforward input to hMT+/V5 comes from V1 (Desimone & Ungerleider, 1986; Rockland, 1989), and since there was reduced connectivity between the early visual cortex and hMT+/V5, then why was there no reduction in the recruitment of hMT+/V5 during visual motion processing in the cataract-reversal patients? Studies demonstrated that in the case of V1 damage, hMT+/V5 still shows significant responses to visual motion stimuli (Ajina, Kennard, et al., 2015). In blindsight individuals, with damaged early visual cortex, the visual information arrives to hMT+/V5 through the intact connections between the lateral geniculate nucleus (LGN) and hMT+/V5 (Ajina & Bridge, 2018, 2019; Bridge et al., 2019). Blindsight individuals were able to discriminate motion directions when they had intact connections between the LGN and hMT+/V5. Oppositely, individuals who couldn't discriminate visual motion directions had impairments in the connections between LGN and hMT+/V5 (Ajina & Bridge, 2018).

As a result of the impairments in the early visual cortex in the cataract-reversal patients, the subcortical route between the LGN and hMT+/V5 could mediate visual information to hMT+/V5. However, this remains to be explored. We did observe some trends in our data to suggest reduced connectivity between the LGN and the early visual

cortex. Despite the absence of difference between the cataract-reversal patients and the controls, the task-based functional connectivity and the resting-state connectivity indicated significant connections between the LGN and the early visual cortex in the controls but not in the cataract. We are currently exploring other techniques, as diffusion tensor imaging (DTI), where we will investigate the structural connections between the LGN, the pulvinar, V1, and hMT+/V5. This could potentially provide more insight regarding the connectivity between the subcortical and the cortical visual regions as observed in the blindsight individuals (Ajina, Pestilli, et al., 2015; Ajina & Bridge, 2018, 2019).

Functional connectivity and plasticity

We demonstrated that visual deprivation even for a short period early in life can have an influence on the connectivity architecture of the visual system. Many studies investigated the effect of long-term visual deprivation on the connectivity profile of the visual system (Liu et al., 2007; Qin et al., 2013; Yu et al., 2008). However, recent studies started to question whether plasticity is what drives connectivity changes, or whether connectivity is what drives plasticity (Hannagan et al., 2015; J. Li et al., 2019). Recent studies suggested that the cortical reorganization observed in the visually deprived follows a pattern that is correlated with the connectivity architecture. Or even more generally, the emergence of a functional specialization in a certain region could be derived by its connectivity architecture (Hannagan et al., 2015; Op de Beeck et al., 2019). For instance, the visual form area (VWFA) in the left hemisphere is specialized in processing visual words (L. Cohen et al., 2000; Dehaene & Cohen, 2011). In the case of visual deprivation, the VWFA is recruited during braille-reading despite the lack of any visual experience. So, is the "visual" word form area really visual? Or is it a language area? What drives the VWFA to process language information? It has been suggested that this functional specialization is due to the connectivity of the VWFA with the language network in the left hemisphere (Bouhali et al., 2014; Stevens et al., 2017). This connectivity is present even in neonates before acquiring any language skills (J. Li et al., 2019). So, this connectivity structure could drive the functional organization of this region. If vision is present, the VWFA, still being a part of the visual system, will process language information from the dominant visual modality (Dehaene et al., 2002). However, if vision is absent, relying on the same connectivity structure, the VWFA will process language-related information from the spared modality (Reich et al., 2011). Looking at the visual motion system, hMT+/V5 is strongly recruited during auditory motion processing in the case of early visual deprivation (Battal et al., 2018; Bedny et al., 2010; Dormal et al., 2016; Jiang et al., 2014; Poirier et al., 2006; Wolbers, Zahorik, et al., 2011). The presence of direct structural connections between hMT+/V5 and PT (Gurtubay-Antolin et al., 2021) support the hypothesis that the reorganized hMT+/V5 might rely on the pre-existing connectivity architecture of hMT+/V5. Therefore, mapping the structural and functional connectivity profile of

hMT+/V5 is necessary to understand its development and its reorganization in the case of visual deprivation.

In chapter 4 of the present thesis, we investigated the resting connectivity architecture of hMT+/V5. Some studies suggested that early visual deprivation triggers a strong reorganization in the resting connectivity profile of the occipital cortex (Burton et al., 2014; Liu et al., 2007; Qin et al., 2013; Yu et al., 2008). Other studies suggested that the connectivity profile of the early visual cortex develops in the same manner, and is not dependent on visual experience (Bock et al., 2015; Striem-amit et al., 2015). However, these studies either focused on the early visual cortex or on large-scale brain networks. In our study, we focused on hMT+/V5 and the organization of its connectivity architecture within the visual motion network, and with the auditory and the tactile networks. Our results suggested that there is a connectivity architecture that is present within the visual motion system regardless of visual experience (Bock et al., 2015; Striem-amit et al., 2015). Oppositely, when investigating the connectivity profile of hMT+/V5 with the non-visual sensory networks, we found a reduced connectivity with the somatosensory network. This result is in line with studies suggesting reduced connectivity between the occipital cortex and the non-visual sensory networks in the EB (Burton et al., 2014; Liu et al., 2007; Yu et al., 2008). We also investigated the impact of blindness onset on the connectivity profile of hMT+/V5. The multisensory connectivity profile of hMT+/V5 was altered in the EB. Moreover, the connectivity fingerprint of hMT+/V5 with different sensory networks in the EB was not similar to that in the sighted. Oppositely, the multisensory connectivity profile of hMT+/V5 in the LB was highly similar to that in the sighted, with no differences between the two groups. These results suggested that late visual deprivation had little effect on the connectivity profile of hMT+/V5. The years of visual experience before blindness onset in the LB developed and stabilized the architecture of the visual motion system, and made it more resistant to reorganization (Bedny et al., 2010).

Limitations of inferring functional reorganization from resting-state connectivity

Resting-state fMRI focuses on the low frequency fluctuations in the blood oxygen-level-dependent (BOLD) signal (Biswal et al., 1995). Early resting-state studies demonstrated that the brain activity in a certain brain region correlated with other regions belonging to the same functional network (Biswal et al., 1995; Biswal, Kylen, et al., 1997; Fox et al., 2005). This suggested that resting-state functional connectivity could reflect the functional organization of the brain (Beckmann et al., 2005; Yeo et al., 2011). Recent studies demonstrated that, indeed, when testing individuals at different cognitive states (as resting-state, or movie-viewing, or performing a motor task), there will be commonalities in the connectivity architecture. However, there will also be state-dependent connectivity differences (Geerligs et al., 2015). Studies also investigated whether functional connectivity

also reflects the structural connectivity between different brain regions. It was demonstrated that the presence of structural connections between different regions is a predictor of high functional connectivity between those regions. however, the opposite is not true. The presence of high functional connectivity between different regions is not an indicator of direct structural connections between them (Honey et al., 2009; Koch et al., 2002). Therefore, inferences from resting-state studies about the structural/functional organization of the brain should be done with caution.

Despite the popularity of using resting-state functional connectivity to understand the reorganization of the brain following visual deprivation, and despite the interesting inferred results from resting-state studies, certain limitations need to be mentioned and discussed. When investigating the reorganization of the brain, some resting-state connectivity results aligned with the functional reorganization of different functionally specialized regions. Regions that showed similar connectivity profiles across groups are the same regions that suggested an abstracted category representation across groups or modalities (X. Wang et al., 2015). The enhanced occipital connectivity with the language network aligns with the EB's occipital recruitment during language processing (Bedny et al., 2011). However, this is not always the case. For example, while the occipital cortex and hMT+/V5 are recruited during performing tactile tasks in the EB (Burton et al., 2004; Ricciardi et al., 2007), the resting-state functional connectivity of the occipital cortex with the somatosensory cortex is strongly reduced (Burton et al., 2014; Liu et al., 2007).

In chapter 4, we discussed two theories that explained why the connectivity between the visual and the tactile networks in the EB is reduced rather than enhanced. The first theory suggests that the reorganized occipital cortex in the EB acts as a multiple demand system (Duncan & Owen, 2000), and is recruited during performing different cognitive tasks (Amedi et al., 2003; Poirier et al., 2006; Ricciardi et al., 2007). During rest, the occipital cortex in the EB will keep switching its connectivity with different brain networks leading to a higher variability of the occipital's connectivity profile across time. However, when performing a specific cognitive task (e.g., as auditory or tactile processing), the occipital cortex will be dedicated to perform the task, and will therefore have less variability in its connectivity profile, and will enhance its connectivity with the non-visual sensory networks (Pelland et al., 2017). This theory works well when speaking about the connectivity of visual areas with the somatosensory or auditory networks. However, it doesn't explain how the visual cortex shows enhanced resting-state connectivity with the language network (Bedny et al., 2011; Watkins et al., 2012). It is unlikely that the visual cortex is constantly shifting its connectivity to different brain networks resulting in the reduced connectivity with the somatosensory cortex, but at the same time systematically increasing its connectivity with the language network.

The second theory suggested that the brain acts as a mixture-of-experts model, where there are different expert networks performing specific functions, and a gating network that assigns different weights to the expert networks. This theory suggested that the reorganized hMT+/V5 becomes an additional expert network for non-visual motion processing. Therefore, the gating network will orthogonalize the output from hMT+/V5 and the auditory/somatosensory network leading to a reduced correlation. However, this theory fails to explain why when performing an auditory/tactile motion task, the connectivity between hMT+/V5 and the auditory/somatosensory network is enhanced (Dormal et al., 2016; Sani et al., 2010). Why would the gating network orthogonalize the outputs from hMT+/V5 and the auditory/tactile expert networks only during rest, but not during performing a task? Moreover, the same theory even fails if applied to another domain. If the occipital cortex in the EB is reorganized to process language related information, wouldn't that lead to the emergence of another expert network in the occipital cortex as was proposed in the case of motion processing? Then this theory should expect reduced connectivity of the occipital cortex in the EB with the frontal language regions, which is not the case (Bedny et al., 2011; Watkins et al., 2012). Both theories work in part when addressing specific examples of cross-modal plasticity. However, they do not generalize to explain the observed reorganization to process different domains.

That is not to undermine the importance of investigating the resting connectivity architecture of the occipital cortex in the EB. Future research should investigate and provide some mechanistic explanation to why the occipital's connectivity changes are different across different domains and networks (e.g., reduced with the tactile network while enhanced with the language network). Nevertheless, mapping the connectivity architecture in the EB is necessary to understand the impact of visual deprivation during the early sensitive period in life. Resting-state analysis is built on the assumption that the resting connectivity profile reflects the functional organization in the brain (Biswal et al., 1995; Fox et al., 2005; Yeo et al., 2011).However, as previously discussed, despite the commonalities in the connectivity architecture across different cognitive states in sighted individuals, there are still some connectivity differences that are modulated by the performed task and the cognitive state (Geerligs et al., 2015). More strikingly, the connectivity between different regions in the EB could even switch its profile at different cognitive states (e.g., reduced connectivity between occipital and the tactile network during rest (Burton et al., 2014; Liu et al., 2007) and enhanced connectivity during performing a tactile motion task (Sani et al., 2010)). Therefore, resting-state connectivity in the EB might not be a perfect reflection of functional connectivity when performing different cognitive tasks. It might be necessary to modify how we test the connectivity between brain regions in the visually deprived. One proposition is to replace resting-state designs with naturalistic complex stimuli (as audio-movies) as this might be a closer reflection of the functional connectivity in the EB when performing certain cognitive tasks (as auditory processing or language processing). It would also be interesting to compare the similarities and

differences between the connectivity profile in the EB during rest and during performing a complex cognitive task (as audio-movie processing). This will directly test if the assumptions used in resting-state analysis are valid in the visually deprived, and whether it's better to use natural stimuli, or combine it with resting-state, to map the connectivity architecture in the blind. Moreover, investigating the link between the changes in the resting-state connectivity and the structural connectivity (Bauer et al., 2017) could potentially connect the missing dots of why the visual system reorganizes in this way following visual deprivation.

Models of the development of the visual motion system

Lastly, we summarize our findings in the present thesis, and integrate it with previous studies investigating the development of the visual motion system and visual deprivation. We propose the following models for the development of the "visual" motion system.

Typical visual development

In individuals who had a typical visual development, visual information reaches the early visual cortex through the LGN (Figure 5.4A). Visual motion information is transmitted to the higher-order visual motion area hMT+/V5 thought feedforward connections (Rockland, 1989, 1995). Additional pathways exist for visual motion information to reach hMT+/V5 through subcortical connections between the LGN or the pulvinar and hMT+/V5, however these pathways are small, compared to the main cortical pathway from the early visual cortex (Maunsell & van Essen, 1983; Sincich et al., 2004). Visual motion directions are represented in hMT+/V5 in an axis-of-motion columnar organization structure (Albright et al., 1984b; Zimmermann et al., 2011). Despite being a dominantly visual area, hMT+/V5 also processes auditory (or tactile) motion information (Battal et al., 2018; Dormal et al., 2016; Hagen et al., 2002; Poirier et al., 2005; Ricciardi et al., 2007; Van Kemenade et al., 2014). The representation of the auditory motion directions follows a similar axis-of-motion organization as that observed in vision. In spite of the similarities between the visual and the auditory motion direction representation in hMT+/V5, there is a distinguishable response code for the auditory and the visual modality (Rezk et al., 2020). This indicates that hMT+/V5 is multimodal in nature, and is not blind to the sensory modality input. The auditory information reaches hMT+/V5 from the auditory motion region PT which also has an axis-of-motion organization (Battal et al., 2019). This information is most likely mediated through the direct structural connections between PT and hMT+/V5 (Gurtubay-Antolin et al., 2021).

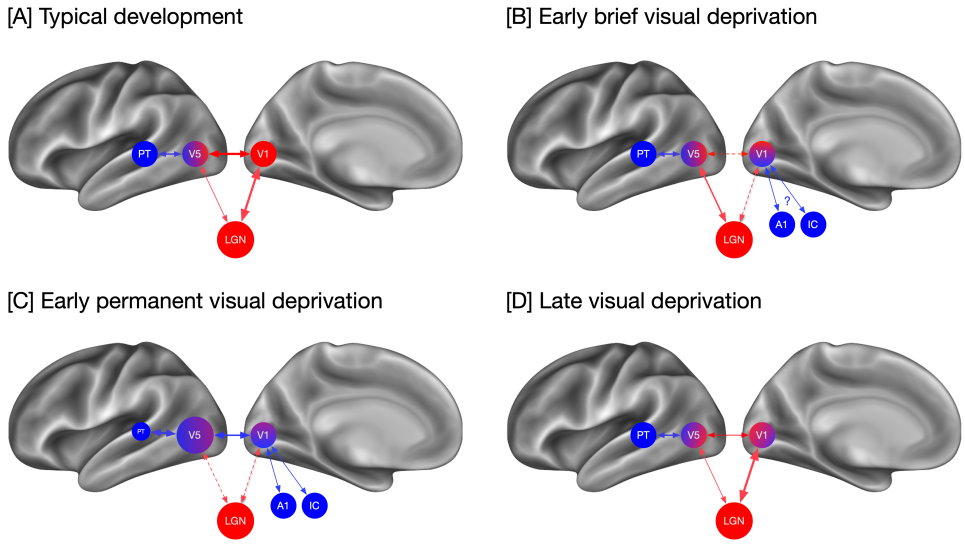


Figure 5.4 Models of the development of the visual motion system.
[A] In the typical development, most of the visual input arriving to V1 comes from the LGN. For hMT/V5, most of the visual input arrive from feedforward connections from V1, in addition to less stronger connections from the LGN. hMT+/V5, a mainly dominant visual motion region, also represents non-visual motion information and is connected to the auditory motion area PT. [B] In the case of early-brief visual deprivation, hMT+/V5 is more resilient to plastic changes than V1 which is strongly impaired in the visual domain and connects less with hMT+/V5 during visual motion processing. Visual motion information could arrive to hMT+/V5 through non-impaired subcortical routes from the LGN. The maladaptive plasticity in V1 is compensated by adaptive beneficial plasticity for non-visual processing. However, the route for auditory information to reach V1 in the case of early brief visual deprivation needs to be investigated. [C] In the case of early permanent blindness, the early visual cortex and hMT+/V5 are massively reorganized to process non-visual information. Auditory motion information processing is enhanced in hMT+/V5 in the EB and therefore reducing the computational load and auditory processing in PT. [D] In the case of late visual deprivation, the visual system has already been developed, and the connections and functions are well established. Cross-modal changes in the dorsal stream might be either absent or present in a smaller magnitude than that in the EB. Red color represents visual processing, while blue color represents auditory processing. Dashed lines represent impaired connections. LGN: lateral geniculate nucleus, PT: planum temporale, IC: inferior colliculus.

Brief early visual deprivation

If brief visual deprivation occurs during the sensitive period early in life, the early visual cortex (V1) is highly reorganized (Collignon et al., 2015; Guerreiro, Erfort, et al., 2015). The recruitment of the early visual cortex for visual motion processing is highly reduced (Figure 5.4B). This reduced recruitment will be correlated with the duration of visual deprivation. Additionally, the connectivity between the early visual cortex and hMT+/V5 will be reduced, as well as the resting-state inter-hemispheric connectivity

between the early visual areas. hMT+/V5 will be more resilient to reorganization following early brief visual deprivation, and will still be able to perform its function without (or with minimal) impairment. This could probably be due to its multi-modal organization that allows it to maintain its role to process motion information from different sensory modalities and to be more resilient to visual deprivation if it occurs for a transient period. Another possibility is that hMT+/V5 receives motion information from alternative subcortical routes, however, this hypothesis needs to be investigated. The produced maladaptive plasticity in the early visual cortex will be compensated by cross-modal plastic changes to allow the early visual cortex to process non-visual information (Collignon et al., 2015). Non-visual motion information will be mainly processed in the auditory motion network (Alink et al., 2012; Baumgart et al., 1999; Lewis et al., 2000), as well as hMT+/V5 just like in the sighted controls (Battal et al., 2018; Dormal et al., 2016; Poirier et al., 2005).

Early permanent visual deprivation

If permanent and long-lasting visual deprivation occurs during the early sensitive period in life, the occipital cortex will be massively reorganized (Büchel et al., 1998; Pietrini et al., 2004; Sadato et al., 1996; Weeks et al., 2000). The early and higher-order visual areas will be reorganized to process auditory (or tactile) motion information. The multi-modal hMT+/V5 will adapt to the absence of visual input and reorganize to have an enhanced processing of non-visual motion information (Battal et al., 2018; Bedny et al., 2010; Dormal et al., 2016; Ricciardi et al., 2007). This will lead to a stronger recruitment of hMT+/V5 to non-visual motion in the EB compared to sighted controls (Figure 5.4C). Non-visual motion direction information in hMT+/V5 will be more reliable in the EB than the sighted. The reorganized hMT+/V5 in the EB will reduce the computational load on PT, and therefore, will lead to reduced auditory motion direction information in PT (Battal et al., 2018; Dormal et al., 2016). The strong reorganization of hMT+/V5 to maintain its functional organization is likely mediated through its organization as a part of dorsal stream which processes spatial and motion information (Goodale & Milner, 1992), and its structural connectivity with PT (Gurtubay-Antolin et al., 2021), which performs a similar functional role in a different modality (Alink et al., 2012; Baumgart et al., 1999; Pavani et al., 2002). The resting connectivity profile of hMT+/V5 within the visual motion network will be similar to that in the sighted. However, it's connectivity with non-visual sensory networks will be modulated by the performed task. During rest, the hMT+/V5 connectivity with the non-visual sensory networks will be reduced (Burton et al., 2014; Liu et al., 2007). During performing a non-visual motion or a spatial task, the connectivity profile will be reversed and enhanced (Dormal et al., 2016; Pelland et al., 2017; Sani et al., 2010).

Late visual deprivation

If visual deprivation occurs late in life, the development of the visual motion system will be well established. Cross-modal reorganization will be minimal. In the presence of cross-modal recruitment of the dorsal stream (including hMT+/V5) in auditory spatial tasks, the recruitment will have a lesser extent, and will not be as functionally selective as in the EB (Collignon et al., 2013). There are also suggestions that hMT+/V5 is not reorganized to process auditory motion information in the LB (Bedny et al., 2010). However, with the more recent techniques as MVPA, and our results in the sighted, we expect to find auditory motion information in hMT+/V5 in the LB. If there is any gain in non-visual motion processing in the LB, it won't be as strong as in the EB. The years of visual experience before visual deprivation will have shaped the visual motion system and sedimented its visual nature. (Figure 5.4D). The connectivity profile of hMT+/V5 during rest will be impacted by late visual deprivation. However, it will be much less than that in the EB. Moreover, it's connectivity with the non-visual sensory networks will be much less impacted.

Summary

The present thesis comprehensively investigated the higher-order motion processing region hMT+/V5. In the first study, we investigated the representation of visual and auditory motion directions in hMT+/V5, and demonstrated that hMT+/V5 represents motion direction information in a multisensory fashion with shared information between the senses. In the second study, we investigated the impact of brief early visual deprivation on the development of the visual motion network. Our results demonstrated that early brief visual deprivation had a region-specific impact on the early visual areas, while hMT+/V5 showed resilience to deprivation. In the third study, we investigated how the onset of permanent visual deprivation impacts the resting-state connectivity profile of hMT+/V5. The results demonstrated that the connectivity profile of hMT+/V5 with different visual regions within the visual motion network was not dependent on visual experience. Oppositely, the connectivity profile of hMT+/V5 with non-visual networks was impacted by the absence of visual experience and the onset of visual deprivation.

References

Ajina, S., & Bridge, H. (2018). Blindsight relies on a functional connection between hMT+ and the lateral geniculate nucleus, not the pulvinar. *PLOS Biology*, *16*(7), e2005769. https://doi.org/10.1371/journal.pbio.2005769

Ajina, S., & Bridge, H. (2019). Subcortical pathways to extrastriate visual cortex underlie residual vision following bilateral damage to V1. *Neuropsychologia*, *128*(January 2018), 140–149. https://doi.org/10.1016/j.neuropsychologia.2018.01.007

Ajina, S., Kennard, C., Rees, G., & Bridge, H. (2015). Motion area V5/MT+ response to global motion in the absence of V1 resembles early visual cortex. *Brain*, *138*(1), 164–178. https://doi.org/10.1093/brain/awu328

Ajina, S., Pestilli, F., Rokem, A., Kennard, C., & Bridge, H. (2015). Human blindsight is mediated by an intact geniculo-extrastriate pathway. *ELife*, *4*(OCTOBER2015), 1–23. https://doi.org/10.7554/eLife.08935

Albright, T. D., Desimone, R., & Gross, C. G. (1984a). Columnar organization of directionally selective cells in visual area MT of the macaque. *Journal of Neurophysiology*, *51*(1), 16–31. https://doi.org/10.1152/jn.1984.51.1.16

Albright, T. D., Desimone, R., & Gross, C. G. (1984b). Columnar organization of directionally selective cells in visual area MT of the macaque. *Journal of Neurophysiology*, *51*(1), 16–31. https://doi.org/10.1152/jn.1984.51.1.16

Alink, A., Euler, F., Kriegeskorte, N., Singer, W., & Kohler, A. (2012). Auditory motion direction encoding in auditory cortex and high-level visual cortex. *Human Brain Mapping*, *33*(4), 969–978. https://doi.org/10.1002/hbm.21263

Alink, A., Singer, W., & Muckli, L. (2008). Capture of Auditory Motion by Vision Is Represented by an Activation Shift from Auditory to Visual Motion Cortex. *Journal of Neuroscience*, *28*(11), 2690–2697. https://doi.org/10.1523/JNEUROSCI.2980-07.2008

Amedi, A., Raz, N., Pianka, P., Malach, R., & Zohary, E. (2003). Early "visual" cortex activation correlates with superior verbal memory performance in the blind. *Nat. Neurosci.*, *6*(7), 758–766. https://doi.org/10.1038/nn1072

Baker, J. F., Petersen, S. E., Newsome, W. T., & Allman, J. M. (1981). Visual response properties of neurons in four extrastriate visual areas of the owl monkey (Aotus trivirgatus): A quantitative comparison of medial, dorsomedial, dorsolateral, and middle temporal areas. *Journal of Neurophysiology*, *45*(3), 397–416. https://doi.org/10.1152/jn.1981.45.3.397

Battal, C., Rezk, M., Mattioni, S., Bottini, R., Bertonati, G., Occelli, V., Targher, S., & Collignon, O. (2018). Decoding auditory motion direction and location in hMT+/V5 and Planum Temporale of sighted and blind individuals. *Journal of Vision*, *18*(10), 436. https://doi.org/10.1167/18.10.436

Battal, C., Rezk, M., Mattioni, S., Vadlamudi, J., & Collignon, O. (2019). Representation of auditory motion directions and sound source locations in the human planum temporale. *The Journal of Neuroscience*, *39*(12), 2218–2289. https://doi.org/10.1523/JNEUROSCI.2289-18.2018

Bauer, C. M., Hirsch, G. V, Zajac, L., Koo, B., Collignon, O., & Merabet, L. B. (2017). Multimodal MR-imaging reveals large-scale structural and functional connectivity changes in profound early blindness. *PLOS ONE*, *12*(3), e0173064. https://doi.org/10.1371/journal.pone.0173064

Baumgart, F., Gaschler-Markefski, B., Woldorff, M. G., Heinze, H.-J., & Scheich, H. (1999). A movement-sensitive area in auditory cortex. *Nature*, *400*(6746), 724–726. https://doi.org/10.1038/23390

Beckers, G., & Zeki, S. (1995). The consequences of inactivating areas V1 and V5 on visual motion perception. *Brain*, *118*(1), 49–60. https://doi.org/10.1093/brain/118.1.49

Beckmann, C. F., DeLuca, M., Devlin, J. T., & Smith, S. M. (2005). Investigations into resting-state connectivity using independent component analysis. *Philosophical Transactions of the Royal Society B: Biological Sciences*. https://doi.org/10.1098/rstb.2005.1634

Bedny, M., Konkle, T., Pelphrey, K., Saxe, R., & Pascual-Leone, A. (2010). Sensitive period for a multimodal response in human visual motion area MT/MST. *Current Biology*, *20*(21), 1900–1906. https://doi.org/10.1016/j.cub.2010.09.044

Bedny, M., Pascual-Leone, A., Dodell-Feder, D., Fedorenko, E., & Saxe, R. (2011). Language processing in the occipital cortex of congenitally blind adults. *Proceedings of the National Academy of Sciences*, *108*(11), 4429–4434. https://doi.org/10.1073/pnas.1014818108

Bedny, M., Pascual-Leone, A., Dravida, S., & Saxe, R. (2012). A sensitive period for language in the visual cortex: Distinct patterns of plasticity in congenitally versus late blind adults. *Brain and Language*, *122*(3), 162–170. https://doi.org/10.1016/j.bandl.2011.10.005

Biswal, B., Kylen, J. Van, & Hyde, J. S. (1997). Simultaneous assessment of flow and BOLD signals in resting-state functional connectivity maps. *NMR in Biomedicine*, *10*(4–5), 165–170. https://doi.org/10.1002/(SICI)1099-

1492(199706/08)10:4/5<165::AID-NBM454>3.0.CO;2-7

Biswal, B., Zerrin Yetkin, F., Haughton, V. M., & Hyde, J. S. (1995). Functional connectivity in the motor cortex of resting human brain using echo-planar mri. *Magnetic Resonance in Medicine*, *34*(4), 537–541. https://doi.org/10.1002/mrm.1910340409

Bock, A. S., Binda, P., Benson, N. C., Bridge, H., Watkins, K. E., & Fine, I. (2015). Resting-State Retinotopic Organization in the Absence of Retinal Input and Visual Experience. *Journal of Neuroscience*, *35*(36), 12366–12382. https://doi.org/10.1523/JNEUROSCI.4715-14.2015

Bottari, D., Kekunnaya, R., Hense, M., Troje, N. F., Sourav, S., & Röder, B. (2018). Motion processing after sight restoration: No competition between visual recovery and auditory compensation. *NeuroImage*, *167*(October 2017), 284–296. https://doi.org/10.1016/j.neuroimage.2017.11.050

Bouhali, F., Schotten, M. T. De, Pinel, P., Poupon, C., Universite, S., Atomique, E., Bm, I., & Yvette, G. (2014). *Anatomical Connections of the Visual Word Form Area*. *34*(46), 15402–15414. https://doi.org/10.1523/JNEUROSCI.4918-13.2014

Braddick, O. J., O'Brien, J. M. D., Wattam-Bell, J., Atkinson, J., Hartley, T., & Turner, R. (2001). Brain areas sensitive to coherent visual motion. *Perception*, *30*(1), 61–72. https://doi.org/10.1068/p3048

Bridge, H., Bell, A. H., Ainsworth, M., Sallet, J., Premereur, E., Ahmed, B., Mitchell, A. S., Schüffelgen, U., Buckley, M., Tendler, B. C., Miller, K. L., Mars, R. B., Parker, A. J., & Krug, K. (2019). Preserved extrastriate visual network in a monkey with substantial, naturally occurring damage to primary visual cortex. *ELife*, *8*, 1–29. https://doi.org/10.7554/eLife.42325

Büchel, C., Price, C. J., Frackowiak, R. S. J., & Friston, K. (1998). Different activation patterns in the visual cortex of late and congentially blind subjects. *Brain*, *121*, 409–419.

Bulthé, J., De Smedt, B., & Op de Beeck, H. P. (2014). Format-dependent representations of symbolic and non-symbolic numbers in the human cortex as revealed by multi-voxel pattern analyses. *NeuroImage*, *87*, 311–322. https://doi.org/10.1016/j.neuroimage.2013.10.049

Burton, H., Sinclair, R. J., & Mclaren, D. G. (2004). *Cortical Activity to Vibrotactile Stimulation : An fMRI Study in Blind and Sighted Individuals*. *228*, 210–228. https://doi.org/10.1002/hbm.20064

Burton, H., Snyder, A. Z., & Raichle, M. E. (2014). Resting state functional connectivity in

early blind humans. *Frontiers in Systems Neuroscience*, *8*(April), 1–13. https://doi.org/10.3389/fnsys.2014.00051

Chawla, D., Phillips, J., Buechel, C., Edwards, R., & Friston, K. J. (1998). Speed-dependent motion-sensitive responses in V5: An fMRI study. *NeuroImage*, *7*(2), 86–96. https://doi.org/10.1006/nimg.1997.0319

Cohen, L., Dehaene, S., Naccache, L., Lehéricy, S., Dehaene-Lambertz, G., Hénaff, M.-A., & Michel, F. (2000). The visual word form area: Spatial and temporal characterization of an initial stage of reading in normal subjects and posterior split-brain patients. *Brain*, *123*(2), 291–307. https://doi.org/10.1093/brain/123.2.291

Collignon, O., Dormal, G., Albouy, G., Vandewalle, G., Voss, P., Phillips, C., & Lepore, F. (2013). Impact of blindness onset on the functional organization and the connectivity of the occipital cortex. *Brain*, *136*(9), 2769–2783. https://doi.org/10.1093/brain/awt176

Collignon, O., Dormal, G., De Heering, A., Lepore, F., Lewis, T. L., & Maurer, D. (2015). Long-Lasting Crossmodal Cortical Reorganization Triggered by Brief Postnatal Visual Deprivation. *Current Biology*, *25*(18), 2379–2383. https://doi.org/10.1016/j.cub.2015.07.036

Collignon, O., Lassonde, M., Lepore, F., Bastien, D., & Veraart, C. (2007). Functional cerebral reorganization for auditory spatial processing and auditory substitution of vision in early blind subjects. *Cerebral Cortex*, *17*(2), 457–465. https://doi.org/10.1093/cercor/bhj162

de Heering, A., Dormal, G., Pelland, M., Lewis, T., Maurer, D., & Collignon, O. (2016). A Brief Period of Postnatal Visual Deprivation Alters the Balance between Auditory and Visual Attention. *Current Biology*, *26*(22), 3101–3105. https://doi.org/10.1016/j.cub.2016.10.014

De Heering, A., & Maurer, D. (2014). Face memory deficits in patients deprived of early visual input by bilateral congenital cataracts. *Developmental Psychobiology*. https://doi.org/10.1002/dev.21094

Dehaene, S., & Cohen, L. (2011). The unique role of the visual word form area in reading. *Trends in Cognitive Sciences*, *15*(6), 254–262. https://doi.org/10.1016/j.tics.2011.04.003

Dehaene, S., Le Clec'H, G., Poline, J. B., Le Bihan, D., & Cohen, L. (2002). The visual word form area: A prelexical representation of visual words in the fusiform gyrus. *NeuroReport*. https://doi.org/10.1097/00001756-200203040-00015

Desimone, R., & Ungerleider, L. G. (1986). Multiple visual areas in the caudal superior

temporal sulcus of the macaque. *Journal of Comparative Neurology*. https://doi.org/10.1002/cne.902480203

Dormal, G., Rezk, M., Yakobov, E., Lepore, F., & Collignon, O. (2016). Auditory motion in the sighted and blind: Early visual deprivation triggers a large-scale imbalance between auditory and "visual" brain regions. *NeuroImage*, *134*, 630–644. https://doi.org/10.1016/j.neuroimage.2016.04.027

Dubner, R., & Zeki, S. (1971). Response properties and receptive fields of cells in an anatomically defined region of the superior temporal sulcus in the monkey. *Brain Research*, *35*(2), 528–532. https://doi.org/10.1016/0006-8993(71)90494-X

Duncan, J., & Owen, A. M. (2000). Common regions of the human frontal lobe recruited by diverse cognitive demands. In *Trends in Neurosciences*. https://doi.org/10.1016/S0166-2236(00)01633-7

Ellemberg, D., Lewis, T. L., Maurer, D., Brar, S., & Brent, H. P. (2002). Better perception of global motion after monocular than after binocular deprivation. *Vision Research*, *42*(2), 169–179. https://doi.org/10.1016/S0042-6989(01)00278-4

Fairhall, S. L., & Caramazza, A. (2013). Brain Regions That Represent Amodal Conceptual Knowledge. *Journal of Neuroscience*, *33*(25), 10552–10558. https://doi.org/10.1523/JNEUROSCI.0051-13.2013

Fox, M. D., Snyder, A. Z., Vincent, J. L., Corbetta, M., Van Essen, D. C., & Raichle, M. E. (2005). The human brain is intrinsically organized into dynamic, anticorrelated functional networks. *Proceedings of the National Academy of Sciences of the United States of America*. https://doi.org/10.1073/pnas.0504136102

Geerligs, L., Rubinov, M., Cam-CAN, & Henson, R. N. (2015). State and Trait Components of Functional Connectivity: Individual Differences Vary with Mental State. *Journal of Neuroscience*, *35*(41), 13949–13961. https://doi.org/10.1523/JNEUROSCI.1324-15.2015

Goodale, M. A., & Milner, A. D. (1992). Separate visual pathways for perception and action. *Trends in Neurosciences*, *15*(1), 20–25. https://doi.org/10.1016/0166-2236(92)90344-8

Guerreiro, M. J. S., Erfort, M. V., Henssler, J., Putzar, L., & Röder, B. (2015). Increased visual cortical thickness in sight-recovery individuals. *Human Brain Mapping*, *36*(12), 5265–5274. https://doi.org/10.1002/hbm.23009

Guerreiro, M. J. S., Putzar, L., & Röder, B. (2015). The effect of early visual deprivation on the neural bases of multisensory processing. *Brain*, *138*(6), 1499–1504. https://doi.org/10.1093/brain/awv076

Gurtubay-Antolin, A., Battal, C., Maffei, C., Rezk, M., Mattioni, S., Jovicich, J., & Collignon, O. (2021). Direct structural connections between auditory and visual motion selective regions in humans. *The Journal of Neuroscience*. https://doi.org/10.1523/jneurosci.1552-20.2021

Hadad, B., Maurer, D., & Lewis, T. L. (2012). Sparing of sensitivity to biological motion but not of global motion after early visual deprivation. *Developmental Science*, *15*(4), 474–481. https://doi.org/10.1111/j.1467-7687.2012.01145.x

Hadad, B., Schwartz, S., Maurer, D., & Lewis, T. L. (2015). Motion perception: a review of developmental changes and the role of early visual experience. *Frontiers in Integrative Neuroscience*, *9*(September). https://doi.org/10.3389/fnint.2015.00049

Hagen, M. C., Franzén, O., McGlone, F., Essick, G., Dancer, C., & Pardo, J. V. (2002). Tactile motion activates the human middle temporal/V5 (MT/V5) complex. *European Journal of Neuroscience*, *16*(5), 957–964. https://doi.org/10.1046/j.1460-9568.2002.02139.x

Hannagan, T., Amedi, A., Cohen, L., Dehaene-lambertz, G., & Dehaene, S. (2015). Origins of the specialization for letters and numbers in ventral occipitotemporal cortex. *Trends in Cognitive Sciences*, *19*(7), 374–382. https://doi.org/10.1016/j.tics.2015.05.006

Honey, C. J., Sporns, O., Cammoun, L., Gigandet, X., Thiran, J. P., Meuli, R., & Hagmann, P. (2009). Predicting human resting-state functional connectivity from structural connectivity. *Proceedings of the National Academy of Sciences of the United States of America*, *106*(6), 2035–2040. https://doi.org/10.1073/pnas.0811168106

Jiang, F., Beauchamp, M. S., & Fine, I. (2015). Re-examining overlap between tactile and visual motion responses within hMT + and STS. *NeuroImage*, *119*, 187–196. https://doi.org/10.1016/j.neuroimage.2015.06.056

Jiang, F., Stecker, G. C., & Fine, I. (2014). Auditory motion processing after early blindness. *Journal of Vision*, *14*(13), 4–4. https://doi.org/10.1167/14.13.4

Kaplan, J. T., Man, K., & Greening, S. G. (2015). Multivariate cross-classification: applying machine learning techniques to characterize abstraction in neural representations. *Frontiers in Human Neuroscience*, *9*, 151. https://doi.org/10.3389/fnhum.2015.00151

Koch, M. A., Norris, D. G., & Hund-Georgiadis, M. (2002). An investigation of functional and anatomical connectivity using magnetic resonance imaging. *NeuroImage*. https://doi.org/10.1006/nimg.2001.1052

Konkle, T., Wang, Q., Hayward, V., & Moore, C. I. (2009). Motion Aftereffects Transfer

between Touch and Vision. *Current Biology*, *19*(9), 745–750. https://doi.org/10.1016/j.cub.2009.03.035

Le Grand, R., Mondloch, C. J., Maurer, D., & Brent, H. P. (2001). Early visual experience and face processing. *Nature*, *410*(6831), 890–890. https://doi.org/10.1038/35073749

Lewis, J. W., Beauchamp, M. S., & DeYoe, E. A. (2000). A comparison of visual and auditory motion processing in human cerebral cortex. *Cerebral Cortex (New York, N.Y. : 1991)*, *10*(9), 873–888. https://doi.org/10.1093/cercor/10.9.873

Lewis, T. L., & Maurer, D. (2009). Effects of early pattern deprivation on visual development. *Optometry and Vision Science*, *86*(6), 640–646. https://doi.org/10.1097/OPX.0b013e3181a7296b

Lewis, T. L., Maurer, D., & Brent, H. P. (1995). Development of grating acuity in children treated for unilateral or bilateral congenital cataract. *Investigative Ophthalmology & Visual Science*, *36*(10), 2080–2095. http://www.ncbi.nlm.nih.gov/pubmed/7657547

Li, J., Osher, D. E., Hansen, H. A., & Saygin, Z. M. (2019). Cortical selectivity driven by connectivity: Innate connectivity patterns of the visual word form area. *BioRxiv*. https://doi.org/10.1101/712455

Liu, Y., Yu, C., Liang, M., Li, J., Tian, L., Zhou, Y., Qin, W., Li, K., & Jiang, T. (2007). Whole brain functional connectivity in the early blind. *Brain*, *130*(8), 2085–2096. https://doi.org/10.1093/brain/awm121

Malonek, D., Tootell, R., & Grinvald, A. (1994). Optical imaging reveals the functional architecture of neurons processing shape and motion in owl monkey area MT. *Proc. R. Soc. Lond. B*, *258*(1352), 109–119.

Maunsell, J. H., & van Essen, D. C. (1983). The connections of the middle temporal visual area (MT) and their relationship to a cortical hierarchy in the macaque monkey. *The Journal of Neuroscience : The Official Journal of the Society for Neuroscience*, *3*(12), 2563–2586.

Maunsell, J. H., & Van Essen, D. C. (1983). Functional properties of neurons in middle temporal visual area of the macaque monkey. I. Selectivity for stimulus direction, speed, and orientation. *Journal of Neurophysiology*, *49*(5), 1127–1147. https://doi.org/10.1152/jn.1983.49.5.1127

Maurer, D. (2017). Critical periods re-examined: Evidence from children treated for dense cataracts. *Cognitive Development*, *42*, 27–36. https://doi.org/10.1016/j.cogdev.2017.02.006

Maurer, D., & Lewis, T. L. (2001). Visual acuity: The role of visual input in inducing

postnatal change. *Clinical Neuroscience Research*. https://doi.org/10.1016/S1566-2772(01)00010-X

Merabet, L. B., Hamilton, R., Schlaug, G., Swisher, J. D., Kiriakopoulos, E. T., Pitskel, N. B., Kauffman, T., & Pascual-Leone, A. (2008). Rapid and reversible recruitment of early visual cortex for touch. *PLoS ONE*, *3*(8). https://doi.org/10.1371/journal.pone.0003046

Mitchell, D. E., Kennie, J., & Kung, D. (2009). Development of Global Motion Perception Requires Early Postnatal Exposure to Patterned Light. *Current Biology*, *19*(8), 645–649. https://doi.org/10.1016/j.cub.2009.02.038

Op de Beeck, H. P., Pillet, I., & Ritchie, J. B. (2019). Factors Determining Where Category-Selective Areas Emerge in Visual Cortex. *Trends in Cognitive Sciences*, 1–14. https://doi.org/10.1016/j.tics.2019.06.006

Pascual-Leone, A., & Hamilton, R. (2001). The metamodal organization of the brain. In *Progress in Brain Research* (pp. 427–445). https://doi.org/10.1016/S0079-6123(01)34028-1

Pavani, F., Macaluso, E., Warren, J. D., Driver, J., & Griffiths, T. D. (2002). A Common Cortical Substrate Activated by Horizontal and Vertical Sound Movement in the Human Brain. *Current Biology*, *12*(18), 1584–1590. https://doi.org/10.1016/S0960-9822(02)01143-0

Pelland, M., Orban, P., Dansereau, C., Lepore, F., Bellec, P., & Collignon, O. (2017). State-dependent modulation of functional connectivity in early blind individuals. *NeuroImage*, *147*(June 2016), 532–541. https://doi.org/10.1016/j.neuroimage.2016.12.053

Pietrini, P., Furey, M. L., Ricciardi, E., Gobbini, M. I., Wu, W.-H. C., Cohen, L., Guazzelli, M., & Haxby, J. V. (2004). Beyond sensory images: Object-based representation in the human ventral pathway. *Proceedings of the National Academy of Sciences*, *101*(15), 5658–5663. https://doi.org/10.1073/pnas.0400707101

Poirier, C., Collignon, O., DeVolder, A. G., Renier, L., Vanlierde, A., Tranduy, D., & Scheiber, C. (2005). Specific activation of the V5 brain area by auditory motion processing: An fMRI study. *Cognitive Brain Research*, *25*(3), 650–658. https://doi.org/10.1016/j.cogbrainres.2005.08.015

Poirier, C., Collignon, O., Scheiber, C., Renier, L., Vanlierde, A., Tranduy, D., Veraart, C., & De Volder, A. G. (2006). Auditory motion perception activates visual motion areas in early blind subjects. *NeuroImage*, *31*(1), 279–285. https://doi.org/10.1016/j.neuroimage.2005.11.036

Qin, W., Liu, Y., Jiang, T., & Yu, C. (2013). The Development of Visual Areas Depends Differently on Visual Experience. *PLoS ONE*, *8*(1), 1–10. https://doi.org/10.1371/journal.pone.0053784

Rees, G., Friston, K., & Koch, C. (2000). A direct quantitative relationship between the functional properties of human and macaque V5. *Nature Neuroscience*, *3*(7), 716–723. https://doi.org/10.1038/76673

Reich, L., Szwed, M., Cohen, L., & Amedi, A. (2011). A ventral visual stream reading center independent of visual experience. *Current Biology*, *21*(5), 363–368. https://doi.org/10.1016/j.cub.2011.01.040

Rezk, M., Cattoir, S., Battal, C., Occelli, V., Mattioni, S., & Collignon, O. (2020). Shared Representation of Visual and Auditory Motion Directions in the Human Middle-Temporal Cortex. *Current Biology*, *30*(12), 2289-2299.e8. https://doi.org/10.1016/j.cub.2020.04.039

Ricciardi, E., Vanello, N., Sani, L., Gentili, C., Scilingo, E. P., Landini, L., Guazzelli, M., Bicchi, A., Haxby, J. V., & Pietrini, P. (2007). The Effect of Visual Experience on the Development of Functional Architecture in hMT+. *Cerebral Cortex*, *17*(12), 2933–2939. https://doi.org/10.1093/cercor/bhm018

Rockland, K. S. (1989). Bistratified Distribution Of Terminal Arbors Of Individual Axons Projecting From Area Vi To Middle Temporal Area (Mt) In The Macaque Monkey. *Visual Neuroscience*. https://doi.org/10.1017/S0952523800004466

Rockland, K. S. (1995). Morphology of individual axons projecting from area V2 to MT in the macaque. *Journal of Comparative Neurology*. https://doi.org/10.1002/cne.903550105

Sadato, N., Pascual-Leone, A., Grafman, J., Ibañez, V., Deiber, M.-P., Dold, G., & Hallett, M. (1996). Activation of the primary visual cortex by Braille reading in blind subjects. *Nature*, *380*(6574), 526–528. https://doi.org/10.1038/380526a0

Saenz, M., Lewis, L. B., Huth, A. G., Fine, I., & Koch, C. (2008). Visual Motion Area MT+/V5 Responds to Auditory Motion in Human Sight-Recovery Subjects. *Journal of Neuroscience*, *28*(20), 5141–5148. https://doi.org/10.1523/JNEUROSCI.0803-08.2008

Sani, L., Ricciardi, E., Gentili, C., Vanello, N., Haxby, J. V., & Pietrini, P. (2010). Effects of Visual Experience on the Human MT+ Functional Connectivity Networks: An fMRI Study of Motion Perception in Sighted and Congenitally Blind Individuals. *Frontiers in Systems Neuroscience*, *4*, 159. https://doi.org/10.3389/fnsys.2010.00159

Scheef, L., Boecker, H., Daamen, M., Fehse, U., Landsberg, M. W., Granath, D. O.,

Mechling, H., & Effenberg, A. O. (2009). Multimodal motion processing in area V5/MT: Evidence from an artificial class of audio-visual events. *Brain Research*, *1252*, 94–104. https://doi.org/10.1016/j.brainres.2008.10.067

Sincich, L. C., Park, K. F., Wohlgemuth, M. J., & Horton, J. C. (2004). Bypassing V1: a direct geniculate input to area MT. *Nature Neuroscience*, *7*(10), 1123–1128. https://doi.org/10.1038/nn1318

Soto-Faraco, S., Kingstone, A., & Spence, C. (2003). Multisensory contributions to the perception of motion. *Neuropsychologia*, *41*(13), 1847–1862. https://doi.org/10.1016/S0028-3932(03)00185-4

Stevens, W. D., Kravitz, D. J., Peng, C. S., Tessler, M. H., & Martin, A. (2017). Privileged functional connectivity between the visual word form area and the language system. *Journal of Neuroscience*. https://doi.org/10.1523/JNEUROSCI.0138-17.2017

Striem-amit, E., Ovadia-caro, S., Caramazza, A., Margulies, S., Villringer, A., & Amedi, A. (2015). *Functional connectivity of visual cortex in the blind follows retinotopic organization principles*. 1–17. https://doi.org/10.1093/brain/awv083

Strnad, L., Peelen, M. V., Bedny, M., & Caramazza, A. (2013). Multivoxel Pattern Analysis Reveals Auditory Motion Information in MT+ of Both Congenitally Blind and Sighted Individuals. *PLoS ONE*, *8*(4). https://doi.org/10.1371/journal.pone.0063198

Van Kemenade, B. M., Seymour, K., Wacker, E., Spitzer, B., Blankenburg, F., & Sterzer, P. (2014). Tactile and visual motion direction processing in hMT+/V5. *NeuroImage*, *84*, 420–427. https://doi.org/10.1016/j.neuroimage.2013.09.004

Voss, P., Gougoux, F., Lassonde, M., Zatorre, R. J., & Lepore, F. (2006). A positron emission tomography study during auditory localization by late-onset blind individuals. *NeuroReport*, *17*(4), 383–388. https://doi.org/10.1097/01.wnr.0000204983.21748.2d

Voss, P., Gougoux, F., Zatorre, R. J., Lassonde, M., & Lepore, F. (2008). Differential occipital responses in early- and late-blind individuals during a sound-source discrimination task. *NeuroImage*, *40*(2), 746–758. https://doi.org/10.1016/j.neuroimage.2007.12.020

Wang, X., Peelen, M. V., Han, Z., He, C., Caramazza, A., & Bi, Y. (2015). How Visual Is the Visual Cortex? Comparing Connectional and Functional Fingerprints between Congenitally Blind and Sighted Individuals. *Journal of Neuroscience*, *35*(36), 12545–12559. https://doi.org/10.1523/JNEUROSCI.3914-14.2015

Watkins, K. E., Cowey, A., Alexander, I., Filippini, N., Kennedy, J. M., Smith, S. M.,

Ragge, N., & Bridge, H. (2012). Language networks in anophthalmia: Maintained hierarchy of processing in "visual" cortex. *Brain*, *135*(5), 1566–1577. https://doi.org/10.1093/brain/aws067

Watson, J. D. G., Myers, R., Frackowiak, R. S. J., Hajnal, J. V., Woods, R. P., Mazziotta, J. C., Shipp, S., & Zeki, S. (1993). Area V5 of the Human Brain: Evidence from a Combined Study Using Positron Emission Tomography and Magnetic Resonance Imaging. *Cerebral Cortex*, *3*(2), 79–94. https://doi.org/10.1093/cercor/3.2.79

Weeks, R., Horwitz, B., Aziz-Sultan, A., Tian, B., Wessinger, C. M., Cohen, L. G., Hallett, M., & Rauschecker, J. P. (2000). A Positron Emission Tomographic Study of Auditory Localization in the Congenitally Blind. *The Journal of Neuroscience*, *20*(7), 2664–2672. https://doi.org/10.1523/JNEUROSCI.20-07-02664.2000

Wolbers, T., Zahorik, P., & Giudice, N. A. (2011). Decoding the direction of auditory motion in blind humans. *NeuroImage*, *56*(2), 681–687. https://doi.org/10.1016/j.neuroimage.2010.04.266

Yeo, B. T. T., Krienen, F. M., Sepulcre, J., Sabuncu, M. R., Lashkari, D., Hollinshead, M., Roffman, J. L., Smoller, J. W., Zöllei, L., Polimeni, J. R., Fischl, B., Liu, H., & Buckner, R. L. (2011). *The organization of the human cerebral cortex estimated by intrinsic functional connectivity*. 1125–1165. https://doi.org/10.1152/jn.00338.2011.

Yu, C., Liu, Y., Li, J., Zhou, Y., Wang, K., Tian, L., Qin, W., Jiang, T., & Li, K. (2008). Altered functional connectivity of primary visual cortex in early blindness. *Human Brain Mapping*, *29*(5), 533–543. https://doi.org/10.1002/hbm.20420

Zeki, S. (1974). Functional organization of a visual area in the posterior bank of the superior temporal sulcus of the rhesus monkey. *The Journal of Physiology*, *236*(3), 549–573. https://doi.org/10.1113/jphysiol.1974.sp010452

Zeki, S. (1980). The response properties of cells in the middle temporal area (area MT) of owl monkey visual cortex. *Proc. R. Soc. Lond. B*, *207*(1167), 239–248.

Zeki, S., Watson, J. D. G., Lueck, C., Friston, K., Kennard, C., & Frackowiak, R. (1991). A direct demonstration of functional specialization in human visual cortex. *The Journal of Neuroscience*, *11*(3), 641–649. https://doi.org/10.1523/JNEUROSCI.11-03-00641.1991

Zihl, J., Von Cramon, D., & Mai, N. (1983). Selective disturbance of movement vision after bilateral brain damage. *Brain*, *106*(2), 313–340. https://doi.org/10.1093/brain/106.2.313

Zihl, J., Von Cramon, D., Mai, N., & Schmid, C. H. (1991). Disturbance of movement vision after bilateral posterior brain damage: Further evidence and follow up

observations. *Brain*, *114*(5), 2235–2252. https://doi.org/10.1093/brain/114.5.2235

Zimmermann, J., Goebel, R., de Martino, F., van de Moortele, P. F., Feinberg, D., Adriany, G., Chaimow, D., Shmuel, A., Uğurbil, K., & Yacoub, E. (2011). Mapping the organization of axis of motion selective features in human area mt using high-field fmri. *PLoS ONE*, *6*(12), 1–10. https://doi.org/10.1371/journal.pone.0028716

List of publications

Rezk, M., Cattoir, S., Battal, C., Occelli, V., Mattioni, S., & Collignon, O. (2020). Shared representation of visual and auditory motion directions in the human middle-temporal cortex. *Current Biology*, 30(12), 2289-2299.

Gurtubay-Antolin, A., Battal, C., Maffei, C., **Rezk, M.**, Mattioni, S., Jovicich, J., & Collignon, O. (2021). Direct structural connections between auditory and visual motion selective regions in humans. *Journal of Neuroscience*.

Benetti, S., Zonca, J., Ferrari, A., **Rezk, M.**, Rabini, G., & Collignon, O. (2021). Visual motion processing recruits regions selective for auditory motion in early deaf individuals. *NeuroImage*, 117816.

Mattioni, S., **Rezk, M.**, Battal, C., Bottini, R., Mendoza, K. E. C., Oosterhof, N. N., & Collignon, O. (2020). Categorical representation from sound and sight in the ventral occipito-temporal cortex of sighted and blind. *Elife*, 9, e50732.

Crollen, V., Lazzouni, L., **Rezk, M.**, Bellemare, A., Lepore, F., Noël, M. P., ... & Collignon, O. (2019). Recruitment of the occipital cortex by arithmetic processing follows computational bias in the congenitally blind. *Neuroimage*, 186, 549-556.

Battal, C., **Rezk, M.**, Mattioni, S., Vadlamudi, J., & Collignon, O. (2019). Representation of auditory motion directions and sound source locations in the human planum temporale. *Journal of Neuroscience*, 39(12), 2208-2220.

Dormal, G., Pelland, M., **Rezk, M.**, Yakobov, E., Lepore, F., & Collignon, O. (2018). Functional preference for object sounds and voices in the brain of early blind and sighted individuals. *Journal of cognitive neuroscience*, 30(1), 86-106.

Davies-Thompson, J., Elli, G. V., **Rezk, M.**, Benetti, S., van Ackeren, M., & Collignon, O. (2019). Hierarchical brain network for face and voice integration of emotion expression. *Cerebral Cortex*, 29(9), 3590-3605.

Benetti, S., van Ackeren, M. J., Rabini, G., Zonca, J., Foa, V., Baruffaldi, F., **Rezk, M.**, & Collignon, O. (2017). Functional selectivity for face processing in the temporal voice area of early deaf individuals. *Proceedings of the National Academy of Sciences*, 114(31), E6437-E6446.

Crollen, V., Lazzouni, L., **Rezk, M.**, Bellemare, A., Lepore, F., & Collignon, O. (2017). Visual experience shapes the neural networks remapping touch into external space. *Journal of neuroscience*, 37(42), 10097-10103.

Dormal, G., **Rezk, M.**, Yakobov, E., Lepore, F., & Collignon, O. (2016). Auditory motion in the sighted and blind: Early visual deprivation triggers a large-scale imbalance between auditory and "visual" brain regions. *Neuroimage*, 134, 630-644